THE ELECTROPHYSIOLOGY OF ADULT RAT FACIAL MOTONEURONES IN A NOVEL IN VITRO BRAINSTEM SLICE : IONIC MECHANISM AND PHARMACOLOGICAL CHARACTERISATION OF SEROTONIN (5-HYDROXYTRYPTAMINE) - EVOKED DEPOLARIZATION

by

Philip M. Larkman

Thesis presented for the degree of

Doctor of Philosophy

University of Edinburgh

1990

DEDICATION

To Fiona, With Love.

In accordance with the requirements of the University of Edinburgh regulation 3.4.7 this thesis has been composed by myself and the work presented herein is my own.

Philip M. Larkman

ACKNOWLEDGEMENTS

There are many people who have provided a great deal of help during my time in Edinburgh. Of great importance has been the love, encouragement and confidence provided by my parents, brothers and sisters especially over the last six months. Their faith and belief in me has been a constant source of inspiration.

A special thanks also to Jennifer and Neil without whom I may never have started, and to Tig who led the way. Their friendship remain an unfailing supply of comfort and strength. Many thanks must go to all my friends both within and outside the Pharmacology Department who have put up with this "boring old sod" from day to day. The lively discussion and endless support they have displayed has been greatly appreciated (even though it may not always have been apparent at the time !).

I am indebted to my supervisor, Professor J.S. Kelly, for his help and support during this research project and especially for the constructive discussion and advice provided during the preparation of this thesis. I am grateful to Miss Audrey Kerr for her assistance in the preparation of the thesis.

The work was supported by a CASE research studentship jointly funded by SERC and Glaxo and by an award from The Wellcome Trust to J.S.K.

ABSTRACT

This study describes intracellular recordings from adult rat cranial motoneurones constituting the Facial Motor Nucleus of the brainstem, using a novel in vitro slice. Facial motoneurones (FMn's) were identified histologically using retrograde labelling with HRP and by antidromic invasion. Antidromically evoked action potentials were overshooting, with initial segment and somato-dendritic components and were often followed by depolarizing potentials. Directly-evoked overshooting action potentials were followed by a fast after hyperpolarization, a brief delayed depolarization and a longer lasting apamin sensitive ahp which was annulled near the predicted equilibrium potential for K^+ ions. Intracellular Cs^+ led to a widening of the spike and a reduction in the amplitude of the ahp. Depolarizing current pulses of longer duration showed a depolarizing prepotential to precede spike generation. Passive membrane properties were investigated using longer duration current pulses and showed the response to be ohmic over a narrow voltage range around rest. The time constant for membrane charging (τ) ranged from 1.5 to 4msec. Larger hyperpolarizing current pulses evoked voltage responses with a time dependent sag characteristic of inward "anomalous" rectification which reached steady state within the pulse. A rebound depolarizing potential occurred subsequent to the current pulse. Voltage clamp studies showed this sag to be the result of a slowly developing inward current.

Intracellular recordings in vitro from a variety of central neuronal types have shown both inhibition and excitation to be modulatory consequences of serotonin receptor activation. Iontophoretic application of 5-HT in vivo on rat facial motoneurones has been shown to evoke a depolarization associated with increased input resistance (Rm). This study has confirmed and further investigated the mechanism and pharmacology of this action in vitro. Superfusion of 5-HT evokes a slow depolarization associated with increased Rm, and a lengthening of τ through a direct action on the post-synaptic membrane. Manual clamping of the membrane potential at the peak of the 5-HT response back to control levels shows a component of the increase in Rm to be due to voltage dependent rectification. Estimated reversal potentials from peak current-voltage plots under these conditions were more negative than the predicted K^+ equilibrium potential. Increasing the extracellular K^+ concentration, $[K^+]_o$, shifted the reversal potential to more positive values in a manner predicted by the Nernst equation for a K^+ conductance. Nor-adrenaline (NA) evoked a similar depolarization associated with increased Rm. However, lower NA concentrations were needed for equivalent size depolarizations and the change in input resistance was usually greater. The estimated reversal potential for the NA effect was more positive than for 5-HT and when manually clamped agreed well with the predicted value. Increasing $[K^+]_o$ changed the reversal potential to a more positive level. Voltage clamp studies show both 5-HT and NA to evoke a slow inward current associated with a decrease in conductance which was greater for NA. 8-OH-DPAT and dipropyl-5-CT, 5-HT_{1A} selective agonists and $2\text{-CH}_3\text{-5-HT}$ a 5-HT_3 agonist were unable to mimic or antagonise 5-HT evoked responses. Methysergide selectively antagonized the 5-HT response leaving the NA response unaffected. LY-53857 also antagonised the 5-HT response while ketanserin was unable to fully abolish 5-HT depolarization even after prolonged exposure. Spiperone, methiothepin and ICS 205-930 were all ineffective antagonists.

CONTENTS

SYNOPSIS

Problems with viability of adult rat spinal cord slices have restricted intracellular investigations of motoneurones *in vitro* to neonatal preparations. As a consequence differences between results of these studies and *in vivo* adult data may largely be developmental. Adult motoneurones constituting the vagal, hypoglossal and ocular motor nuclei of the brainstem have been shown to be viable *in vitro* and possess many of the properties attributed to both cranial and spinal motoneurones studied *in vivo*. This study describes intracellular recordings from motoneurones constituting the Facial Motor Nucleus of the brainstem, using a novel *in vitro* slice.

Facial motoneurones (FM's) were identified histologically using retrograde labelling with HRP and by antidromic invasion following stimulation with a bipolar electrode placed in the region of the genu of the facial nerve. Slice preparation, motoneurone identification and intracellular recording methods are described in Chapter 2. In Chapter 3 intracellular current and voltage clamp records have been used to illustrate the characteristic electrophysiological profile of adult rat FM's *in vitro*.

Antidromically evoked action potentials were overshooting and had initial segment and somato-dendritic components which could be dissociated by hyperpolarisation and more clearly by using a double stimulation protocol. Frequently, antidromic spikes were followed by depolarising synaptic potentials which if of sufficient magnitude evoked an orthodromic spike. The nature of these potentials was not investigated in detail. Directly-evoked overshooting action potentials were about 0.5ms in duration and TTX sensitive. They were followed by a fast after hyperpolarisation (fahp) seen to be

more prominent at depolarised membrane potentials where it appeared to be a continuation of the repolarising phase of the spike, a brief delayed depolarisation (DD) and a longer lasting, apamin sensitive, ahp (~ 50 - 80msec duration) which was annulled near the predicted equilibrium potential for K^+ ions. Intracellular Cs^+ led to a widening of the spike and a reduction in the amplitude of the fast ahp. Depolarising current pulses of longer duration (120msec) showed a depolarising prepotential to often precede spike generation. The first spike could also be seen to be delayed by a slowly rising potential in some motoneurones studied. Sustained repetitive discharge of spikes followed the first spike and continued for the duration of the current pulse, the frequency being dependent on the amplitude of the injected current pulse.

Passive membrane properties were investigated using longer duration hyperpolarising and sub-threshold depolarising current pulses (100-200msec duration). Electrotonic potentials so obtained showed ohmic responses in only a narrow voltage range around rest. The time constant for membrane charging (τ) measured from these responses was about 3ms. Larger hyperpolarising current pulses evoked voltage responses with a time dependent sag characteristic of inward "anomalous" rectification (IR) which reached steady state within the pulse. Voltage clamp studies showed this sag to be the result of a slowly developing inward current. A rebound depolarising potential occurred subsequent to the current pulse. Current voltage (I/V) plots at the peak of the voltage response were linear over a wide range indicating that the inward rectifier obeys ohm's law during steps from a given potential. Neurones held at more negative membrane potentials demonstrated time-dependent sag in response to depolarising current pulses which were followed by

hyperpolarising rebound potentials. Nevertheless the steady-state I/V curve showed an increasing slope with depolarisation thus demonstrating that IR operates in the depolarising direction. In some cases at subthreshold potentials anomalous rectification was observed which may be blocked by TTX. The results are discussed in relation to other central neuronal types with particular reference to the data obtained from other cranial motoneurones in vitro and spinal motoneurones of both the neonate in vitro and adult in vivo.

The first detailed studies on the actions of neurotransmitters classically describe their ability to open non-voltage dependent ion channels which, depending on the ionic selectivity of the channel, led to rapid neuronal excitation or inhibition. These events are fast activating and involve integral receptor ion channel membrane proteins of which the nicotinic acetylcholine receptor provides probably the most investigated example. Further studies have shown the same as well as other putative neurotransmitters to evoke responses with slower activation and longer duration not only by increasing membrane conductance but also by closing channels normally open under resting conditions. These actions appear to be mediated by receptors which are linked to the ion channels by a G protein either directly or through an interaction with a diffusable intracellular second messenger.

Intracellular recordings in vitro from a variety of central neuronal types have shown both inhibition and excitation to be modulatory consequences of serotonin receptor activation. These responses can be seen in isolation or in some cases (e.g. hippocampal pyramidal cells) as a complex biphasic combination of hyperpolarisation followed by depolarisation, suggesting overall control of neuronal excitability may be dependent on the interaction

between activation of more than one post-synaptic receptor and/or mechanism. Inhibitory actions of 5-HT have been studied in detail and are mediated through neuronal hyperpolarisation due to an increase in a K^+ conductance. Details of the mechanism of the central excitatory effect of 5-HT at the start of this study were less comprehensive and are reviewed in Chapter 5. Briefly, depolarisation accompanied by an increase in input resistance (R_m) suggested a mechanism involving K^+ channel closure in the hippocampus though detailed investigation was compromised by the pharmacological manipulation required to isolate this response from the accompanying hyperpolarisation.

The slow depolarisation evoked by 5-HT compares with that elicited by cholinergic agonists acting through muscarinic receptors in several central neuronal types which have been investigated in greater detail (Dodd et al, 1981; Halliwell & Adams, 1982; Madison et al, 1987; Benson et al, 1988; Dutar & Nicoll, 1988). Several components of the muscarinic response have been identified in hippocampal pyramidal cells. When the neurone is held at potentials more negative than the threshold of activation for I_M, activation of an M_1 receptor evokes a depolarisation associated with increased cell input resistance. This is due primarily to the closure of "leak" K^+ channels. More recently a second concomitant increase in a dendritically located Na^+ and/or Ca^{++} conductance, which may or may not be voltage dependent, has also been suggested to contribute to the depolarisation evoked by carbachol but not yet associated with the 5-HT response. Modulation of voltage dependent conductances also contribute to the effects of mAChR activation. Thus at potentials where I_M is active stimulation of an M_2 receptor leads to its suppression thereby reinforcing the depolarisation due

to closure of the "leak" K^+ conductance. In addition M_1 receptor activation also leads to a suppression of the current underlying the slow calcium dependent ahp leading to reduced accommodation of spike firing an effect which may also be added to by M-current suppression.

Iontophoretic application of 5-HT or noradrenaline (NAd) in vivo on rat facial motoneurones evoke a depolarisation associated with increased input resistance. In chapter 6 of Part II of this study the FMN slice was used to help elucidate in greater detail the mechanisms by which 5-HT and NAd evoke monophasic depolarisations of FM's. Superfusion of 5-HT (100 - 250μM) evokes a dose-dependent slow depolarisation (1 - 16mV) associated with increased R_m, and a lengthening of τ through a direct action on the post-synaptic membrane as it is largely unaffected by the presence of TTX in the aCSF. The ratio of the R_m in the presence of 5-HT over that in its absence appeared to be meaningful in relation to the depolarisation though some deviation occurred as the depolarisation amplitude increased. Manual clamping of the membrane potential at the peak of the 5-HT response back to control levels shows a component of the increase in R_m to be due to voltage dependent rectification. Estimated reversal potentials from peak current-voltage plots under these conditions were more negative than the predicted K^+ equilibrium potential, but given the use of 3M KCl filled microelectrodes, indicated that a suppression of a K^+ conductance is the primary mechanism for this effect. Increasing the extracellular K^+ concentration, $[K^+]_o$, shifted the reversal potential to more positive values in a manner predicted by the Nernst equation for a K^+ conductance. Nor-adrenaline (NAd) (10-100μM) evokes a similar depolarisation associated with increased R_m

that differed from the 5-HT response in two ways. Firstly lower NAd concentrations were needed for equivalent size depolarisations and secondly the change in input resistance for a given size depolarisation was greater for NAd than for 5-HT. As such the estimated reversal potential for the NAd effect as more positive than for the 5-HT depolarisation and when manually clamped agreed well with the predicted value. Increasing $[K^+]_o$ to 10mM changed the NAd reversal potential to a more positive level. Voltage clamp studies show both 5-HT and NAd to evoke a slow inward current associated with a decrease in conductance which was greater for NAd. The reversal potential for NAd under these conditions was less negative than for 5-HT as observed with current clamp methods. No evidence was obtained for modulation of the time and voltage dependent inward rectifier or the action potential ahp by either neurotransmitter.

8-OH-DPAT (10μM) a 5-HT_{1A} selective agonist/partial agonist was unable to mimic the 5-HT depolarisation or antagonise a 5-HT evoked response. Likewise dipropyl-5-CT a highly potent 5-HT_{1A} agonist and 2-methyl-5-HT a 5-HT_3 agonist were unable to mimic the 5-HT depolarisation even at equimolar concentrations. The 5-HT response was selectively and competitively antagonised by Methysergide (10-100μM) leaving the NAd response unaffected. LY 53857 (50-100μM) a methysergide analogue with greater 5-$HT_{1C/2}$ receptor selectivity also antagonised the response. Ketanserin (1-100μM) which has high affinity for 5-HT_2 receptors was unable to fully abolish 5-HT responses even after prolonged exposure. Spiperone (10-100μM) a 5-HT_{1A} and 5-HT_2 antagonist and Methiothepin a 5-$HT_{1/2}$ antagonist were both ineffective against the 5-HT evoked depolarisation. During the course of this study a detailed examination of 5-HT evoked

depolarisation of nucleus accumbens neurones was published (North and Uchimura, 1989). The results presented here are discussed in relation to this and other studies of 5-HT evoked excitation.

It is concluded that motoneurones with extensive dendritic morphologies such as FM's maintained in vitro retain the specific biophysical and pharmacological properties observed in vivo and are comparable with other cranial and spinal motoneurones both in vivo and in vitro. The ionic mechanisms of 5-HT and NAd evoked depolarisation can be attributed to a closure of a resting K^+ conductance possibly mediated at different dendritic locations though an additional unidentified conductance increase evoked by 5-HT cannot be excluded. The data presented cannot distinguish between a 5-HT_{1C} and 5-HT_2 identity for the receptor mediating this event though the results with Spiperone and Ketanserin suggest a 1C identity to be more probable. Recent molecular biological discoveries coupled with pharmacological and biochemical evidence indicate that this ambiguity obtained with electrophysiological techniques is not surprising given the similarities between the two receptor subtypes.

PART I

The Electrophysiology of Adult Rat Facial Motoneurones *in vitro*

CHAPTER 1 INTRODUCTION

The development of the in vitro brain slice technique has facilitated detailed studies of the electrophysiology of a wide range of neuronal types in the adult vertebrate central nervous system (CNS). In addition to the greater stability that this preparation provides over in vivo models, control over the composition of the extracellular artificial cerebrospinal fluid (aCSF) has enabled detailed pharmacological investigation of the passive and active membrane properties of central neurones using intracellular recording methods. Studies of this nature have made it clear that as well as possessing fast sodium and delayed rectifier type potassium conductances similar to those shown to underlie the action potential (AP) in the squid giant axon (Hodgkin and Huxley, 1952a,b), the cell soma and dendrites display a wide array of other voltage and ligand gated channels. Combined with the passive electrotonic properties of the cell membrane, these conductances, and their modulation, allow detailed integration of spatially and temporally distinct synaptic potentials leading to frequency coded AP output by the neurone. Indeed instances of direct neurotransmitter modulation of voltage dependent conductances are apparent.

The resistance and capacitance of the neuronal membrane control the passive electrotonic propagation of post-synaptic potentials (psp's). The membrane time constant, τ, governs the temporal propagation of a psp. The value of τ is the product of neuronal resistance and capacitance and can be experimentally determined as the time taken for an evoked voltage response to reach 63% of its steady state value under purely passive conditions. Conduction of

a psp along the length of a dendrite is determined by a proportional ratio of the membrane and cytoplasmic resistances. This is described by the length constant, λ, which is determined from the equation:

$$\lambda = \sqrt{\frac{r_m}{r_a}}$$

r_m = membrane resistance x unit length (Ωcm)
r_a = cytoplasmic resistance/unit length (Ω/cm)

The value of λ is the distance over which the amplitude of a potential falls to 37% of its original level. Thus λ will be smaller as dendritic length increases for a constant diameter, i.e. as r_m decreases and r_a increases. Even though the capacitance per unit length (F/cm) (C_m) of the membrane increases with membrane area, λ is independent of C_m because it can be assumed that at the steady-state potential the capacitance is fully charged.

By far the most detailed studies of active properties of the soma-dendritic membrane using the brain slice technique have been performed on hippocampal pyramidal neurones. In contrast the investigation of adult spinal motoneurones has suffered from the poor viability of spinal cord slices, thus studies have been largely restricted to immature motoneurones of neonatal rat hemisected or sliced spinal cord (Takahashi, 1978; Harada and Takahashi, 1983; Fulton and Walton, 1986; Walton and Fulton, 1986). Differences between the results obtained from these studies compared to <u>in vivo</u> adult data may largely be developmental.

The AP depolarisation in both adult cat and neonatal rat motoneurones appears to be mediated by a tetrodotoxin (TTX) sensitive transient sodium conductance I_{NaT} (Barrett and Crill, 1980; Crill and Schwindt, 1983; Harada and Takahashi, 1983). Repolarisation is attributed to a combination of the rapid

inactivation displayed by I_{NaT}, a large leak conductance provided by the soma-dendritic tree and the activation of an outward potassium conductance, I_{Kf} (Barrett, Barrett and Crill, 1980). This conductance can be blocked by tetraethylammonium (TEA) and may also show some sensitivity to Co^{2+} and Mn^{2+} suggesting some calcium dependence (Schwindt and Crill, 1981). However a small narrowing of the action potential of neonatal motoneurones in the presence of Cd^{++} was attributed to an effect on Na^{+} channels (Walton and Fulton, 1986). In hippocampal pyramidal cells a somatic transient sodium conductance is also responsible for AP depolarisation but while a delayed rectifier I_K conductance with slow steady-state inactivation has been characterised its role in AP repolarisation is thought to be not as important as in the squid axon (Storm, 1987). Two other outward currents have been shown to be important in AP repolarisation and probably also underlie the initial fast afterhyperpolarisation (fahp). I_c is a rapidly activating calcium dependent potassium current which can be blocked with TEA, suggesting similarity to I_{Kf} of motoneurones described earlier (Brown and Griffith, 1983a). AP repolarisation was slowed by both Ca^{2+} channel blockers and TEA both of which showed mutual occlusion suggesting a role for I_c. A rapidly activating transient outward current which requires hyperpolarisation to remove steady-state inactivation and is sensitive to 4-aminopyridine (4-AP) is termed I_A and also contributes to repolarisation. Both 4-AP and depolarising prepulses widen the last two thirds of the AP and abolish the fahp (Storm, 1987). An I_A like current has only tentatively been identified in adult cat motoneurones and as such a role for it has not been speculated on (Schwindt and Crill, 1980). While 4-AP has been shown to widen the AP in spinal motoneurones <u>in vivo</u> (Zhang and

Krnjevic, 1986) the specificity of this action cannot at this stage be attributed to an action on an I_A-like current.

In both adult and neonatal motoneurones the firing rate is dependent on calcium entry through its influence on the slower activating calcium dependent potassium conductance I_{Ks}, (Barrett, Barrett and Crill, 1980; Walton and Fulton, 1986), which underlies the slow ahp seen in these neurones. Similarities of this current to I_{AHP} located in hippocampal cells (Lancaster and Adams, 1986) exist. While the calcium dependence of I_{Ks} in adult motoneurones is only inferred this current is blocked by apamin (Zhang and Krnjevic, 1987) in common with I_{AHP} of pyramidal cells. I_{Ks} is activated 10mV or so above resting potential where it is responsible for a sag seen in the sub-threshold depolarising voltage response. I_{AHP} has also been suggested to be tonically active in a similar voltage range. Given the similarities in the underlying conductances it is of interest that the ahp of neonatal rat motoneurones is considerably longer than that seen in the adult rat and as such may contribute to the lower firing rates observed (Fulton and Walton, 1986).

Many central neurones display complex response properties, however cat spinal motoneurones <u>in vivo</u> appear to be more limited in the firing patterns they express. In response to depolarising current, adult cat motoneurones fire tonically at a relatively slow rate. The frequency intensity (f/I) relationship is linear and generally shows two ranges, the secondary higher frequency range being steeper than the primary range (Schwindt and Crill, 1982). Neonatal rat motoneurones <u>in vitro</u> show only a single range with lower maximum firing rates, in this respect similar to the primary range of adult motoneurones. However, the slope of the neonatal

f/I relationship is steeper than the secondary range observed in adults which is a likely consequence of the higher input resistance of neonatal motoneurones (Walton and Fulton, 1986).

Whether the absence of a secondary firing range in neonates is a developmental or species difference has not been satisfactorily resolved. A steady inward current, I_i, activated 10mV positive to rest in adult cat spinal motoneurones in vivo is carried largely by Ca^{++} and shows similarities to low threshold calcium currents in other neurones. It shows no voltage dependent inactivation such that it has been suggested that this inward current, by opposing outward current flow, maintains linear firing at high frequencies and where I_i is more prominent it can promote the secondary firing range (Schwindt and Crill, 1980, 1982). However, in the neonatal rat a different emphasis of voltage dependent conductance interaction is suggested (Walton and Fulton, 1986). Here the sustained inward calcium current I_i leads to activation of outward calcium dependent potassium conductances which prevent a secondary firing range.

In the neonatal preparation blockade of sodium and outward potassium conductances allowed Ca^{++} dependent action potentials to be evoked which could in certain instances be sustained for several seconds (Walton and Fulton, 1986). In older animals these potentials became progressively less prominent. The occurrence of Ca^{++} AP's under these conditions coincided temporally with the delayed depolarisation (DD) seen following sodium AP's. As the DD was also suppressed by Mn^{++} or Co^{++} it is suggested that it is a calcium dependent potential which is normally suppressed by outward K^{+} conductances (Harada and Takahashi, 1983).

In addition to a low threshold calcium conductance pyramidal cells also possess a slowly rising high threshold inward current which may be partially or even totally dendritic. It is evoked from potentials more depolarised than the low threshold Ca^{++} current (Brown and Griffith, 1983b) and may be subject to calcium mediated inactivation (Pitler and Landfield, 1987). Hippocampal neurones also possess two conductances not identified in spinal motoneurones. I_M is a Ba^{++} sensitive-slowly activating outward K^+ current observed between potentials of -70 to -30mV. As well as being subject to modulation by neurotransmitters, notably via the muscarinic acetylcholine receptor subtype, it is proposed to be responsible for an early component of AP adaptation during sustained depolarisation (Halliwell and Adams, 1982). A sustained TTX sensitive sodium current I_{NaS} has also been seen in pyramidal cells where it contributes to the observed anomalous rectification of depolarising membrane potential responses as threshold is approached (Hotson et al, 1979).

Finally both adult cat motoneurones and hippocampal pyramidal cells display a time dependent sag in hyperpolarising voltage responses. This is mediated probably in both cases by a mixed Na^+/K^+ inward current which is activated slowly by hyperpolarisation. In the hippocampus this inward rectifier current is termed I_Q and is not observed at potentials more positive than -80mV (Halliwell and Adams, 1982) whereas in adult cat motoneurones it is observed at more positive potentials (Barrett, Barrett and Crill, 1980). The depolarising action of the inward rectifier may serve to maintain the resting potential at a level positive to the potassium equilibrium potential (E_{K+}) and thus close

to action potential threshold. Modulation of firing rate by influencing the duration and amplitude of ahp's has also been suggested.

Fears that intracellular recordings in the brain slice would be restricted to cell types with compact dendritic field were allayed by recent studies of adult mammalian cranial motoneurones contemporary with this project. Rat ocular motoneurones (Gueritaud, 1988) and guinea-pig hypoglossal motoneurones (Mosfeldt-Laursen and Rekling, 1989) have been successfully investigated using coronal brainstem slices despite their extensive dendritic morphologies. Similarly adult cat spinal cord slices have enabled intracellular studies of sympathetic preganglionic neurones whose dendritic fields extend at least 2mm in the longitudinal direction (Yoshimura et al, 1986).

This study describes intracellular recordings from motoneurones constituting the Facial Motor Nucleus (FMN) using a novel <u>in vitro</u> slice from the brainstem of the adult rat. Axons of facial motoneurones (FM's) form the major branches of the seventh cranial nerve supplying the superficial and some deeper muscles of the head and neck. Chromatolytic and retrograde tracing, as well as electrophysiological techniques have shown a topographic representation of the facial muscles and nerve branches on four or five sub-divisions of the FMN (Courville, 1966; Martin and Lodge, 1977; Watson et al, 1982; Friauf and Herbert, 1985; Semba and Egger, 1986). Temporal and zygomatic branches which supply axons to muscles of the dorsal head region and eyes are largely represented in the dorsal subdivision; cell bodies contributing axons to the marginal mandibular and buccal branches innervating the nasolabial muscles, including those controlling vibrissal movement,

are in the intermediate and lateral subdivisions, while the medial subdivision is occupied by motoneurones sending axons to the muscles governing pinna movement via the posterior auricular branch. An additional group of motoneurones located dorsally to the main FMN and referred to as the suprafacial nucleus supplies axons to the deeper muscles of the neck (Semba and Egger, 1986; Friauf and Herbert, 1985).

The discrete topographical respresentation of facial muscles within the FMN has been related to differential afferent synaptic input. For example, retrograde tracing has shown the lateral subdivision to receive selective afferent projections from the parabrachial nuclear complex (involved in pneumotaxic function) the nucleus ambiguus (containing respiratory neurones) and the contralateral red nucleus, thus implicating roles for sensorimotor integration of vibrissal and nasal movement (Hinrichsen and Watson, 1983). However, these studies generally present a less clear picture with more general innervation to all subdivisions from other brain regions (Isokawa-Akesson and Komisaruk, 1987).

Until recently despite detailed morphological studies in a variety of species, the electrophysiology of the FMN had been confined to <u>in vivo</u> studies in the rat and cat which were principally concerned with the excitability and synaptic activation of FM's (Iwata et al, 1972; McCall and Aghajanian, 1979a,b, 1980a,b; Fanardjian et al, 1983a,b; Fanardjian and Manvelyan, 1987a,b). Virtually no data existed on the specific membrane properties of rat FM's. This study describes the passive and active membrane properties of adult rat FM's <u>in vitro</u> and discusses these characteristics in relation to other adult cranial and spinal motoneurones. Some of this work has already been published

(Larkman et al, 1989) or presented in abstract form (Larkman et al, 1988; Larkman and Kelly, 1988). While in progress two other relevant in vitro studies have also recently appeared, one studying FM's in the rat (Aghajanian and Rasmussen, 1989) and the other using a guinea-pig slice (Nishimura et al, 1989).

CHAPTER 2 METHODS

Preparation of the Facial Motor Nucleus (FMN) slice

Drug preparation and administration

Identification of motoneurones in the FMN

Intracellular Recordings:

i) Current clamp

ii) Discontinuous current clamp: Optimal setting of negative capacitance compensation

iii) Voltage clamp

Data storage and analysis

Figures 2.1 - 2.5

Table 2.1

Preparation and maintenance of the facial motor nucleus (FMN) slice

Adult Cob Wistar rats (160-250g) were decapitated using a small animal guillotine and the dorsal part of the cranium removed. The brain was sectioned at the level of the inferior colliculus, the cranial nerves cut, and the brainstem with attached cerebellum quickly removed and placed in pre-oxygenated artificial cerebrospinal fluid (aCSF) at 4°C (Llinas and Yarom, 1981). The tissue was placed on aCSF moistened filter paper, the cerebellum removed and the rostral end of the brainstem glued to a plastic block using cyanoacrylate glue, with an agar block supporting the dorsal surface. After attaching the plastic block to an aCSF (4°C) filled plexiglass chamber the brainstem was sliced coronally in the ventral to dorsal direction using a Vibroslice (Cambden Inst.).

The composition of aCSF in mM was; NaCl 124, KCl 5, $MgSO_4$ 2, $CaCl_2$ 2, $NaHCO_3$ 26, HEPES 1.25, D-Glucose 10, and pH was 7.4 after equilibration with a 95% oxygen : 5% carbon dioxide gas mixture. In early experiments, to provide protection against anoxia, hydrogen peroxide (0.003% w/v) was added to the aCSF. This concentration of H_2O_2 was lower than that seen to affect synaptic transmission in hippocampal slices in vitro (Pellmar, 1987) and has been used in other studies to maintain central preparation viability (Llinas et al, 1981; Walton and Fulton, 1983). However, to allow the superfusion of noradrenaline (NAd), which is rapidly oxidised in the presence of H_2O_2, this was later abandoned without prejudicing FM viability though the proportion of successfully viable slices obtained was reduced.

In experiments designed to determine the effects of the potassium ion concentration $[K^+]$ on 5-HT and NAd evoked depolarisations, changes in the KCl concentration of the aCSF were

accommodated by equimolar changes in NaCl, to maintain the overall monovalent ion concentration. Likewise when CsCl was added to the aCSF equimolar concentrations of NaCl were removed.

Since the facial nuclei of a 200g rat measures approximately 2.3mm mediolaterally, 1.7mm dorsoventrally, and 1.5mm rostrocaudally, 3 to 4 slices (~ 350μM thick) can be obtained. The nuclei are located near the ventral surface of the brainstem either side of the midline (Fig.2.1). Their rostral boundaries are marked by the descending fibres of the facial nerve and the superior olivary complex, while caudally they are associated with the rostral boundaries of the Nucleus Ambiguus and the Inferior Olivary Complex.

The slices were quickly transferred to a Haas type interface chamber (Fig.2.2) (Haas et al, 1979) and perfused at a rate of 0.5 - 1.0ml min^{-1} with aCSF at 37°C. Briefly, the incubation chamber sits above a thermostatically controlled water bath maintained at approximately 37°C. aCSF is fed by gravity from a series of reservoirs, interconnected by three-way taps, via an adjustable membrane flow regulator (Regu-Flo 300) and polypropylene tubing (i.d. 1mm) to the incubation chamber. The tubing runs through the water bath and enters a small reservoir at the head of the incubation chamber. The pre-warmed aCSF is then run through a nylon mesh on the base of the chamber, upon which the slices rest, and subsequently drained off via a tissue paper wick. A humidified 95% oxygen : 5% carbon dioxide atmosphere is maintained above the slices by bubbling the gas mixture through the water bath and allowing access to the slices through a port at the head of the incubation chamber. The whole procedure lasted about 10 minutes and slices were incubated for at least one hour before attempting intracellular recording.

Later experiments utilised the method of Aghajanian and Rasmussen (1989) in an attempt to increase the proportion of viable slices without using H_2O_2. Based on the principle that it is passive chloride entry which is acutely responsible for neurotoxicity during slice preparation, the cutting and incubating aCSF was modified such that all the NaCl (126mM) was replaced by equimolar sucrose (252mM). Only after 1h incubation in this modified aCSF was perfusion with normal aCSF started. Intracellular recordings were attempted after a further 30 minutes incubation. The quality of intracellular recordings achieved using this method were the same as with the original procedure though the proportion of viable slices overall was increased.

Drug preparation and administration

All drugs were applied to FM's by addition to the superfusing aCSF. 5-HT creatinine sulphate was diluted to the required concentration immediately prior to use from a 20mM stock solution in deionised distilled water which had been stored at -20°C. Noradrenaline (NAd) was prepared as a 10mM stock solution in 10^{-4}M ascorbic acid (pH = 4), to prevent oxidation, and stored as for 5-HT. A 10mM frozen stock solution of Spiperone (free-base) was prepared in 6.7 x 10^{-3}M (1mg/ml) tartaric acid. Ketanserin tartrate was prepared immediately prior to use either as a 5mM solution in 0.01M HCl or as a 50mM solution in DMSO. When diluted to use concentrations in aCSF the final concentration of DMSO was 0.1% or less. Tetrodotoxin was stored as a 313μM stock solution in equimolar acetic acid. All other drugs were prepared and stored as described for 5-HT though the stock concentration depended on each individual drug solubility (See table 2.1).

The onset of action and time to equilibration of drugs applied via the superfusing aCSF was dependent on both the flow rate and the dead-space between the reservoir containing the drug/aCSF mixture and the incubation chamber. The dead-space was measured at 2ml which led to a 2 to 4 minutes delay between switching to drug-containing aCSF and its appearance in the incubation chamber (based on the maximum and minimum flow rates described earlier). In all figures the onset of drug application refers to the time at which the perfusion reservoirs were switched and not the point at which drug enters the chamber.

The time to equilibration was dependent on several factors including flow rate, active uptake within the slice and drug lipophilicity. The latter two are discussed in a later section. The volume of the incubation chamber was approximately 250μl thus based on the flow rates achieved its volume will be replaced every 15 to 30 seconds suggesting that this variation will affect time taken to achieve equilibration. While equilibration of an agonist can be determined by attainment of a steady-state response equilibration of an antagonist is less easy to determine such that this may explain some of the poor antagonistic effects of some putative 5-HT receptor blockers.

Identification of motoneurones in the FMN

In a preliminary study motoneurones in the FMN were identified by retrograde transport of Horse Radish Peroxidase (HRP) (Type VI, Sigma), from peripheral branches of the ipsilateral facial nerve. Rats were anaesthetised with a Fentanyl-Fluanisone (Hypnorm), Midazolam (Hypnoval), water mixture (1:1:1) (3.3mlkg^{-1} i.p.) and the peripheral branches of the facial nerve exposed. Branches were dissected away from underlying and overlying tissue and transected.

The proximal stump was washed with sterile water, dried thoroughly, placed on a piece of plastic sheet and an HRP-agar pellet applied to the cut end (Enevoldson et al, 1984; Semba et al, 1984). This was sealed in place using cyanoacrylate glue and the wound sutured. The animals were left for 36 hours before being deeply anaesthetised with Methohexitone Sodium (Brietal Sodium) and transcardially perfused with the following solutions: (Rosene and Mesulam, 1978).

1. Buffered saline solution (gl^{-1}): $NaH_2PO_4.2H_2O$ 2.03, Na_2HPO_4 12.32, NaCl 5. Heparin 1ml l^{-1} (Heparin Injection 5000Uml^{-1} Weddel Pharm Ltd.) 100ml.
2. Fixative Solution: 1.25% Glutaraldehyde, 0.4% Paraformaldehyde, 5% Sucrose in buffered saline solution. 500ml rate adjusted to last 30 minutes.

The brain was then removed, placed in a fixative solution with 10% sucrose at 4°C for 2-4 hours and then soaked overnight in buffered saline solution with 10% sucrose at 4°C. Coronal sections (50μm) through the brainstem were cut using a freezing microtome and then processed for HRP using the 3,3', 5,5'-tetramethylbenzidine method of Mesulam (1978). Sections were mounted on chrome-alum subbed slides and coverslipped with DPX.

Fig.2.3 shows labelled FM's in the lateral, intermediate and dorsal subdivisions of the FMN after HRP application to the buccolabial branch of the facial nerve. This confirms the work of Semba and Egger (1986) and also Watson et al (1982) who injected HRP into the nasolabialis muscle bed and showed a similar localisation of labelled motoneurones.

Intracellular Recording

The slices were illuminated with fibre optics and the FMN identified as a darker grey area in the ventral brainstem in the area identified by the previous HRP studies. Identification was often aided by observation of ascending nerve fibres climbing towards the genu of the facial nerve in the dorsal aspect of the slice (Fig.2.1). Intracellular recordings were made using microelectrodes pulled on a Flaming-Brown horizontal puller (Sutter Inst.) using 1.2mm outside diameter, thin walled fibre, glass capillaries (Clark Electromedical). They were filled with 3M KCl and had D.C. resistances of 10-50MΩ. The general layout of the electrical recording apparatus is shown in Fig.2.4. In some experiments 2M CsCl filled microelectrodes with similar DC resistances were used to block outward K^+ conductances by allowing leakage of Cs^+ into the neurone. Electrodes were placed on the surface of the slice in the region of the FMN under microscopic control (Wilde M5 Stereomicroscope). The microelectrode was moved through the slice in 2μM steps.

Earlier experiments utilised a "Dick Vet" microdrive but this was replaced in later studies by a Burleigh Inchworm system. An apparent increase in the electrode resistance, indicated by a small voltage deflection in response to a brief (100msec) current pulse, was taken as an indication that the electrode may be close to a neuronal membrane. FM's were impaled by briefly increasing the negative capacity compensation. "Sealing" was often aided by passage of constant hyperpolarising current (about 1nA) through the electrode. Membrane potentials were calculated by withdrawal of

the microelectrode from the cell after recording and where necessary any residual resistance was subtracted from the calculated cell resistance.

Current-Clamp

All intracellular current-clamp recordings from FM's were performed using a high input resistance amplifier, the Axoclamp 2A (Axon Inst.) operating in the bridge mode. This allows microelectrode voltages to be monitored continuously while simultaneously allowing current injection. During intracellular recording any voltage deflection (V) observed in response to an injected current (I) is the sum of the voltage (Vm) set up across the resistance of the cell membrane (R_m) and the voltage (Ve) set up across the microelectrode resistance (Re) according to Ohm's law

$$\therefore \quad V = V_m + V_e = I\,(R_m + R_e)$$

In bridge mode accurate measurement of V_m is achieved by eliminating V_e using a bridge balancing method. This refers to the original Wheatstone bridge circuitry used to compensate for the R_e but which has been superceded by operational amplifier techniques in the Axoclamp 2A. The contribution of V_e to the total voltage drop in response to an injected current pulse is identified as the time independent drop seen at the onset and offset of the current pulse prior to the slower charging and discharging curves generated as a result of the neuronal resistance and capacitance. Elimination of this component of the voltage drop was performed by observing the onset of the voltage deflection, in response to a repetitive current pulse, on a oscilloscope using a brief time base, and subsequent appropriate adjustment of the bridge balance potentiometer. Once

V_e is fully eliminated the bridge potentiometer gives a reading equivalent to R_e. At this point a fast transient was observed at the beginning and end of the voltage deflection and was the result of the finite response speed of the microelectrode due to capacitative currents set up at the headstage input and at the capacitance of the electrode to ground. Capacitance at the headstage input is minimised by the Axoclamp circuitry while electrode capacitance can be minimised by optimum use of negative capacity compensation (capacity neutralisation) (see later).

The bridge was routinely balanced after impalement of FM's and thereafter monitored continuously on an oscilloscope. Current-voltage responses generated in control and drug treated conditions by measuring voltage deflections in response to current pulses of varying amplitude were only compared when R_e remained balanced throughout treatment.

Discontinuous Current Clamp : Optimal setting of negative capacitance compensation

Discontinuous current clamp (DCC) and dSEVC modes differ from the bridge (or continuous) mode in the use of a switching system which rapidly cycles the functioning of the microelectrode from current passing to voltage recording on a time-shared basis. The length of the current passing period within each cycle is referred to as the duty cycle and this is set at 30% in the Axoclamp 2A. V_m can only be recorded independently provided the voltage (Ve) set up across the electrode resistance (Re) has decayed to a value close to zero at the end of each cycle. This decay is dependent on the time constant of the microelectrode capacitance (τe) and headstage input capacitance. Decay of Ve can be optimised by injecting current into the headstage to compensate for the loss of current due to the

charging of these capacitances. This is termed negative capacity compensation. Optimal negative capacitance compensation plays an integral role in minimising transients in current-clamp bridge mode and also in the prevention of "false clamp" when using discontinuous single electrode voltage clamp mode (dSEVC).

Figure 2.5 illustrates the principles of operation of DCC and dSEVC modes employed by the Axoclamp 2A including correct setting of the negative capacity compensation. A DCC system is implemented when switch S3 is in the DCC position (Fig.2.5A). At the start of the illustrated timing cycle the voltage (Ve + Vm) across the headstage amplifier (A1) is equal to Vm. At this point switch S2 is briefly closed allowing C_H and A2, which together constitute a sample and hold amplifier, to sample the membrane potential (Vms) which it then holds for the duration of the following cycle (T). Immediately after S2 opens, S1 switches to the current command voltage position (-Vc). Differential amplifier A5 in series with R_o and A1 becomes a constant current source (CCS) whose output is directly proportional to the voltage at its input (Ve + Vm + Vc) irrespective of microelectrode resistance. As such the voltage across R_o equals Vc thus forcing the current (I_o) into the microelectrode to be equal to Vc/Ro. A3 is a differential amplifier which monitors instantaneous I_o. This is subsequently averaged and scaled to give a continuous measurement (Im). During this period Ve + Vm charges to a final value which consists mainly of the voltage drop across Re, which is monitored on the head stage oscilloscope (Vmon). The duration of the current passing period (Ti) should be 2 orders of magnitude briefer than τm leading to only a small, linear change in Vm. Current passing is terminated when S1 switches to the 0 volts position and Ve decays passively.

Before a new sample of Vms can be obtained Ve must decay to almost zero, which usually requires 9 electrode time constants. A plateau at Vm will only be achieved with correct negative capacitance compensation and cycle duration (determined by the switching frequency, fs). Incorrect setting of negative capacitance compensation at this stage will be observed as overshoot of Ve or failure of Ve to decay almost completely to a plateau. In addition a minimum cycle duration compatible with a return of Ve + Vm to Vm must be set which should be at least ten times less than τm so that the membrane voltage response can be smoothed by its capacitance. In these studies fs was approximately 10kHz giving a cycle duration of 100μsec which fulfilled these criteria as τm was 2.9 ± 1.2 msec (n = 99).

Voltage Clamp

A dSEVC system is operational when switch S3 is in the dSEVC position. Again Vms is sampled when Ve has decayed to very nearly zero, however the held Vms then becomes the input to a differential amplifier A4 where it is compared to a command voltage, Vc. These values are subtracted and the output of A4 (i.e. the difference between Vms and Vc) when S1 is in the current passing position, provides the input to the CCS (A5, Ro) which leads to the injection of an appropriate current into the microelectrode irrespective of Re. The gain of the CCS is G_T. The output of the CCS represents the current flow across the clamped membrane and is monitored by A3 whose output is sampled, smoothed and scaled by an averager (not shown) giving Im. As in DCC mode, before a new value of Vms can be obtained the voltage set up across Re by the current injection must decay to a negligable value. The negative feedback provided by A4 clamps Vms close to Vc. However, Vms moves in small increments

around the average Vms (Vms(ave)). In addition, Vms(ave) is not exactly equal to Ve due to the finite gain of the CCS. In practice this steady state error ϵ can be minimised by increasing G_T to the maximum still consistent with a stable clamp which can be defined by the equation:-

$$0 < \frac{G_T\ DT}{Cm} < 2$$

where G_T = CCS gain

D = duty cycle

T = cycle duration

C_m = neuronal capacitance

Thus maximum gain consistent with stability is determined by the duration of the current passing period (DT) and neuronal capacitance. However, the minimum time required to achieve a steady-state voltage after a step command is fulfilled only when:-

$$\frac{G_T\ D\ T}{Cm} = 1$$

In this condition the clamp is said to be critically damped. Given the constraints on T previously described, T should be as small as possible while allowing G_T to increase to achieve critical damping. dSEVC of FM's required the introduction of phase lag into the feedback path of the clamp circuit at A4 (not shown). This allowed G_T to be increased to higher values and a faster squarer step voltage response to be achieved. Negative capacity compensation and T were optimised prior to the introduction of phase shift. The headstage voltage (Ve + Vm) was continually monitored on Vmon to

warn of the development of a false clamp due to insufficient decay of Ve prior to obtaining Vms. Such a scenario may occur if a change in Re led to underutilisation of negative capacity compensation.

In this study Cm could be calculated from current-clamp data according to

$$\tau m = Rm\ Cm$$

and gave a value of 276pF. A mean sample rate of 10kHZ (n = 9) gave a value of 100μsec for T. For critical damping to be achieved a value of G_T equal to 9.2nA/mV would be required. In practice values of between 3 and 8nA/mV were achieved. This implies that the system was overdamped and thus required more cycles to reach steady-state after Vc changes. However, such a situation was considered essential to maintain stable clamp conditions. The increase in the settling time after command voltage steps due to this overdamping was not considered important as the time course of events being monitored were much slower (Instantaneous current measurements were made after about 10ms and steady state measurements after 250msec to 1sec). FM's were routinely clamped at or close to the resting potential and step hyperpolarising and depolarising voltage commands were imposed to study both the time and voltage dependent inward rectifier prominent in these cells, as well as conductance changes as a result of 5-HT and NAd application. Downward deflections of the current traces are indicative of inward current flow in all records.

The ideal voltage-clamp necessitates that the whole membrane of the neurone is isopotential. In practice the use of a single point source for the clamp means that this spatial voltage uniformity may

not be achieved. As such currents generated in electrotonically distant parts of the cell may be subject to significant error when measured by an electrode located in the soma. Given the large size and dendritic extent of FM's this problem should be given due consideration when interpreting measured currents.

Data Storage and Analysis

All parameters measured during intracellular recordings including membrane potential responses to injected current pulses or extracellular stimulation in current-clamp, and evoked currents in response to step voltage commands in voltage clamp were continuously observed on a digital storage oscilloscope (Gould, 1425) and stored on video-tape, using an analog interfaced digital audio signal processor (Sony PCM 701ES) - video cassette recorder (Sony SLF 30) system (Lamb, 1985) for computer aided analysis using a CED 502 interfaced to a PDP 11 (Crunelli et al, 1983). A DC pen recorder (Linear Corder MkV Watanabe) was used for a continuous record of resting membrane potential and responses to intracellular current pulse injection (Fig.2.4).

Stored data was reviewed using a real time FORTRAN package (DA6.FOR) and electrotonic potentials or evoked currents were averaged, to reduce high frequency noise, (usually from 6 individual records) and used to construct current-voltage relations with a range of "in-house" written sub-routines.

Time constants for the charging of the membrane capacitance (τ) were obtained by determining the time taken for voltage deflections to reach 63% of its peak value. Only small ohmic responses not displaying time dependent sag were used for these values. The linearity of a computer-generated semilogarithmic plot of ln (1-

V/Vmax) against time indicated the single exponential nature of the charging curve and was used to determine the value of the time constant.

Figure 2.1

A line drawing of a coronal section through the rat brainstem adapted from Paxinos and Watson (1982) showing the location of the Facial Motor Nucleus (FMN (7)) in relation to other brainstem structures.
Abbreviations: asc 7, ascending fibres facial nerve; bas, basilar artery; FMN (7), facial motor nucleus; g7, genu facial nerve; icp, inferior cerebellar peduncle; LVe, lateral vestibular nucleus; mlf, medial longitudinal fasciculus; Mve, medial vestibular nucleus; PGi, nucleus paragigantocellularis; PrH, prepositus hypoglossal nucleus; py, pyramidal tract; RMg, raphe magnus; RPa, raphe pallidus; Sp50, nu. spinal tr. trigeminal nerve, oral; Sp5, spinal tr. trigeminal nerve; SuVe, supravestibular nucleus; VCo, ventral cochlear nucleus; 4V, fourth ventricle.

Fig. 2.1

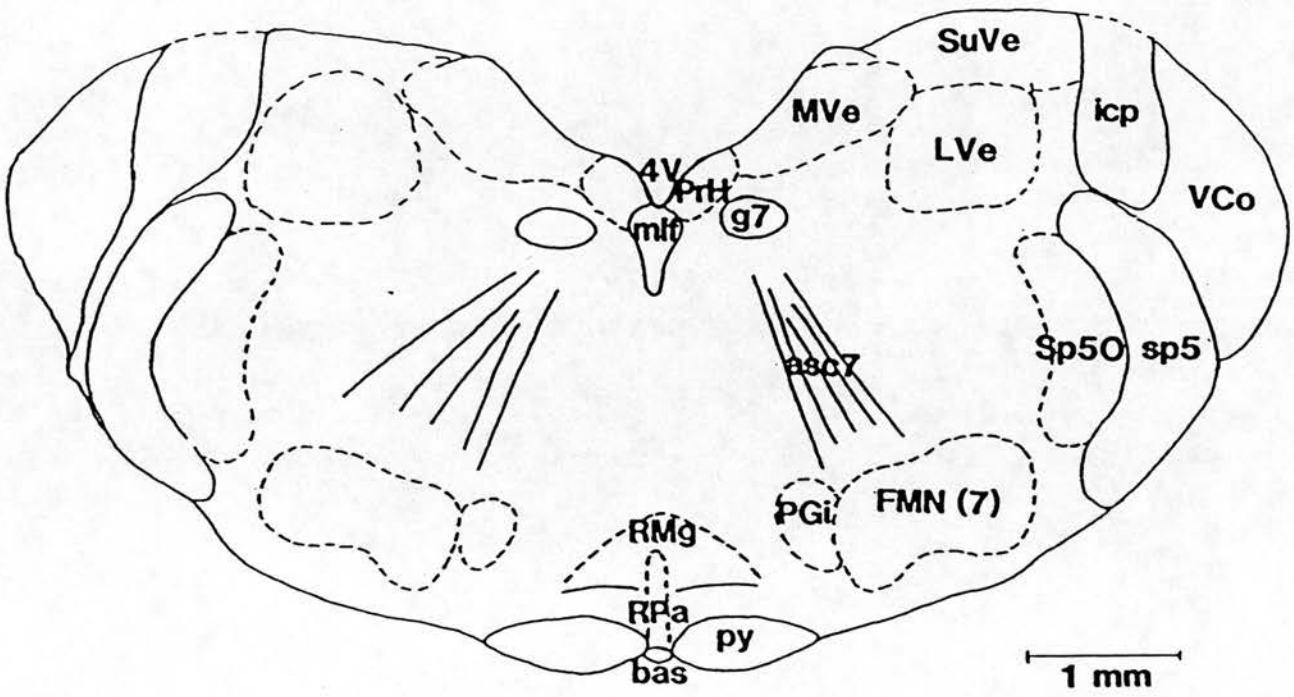
SuVe
MVe
LVe
icp
VCo
4V
PrH
mlf
g7
asc7
Sp5O
sp5
PGi
FMN (7)
RMg
RPa
py
bas
1 mm

Figure 2.2

The Incubation/Recording Chamber
350μm thick brainstem slices (BS) were placed on the nylon mesh and superfused with prewarmed (37^{o}C) oxygenated aCSF supplied through the polypropylene tubing (A) and entering the chamber at B. The water bath, filled with distilled water to the level indicated by the dashed line, was heated by a thermopad (C) (Minco Caval Components Ltd. USA) which was controlled thermostatically by probe D. aCSF was drained from the chamber by the tissue paper wick and funnel at E. A silver chloride reference ground electrode (F) connected the tissue wick to the headstage unit (not shown). A 95% oxygen, 5% carbon dioxide gas mixture was bubbled through the water bath at G and was directed over the slices through a port at H. A humidified atmosphere was maintained in the recording chamber by a glass cover (J) which had a small aperture to allow the recording microelectrode access.

Fig. 2.2

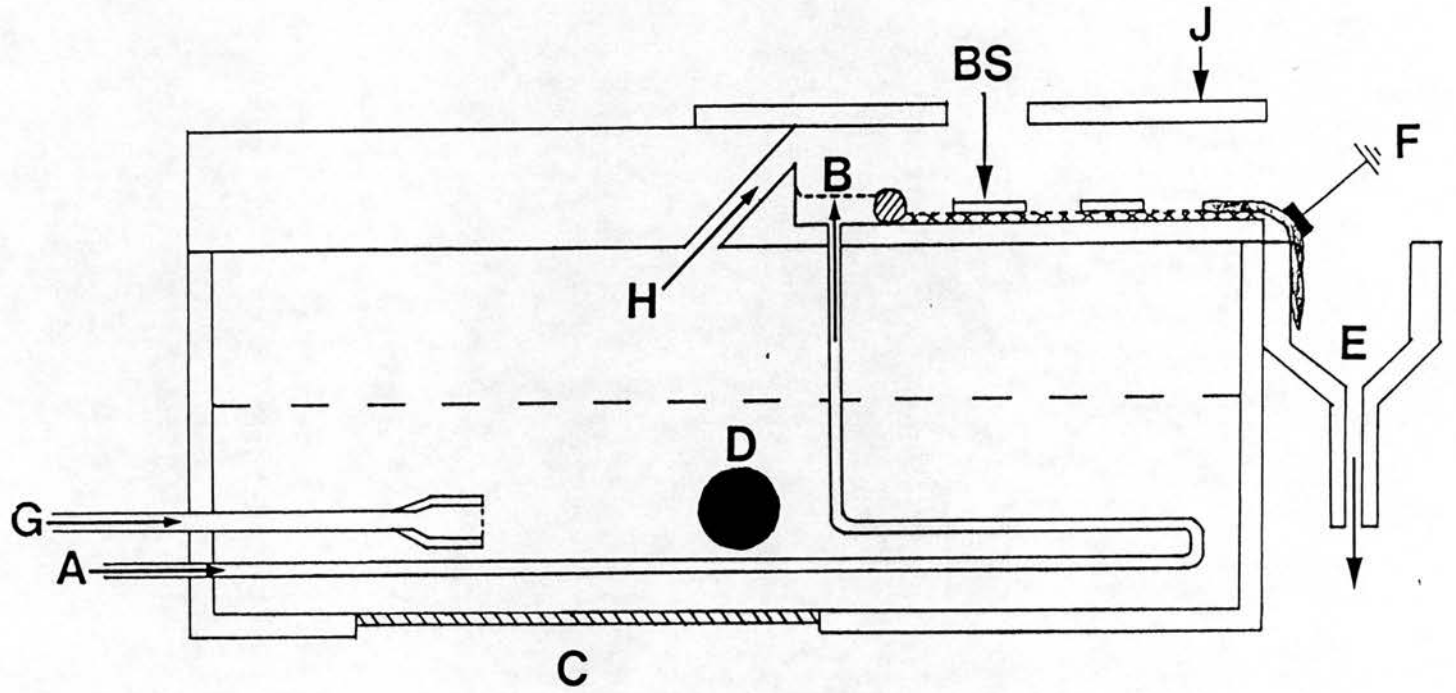

Figure 2.3

Morphology of facial motoneurones in the adult rat brainstem

A) A 50μm thick coronal section through the FMN. Labelled neurones were identified in the lateral, intermediate and dorsal subdivisions following retrograde transport of HRP applied to the ipsilateral buccolabial branch of the facial nerve 36 hours before perfusion fixation and subsequent histochemical processing. The calibration bar is 100μM. M and D represent medial and dorsal directions respectively.

B) Higher magnification photomicrograph of a labelled facial motoneurone. Five primary dendrites can be seen on the densely labelled soma. Note also labelling of the dorsally directed axon (arrowed). Calibration is 25μM.

Fig. 2.3

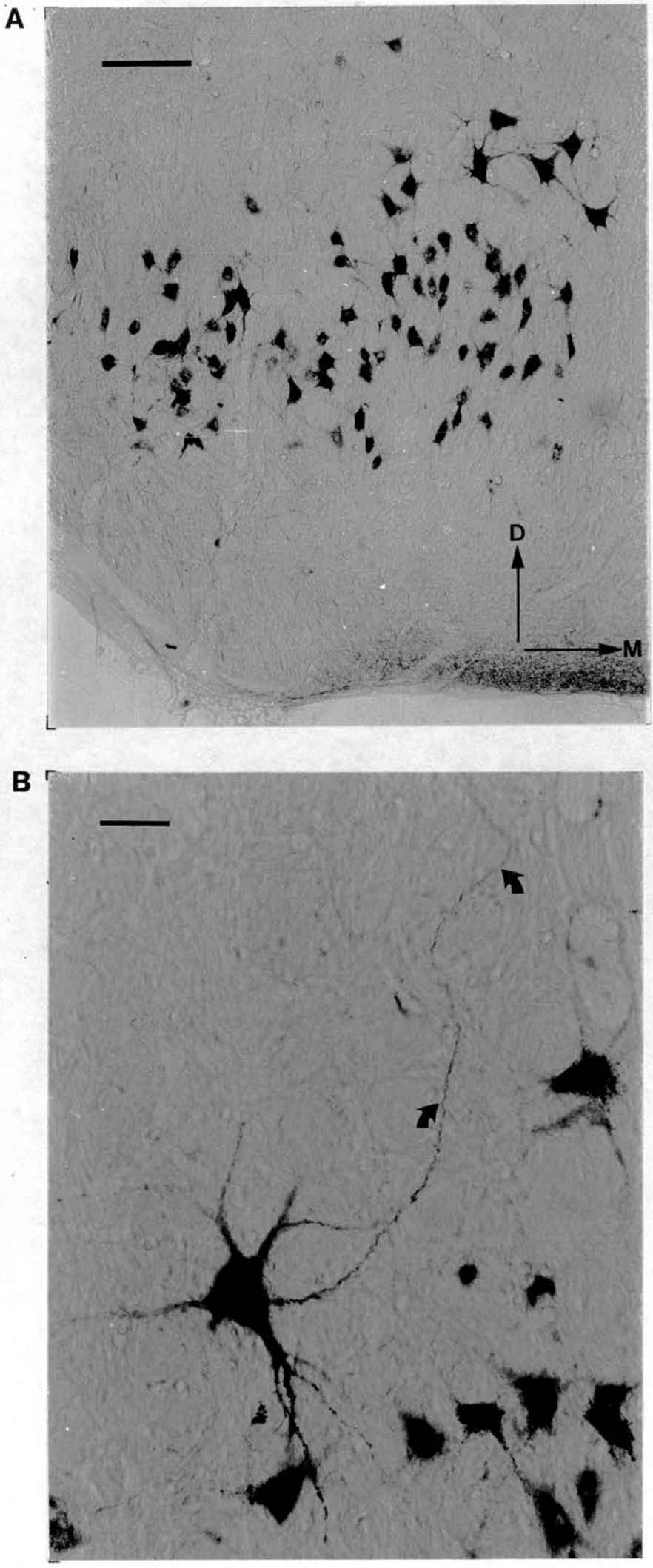

Figure 2.4

Intracellular recording apparatus

Intracellular recordings from FM's were made using 3M KCl filled glass microelectrodes and all measurements were with respect to a Ag/AgCl reference ground in contact with the superfusing aCSF in the recording chamber. A high input resistance preamplifier (Axoclamp 2A) was used to generate current step commands in current clamp and voltage step commands in dSEVC. Responses of neuronal membrane potential and current in the two modes were buffered by a unity current gain headstage and amplified by the preamplifier and a second amplifier (amp 2). Generated waveforms were monitored on a digital storage oscilloscope (scope 1) and stored on video tape using an analog-interfaced digital audio signal processor (A/D proc; Sony PCM 701 ES) - video cassette recorder (vcr; Sony SLF 30) system. A DC chart recorder (chart rec; Linear Corder MkV Watanabe) was used to obtain a continuous record of membrane potential. The digitimer controlled the onset and duration of all command current and voltage steps. At the start of each experiment calibration signals of 1nA, 1mV and 10nA, 10mV were generated by the preamplifier triggered by a pulse from an isolated stimulator (cal; Digitimer DS2). Headstage voltages were monitored on a second oscilloscope (scope 2) during DCC and dSEVC modes to ensure complete decay of the voltage set up across the electrode resistance. A Schmitt trigger was placed between the digitimer and A/D processor to guarantee that the trigger signal would drive the PDP 11/73 used for data analysis. A second stimulator (stim; Digitimer DS2) was connected to a bipolar stimulating electrode used in antidromic identification of the FM's.

Fig. 2.4

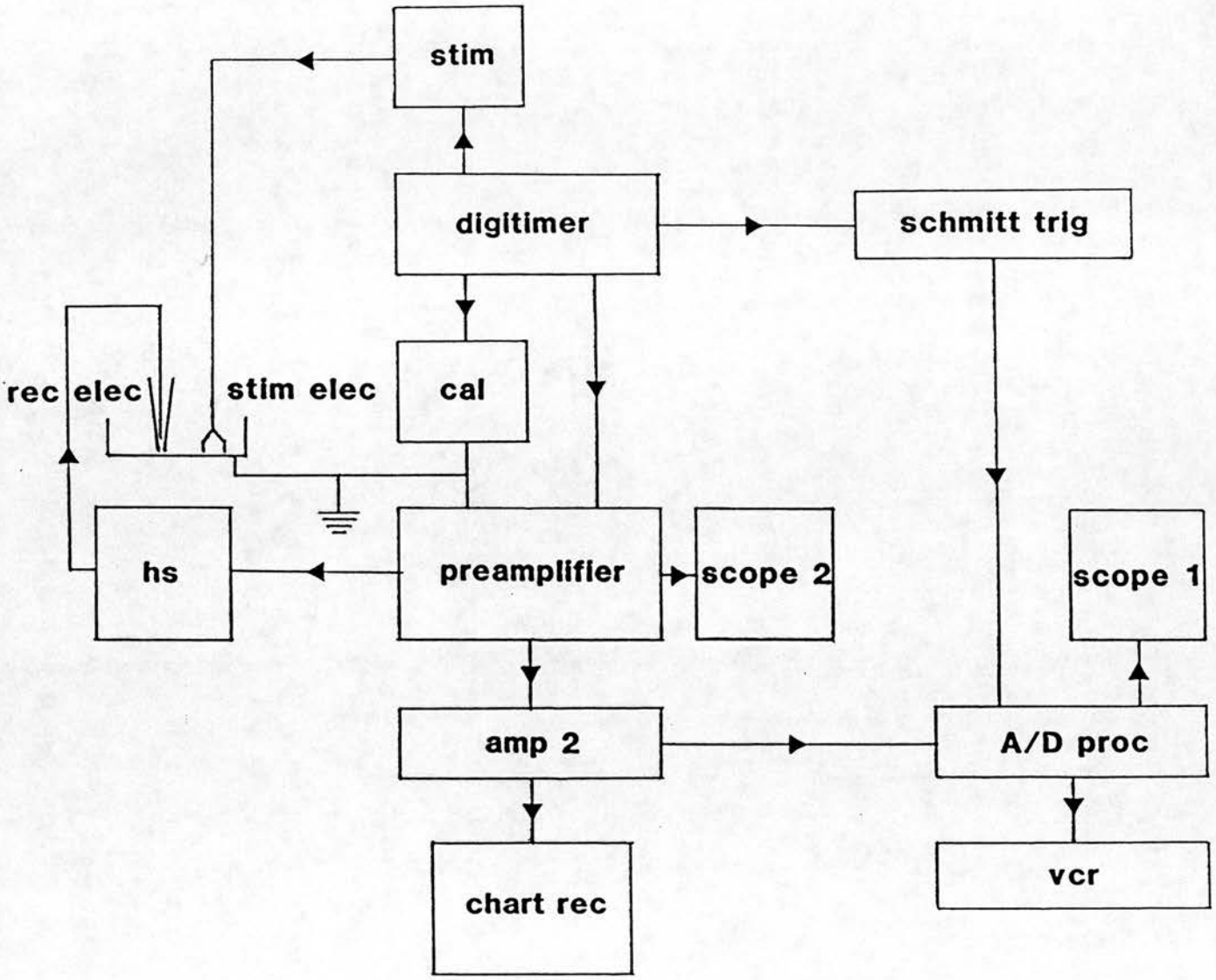
stim
digitimer
schmitt trig
rec elec
stim elec
cal
hs
preamplifier
scope 2
scope 1
amp 2
A/D proc
chart rec
vcr

Figure 2.5

A block diagram, A, and timing sequence, B, showing the principles underlying the operation of the discontinuous current clamp (DCC) and voltage clamp (dSEVC) using a single microelectrode

Switch S1 opens and closes at the sampling frequency (fs) which determines the length of each cycle (T). When closed, S1 allows the passage of current during Ti, and when open is grounded (Vo) allowing voltage recording for the rest of the cycle, Tv. During Ti, Ve increases exponentially and decays in the same fashion during Tv, changes which can be observed on the oscilloscope, Vmon. Membrane potential (Vm) changes are linear during the cycle T because the membrane time constant (τm) is much greater than T. Vm is sampled and held, as Vms when S2 closes but is only an accurate measure of Vm if Ve has decayed to a negligible value. In dSEVC mode (S3) the output of the sample and hold amplifier (S2, CH, A2) provides the input to A4 where it is compared with the command voltage, Vc. The difference between the signals, Vc-Vms, provides the input to the controlled current source (CCS; A5, Ro, A1). During Ti the current generated by the CCS is directly proportional to Vc-Vms and can be monitored via A3 (Im). Vms(ave) is the average value of Vms and differs from Vc by a steady-state error ϵ which is the result of the finite gain (G_T) of the CCS. In DCC mode (S3) the output of the CCS is determined by a current command voltage, -Vc, and Vms(ave) is a reliable measure of Vm providing Ve decays to zero by the time S2 closes again.

Fig. 2.5

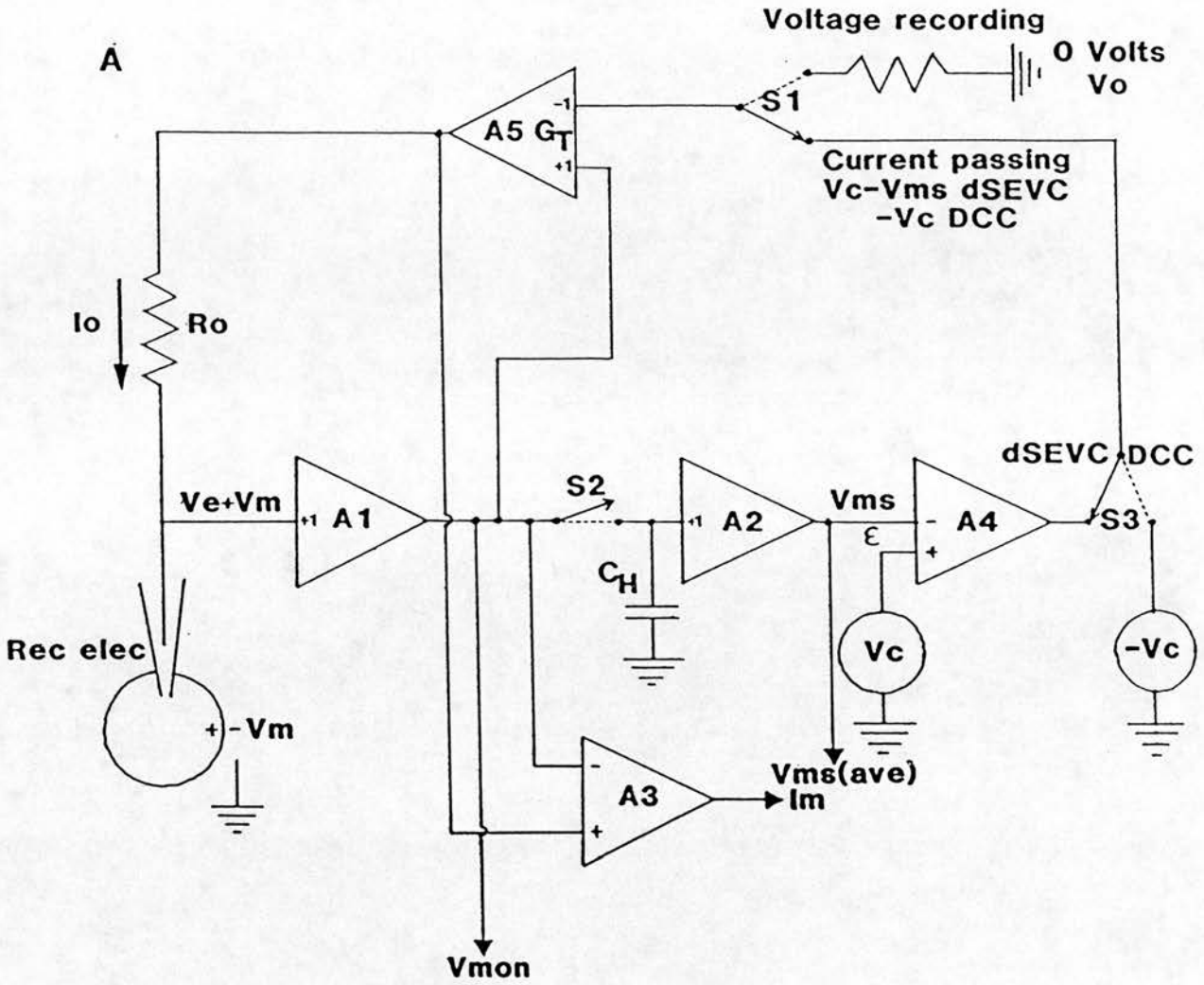
A
Voltage recording
0 Volts
Vo
S1
A5 G_T
-1
+1
Current passing
Vc-Vms dSEVC
-Vc DCC
Io
Ro
dSEVC
DCC
Ve+Vm
+1 A1
S2
+1 A2
Vms
ε
- A4
+
S3
C_H
Rec elec
+ -Vm
Vc
-Vc
A3
Vms(ave)
Im
Vmon

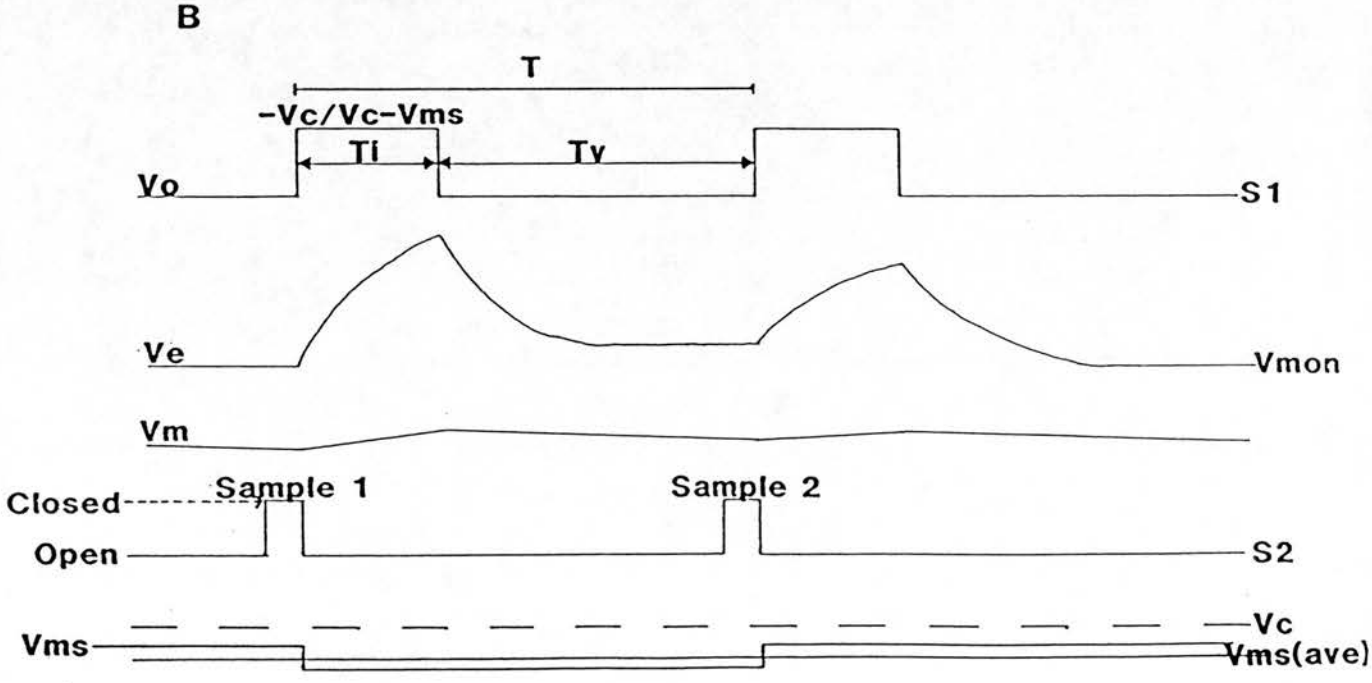
B
T
-Vc/Vc-Vms
Ti
Ty
Vo
S1
Ve
Vmon
Vm
Closed
Sample 1
Sample 2
Open
S2
Vc
Vms
Vms(ave)

TABLE 2.1

DRUG	SOURCE	STOCK []	TEST []
Apamin	Sigma	10μM	25nM
CsCl	Sigma		2mM
dipropyl-5-CT	Sandoz	10mM	10-200μM
5-HT creatinine sulphate	Sigma	20mM	100-250μM
8-OH-DPAT	Research Biochemicals Inc.	10mM	10μM
ICS 205 930	Sandoz	10mM	1-100μM
Ketanserin tartrate	Janssen	10mM 50mM/DMSO	1-100μM
LY-53857	Eli Lilly	10mM	50-100μM
2-methyl-5-HT	Sandoz	10mM	100-200μM
Methiothepin maleate	Roche	10mM	1-100μM
Methysergide	Sandoz	2mM	10-100μM
Noradrenaline	Sigma	20mM	10-100μM
Spiperone	Janssen	10mM	10-100μM
Tetrodotoxin	Sigma	300μM	1μM

CHAPTER 3 RESULTS

Intracellular current clamp recordings lasting 0.3 to 6 hours from 201 facial motoneurones with stable membrane potentials were obtained in all sub-divisions of the FMN. Records from motoneurones with resting potentials exceeding -60mV and with short duration overshooting action potentials were selected for further analysis. These selection criteria were compatible with long term, stable recording from FM's. FM's with less negative membrane potentials were in general less stable and could not be impaled for periods long enough to compile sufficient basic biophysical data for further analysis. In addition, these neurones displayed little or no sag in membrane voltage responses even at artificially hyperpolarised levels which was taken as an indication that they were unhealthy and not suitable for further investigation. All FM's were silent at their apparent resting potential though in some cases spontaneous synaptic events were observed. The resting potential of FM's ranged from -60 to -88mV with a mean value of -70.6 ± 6.2mV (n = 201) (This and other values are mean ± population S.D. for the number of values, n).

Passive Membrane Properties of Facial Motoneurones

The passive membrane properties of facial motoneurones were determined by examining voltage responses to intracellular injection of current pulses of varying amplitude 100-120msec in duration. Superimposed electrotonic potentials from three different FM's obtained in this way are illustrated in figures 3.1, 3.3A and 3.5. These neurones will be referred to specifically in this section though similar records can be seen throughout this and subsequent chapters. Small hyperpolarising current pulses (-0.3nA, Fig.3.3A) produced linear ohmic voltage responses in some FM's. However, more commonly and with greater prominence as hyperpolarising current

amplitude was increased, voltage responses peaked after a delay of 10-20msec and then displayed a time-dependent "sag" towards the resting potential, reaching a steady state voltage level at the end of the current pulse (Fig.3.1, 3.3A, 3.5B). The magnitude of the sag increased as the magnitude of the test pulse increased. This type of response is characteristic of inward "anomalous" rectification of the kind seen in several other cell types (see discussion). The prominence of the inward rectification varied from cell to cell but was in general greater in neurones with more negative resting potentials.

Time-dependent voltage sag was also seen in response to depolarising current pulses (Fig.3.1) though it was commonly less prominent than that seen in the hyperpolarising direction (Fig.3.1, 3.3A). In figure 3.1 the FM shows prominent time dependent "sag" even at threshold for action potential (AP) generation, though the steady state slope resistance is steeper in the depolarising than the hyperpolarising direction (Fig.3.2). However, this was not the case for all cells. The FM in figure 3.3A shows only a small time-dependent sag of membrane potential in response to small amplitude depolarising current pulses while at more depolarised levels the steady state and peak current-voltage curves converge showing the absence of any time-dependent rectification in this region of membrane potential (Fig.3.4). A third form of time dependent rectification in the potential range between rest and threshold was observed in FM's and is illustrated in figure 3.6b,c. This FM demonstrates sag of small amplitude depolarising voltage responses. When larger amplitude depolarising current pulses are applied a slowly developing depolarising potential can be seen. This is reflected in the non-linear steady-state current voltage

relationship which displays an increasing slope with increased depolarisation (Fig.3.7B, filled squares) indicative of inward rectification in the depolarising direction from resting potential. Hyperpolarising and depolarising current test pulses, were followed by depolarising and hyperpolarising rebound tail potentials respectively.

Current voltage relations measured at the peak of the voltage response were linear over a wide voltage range around the resting potential only showing non-linearity at potentials of -90mV and greater (Fig.3.2, 3.4A). This non-linearity occurred simultaneously with the peak of the voltage response starting to occur at an earlier point after onset of the current pulse. The FM illustrated in Figure 3.1 had an apparent input resistance, taken from the slope of the peak voltage deflection current-voltage plot, ($R_{m(pk)}$) of 4.2MΩ (Fig.3.2 open squares), while the neurone depicted in figure 3.3A had a value for $R_{m(pk)}$ of 14.8MΩ (Fig.3.4A, asterisks). The linearity of steady-state (ss) current voltage plots was variable from cell to cell and in general restricted to a narrower voltage range near the resting potential. The neurone in figures 3.1 and 3.2 showed two linear ranges for the ss current voltage relationship giving an $R_{m(ss)}$ of 1.8MΩ in the hyperpolarising direction and 2.7MΩ in the depolarising direction. The ss current voltage relation for cell in figure 3.3A (Fig.3.4A) showed non-linearity throughout the tested range such that an accurate slope $R_{m(ss)}$ could not be established. In both cases the divergence of the peak and steady-state current-voltage curves in both the hyperpolarising and depolarising directions indicates that

the time dependent inward rectifier is active at the resting potential and thus has a role to play in maintaining resting potential in these neurones.

In a sample of 188 FM's, $R_{m(pk)}$ ranged between 3.1MΩ and 25.7MΩ with a mean value of 10 ± 3.9MΩ. The minimum and maximum $R_{m(ss)}$ was 1.5MΩ and 17.9MΩ respectively. The mean value for $R_{m(ss)}$ was 7 ± 3.6MΩ which compared with an $R_{m(pk)}$ of 9.4 ± 3.5MΩ for the same population of FM's (n = 97).

Membrane Time Constant

The measurement of the membrane time constant (τ) from hyperpolarising voltage deflections was complicated in many cells by the presence of time-dependent inward rectification. τ was thus evaluated by one of two methods; either by using small amplitude voltage deflections which did not evoke an inwardly rectifying response or by monitoring the decay of a depolarising response evoked by a brief current pulse of insufficient duration to activate the time dependent rectification. Both methods gave similar values for τ ranging from 1.3msec to 8.9msec with a mean of 2.9 ± 1.2msec (n = 99).

Voltage clamp studies

Inward rectification observed in current-clamp experiments was also studied in single electrode voltage-clamp. Figure 3.3B shows records obtained in voltage clamp from the same cell as the current-clamp records shown in Figure 3.3A. Step hyperpolarising voltage commands 5 to 50mV in amplitude and 250msec long from a holding potential of -72mV (resting potential in current-clamp, -73mV) elicited a slowly developing inward current. After the initial capacitative transient (attenuated in Fig.3.3B due to record averaging) an instantaneous (inst) current peak occurred after about

10ms, which was followed by development of the slow inward current reaching a plateau steady state (ss) at the end of the voltage command. While not studied in detail the onset of this slow inward current became faster with increasing step amplitude (see also Figure 3.14A and 3.17B). Termination of the voltage command resulted in an inward tail current peaking after about 20ms and decaying back to baseline over the following 150 to 200ms. As seen in other neuronal types (Spain et al, 1987; Mayer and Westbrook, 1983) this inward relaxation is associated with an increase in conductance since the current jump at the end of the voltage step is greater than that seen at the onset of the voltage step (Fig.3.3B), thereby differentiating it from inward relaxations seen as a result of channel closure (e.g. M-current, Halliwell and Adams, 1982). Current-voltage plots (Fig.3.4B) taken at the beginning (inst) and steady-state (ss) of the evoked currents show divergence throughout the tested range indicating that this current is activated close to if not at resting potential and is further activated by hyperpolarisation. Measurements of conductance for the cell shown in figure 3.3B were taken from the linear ranges of the inst. and ss current-voltage curves shown in figure 3.4B, and were 66.1nS and 93.5nS respectively. The instantaneous conductance correlates well with that predicted from the $R_{m(pk)}$ obtained in current clamp. In 9 neurones held at a mean potential of -68.8 ± 4.4mV, which was at or close to the resting potential, the mean instantaneous conductance was 88.4 ± 18.9nS.

Inward rectification in facial motoneurones

The properties of the inward "anomalous" rectification seen in FM's were further studied by changing the membrane potential using the passage of continuous inward or outward current through the

recording microelectrode. An example of this is illustrated in Figure 3.6. Electrotonic responses obtained at resting potential are shown in Figure 3.6c. Similar electrotonic responses were obtained at membrane potentials of -58, -69 and -80mV (Fig.3.6a,b and d respectively). Current-voltage plots taken at the peak and steady state levels at each membrane potential are plotted in figures 3.7A and B. As seen previously peak deflection current voltage plots were linear at each membrane potential showing non-linearity only at potentials more negative than -90mV. It was observed that the time to peak voltage deflection was progressively reduced with membrane hyperpolarisation being 19.7msec at -58mV, 15.4msec at -69mV, 12.2msec at -76mV and 10.2msec at -80msec. The slope of the peak deflection current-voltage plots became progressively steeper with membrane potential depolarisation. $R_{m(pk)}$ values were 13.1, 11.8, 9.9 and 7.9MΩ for holding membrane potentials of -58mV, -69mV, -76mV and -80mV respectively. These changes in resistance were largely reflected in a decrease in the value of τ with hyperpolarisation, though the value obtained at -58mV did not follow the predicted trend. Thus at -80mV, τ measured 2.5msec at -76mV, 3.2msec at -69mV, 4.4msec and at -58mV, 3.3msec. When the steady-state current-voltage curves were plotted (Fig.3.7B) non-linear relationships are observed at each membrane potential. Each shows an increase in slope with depolarisation which is more prominent at -58mV than at -80mV.

When the FM was held at -58mV hyperpolarising voltage responses up to 10mV in amplitude showed no sag over the entire current pulse duration (Fig.3.6A). Stepping to more hyperpolarised levels evoked some sag suggesting that the inward rectifier shows an activation threshold around -68mV on this neurone. This is further supported

by the absence of hyperpolarising tail potentials after depolarising voltage responses from a resting potential of -69mV (Fig.3.6B). Similar observations in other neurones indicated a mean threshold for IR of -62 ± 5mV (n = 12). That the steady-state current-voltage curve obtained at -80mV (Fig.3.7B, asterisks) was non-linear throughout the tested range indicates that IR is not fully activated even at -90mV. (Once fully activated the ss relationship would be expected to become linear).

Since the peak deflection current-voltage curves are linear over the ranges tested it is apparent that no voltage dependent conductances other than that mediating IR are active, and that at any given membrane potential the membrane response obeys ohms law irrespective of the state of activation of the IR. Thus an estimate of the reversal potential of IR can be obtained by extrapolating the lines of regression for peak current-voltage curves at different membrane potentials and hence different states of IR activation. Such a plot is shown in Fig.3.8 where the peak I/V curves for the neurones in figure 3.6 have been plotted taking the offset DC into account. The points of intersection lay between -49 and -56mV. This procedure was carried out on 13 FM's and a mean reversal potential for the IR (E_{IR}) of -46 ± 10mV was obtained.

When performed in voltage-clamp, results were similar. Figure 3.10Aa shows a FM normally resting at -66mV clamped at a potential of -55mV with +0.9nA holding current. Instantaneous currents evoked by hyperpolarising voltage step commands were linear over the range -55 to -115mV and gave a slope conductance of 78.7nS (Fig. 3.10B closed squares). The motoneurone was then reclamped at -85mV requiring -4.4nA holding current. The instantaneous currents evoked by depolarising step voltage commands +10 to +40mV in

amplitude were obtained giving a slope conductance of 135.1nS (Fig.3.10Ab, 3.10B, asterisks). Extrapolation of the inst. current linear lines of regression at these two holding potentials gave an estimated reversal potential for IR of -31mV (Fig.3.10B). The mean value obtained by this method for the reversal potential of IR was -37.4 ± 18.3mV (n = 3) in agreement with current-clamp estimates.

Rebound Tail Potentials

At the end of hyperpolarising current pulses a depolarising rebound tail potential, which peaked after about 10msec and returned to the resting potential over the following 100msec, was observed (Fig.3.1, 3.3A). The mean values for the time to peak and duration of these potentials were 11 ± 4.2ms and 144 ± 19.7ms respectively (n = 26). The amplitude of the tail potential increased with increasing amplitude of the preceding current pulse (and hence the amount of 'sag' in the voltage response) (Fig.3.1, 3.3A). At the cessation of depolarising current pulses most neurones displayed hyperpolarising rebound tail potentials which peaked slightly later than the corresponding depolarising potentials (mean time to peak, 16.4 ± 6.9msec) and had a duration of 141 ± 18.3msec (n = 23). Comparing hyperpolarising potentials seen in figures 3.1, 3.3A, and 3.5A shows their prominence to vary between cells. Amplitude was related to current pulse amplitude, as for the depolarising potentials, up to a point, after which further depolarisation did not further increase hyperpolarising tail potential amplitude (Fig.3.3A, 3.6C).

The amplitude of hyperpolarising and depolarising tail potentials was studied at different membrane potentials in the same FM (Fig.3.6). At the resting potential (-76mV; Fig.3.6C) the depolarising rebound potential peaked after 10.5msec, had a duration

of about 150msec and increased in amplitude with increasing current strength. Hyperpolarising tail potentials peaked after 20msec, had a similar duration to depolarising tail potentials and increased in amplitude with increasing stimulus intensity but with a tendency towards a plateau amplitude as indicated by the decreasing slope of the curve shown in figure 3.9A (triangles). When the membrane potential was hyperpolarised to -80mV (Fig.3.6d) with continuous hyperpolarising DC the relationship between current pulse intensity and depolarising tail potential amplitude was unchanged (Fig.3.9A, #). However, the linear range of hyperpolarising potential amplitude against stimulus intensity was extended with only a small reduction in the slope as AP threshold was approached. Depolarisation of the membrane potential to -69mV (Fig.3.6b) led to a reduction in the early part of the slope of the relationship between depolarising potential amplitude and current amplitude. This correlated to the absence of 'sag' in the preceding hyperpolarising voltage response. As current intensity was increased sag developed in the membrane voltage response and the slope of the relationship increased (Fig.3.9A; crosses). No hyperpolarising tail potentials were observed in response to depolarising current pulses. Further depolarisation to -58mV (Fig.3.6a) led to the loss of any depolarising tail potentials even when a sag response was observed in the preceding voltage response. Instead, a biphasic repolarisation to the resting potential composed of a rapid initial phase and a slower second phase, the amplitude of which was not significantly affected by the preceding current pulse (Fig.3.9A; squares).

When the amplitude of the tail potentials is plotted against the potential achieved at steady-state during the preceding voltage deflection the effects of different membrane potential can be seen (Fig.3.9B). The amplitude of hyperpolarising tail potentials after the same steady state potential is progressively reduced as the membrane potential is depolarised. Depolarising tail potentials are similar at holding potentials of -80 and -76mV, slightly reduced at -69mV and completely absent at -58mV.

Effects of Extracellular Cs^+ on Inward Rectification

Extracellular Cs^+ has been shown to be an effective blocker of similar inward rectifier currents in other neuronal types (Spain et al, 1987; Mayer and Westbrook, 1983; Halliwell and Adams, 1982). The effects of extracellular Cs^+ on IR in FM's was examined in both current clamp (Fig.3.11) and voltage clamp (Fig.3.14). Under control conditions the FM shown in figure 3.11A displayed prominent IR at a resting potential of -62mV and had a $R_{m(pk)}$ and $R_{m(ss)}$ of 5.9 and 2.1MΩ respectively (Fig.3.12A, 3.12B; closed circles). When superfused with aCSF containing 2mM Cs^+ the cell depolarised by 1mV and showed large increases in $R_{m(pk)}$ and $R_{m(ss)}$ (13 and 9.3MΩ respectively) (Fig.3.11B, 3.12A,B; asterisks). Over the voltage range tested in the control condition, IR was almost completely blocked by Cs^+ (compare the first two voltage records in Cs^+ (Fig.3.11B) with those in control (Fig.3.11A)). However, the increase in R_m in the presence of Cs^+ enabled more negative potentials to be reached where some sag due to inward rectification remained. The depolarising tail potentials were also greatly reduced over the control voltage range but could still be evoked by

the larger hyperpolarising voltage responses as shown in figure 3.13 where tail potential amplitude is again plotted against the steady state potential achieved in the preceding voltage response.

Figure 3.14 shows the same treatment of a different FM this time in voltage-clamp. The neuron was held at a potential of -74mV and displayed prominent time dependent inward currents in response to -20 to -70mV voltage steps 1sec in duration. Steady state and instantaneous current-voltage curves were only seen to diverge below -90mV. Cs^+ (2mM) evoked a small change in holding current but did not alter the slope of the current voltage curves in the linear region. Conductance of the cell in this region was 81.4nS in control and 79.5nS in Cs^+ (Fig.3.14B). However, the current traces of figure 3.14Ab show a significant reduction in the amplitude of the inward current relaxation at more hyperpolarised levels. Additionally the non-linearity of the instantaneous current-voltage curve was lost in the presence of Cs^+. As seen in current-clamp, at very negative potentials some time dependent inward current remained. The inward tail currents were also reduced in amplitude but not abolished by Cs^+.

<u>The Effects of Intracellular Cs^+ on IR and tail potentials</u>

In common with other time dependent inward rectifiers the sag seen in response to hyperpolarising current steps was not sensitive to Cs^+ applied intracellularly from the recording microelectrode (Figs.3.15, 3.16A). $R_{m(pk)}$ and $R_{m(ss)}$ immediately after impalement (Fig.3.15A, 3.16A) were 7.3MΩ and 4.1MΩ respectively. After 15 minutes the neurones were seen to be Cs^+ loaded indicated by widening of the AP, the blockade of the fast ahp and the prominence

of the DD and depolarising tail currents (Fig.3.15C). Under these conditions $R_{m(pk)}$ and $R_{m(ss)}$ measured in the hyperpolarising direction were 7.1MΩ and 4.9MΩ respectively (Fig.3.16A).

The biphasic return to resting potential seen in figures 3.6a and 3.24Bb is similar to that seen in other central neuronal types where activation of voltage sensitive outward K^+ currents have been shown to be responsible. In this study similar potentials have also been observed on depolarising tail potentials evoked from some FMs depolarised with 5-HT, (Figs.6.23Ab, 6.27Bb,Cb) thereby attenuating the maximum amplitude of the rebound potential. In an attempt to evaluate a role of K^+ mediated outward currents in the loss of depolarising tail potentials at depolarised membrane potentials, FMs were impaled with 2M CsCl filled microelectrodes and subsequently Cs^+ loaded, thereby blocking most potassium conductances of the neuron. At more negative resting potentials (-66mV) the amplitude of tail potentials was unaffected by Cs^+ loading (compare figs. 3.15A and 3.15B). However, when held at a more depolarised level (-61mV, Fig.3.15C) instead of seeing a reduction in the amplitude of depolarising potentials described earlier the amplitude of the tail potentials was unaffected and even increased with greater stimulus intensity (Fig.3.16B,C). These effects were independent of a change in neuronal R_m (Fig.3.16A) indicating that inward rectification is not affected by Cs^+ loading. The implication appears to be that the absence of depolarising tail potentials in FM's held at depolarised membrane potentials under normal conditions may in part be due to the dominance of Cs^+ sensitive outward potassium currents at these potentials. As seen later these may also play a role in delaying the first AP in response to depolarising stimuli.

The effects of Tetrodotoxin on FM passive membrane properties

Tetrodotoxin is known to block sodium conductances in central neurones. Its ability to block Na^+ dependent fast action potentials has led to its use as a blocker of synaptic transmission in this study. Figure 3.17 shows 1μM TTX in the superfusing aCSF to successfully prevent the production of a fast action potential in response to depolarising current pulses (See also Figs.6.22, 6.23). Voltage responses in the hyperpolarising direction display the prominent "sag" described earlier indicating that hyperpolarising inward rectification is not affected by TTX (Fig.3.17A). Similarly the slow inward current seen in voltage clamp is also unaffected by TTX (Fig.3.17B). Membrane potential and $R_{m(pk)}$ are likewise unaffected (see Chapter 6; Figs.6.22, 6.23). The FM in figure 3.17A had a $R_{m(pk)}$ of 7MΩ (Fig.3.18A) at a resting potential of -68mV compared to a control value of 7.6MΩ. When voltage clamped at -66mV (Fig.3.17B) the instantaneous conductance over the same potential range was 134.9nS (Fig.3.18B). Steady-state I/V relationships in the hyperpolarising direction were non-linear (Fig.3.18A,B). In the depolarising direction, however, some cells showed the development of prominent outward rectification of the steady-state current-voltage relationship in the presence of TTX (Fig.3.18A and 6.23D), suggesting that a TTX sensitive Na^+ component may play a role in anomalous rectification in the membrane potential region near threshold. Voltage clamp studies show that normally suprathreshold depolarising voltage steps when applied in the presence of TTX evoked large outward current with inwardly relaxing tails which were inadequately clamped (Fig.3.17B).

Active Membrane Properties of Facial Motoneurones

Antidromic Action Potentials

In addition to histological identification, FMs were also identified by antidromic invasion following stimulation of axon fibre bundles with a bipolar stimulating electrode placed dorsal to the FMN, over the route axons of FMs take to the genu of the VIIth nerve (see Fig.2.1). Latency of the antidromic spike after the stimulus artefact was short probably due to the small spatial separation of recording and stimulating electrodes. Often no clear latency was observed (Fig.3.19) with the antidromic spike being evoked simultaneously with the end of the stimulus artefact. The antidromic nature of these action potentials was confirmed by differentiation of the two classically defined initial segment (IS) and somato-dendritic (SD) components of the somatically recorded action potential. The IS component could be initially identified as an inflection on the rising phase of the action potential (Figs.3.19A, 3.20A, 3.21A) which further developed when the somatic membrane was hyperpolarised with continuously injected outward current. Figure 3.19 shows an antidromic action potential evoked from a membrane potential of -81mV. It had an amplitude of 96mV and the IS component could be identified as an inflection on its rising phase. Further hyperpolarisation of the membrane potential to -83mV with 0.9nA D.C. was sufficient to enhance the IS-SD break. Increasing hyperpolarisation to -85mV (-1.1nA D.C.) led to failure of the action potential to invade the soma and dendrites leaving only the IS component which had an amplitude of 36mV. Differentiation of an M-component from the myelinated membrane of the motor axon was not observed in any of the cells tested.

Figure 3.20 shows a second antidromically identified FM which demonstrated a latency of 0.14ms between stimulus and initiation of the action potential. Clear separation of the IS-SD components was obtained using a double stimulation paradigm combined with neuronal hyperpolarisation. The first action potential evoked from a resting potential of -68mV had an amplitude of 94mV and an inflection on its rising phase. The second action potential evoked with a stimulus interval of 1.8ms had a slightly smaller amplitude of 90mV and an even more pronounced IS inflection on its rising phase (Fig.3.20A). Hyperpolarisation of only 4mV was sufficient first to draw out (Fig.3.20B) the IS component and then lose the SD action potential completely leaving an IS component with an amplitude of 39mV (Fig.3.20C).

When paired stimuli of the same intensity were delivered at decreasing interstimulus intervals (Fig.3.21B) the amplitude of the second spike decreased and the IS-SD inflection became more apparent. At an interstimulus interval of 3ms the second spike had an amplitude of 93mV from a membrane potential of -63mV compared to the first spike amplitude of 98mV (Figs.3.21A,B). Reducing the interval to 2ms emphasised the IS inflection on the rising phase of the spike and the amplitude of the second somatodendritic spike was further reduced to 87mV (Fig.3.21B). Further narrowing of the interstimulus interval to 1.4ms led to only an IS spike being evoked with an amplitude of 30mV. Further shortening of the stimulus interval led to total loss of the IS component (not shown).

Twenty-one out of twenty-five FMs were successfully invaded antidromically using this method. The mean antidromic action potential amplitude was 92 ± 6.5mV (n = 21) and where separation of the IS component was achieved it had a mean amplitude of 33.7 ± 3.5mV (n = 12).

When viewed on a longer time base (Fig.3.21C) the antidromic action potential was followed by a prominent depolarising potential (delayed depolarisation, DD), which had an amplitude of 7.3mV, and a longer lasting afterhyperpolarisation (ahp) approximately 50ms in duration and with a peak amplitude of 3.9mV. The ahp prevented the generation of a second antidromic action potential with the same stimulus intensity used to generate the first. The mean amplitude of the slow ahp and DD were -3.1 ± 0.8mV and 8.1 ± 3.4mV (n = 11) respectively evoked after spikes with an amplitude of 96 ± 4mV from a resting potential of -65.4 ± 5.6mV. The ahp had a mean duration of 39 ± 7ms.

In the remaining FMs which were antidromically activated the spike after-potentials were obscured by depolarising synaptic potentials presumably evoked as a result of afferent stimulation by the stimulating electrode (Fig.3.22A). The presence of FM axon collaterals has been discounted in the cat (Fanardjian et al, 1983a) as well as their absence being inferred in the rat (Martin and Biscoe, 1977). In figure 3.22B synaptic potentials could be evoked in the absence of an antidromic potential when the cell was resting at -71mV. The amplitude of the depolarising potential was increased with increasing stimulus intensity to the point where an orthodromic action potential could be evoked. The action potential had an amplitude of 94mV and a duration of 0.5ms and was followed by a fast ahp, DD and a slow ahp. The evoked potentials had a time

course of about 20ms and were additive such that an action potential could be evoked by a second normally sub-threshold stimulus superimposed on a decaying synaptic potential (Fig.3.22C).

Directly Evoked Action Potentials

Action potentials (AP) could be evoked by increasing the amplitude of rectangular injected depolarising current pulses. In some cells a slowly depolarising prepotential was observed at sub-threshold levels upon which an action potential was evoked when the current amplitude was increased (Figs.3.5A, 3.25A).

The delay to the first spike after injection of a depolarising current pulse varied between neurones as can be seen by comparing figures 3.1, 3.5A and 3.28Ab. This delay appeared to be the result of a slowly rising potential which could be observed more clearly when the neurone was held at hyperpolarised membrane potentials and large amplitude current pulses used to evoke depolarising voltage responses in the region close to threshold. The neurone in figure 3.24Aa when held at -81mV showed a slowly rising potential in response to a 3.5nA depolarising current step. When held at -57mV a similar potential could be observed on the repolarising phase of a large hyperpolarising voltage response but not on smaller hyperpolarising responses (Fig.3.24Bb). This response appeared to be different to slower depolarising potentials observed in other FM's (Fig.3.6, 6.14B, 6.32) however, no pharmacological studies were performed to confirm this.

Figure 3.23A shows an action potential evoked by a continuous depolarising current of 1.3nA. The spike had an amplitude of 94mV and a duration at its base of 0.6ms and arose from a threshold of -51mV. The neurone had a resting potential of -69mV. Action potentials evoked by continuous current pulses had a mean amplitude

measured from the resting potential of 83.4 ± 8.9mV (n = 20) an overshoot of 12mV from a threshold of -53.6 ± 4.7mV (n = 20). Duration of AP's was 0.5msec and their Na^+ dependence inferred by their sensitivity to Tetrodotoxin (TTX).

The directly evoked AP was followed by a fast and slow after-hyperpolarisation (ahp) and a delayed depolarisation (DD) (Fig.3.23A). The fast ahp appeared to be a direct continuation of the repolarising phase of the AP and was brief in duration. The slow ahp peaked later and had an average amplitude of -10.2 ± 3mV from threshold voltage level and a duration of 57.7 ± 14.7msec measured from where the repolarising phase of the AP crossed the threshold voltage. The delayed depolarisation was identified as a small hump of short duration and small amplitude between the fast and slow ahp's (Fig.3.23A).

Figure 3.23B shows an action potential evoked by a brief 2ms current pulse from the same neurone as in Figure 3.23A. In this case AP amplitude and afterpotentials were measured in the absence of any injected current. The AP had an amplitude of 95mV and duration of 0.44ms. The fast ahp is represented as a negative notch prior to the DD which fails to overshoot the resting potential, while in cells held at higher membrane potentials the fast ahp was a genuine hyperpolarisation (Fig.3.26a). The DD had an amplitude of 5.7mV (Fig.3.23B) and was followed by a slower ahp which peaked later and had an amplitude of -2.9mV at the resting potential of -69mV showing that it was a true afterhyperpolarisation. Slow ahp duration was 46ms. The mean amplitude of the AP evoked in this way was 94.1 ± 5.8mV from a resting potential of -69.1 ± 5.2mV (n = 44). AP duration was 0.52

± 0.1ms, the DD had an amplitude of 6.1 ± 3.6mV (n = 41) while the slow ahp had an amplitude of -3.7 ± 1.8mV and a duration of 52.5 ± 12.4msec (n = 44).

Where antidromic and directly evoked action potentials were elicited in the same neurones AP amplitude, slow ahp amplitude and duration showed similar values. Thus antidromic AP had an amplitude of 95.4 ± 3.8mV compared with a directly evoked AP amplitude of 94.3 ± 3.6mV, the ahps had amplitudes of 3.1 ± 0.8 and 3.9 ± 0.9mV with durations of 39 ± 7 and 46.6 ± 4.1ms respectively (n = 8). All neurones displayed the characteristic membrane properties described previously and where tested were depolarised by 5-HT (n = 3). (See later).

The Effects of membrane potential and intracellular Cs^+ on FM ahp's

Figure 3.26 shows the reduction in amplitude of the slow ahp following directly evoked AP's as the holding membrane potential was hyperpolarised (Resting potential was -66mV). A plot of amplitude of the ahp against membrane potential indicated that the ahp reversed at about -80mV, using a linear regression analysis (Fig.3.27). This procedure was performed on 13 neurones and the mean estimated reversal potential was -80.6 ± 3mV. The use of KCl filled microelectrodes suggests that the mediating ion of the slow ahp is potassium in common with similar ahp's seen in other central neurones (Llinas, 1988).

The involvement of K^+ ions in the fast ahp is indicated by its sensitivity to intracellular Cs^+ (Fig.3.15). Immediately after impalement with a 2M CsCl filled microelectrode AP's with prominent fast ahps and slow ahp's could be evoked with depolarising current pulses (Fig.3.15A). The DD showed a reduced prominence in this neurone. In general, the low resistance electrodes used, led to

rapid Cs^+ loading such that a progressive blockade of the ahp was rarely seen. In this neurone the electrode resistance was higher than usual which led to a slower Cs^+ loading process. After 10 minutes the fast ahp was reduced to a brief notch prior to a greatly pronounced DD while the slow ahp remained but was less well defined which may be due to a direct effect of Cs^+ or the increased DD (Fig.3.15B). When held at a slightly more depolarised membrane potential a second spike could be seen to be evoked on the prominent DD (Fig.3.15C). Over this period of Cs^+ loading the AP duration also increased from 0.7msec to 2.1msec indicating a role for Cs^+ sensitive outward K^+ conductances in spike repolarisation and the fast ahp.

The Effects of Apamin on FM ahp's

Apamin has been shown to selectively block the Ca^{++} dependent K^+ conductance responsible for the slow ahp in several cell types including spinal motoneurones (Zhang & Krinjevic, 1987). Figure 3.28 shows the effects of apamin on slow ahp's of FMs. The AP evoked by a brief depolarising current pulse from a holding potential of -50mV had an amplitude of 73mV and was followed by a slow ahp -11.8mV in amplitude and 50ms long (Fig.3.28Aa). The normal resting potential of this neurone was -65mV and it had a $R_{m(pk)}$ of 10.6MΩ (not shown). A 1.5nA current step 100ms in duration evoked two AP's with prominent ahp's (Fig.3.28Ab). Apamin, 25nM, was superfused for 20 minutes without any effect on resting potential (-65mV) or $R_{m(pk)}$ (10.1MΩ). The amplitude of the AP evoked at -50mV was unaffected by apamin (78mV) however the slow ahp was greatly reduced in both amplitude (7.7mV) and duration (21msec) (Fig.3.28Ba). The fast ahp appeared to be unaffected by apamin. When a 1.5nA depolarising current pulse from the resting

potential was applied four AP's were evoked which had much steeper interspike trajectories indicating reduced accommodation due to apamin induced suppression of the slow ahp (Fig.3.28Bb).

Repetitive Firing of Facial Motoneurones

The AP firing responses were not analysed in great detail, however, figure 3.25, shows the characteristic properties of FM firing in vitro. As mentioned earlier a sub-threshold depolarising current pulse elicited a prepotential (Fig.3.25A) on which a single AP can be evoked when the current amplitude is increased (Fig.3.25B). The AP was followed by a pronounced ahp which had not decayed fully by the end of the current pulse thereby preventing a second AP being generated. Further depolarisation led to an increase in the gradient of the trajectory following the first AP such that threshold for a second AP was reached 38msec after the first AP. The ahp following the second AP had a more concave appearance than the first and a less steep repolarising phase though its peak amplitude was less negative than the first ahp. This led to an increased interval of 45ms before a third AP was evoked (Fig.3.25C). The threshold for the second and third AP's was higher than that for the first. Increased depolarisation led to further reduction in the first and subsequent interspike intervals reflected in steeper trajectories between AP's and reduced peak amplitude of the ahp's (Fig.3.25D,E). While the first interspike interval was shorter than the second which was concomitantly briefer than the third, subsequent interspike intervals were of equal duration leading to sustained tonic AP generation.

Fig. 3.1

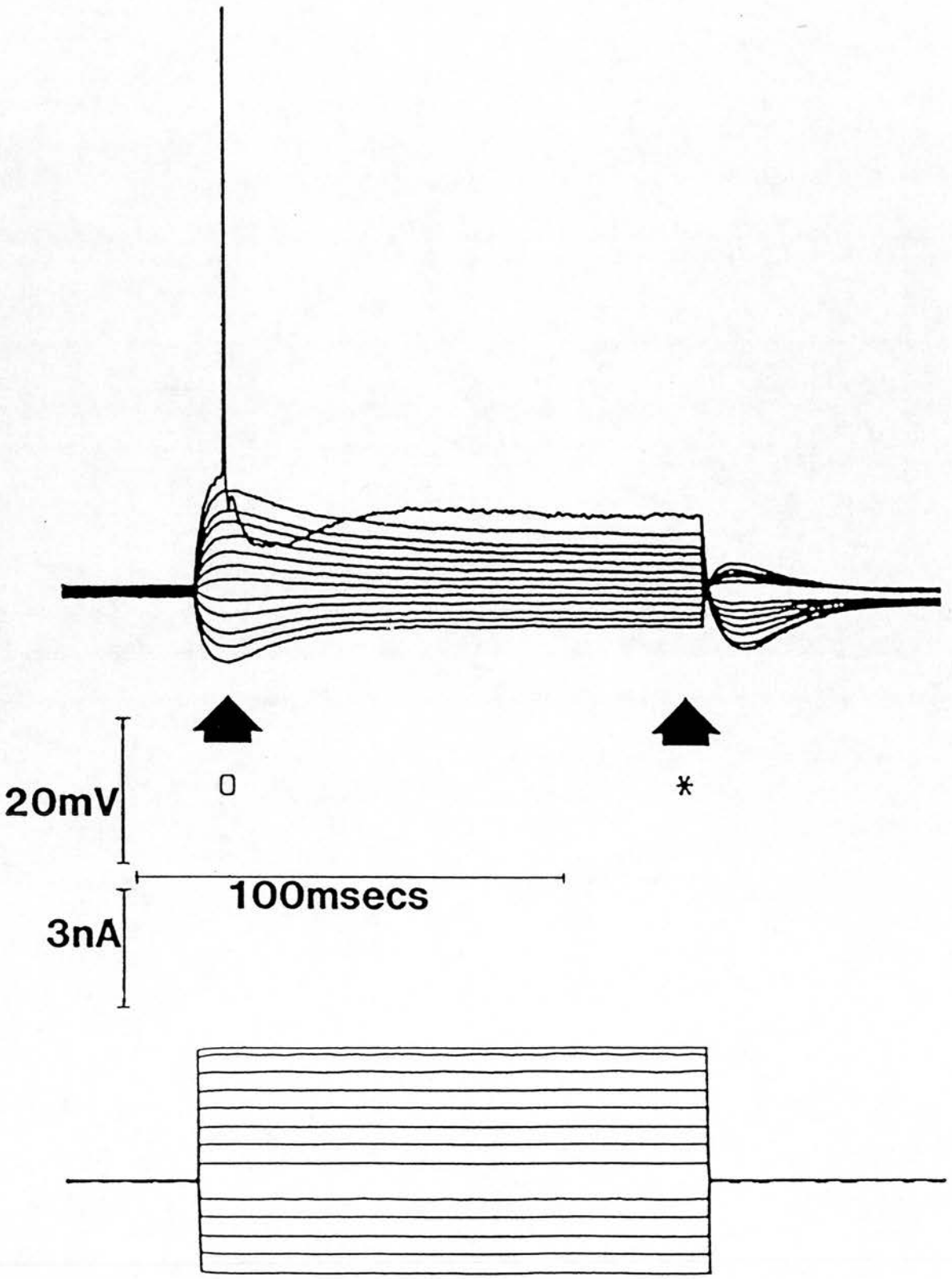

Figure 3.1

Membrane properties of a Facial Motoneurone (FM) I

Superimposed, averaged traces of membrane potential (upper record) during intracellular injection of graded hyperpolarising and depolarising current pulses (lower record) applied from a resting potential of -74mV. Hyperpolarising voltage responses show a time dependent "sag" characteristic of inward "anomalous" rectification (IR), which reaches steady-state within the 120ms current pulse, and is followed by a depolarising rebound tail potential. Depolarising voltage responses display a time dependent sag towards resting potential and these responses are followed by hyperpolarising tail potentials. Action potential (AP) amplitude is attenuated on this and all subsequent records, unless otherwise stated, due to the slow sampling rate used for examining the membrane responses of longer duration. The AP overshoots by 19mV and is evoked from a threshold of -58mV. It is followed by a series of afterpotentials including fast and slow afterhyperpolarisations (ahp) separated by a brief delayed depolarisation (DD). The arrows indicate the points at which measurements are taken to construct the peak (open square) and steady-state (asterisk) voltage deflection current-voltage (I/V) relationships shown in figure 3.2. (This convention is used throughout for current clamp records).

Fig. 3.2

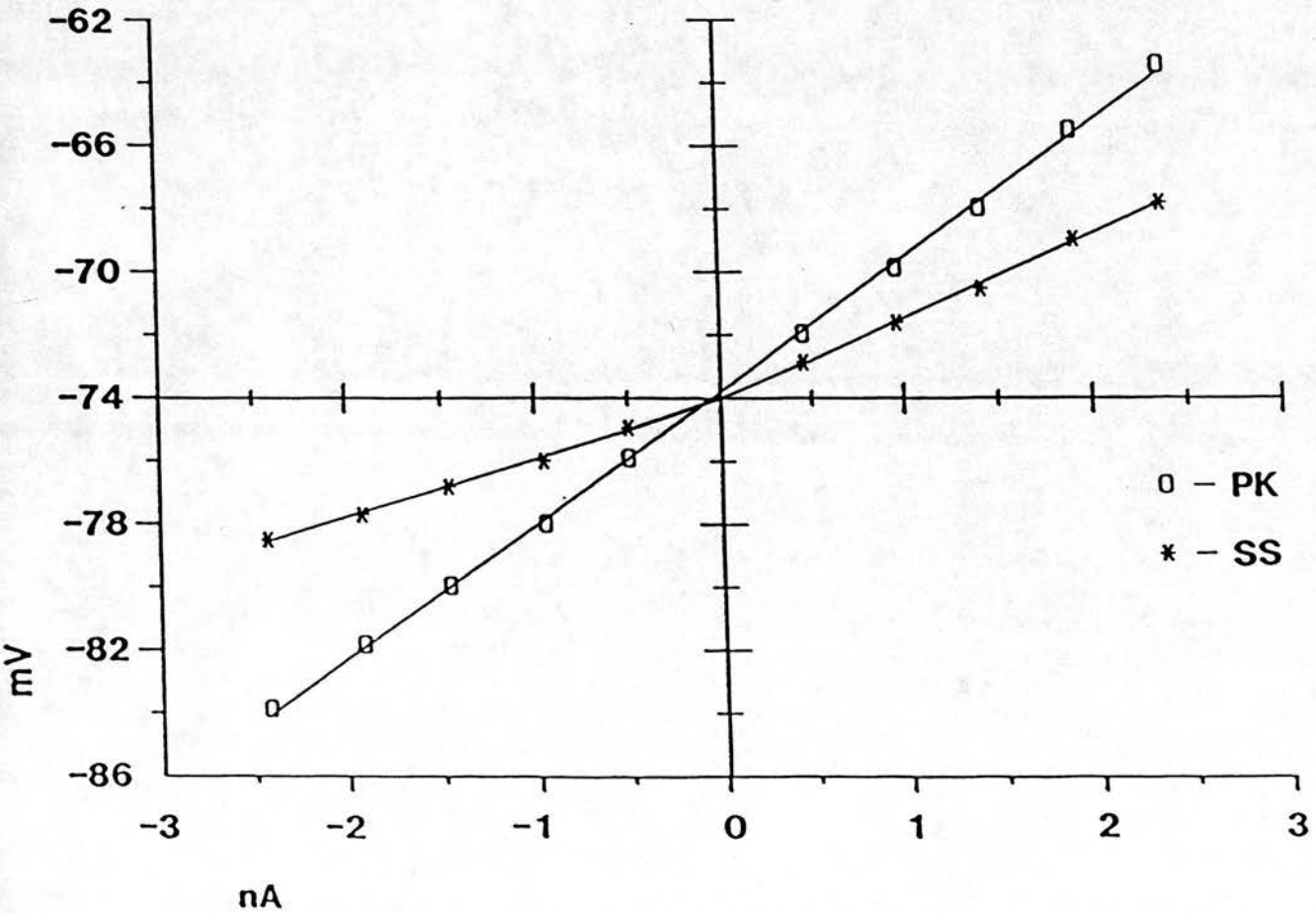

Figure 3.2

Current-voltage relationships for the FM shown in Figure 3.1
The I/V plot of peak voltage deflections (open squares) is linear throughout the tested range (~ 10mV around resting potential) and its slope gives a value for neuronal input resistance ($R_{m(pk)}$) of 4.24MΩ. Plots of steady-state voltage deflections (asterisks) were also linear but had different slopes in the depolarising and hyperpolarising direction giving values of $R_{m(ss)}$ of 2.66 and 1.84MΩ respectively.

Fig. 3.3

A Current-clamp Vm-72mV

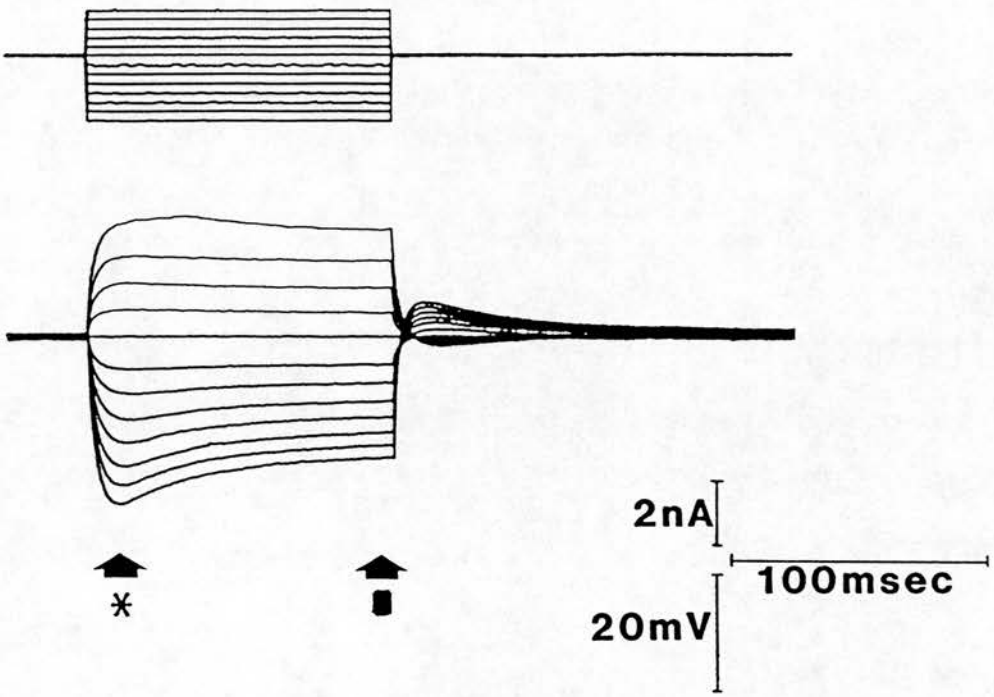

B Voltage-clamp Vm-73mV

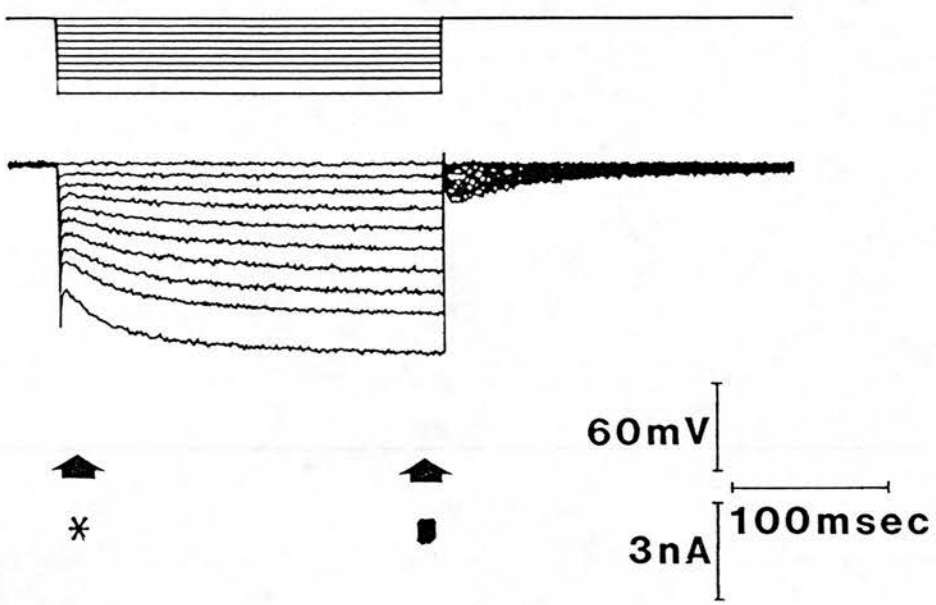

Figure 3.3

Membrane properties of a Facial Motoneurone (II)

A) Membrane voltage responses (lower traces) in response to injected current pulses (upper traces) recorded from a FM resting at -72mV. Hyperpolarising voltage responses show time dependent IR and are followed by depolarising tail potentials which decay to resting potential over the following 100 to 120msec. Depolarising voltage responses show little time-dependent "sag" and are followed by only small hyperpolarising rebound potentials. At just sub-threshold levels for AP generation a small prepotential can be seen on the depolarising voltage response.

B) Membrane currents (lower traces) evoked by hyperpolarising voltage step commands (upper traces) from the same FM as in A, voltage-clamped at -73mV (resting potential). As the amplitude of the voltage command increases after an initial instantaneous (asterisk) current level, a slower time-dependent inward current develops which reaches steady-state (closed squares) at the end of the pulse. The amplitude of the inward current and its activation rate increase with hyperpolarisation as does the amplitude of the associated inward tail current observed at the offset of the voltage command.

Fig. 3.4

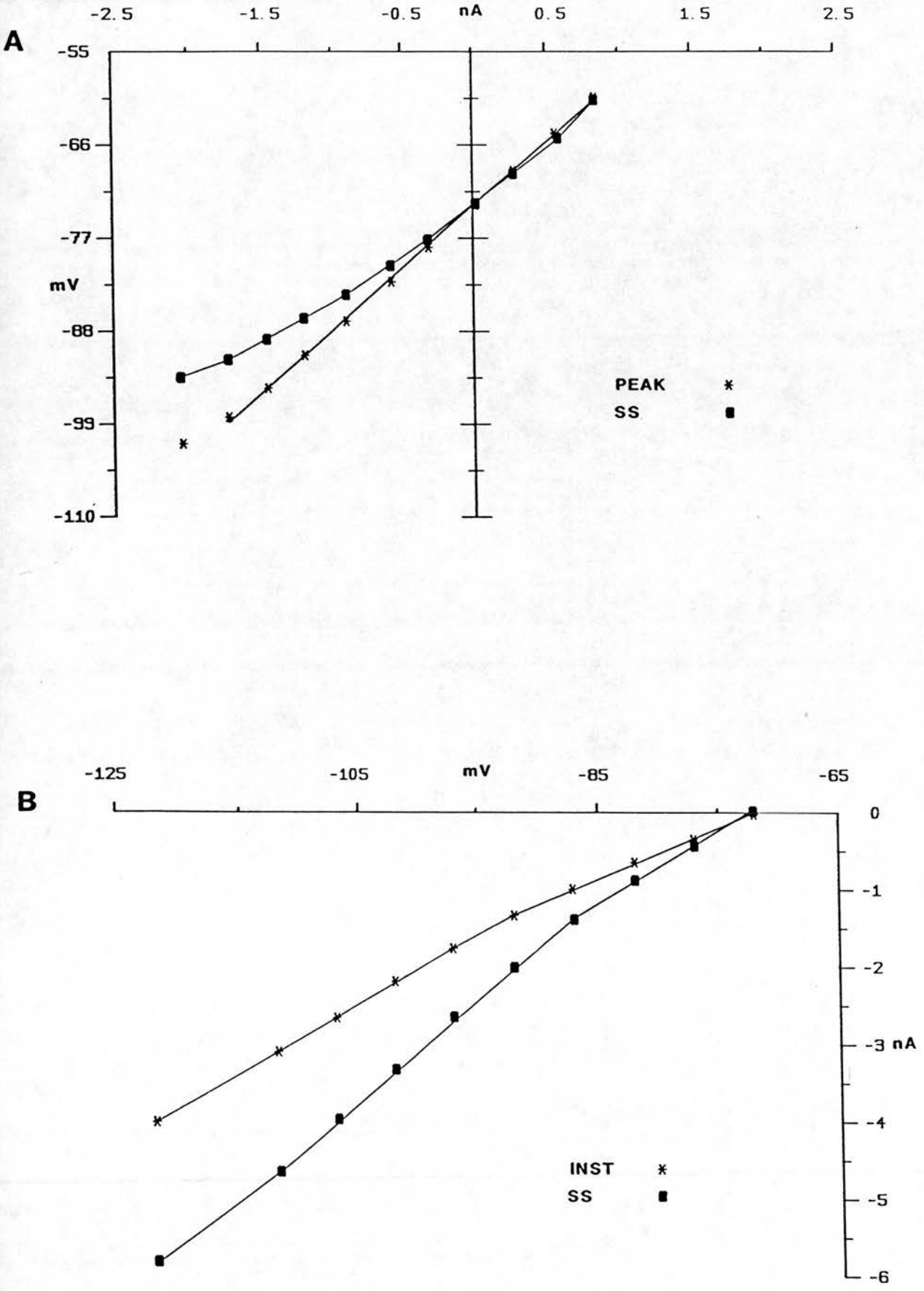
A
-2.5
-1.5
-0.5
nA
0.5
1.5
2.5
-55
-66
-77
mV
-88
-99
-110
PEAK
SS
B
-125
-105
mV
-85
-65
0
-1
-2
-3 nA
-4
-5
-6
INST
SS

Figure 3.4

Facial motoneurone current-voltage relationships

A) Peak and steady state current-voltage relationships obtained from measurements of the electrotonic potentials in Fig.3.3A. The peak I/V plot (asterisks) was linear throughout virtually its whole range showing only small rectification at potentials more negative than -99mV. $R_{m(pk)}$ was 14.8MΩ. A value of $R_{m(ss)}$ was not obtained as the steady-state I/V relationship was non-linear throughout the hyperpolarising range. The lack of "sag" in the depolarising responses is illustrated by the similarity between steady-state and peak deflection curves in this potential range.

B) Voltage-current relationships measured in voltage-clamp for the records shown in figure 3.3B. The instantaneous current (asterisks) shows linearity up to approximately -93mV and gave a slope conductance of 66.1nS. The steady-state current (closed squares) diverged from the instantaneous current throughout the measured range and was linear over the range -73 to -88mV giving a steady-state conductance of 93.5nS.

Fig. 3.5

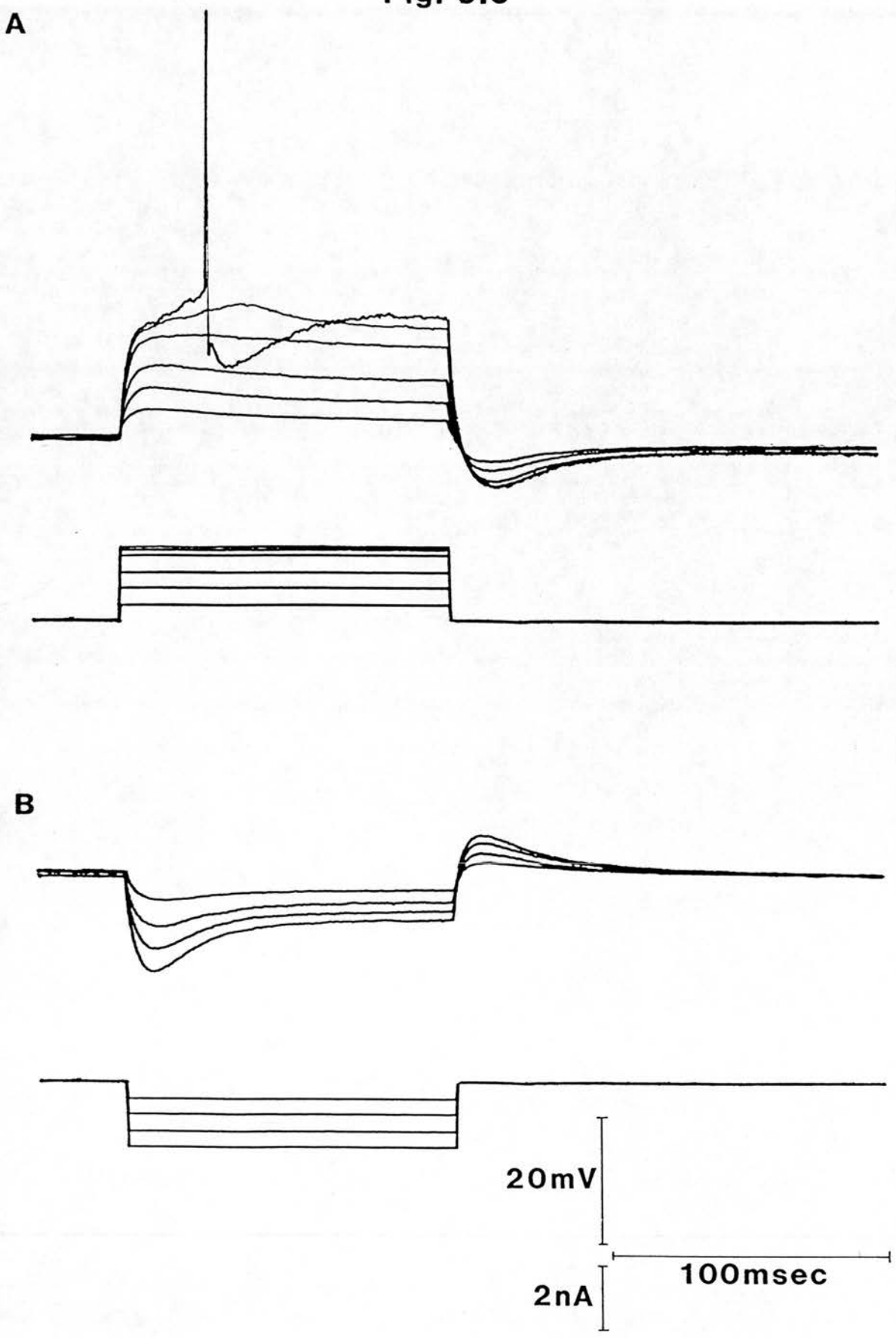

Figure 3.5

Membrane properties of a FM (III)
A) Depolarising voltage responses (upper traces) evoked by current pulses (lower traces) from a resting potential of -75mV, show a small amount of membrane potential sag and are followed by prominent hyperpolarising tail potentials. A just sub-threshold depolarising current pulse (+2.4nA) evokes a prepotential but not an AP. Increasing the current pulse amplitude to +2.5nA evokes an action potential on this prepotential. Unlike Fig.3.1, the AP is delayed after the initial rapid depolarisation.
B) In the hyperpolarising direction the FM demonstrates the characteristic IR and depolarising tail potentials seen in earlier figures. $R_{m(pk)}$ was 8.1MΩ over its linear range.

Fig. 3.6

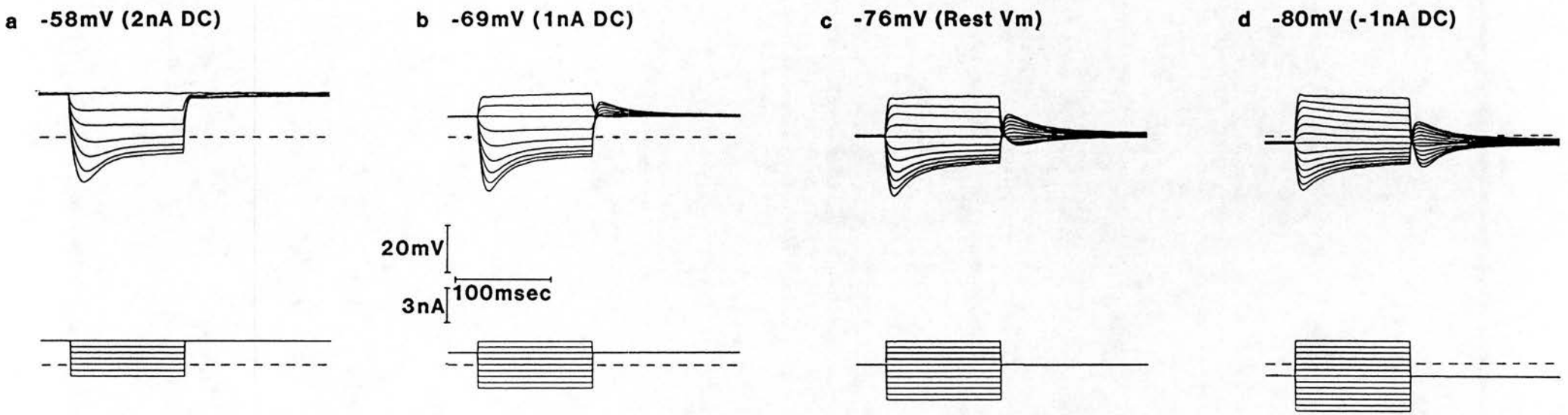
a -58mV (2nA DC)
b -69mV (1nA DC)
c -76mV (Rest Vm)
d -80mV (-1nA DC)
20mV
100msec
3nA

Figure 3.6

The effects of changing the membrane potential on the membrane properties of FM's

Membrane voltage responses (upper records) were obtained from the same FM held at -58, -69, -76 and -80mV by the passage of +2, +1, 0 and -1nA continuous DC through the recording microelectrode respectively (a to d). The dashed line in the voltage records indicates the true resting potential (-76mV) while in the current records it represents the passage of zero current. At resting potential (-76mV, c) the neurone displayed the membrane properties described earlier. Hyperpolarising responses displayed prominent IR and were followed by depolarising tail potentials. Depolarising voltage responses displayed time dependent sag and were followed by hyperpolarising tail potentials which tended towards a maximum amplitude. Larger amplitude depolarising responses displayed a slowly developing anomalous rectification at potentials just sub-threshold for AP's. A new holding potential of -80mV was achieved with -1nA DC (d). At this potential all the membrane properties seen at rest were retained though hyperpolarising tail potentials were seen to increase linearly in amplitude without a maximum response being determined. Injection of +1nA DC depolarised the FM to a holding potential of -69mV (b). Hyperpolarising voltage responses showed an increased amplitude in response to the test current pulses though IR was still apparent in all the responses. The amplitude of depolarising tail potentials was reduced at this holding potential. Membrane potential sag was not observed with depolarising current pulses and neither were hyperpolarising tail potentials though anomalous rectification was seen in the range just sub-threshold for AP generation. With +2nA continuous depolarising current the FM rested at -58mV(a). Further depolarisation to -56mV led to spontaneous firing of AP's (not shown). Voltage responses evoked by -0.5 and -1nA current pulses showed no time dependent sag. Larger currents evoked voltage responses displaying IR however depolarising rebound potentials were not observed. In their place a biphasic return to the resting potential was observed. The largest component of this repolarisation was rapid while the final 2 to 3mV took longer than 100msec and showed similarities to the outward rectification seen on sub-threshold depolarising responses from more negative holding potentials.

Fig. 3.7

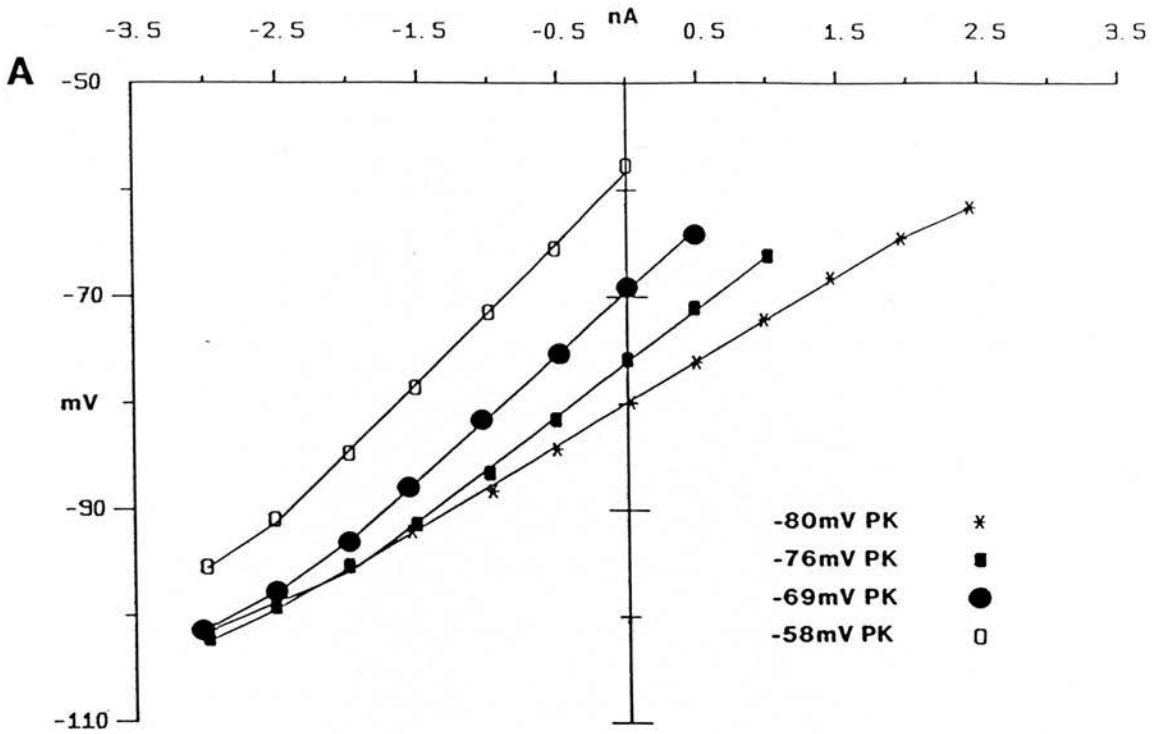
A
-3.5
-2.5
-1.5
-0.5
nA
0.5
1.5
2.5
3.5
-50
-70
mV
-90
-110
-80mV PK
-76mV PK
-69mV PK
-58mV PK

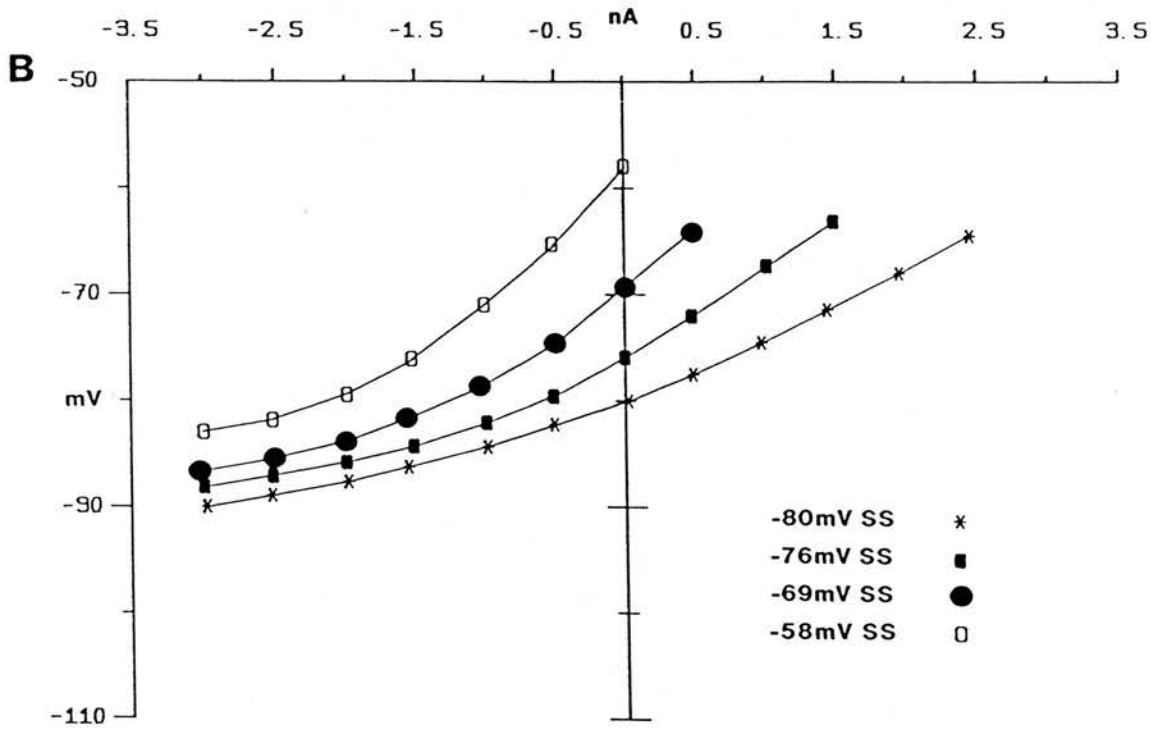
B
-3.5
-2.5
-1.5
-0.5
nA
0.5
1.5
2.5
3.5
-50
-70
mV
-90
-110
-80mV SS
-76mV SS
-69mV SS
-58mV SS

Figure 3.7

Peak voltage deflection and steady-state voltage deflection current-voltage relationships at different membrane potentials taken from the records illustrated in figure 3.6

A) Peak I/V plots at each potential were linear over most of the potential range but showed rectification at more negative potentials. The slope of these relationships decreased with hyperpolarisation of the holding potential, giving values of $R_{m(pk)}$ of 13.1, 11.8, 9.9 and 7.9MΩ at -58, -69, -76 and -80mV respectively.

B) Steady-state I/V plots are non-linear throughout the tested range at each holding potential and showed an increase in slope with depolarisation. This indicates that IR is active throughout the tested range and has not reached its maximum conductance state even at the most negative potentials attained (-90mV).

Fig. 3.8

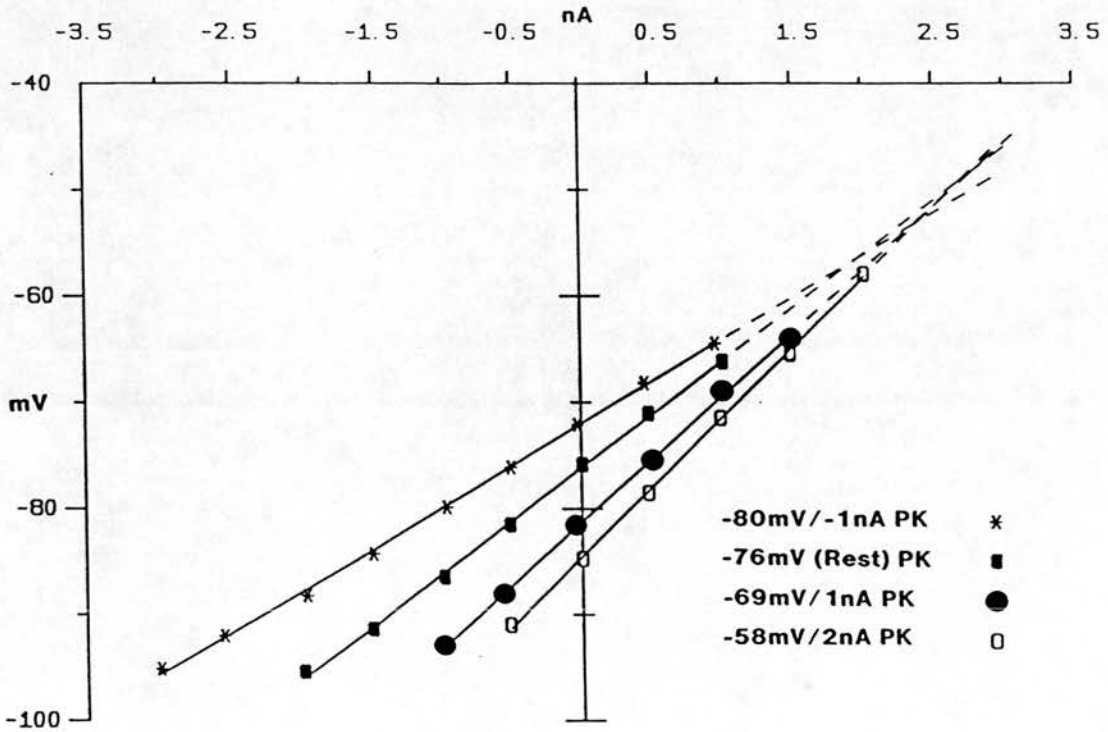
nA
-3.5
-2.5
-1.5
-0.5
0.5
1.5
2.5
3.5
-40
-60
-80
-100
mV
-80mV/-1nA PK
-76mV (Rest) PK
-69mV/1nA PK
-58mV/2nA PK

Figure 3.8

Peak deflection I/V plots as in figure 3.7A this time plotted against offset current

Linearity of these plots indicates that no voltage-dependent conductances are activated over this potential range within the time taken for the peak voltage deflection to be reached. The slope is therefore determined by the activation state of IR and thus the extrapolated point of intersection of these plots at potentials between -49 and -56mV can be taken to be the reversal potential for IR.

Fig. 3.9

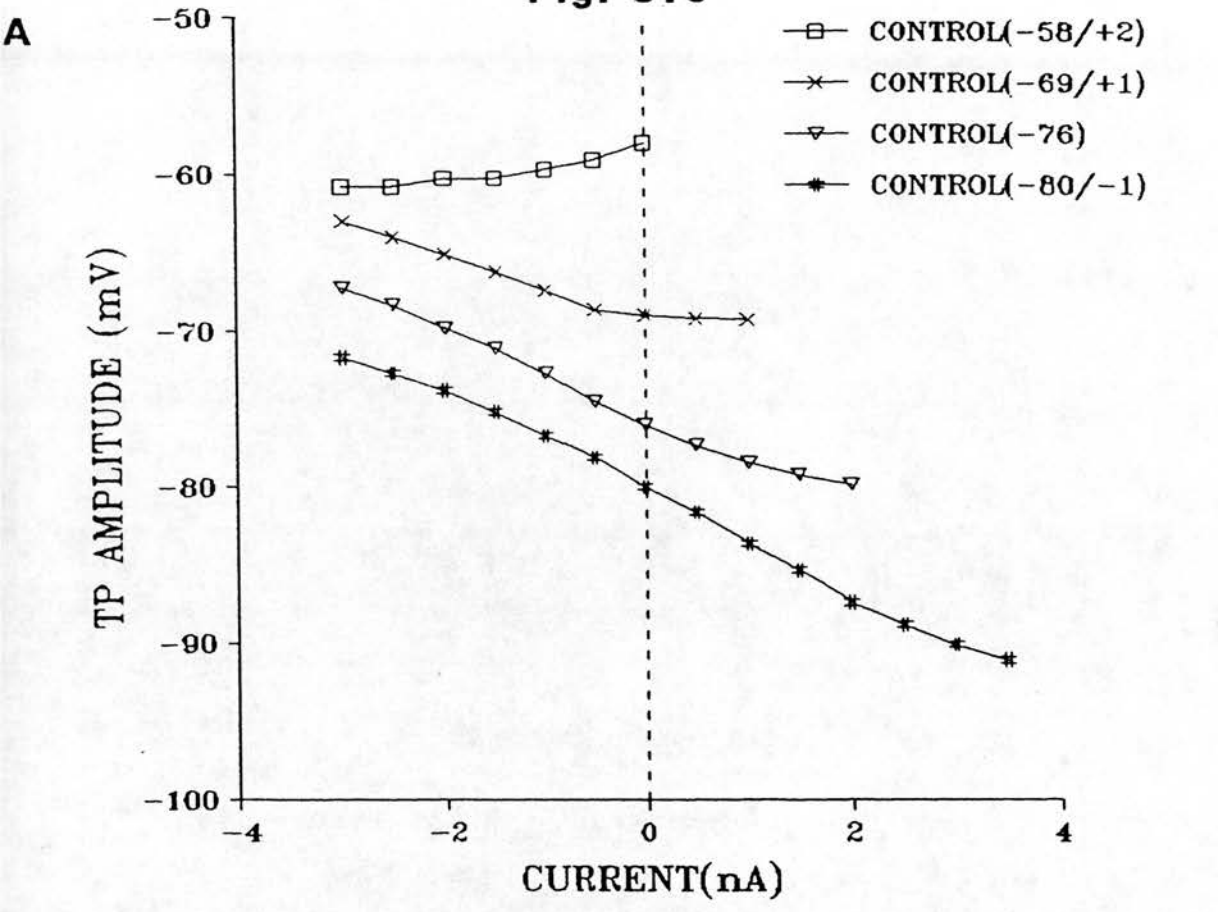
A
CONTROL(-58/+2)
CONTROL(-69/+1)
CONTROL(-76)
CONTROL(-80/-1)
TP AMPLITUDE (mV)
-50
-60
-70
-80
-90
-100
-4
-2
0
2
4
CURRENT(nA)

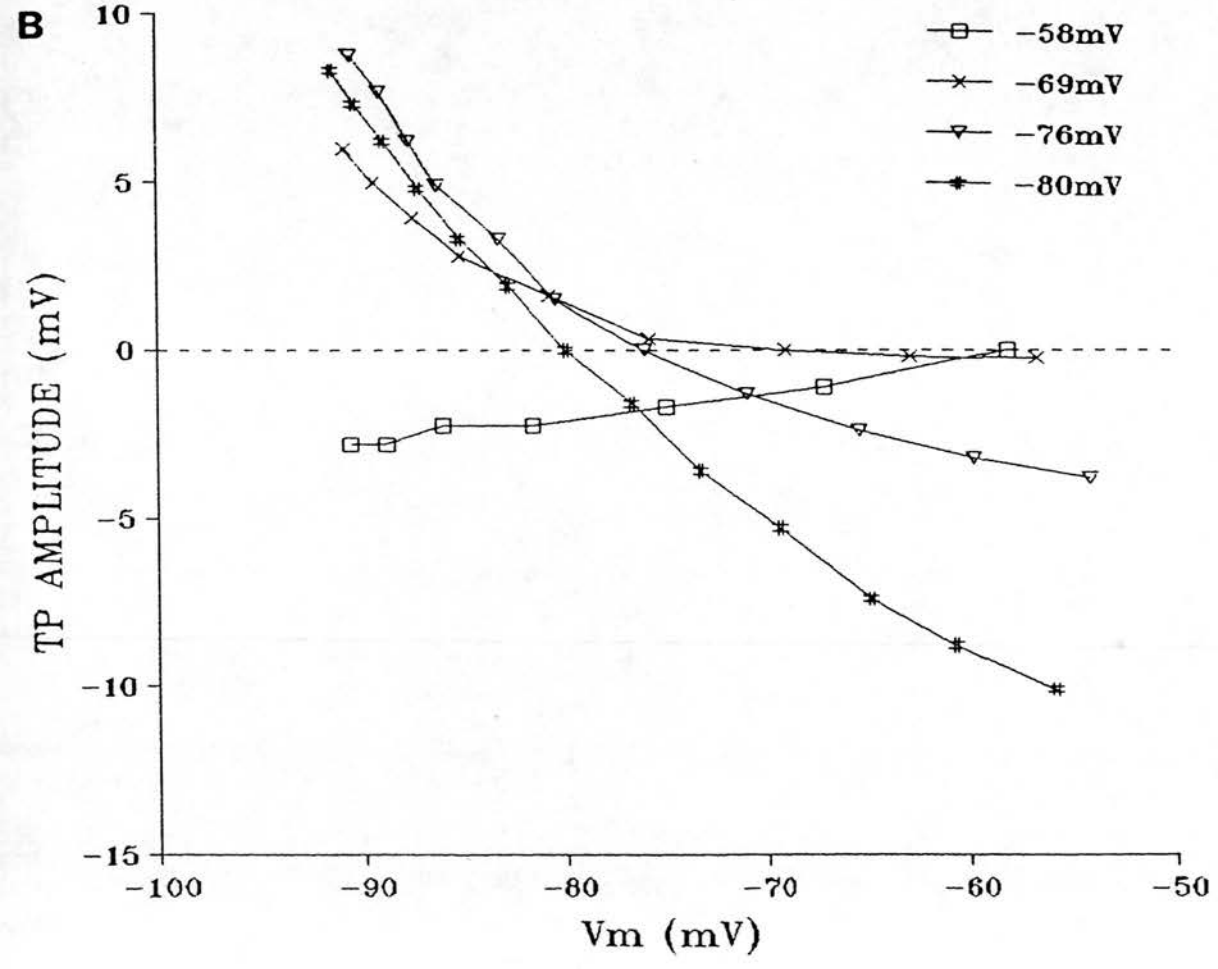
B
-58mV
-69mV
-76mV
-80mV
TP AMPLITUDE (mV)
10
5
0
-5
-10
-15
-100
-90
-80
-70
-60
-50
Vm (mV)

Figure 3.9

The effects of membrane potential on the amplitude of rebound tail potentials

A) The voltage reached at the peak of the rebound tail potential is plotted against the amplitude of the preceding current pulse. At -80mV (#) the relationship is roughly linear throughout the whole range. At -76mV (triangles) depolarising potentials show a linear relationship with a slope similar to that seen at -80mV while hyperpolarising potentials tend towards a plateau. Holding at -68mV (crosses) shows a biphasic relationship. No tail potentials are seen in the range -0.5 to +1.0nA while hyperpolarising currents of greater amplitude than 0.5nA evoked a linearly increasing depolarising tail potential amplitude but with a less steep slope to that seen at more negative holding potentials. When held at -58mV (squares) hyperpolarising current pulses did not evoke depolarising tail potentials but showed a slow component of the repolarising phase which had an amplitude relatively independent of current amplitude.

B) Absolute amplitude of the tail potential is plotted against the steady-state membrane potential achieved during the preceding current pulse, showing the dependence on both this potential and the holding membrane potential.

Fig. 3.10

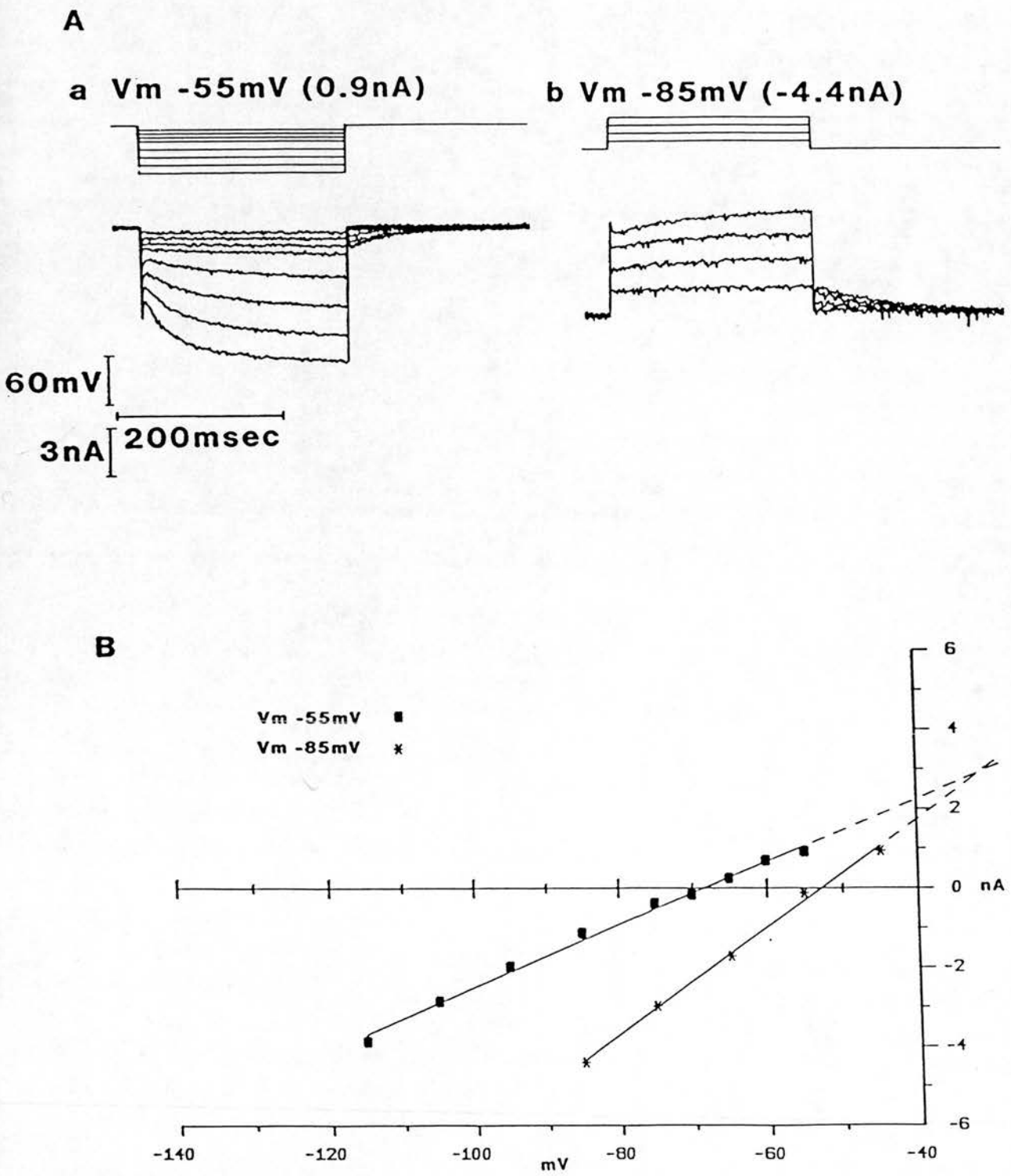
A
a Vm -55mV (0.9nA)
b Vm -85mV (-4.4nA)
60mV
3nA
200msec
B
Vm -55mV
Vm -85mV
6
4
2
0 nA
-2
-4
-6
-140
-120
-100
mV
-80
-60
-40

Figure 3.10

FM instantaneous current-voltage relations
Aa) Membrane current records (lower traces) evoked by 250msec hyperpolarising voltage step commands (upper traces) from a holding potential of -55mV. Ab) Membrane currents evoked by depolarising voltage step commands from a holding potential of -85mV. Note the slow outward relaxation indicative of inactivation of IR and also the outward tail currents. B) Plot of instantaneous current jumps obtained from the records in A were linear giving conductances of 78.7 and 135.1nS at -55 and -85mV, respectively. The reversal potential for IR is -31mV obtained from the extrapolated point of intersection of the relationships, i.e. where IR is weakly (-55mV) and strongly (-85mV) activated.

Fig. 3.11

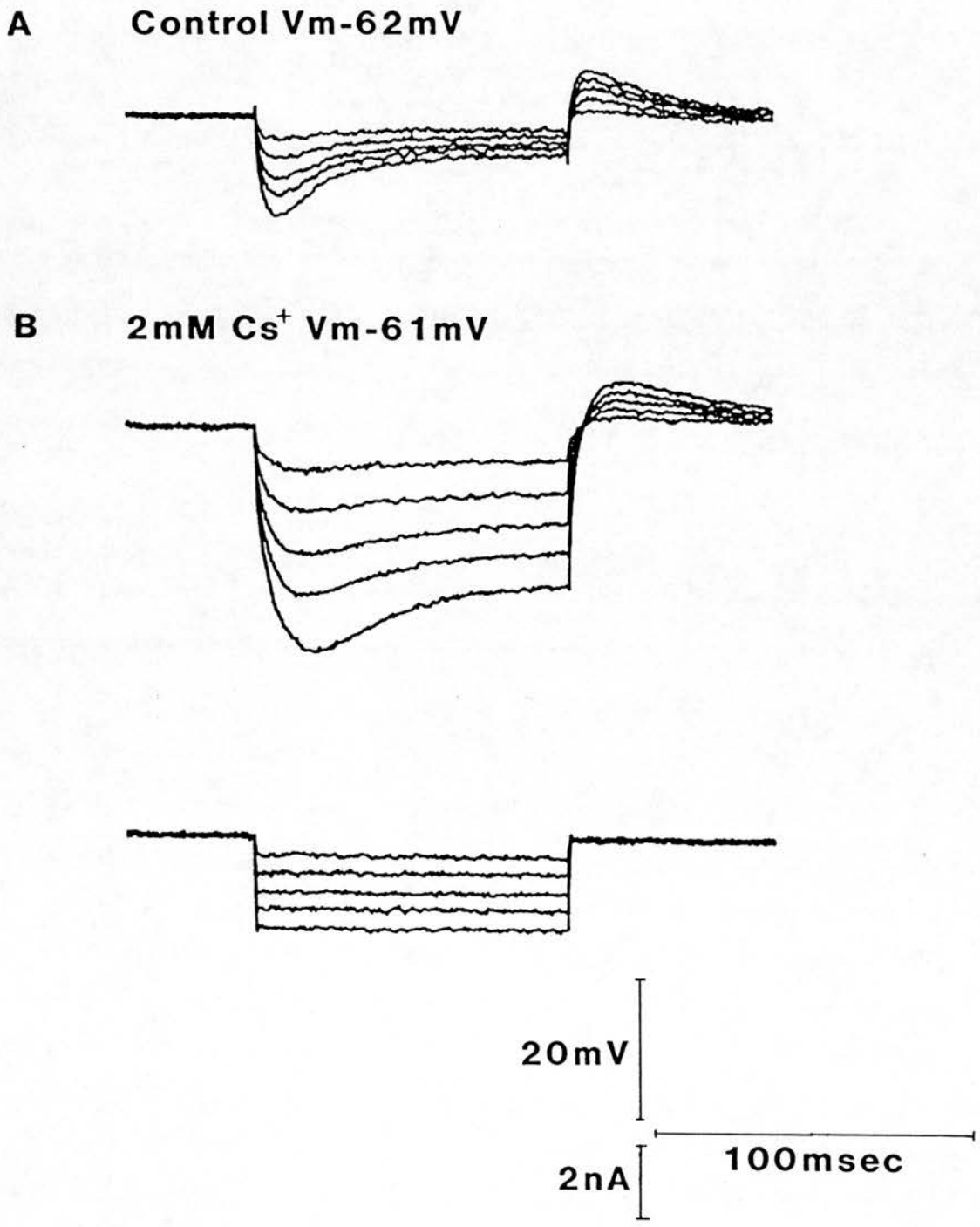

Figure 3.11

The effects of Cs^+ (2mM) on FM membrane voltage responses
A) Hyperpolarising voltage responses displayed the characteristic properties of FM's described earlier. Resting potential was -62mV. B) Superfusion of Cs^+ (2mM) led to an increase in both the peak and steady-state voltage deflections to the test current pulses along with a small depolarisation to -61mV. Over the control voltage range IR was greatly suppressed. However, at more negative potentials (achieved because of the increase in R_m) incomplete blockade was observed.

Fig. 3.12

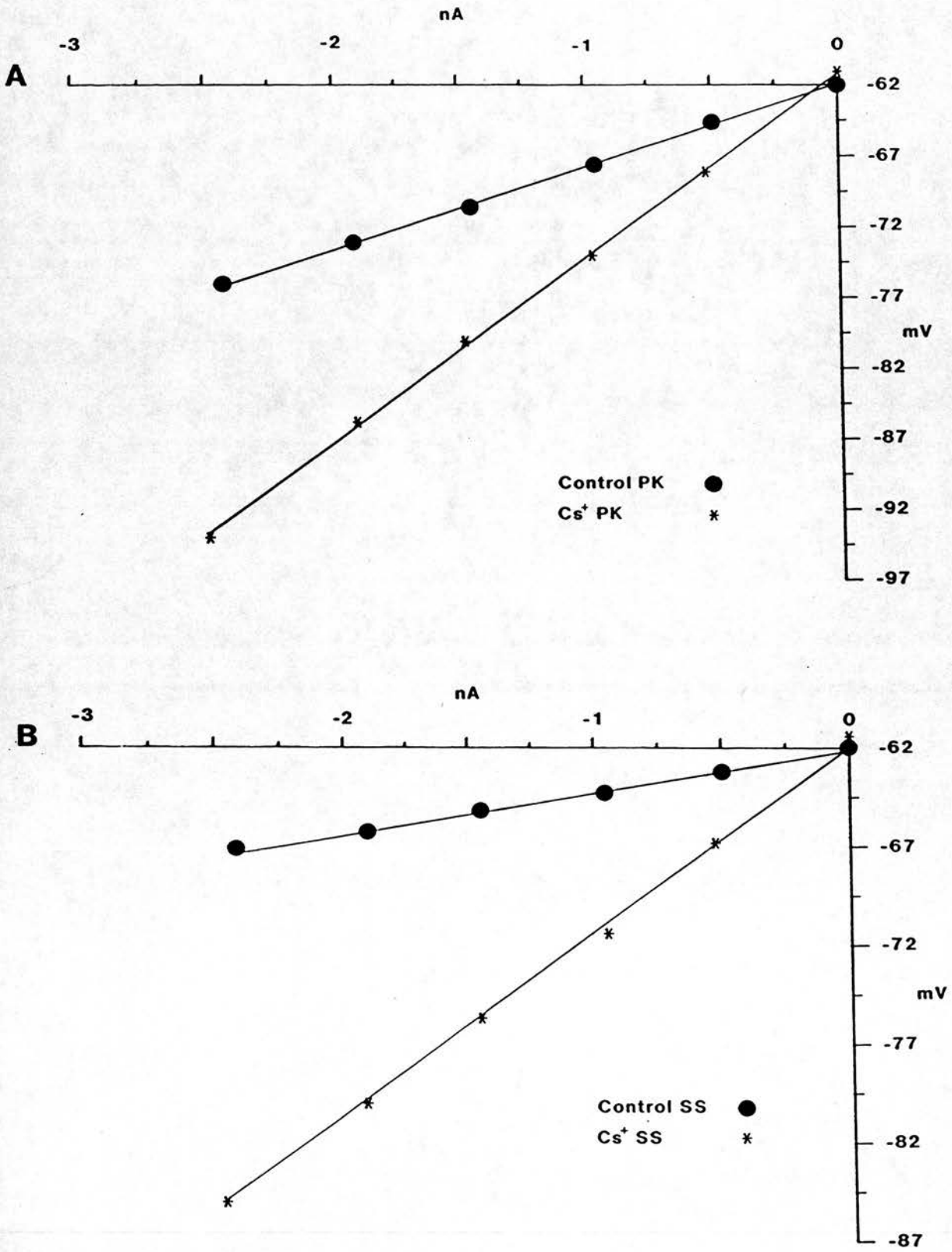
A
nA
-3
-2
-1
0
-62
-67
-72
-77
mV
-82
-87
-92
-97
Control PK
Cs+ PK
B
nA
-3
-2
-1
0
-62
-67
-72
mV
-77
-82
-87
Control SS
Cs+ SS

Figure 3.12

Facial motoneurone I/V relationships in the absence and presence of Cs^+

Peak voltage deflection (A) and steady-state voltage deflection (B) I/V plots in the absence (closed circles) and presence (asterisks) of Cs^+ (2mM). $R_{m(pk)}$ measured from the slope of the plots increased from 5.9 to 13MΩ in the presence of Cs^+ while $R_{m(ss)}$ increased from 2.1 to 9.3MΩ indicating that IR active at the resting potential as well as that activated by hyperpolarisation is blocked by Cs^+ (2mM).

Fig. 3.13

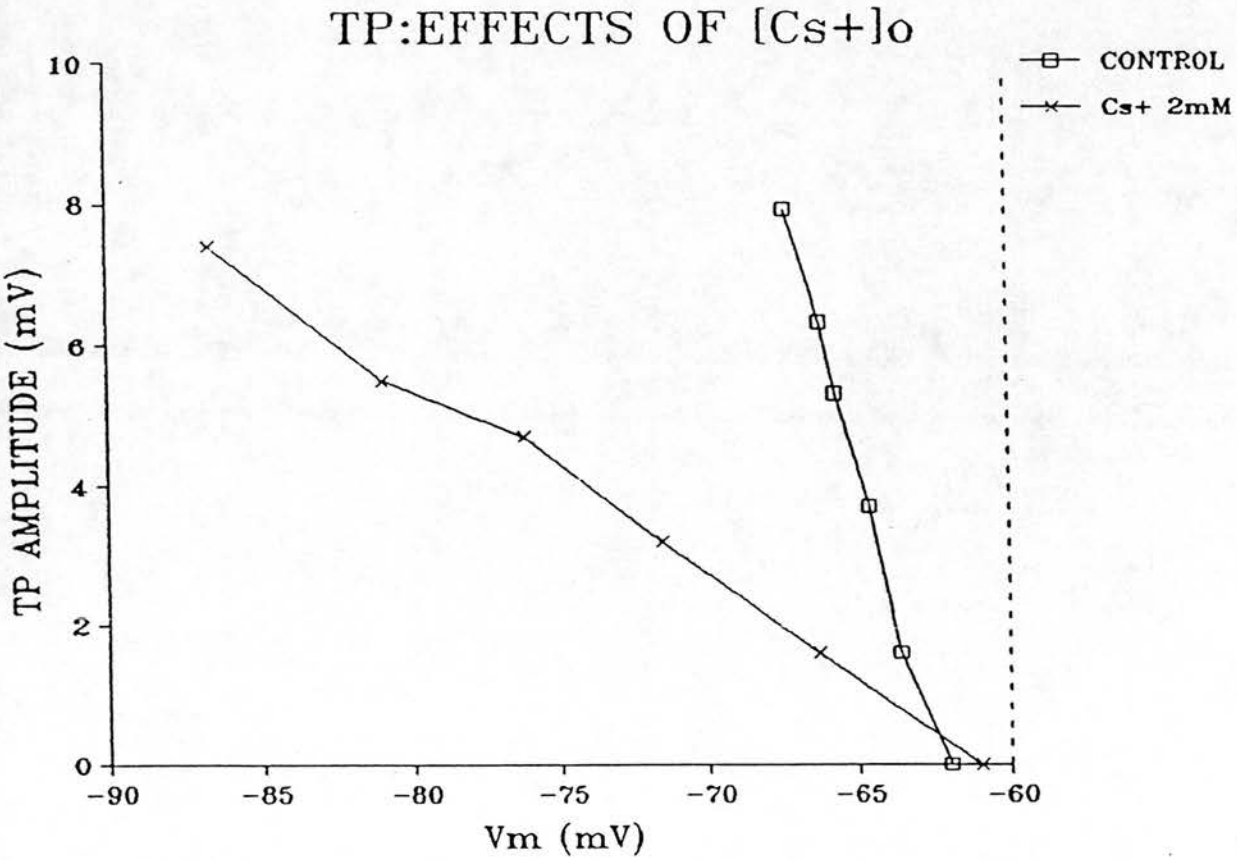
TP:EFFECTS OF [Cs+]o
CONTROL
Cs+ 2mM
TP AMPLITUDE (mV)
10
8
6
4
2
0
−90
−85
−80
−75
−70
−65
−60
Vm (mV)

Figure 3.13

The effects of Cs^+ on tail potential amplitude
Depolarising tail potential amplitude from resting potential plotted against the steady-state membrane potential achieved during the preceding membrane voltage response, in the absence (open squares) and presence (crosses) of Cs^+ (2mM). Suppression of IR by Cs^+ is accompanied by a depression of the tail potential when compared over similar voltage ranges. Greater preceding hyperpolarisation in the presence of Cs^+ is required to evoke tail potentials of similar amplitude to those seen in control conditions.

Fig. 3.14

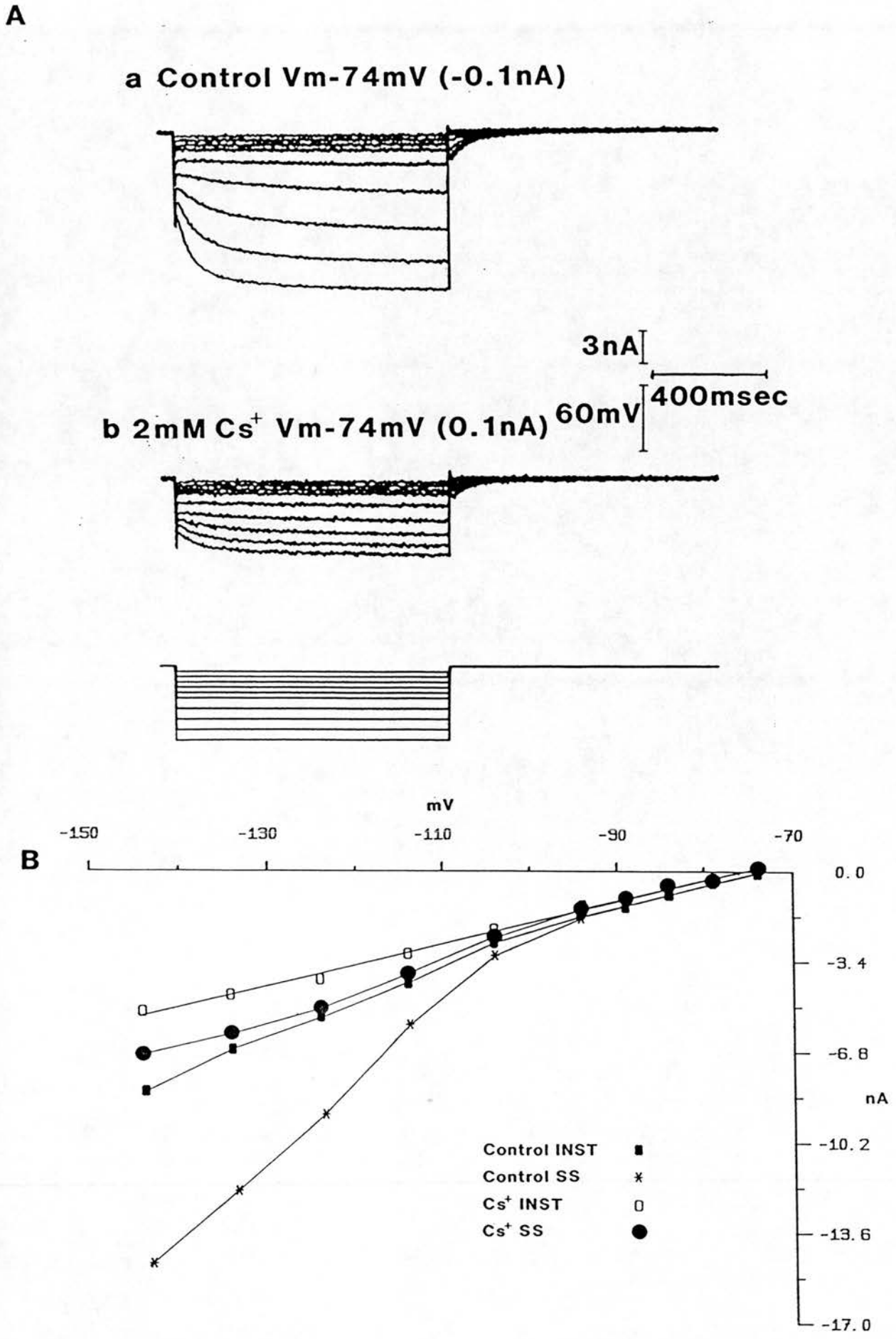
A
a Control Vm-74mV (-0.1nA)
3nA
400msec
60mV
b 2mM Cs+ Vm-74mV (0.1nA)
B
mV
-150
-130
-110
-90
-70
0.0
-3.4
-6.8
nA
-10.2
-13.6
-17.0
Control INST
Control SS
Cs+ INST
Cs+ SS

Figure 3.14

The effects of Cs^+ (2mM) on FM membrane currents

A) Currents evoked by hyperpolarising voltage step commands 1 sec in duration from a holding potential of -74mV show a time and voltage dependent inward current. Cs^+ (2mM) suppresses both the instantaneous current jump and the time and voltage dependent inward current.

B) Instantaneous and steady-state current voltage plots in the presence and absence of Cs^+ (2mM). Cs^+ has no effect over the range -74 to -94mV where no time dependent current is observed. At potentials more negative than -94mV both control instantaneous (closed squares) and steady-state (crosses) plots show non-linearity and diverge as hyperpolarisation is increased. Cs^+ leads to the instantaneous plot (open squares) being linear throughout its range while the slope of the steady-state plot (closed circles) is greatly reduced.

Fig. 3.15

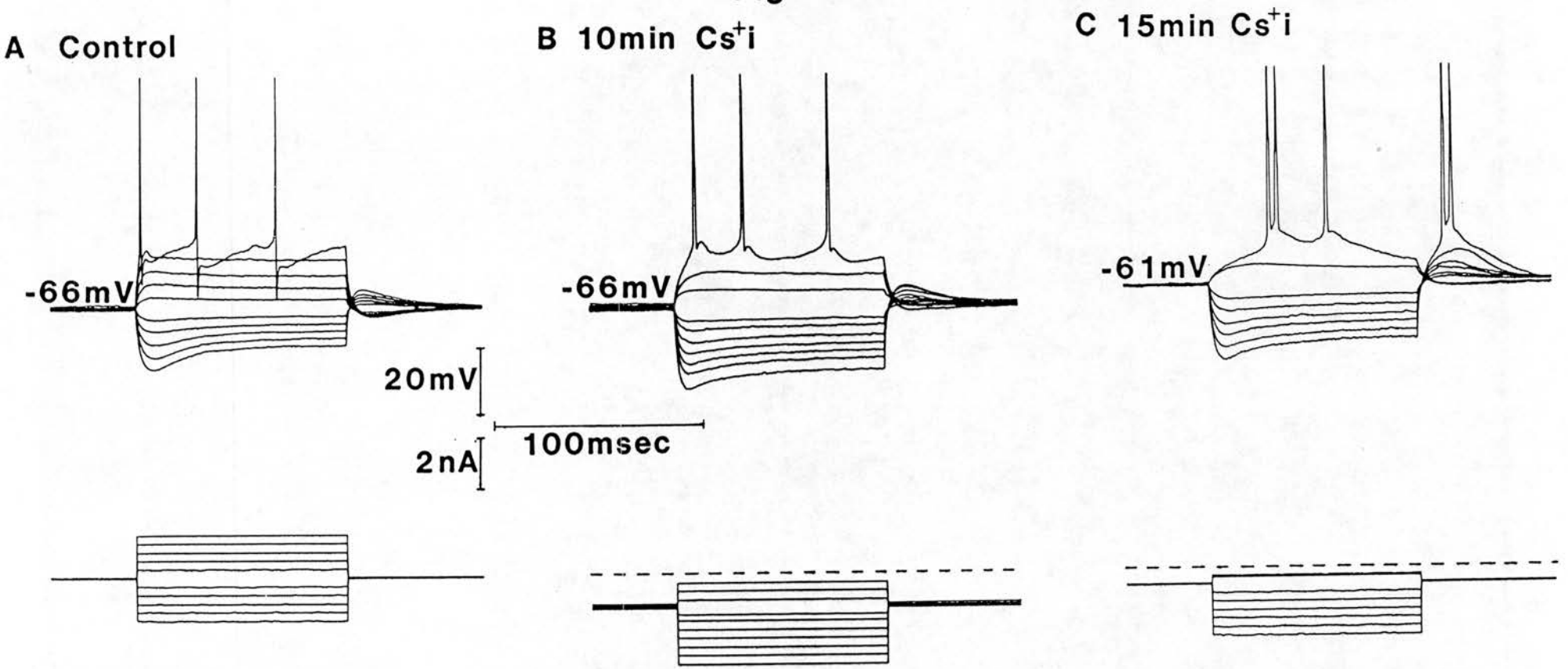
A Control
B 10min Cs+i
C 15min Cs+i
-66mV
-66mV
-61mV
20mV
2nA
100msec

Figure 3.15

The effects of intracellular Cs^+-loading of a FM

A) Immediately after impalement with a 2M CsCl filled microelectrode electrotonic potentials obtained from a resting potential of -66mV showed properties characteristic of FM's. Importantly AP's were brief in duration (0.7ms) and followed by the fast and slow ahp's separated by a DD.

B) After 10 mins as Cs^+ diffused into the soma, the FM depolarised from rest. Continuously applied-DC was used to maintain the resting potential at -66mV. In the hyperpolarising direction membrane voltage responses were similar to control. In the depolarising direction voltage responses to test current pulses were increased in amplitude. At threshold AP duration increased (2.1ms) and the fast ahp was suppressed. The DD appeared to increase in prominence while the slow ahp also showed a reduced amplitude.

C) When held closer to threshold (-61mV) the depolarising tail potentials seen after hyperpolarising voltage responses showed an increase in amplitude and duration. Larger hyperpolarising current steps led to AP generation on the rebound potential. Depolarising current pulses to threshold evoked AP's which were followed by a pronounced DD upon which a second AP could be evoked.

Fig. 3.16

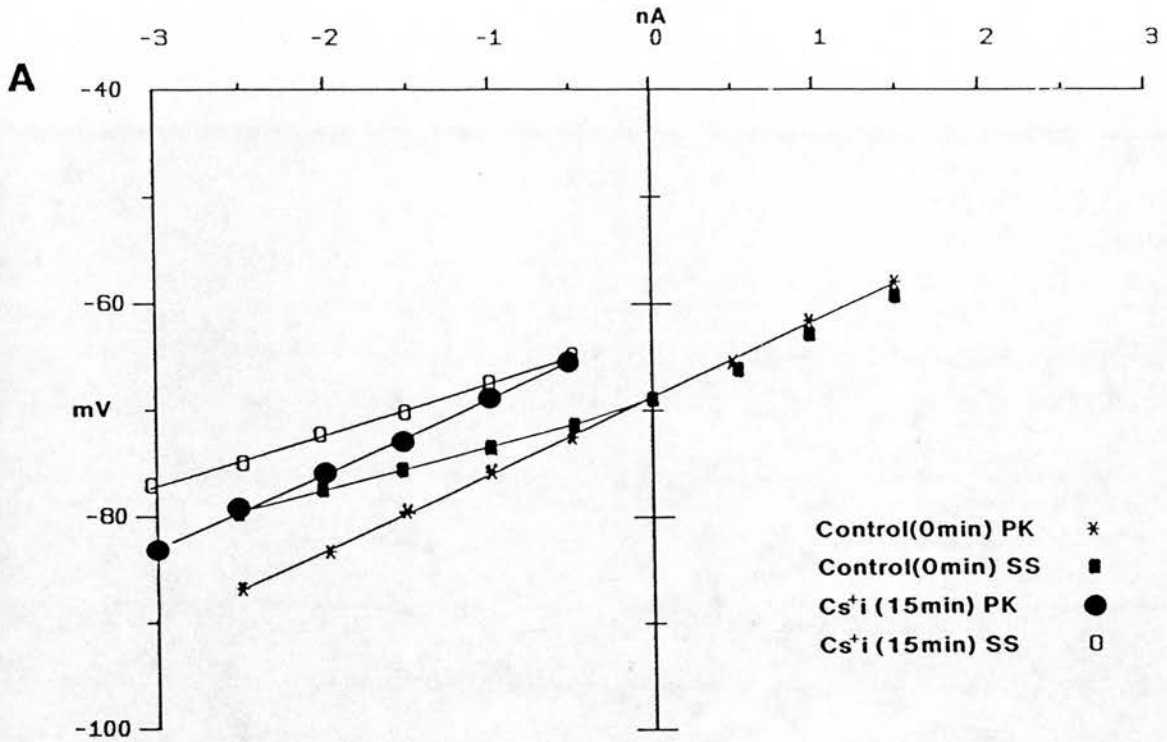
A
nA
-3
-2
-1
0
1
2
3
-40
-60
mV
-80
-100
Control(0min) PK
Control(0min) SS
Cs+i (15min) PK
Cs+i (15min) SS

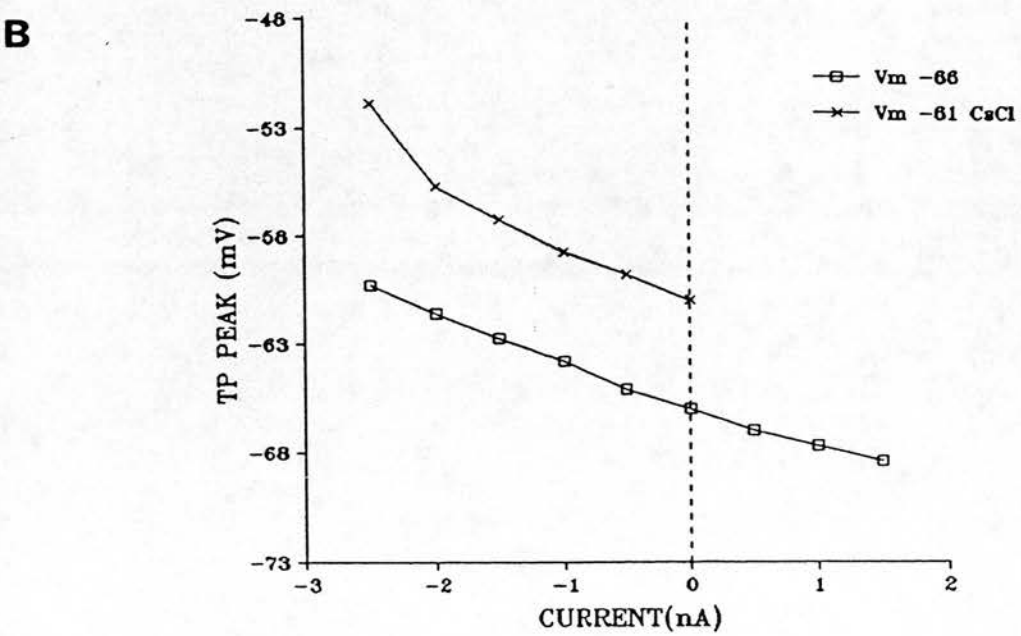
B
-48
-53
-58
-63
-68
-73
TP PEAK (mV)
-3
-2
-1
0
1
2
CURRENT(nA)
Vm -66
Vm -61 CsCl

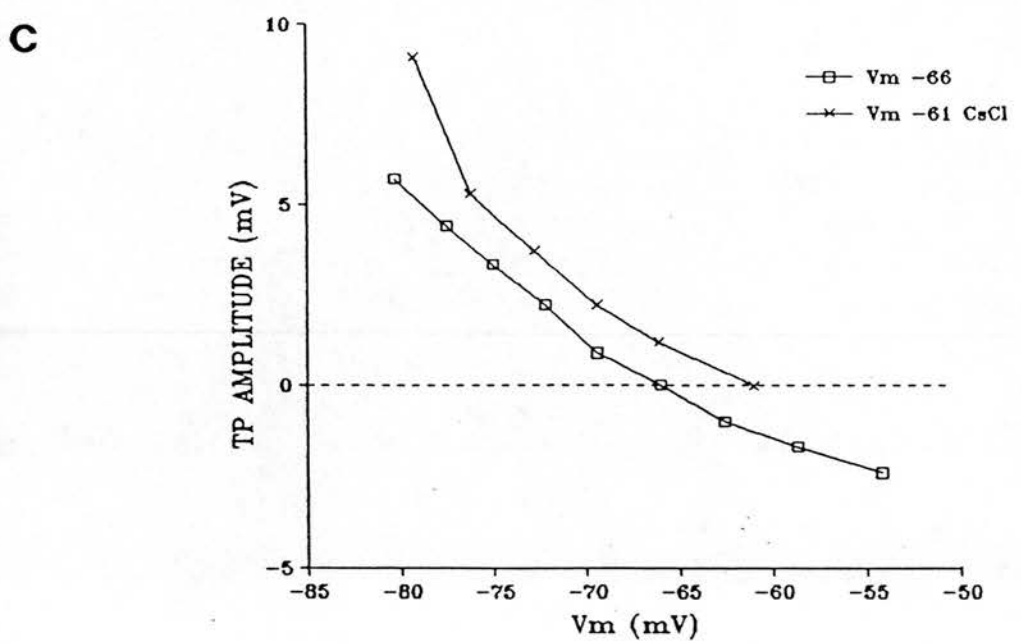
C
10
5
0
-5
TP AMPLITUDE (mV)
-85
-80
-75
-70
-65
-60
-55
-50
Vm (mV)
Vm -66
Vm -61 CsCl

Figure 3.16

Peak and steady-state voltage deflection I/V plots before and after Cs^+ loading of a FM

A) All plots were linear and despite Cs^+ loading and a small depolarisation from -66 to -61mV the slopes were essentially unaltered indicating that intracellular Cs^+ does not block the inward rectifier. Control $R_{m(pk)}$ and $R_{m(ss)}$ were 7.3 and 4.1MΩ compared to Cs^+ loaded values of 7.1 and 4.9MΩ respectively. The small increase in input resistance and depolarisation can be attributed to Cs^+ blockade of a resting "leak" K^+ conductance.

B) and C) Depolarising tail potential amplitude in Cs^+ loaded neurones. In B the peak amplitude of the tail potential is plotted against preceding current pulse amplitude while in C) absolute tail potential amplitude is plotted against the membrane potential achieved during the preceding voltage deflection. Note that even at holding potentials close to threshold (crosses) tail potential amplitude increased with an increasing slope suggesting that Cs^+ blocks outward currents which normally suppress the tail potential in this membrane potential range.

Fig. 3.17

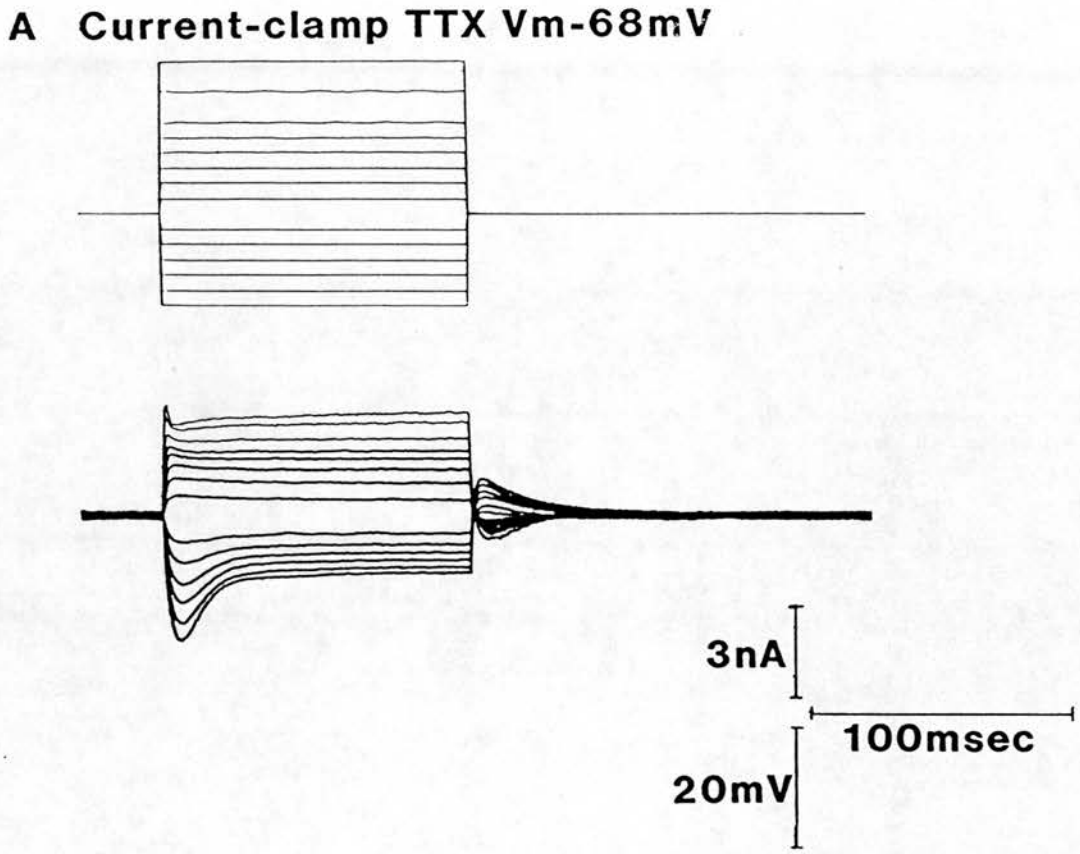
A Current-clamp TTX Vm-68mV
3nA
100msec
20mV
B Voltage-clamp TTX Vm-66mV
3nA
100msec
40mV

Figure. 3.17

The effects of TTX (1μM) on FM membrane voltage and current response
A) Current-clamp records showing that TTX does not affect the IR in the hyperpolarising direction or depolarising tail potentials from a FM resting at -68mV. In the depolarising direction, Na^+ dependent action potentials are blocked and marked outward rectification of voltage responses is observed.
B) Membrane currents (upper traces) evoked by voltage step command (lower traces) from the same neurone as in A, in the presence of TTX. The holding potential was -66mV and the slow inward current evoked by hyperpolarising voltage step commands was not affected by TTX. Depolarising voltage steps evoked progressively larger outward currents which showed an initial peak amplitude followed by a slow inward decay to a steady-state level. Steps greater than +20mV evoked a large time-dependent outward current which could not be adequately clamped (see voltage record).

Fig. 3.18

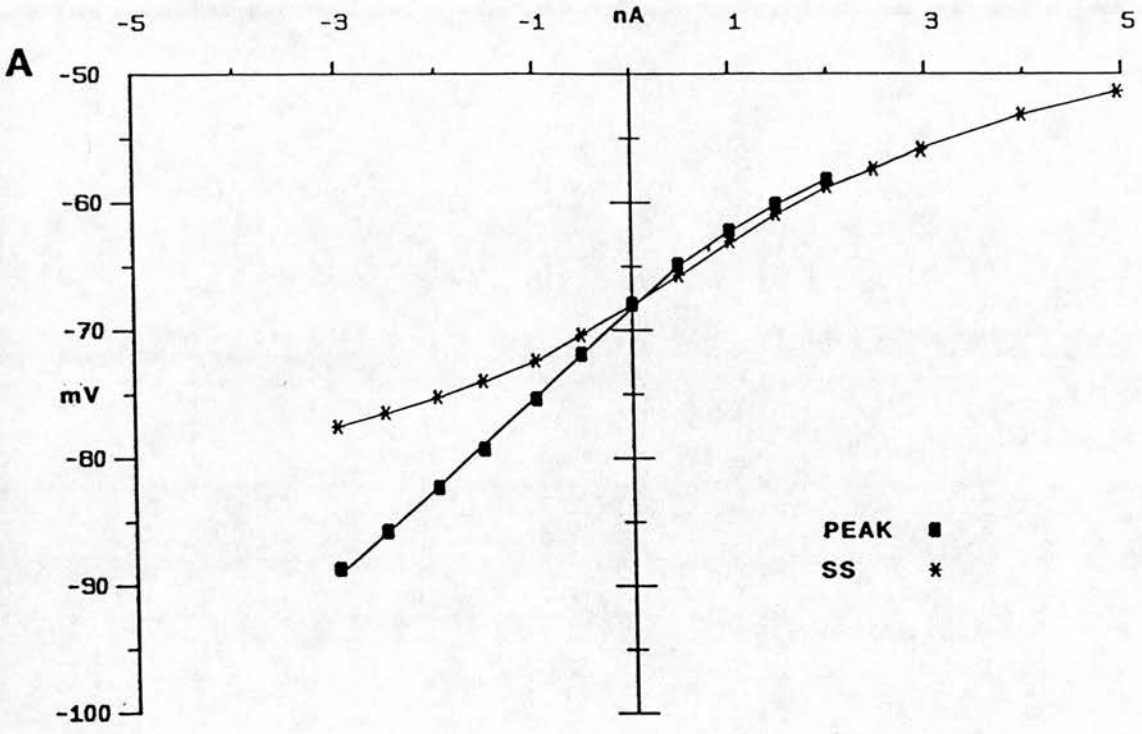
A
-5
-3
-1
nA
1
3
5
-50
-60
-70
mV
-80
-90
-100
PEAK
SS

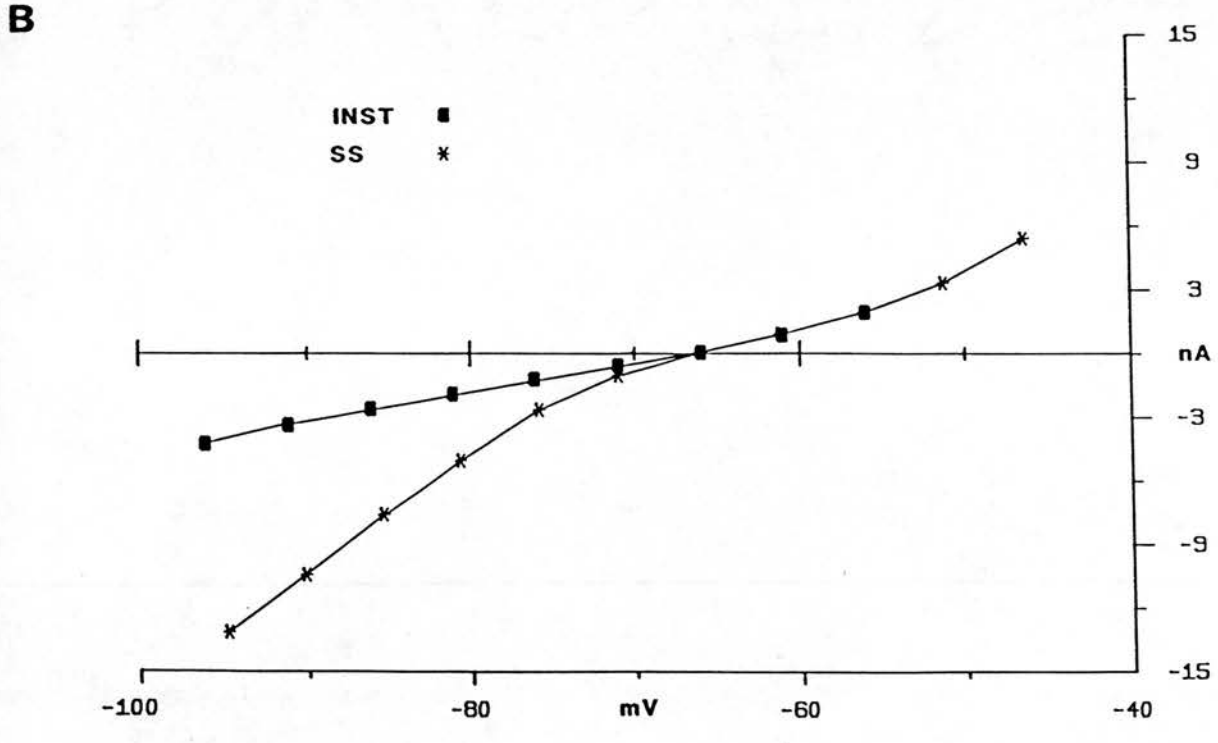
B
INST
SS
15
9
3
nA
-3
-9
-15
-100
-80
mV
-60
-40

Figure 3.18

Current-voltage plots in the presence of TTX obtained from the current and voltage clamp records of figure 3.17

A) In current clamp the peak deflection relationship (closed squares) is linear from rest (-68mV) to -90mV with a $R_{m(pk)}$ of 7MΩ. In the depolarising direction the plot displays outward rectification. The steady-state I/V plots (asterisks) shows non-linearity throughout the tested range rectifying inwardly in the hyperpolarising direction and outwardly in the depolarising direction.

B) The instantaneous current jump relationship (closed squares) was also linear giving a slope conductance of 134.9nS, while the steady-state I/V relationship (asterisks) showed non-linearity similar to that observed in current-clamp (A).

Fig. 3.19

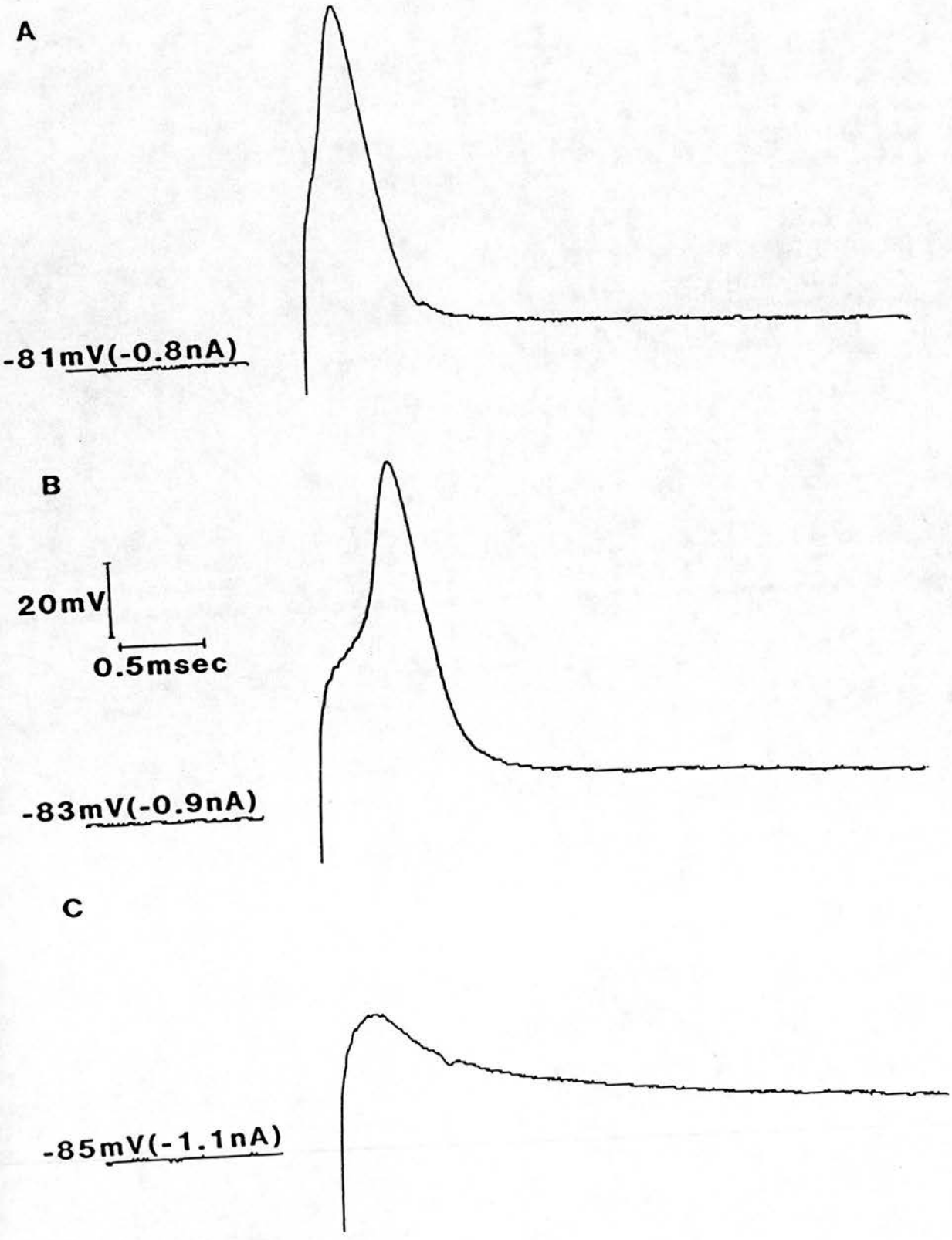

Figure 3.19

Antidromic activation of facial motoneurones (I)
A) The FM was resting at -76mV. Stimulation in the region of the ascending axon fibres with a bipolar simulating electrode evoked an action potential which was better separated from the stimulus artefact when the neurone was manually hyperpolarised to -81mV with -0.8nA DC. The gap in the trace prior to the action potential indicates where the stimulus artefact has been deleted for improved clarity. The soma-dendritic (SD) antidromic action potential had an amplitude of 96mV was followed by a delayed depolarisation and a slow ahp (not shown). On its rising phase a small inflection due to the initial segment (IS) component of the AP was observed.
B) Increasing hyperpolarisation of the membrane potential to -83mV markedly enhanced the inflection seen on the rising phase of the AP.
C) Further hyperpolarisation of the neurone (-85mV) led to failure of the AP to invade the soma leaving an IS component with an amplitude of 36mV.

Fig. 3.20

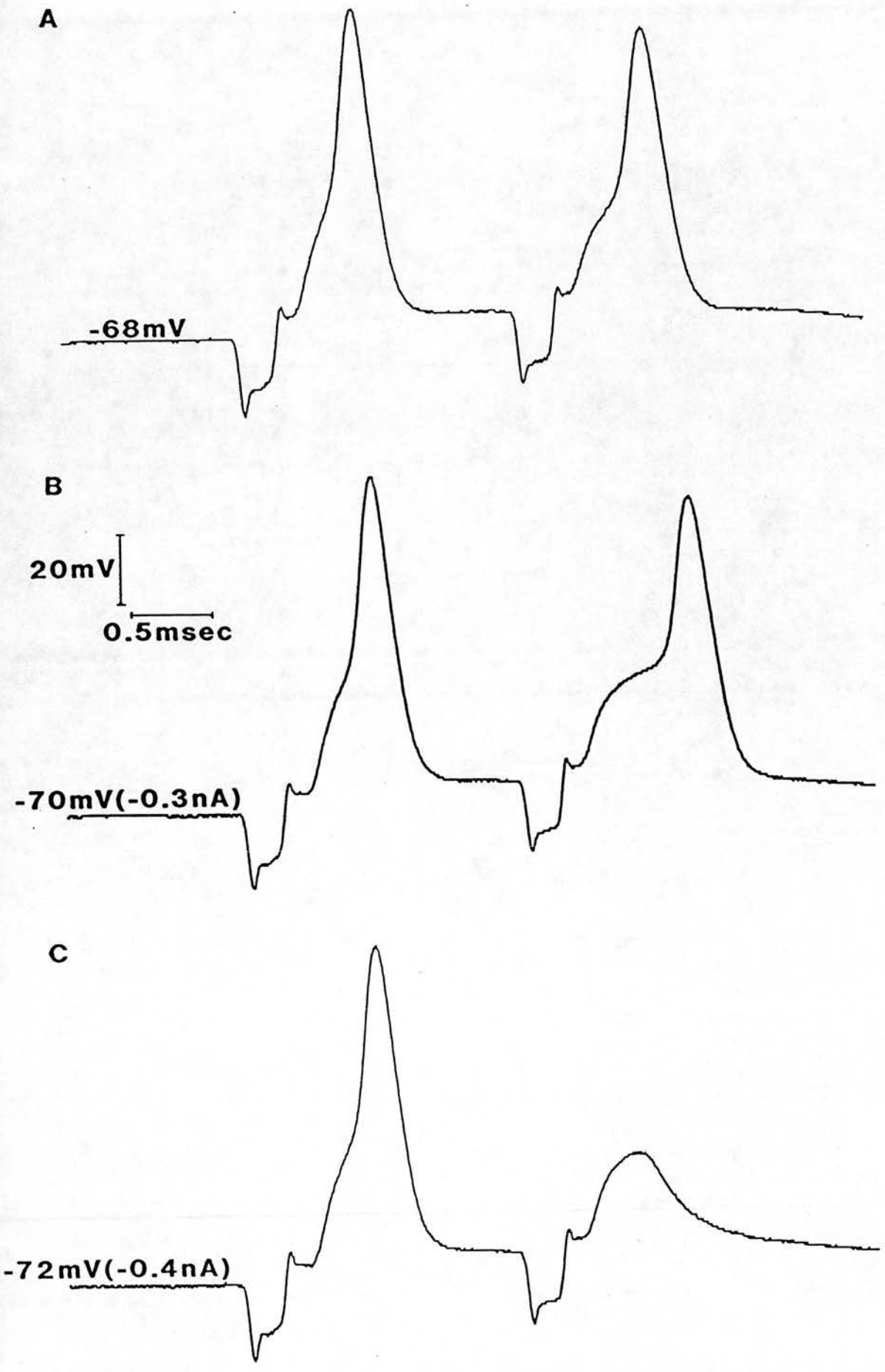

Figure 3.20

Antidromic activation of facial motoneurones (II)
A) The FM had a resting potential of -68mV. Double stimulation (stimulus interval 1.8ms) of the ascending axon fibres in the region dorsal to the FMN produces double antidromic activation.
B) and C) Hyperpolarisation of the membrane potential allows progressive dissociation of the IS and SD components eventually leading to complete blockade of the SD action potential. The artefact preceding the AP indicates a brief latency of 0.14ms between stimulus and antidromic invasion. The first antidromic SD action potential in A, had an amplitude of 94mV while the second was slightly smaller (90mV). The IS component in C had a peak amplitude of 39mV.

Fig. 3.21

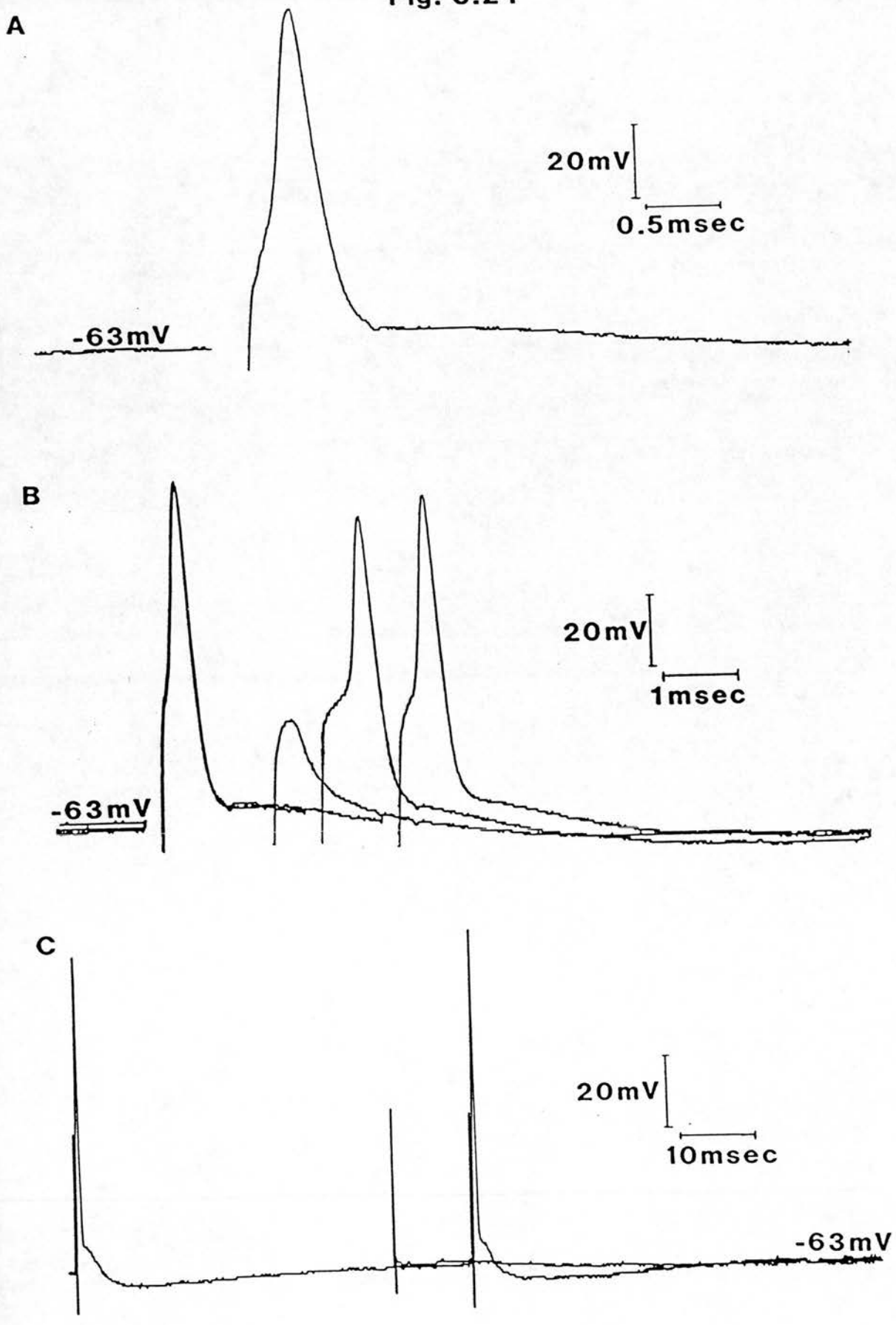

Figure 3.21

Antidromic activation of facial motoneurones (III)

A, B and C show antidromic activation of the same FM with a progressively longer time base.

A) A single antidromic action potential evoked from a resting potential of -63mV had a peak amplitude of 98mV. The stimulus artefact has been deleted for clarity but indicates little latency to antidromic activation.

B) Superimposed records from a double stimulus protocol showing differentiation of IS and SD components (3 and 2ms stimulus interval) followed by complete blockade of the SD component (1.4ms stimulus interval) of the antidromic action potential by refractoriness. A constant stimulus intensity was used in this procedure. Further narrowing of the interstimulus interval led to complete loss of the IS component (not shown).

C) Antidromic activation shown on a longer time base illustrates the delayed depolarisation (peak amplitude 7.3mV) and the ahp (peak amplitude -3.9mV) following the antidromic action potential. The stimulus artefact has been left on the trace to show that a second antidromic invasion cannot be evoked with the same stimulus intensity for 50ms following a successful invasion.

Fig. 3.22

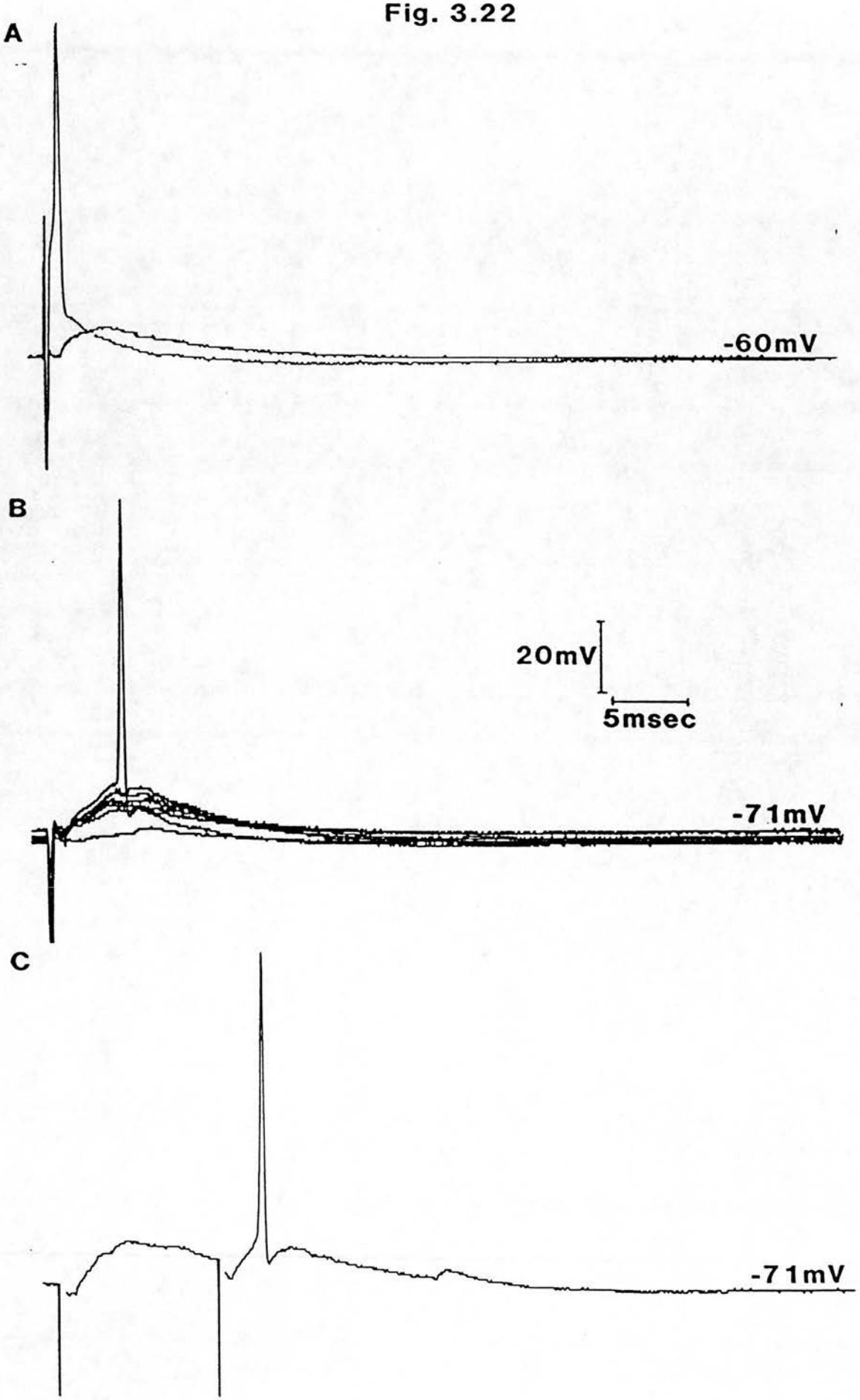

Figure 3.22

Synaptic potentials recorded from FM's

A) Superimposed records showing antidromic activation of a FM at a resting potential of -60mV. Stimuli sub-threshold for antidromic activation evoked a depolarising synaptic potential which arose after a delay of about 1msec and was about 35msec in duration.

B) In a different FM resting at -71mV depolarising synaptic potentials could be evoked in the absence of an antidromic action potential. Increasing stimulus intensity increased the amplitude of the depolarisation up to threshold where an orthodromic action potential with an amplitude of 94mV was evoked.

C) Addition of synaptic potentials indicating that a second normally sub-threshold stimulus could evoke an action potential when superimposed on the decaying phase of an earlier depolarising potential.

Fig. 3.23

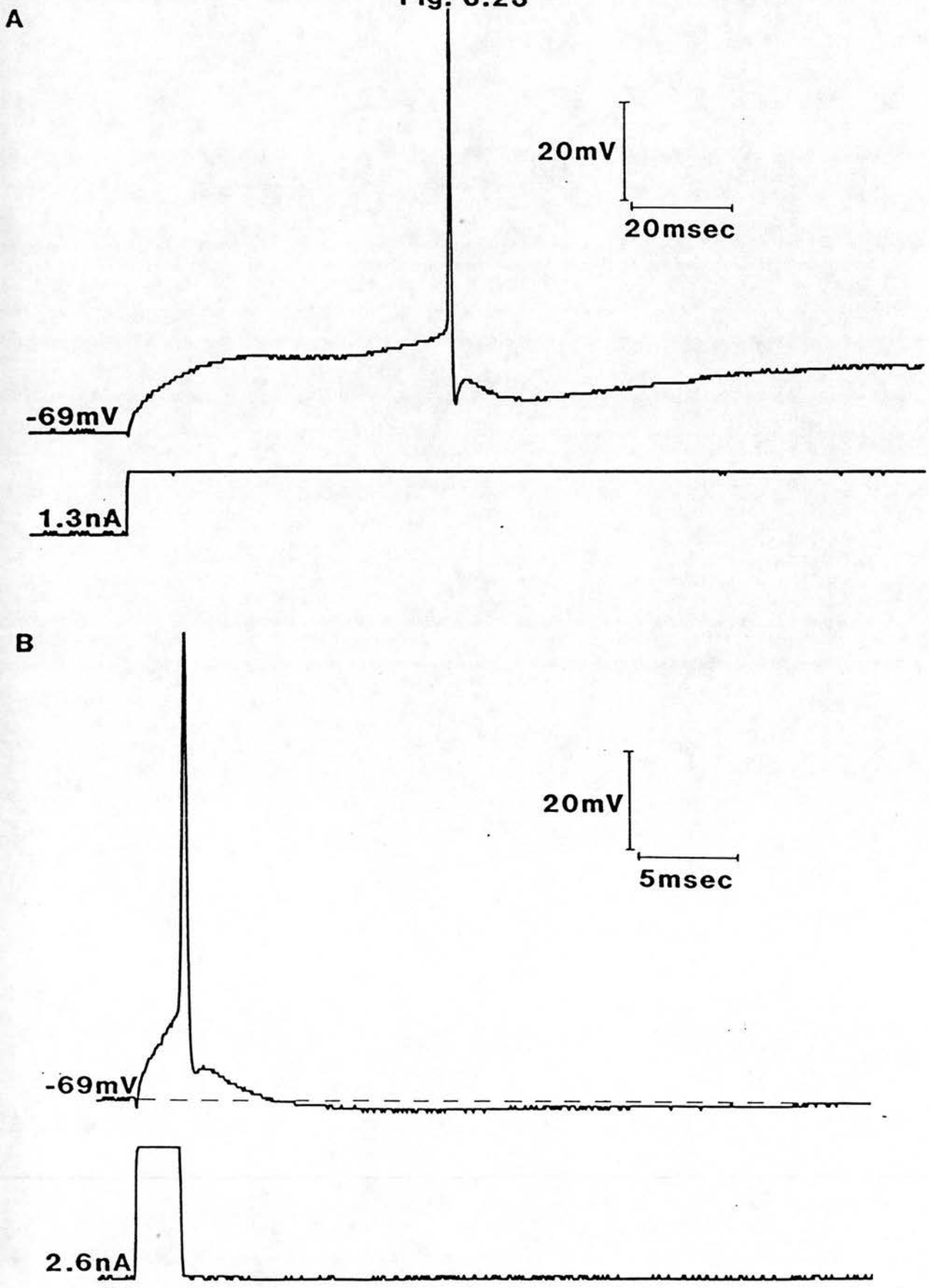

Figure 3.23

Directly evoked action potentials of facial motoneurones
A) An action potential evoked by a continuous depolarising current pulse of +1.3nA. It is followed by fast and slow ahp's separated by a delayed depolarisation. Action potential amplitude is 94mV from a resting potential of -69mV but is attenuated on this record. The threshold for AP activation is -51mV.
B) An action potential evoked by a brief depolarising current pulse of 2.6nA, 2msec from the same cell as in A. Action potential amplitude of 95mV is fully reproduced here. The fast ahp is identified as a brief notch which does not undershoot resting potential prior to the prominent DD. The slow ahp has a peak undershoot of -2.9mV and returns to resting potential after 46msec.

Fig. 3.24

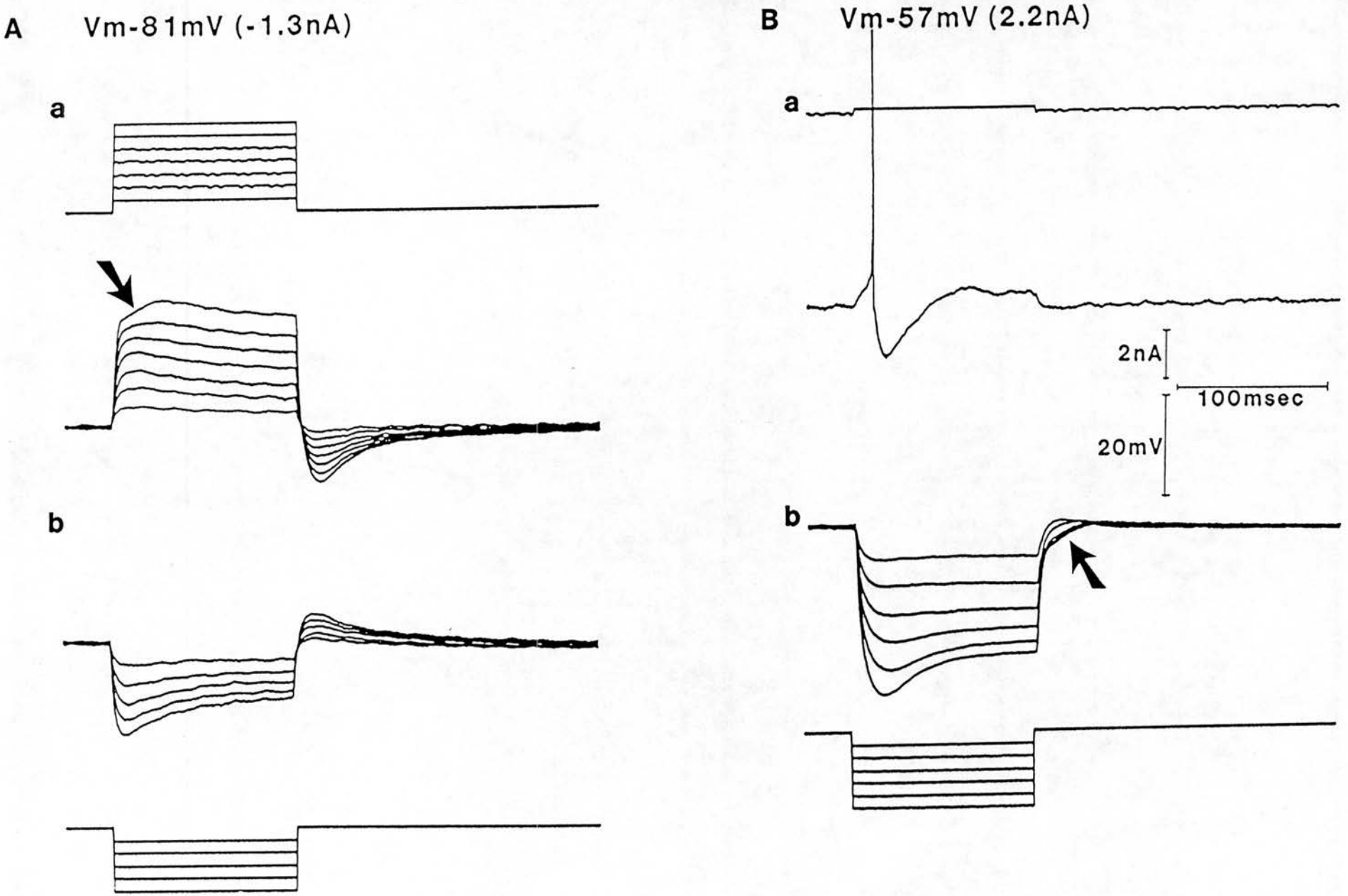

Figure 3.24

Observations on the latency to the first spike evoked by depolarising current pulses

Aa) The FM was held at -81mV with -1.3nA D.C. Small amplitude depolarisations showed an initial rapid voltage deflection which was followed by time-dependent sag. Current steps 3 and 3.5nA in amplitude evoked a depolarisating potential close to threshold which displayed two components. The largest part of the depolarisation was rapid whereas the second smaller component (arrowed) had a much slower time course and after a delay triggered the first spike (not shown). Ab) Hyperpolarising responses at -81mV were as described for other FM's. $R_{m(pk)}$ of this neurone was 7.5MΩ at -81mV.

Ba,b) The same neurone as in A this time held at -57mV with +2.2nA DC. A small depolarising current pulse evoked a single spike without any noticeable delay (Ba). Test hyperpolarising current steps evoked much greater voltage deflections due to the reduced activation of IR at this potential. $R_{m(pk)}$ was 11.3MΩ. Current pulses -0.5 and -1nA in amplitude evoked voltage responses which returned to resting potential in the manner previously described. Large amplitude hyperpolarisations showed a biphasic repolarisation of which the slow component (arrowed) was very similar to the slow depolarising component seen in (Aa).

Fig. 3.25

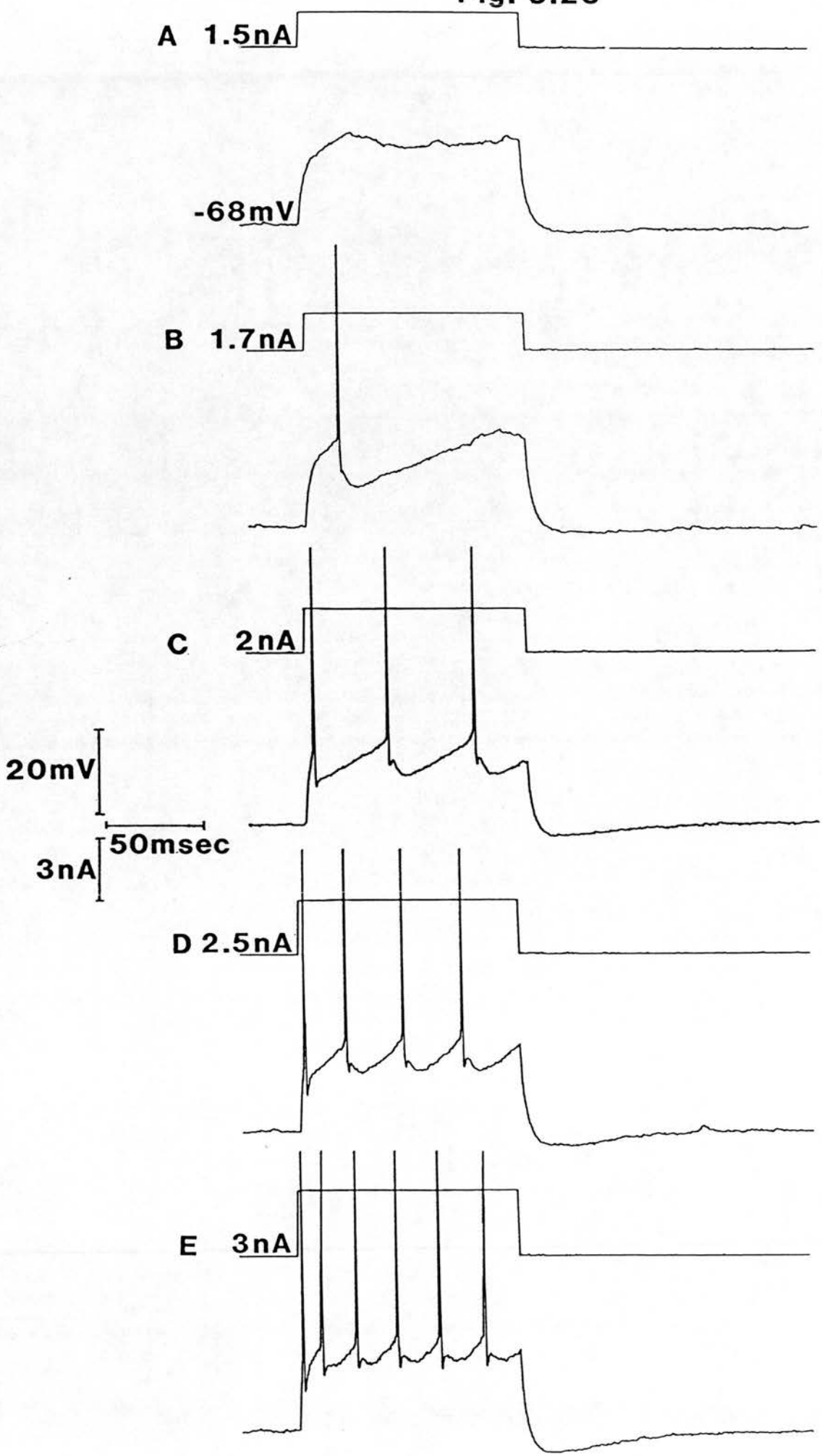

Figure 3.25

Firing response of a facial motoneurone
Increasing the amplitude of the depolarising current pulse leads to tonic repetitive firing of the FM.
A) Subthreshold response illustrating the biphasic depolarisation and AP prepotential. B) A single AP evoked with a short delay followed by a pronounced ahp. C) Increasing current amplitude leads to three AP's being evoked. The voltage trajectory between the first and second spike is steeper than between the second and third resulting in a shorter interval. Threshold for the second and third AP's is higher than for the first. D and E) Increasing the stimulus intensity further increased the number of evoked AP's. The time between AP's progressively increases over the first, second and third intervals thereafter remaining constant leading to tonic repetitive firing.

Fig. 3.26

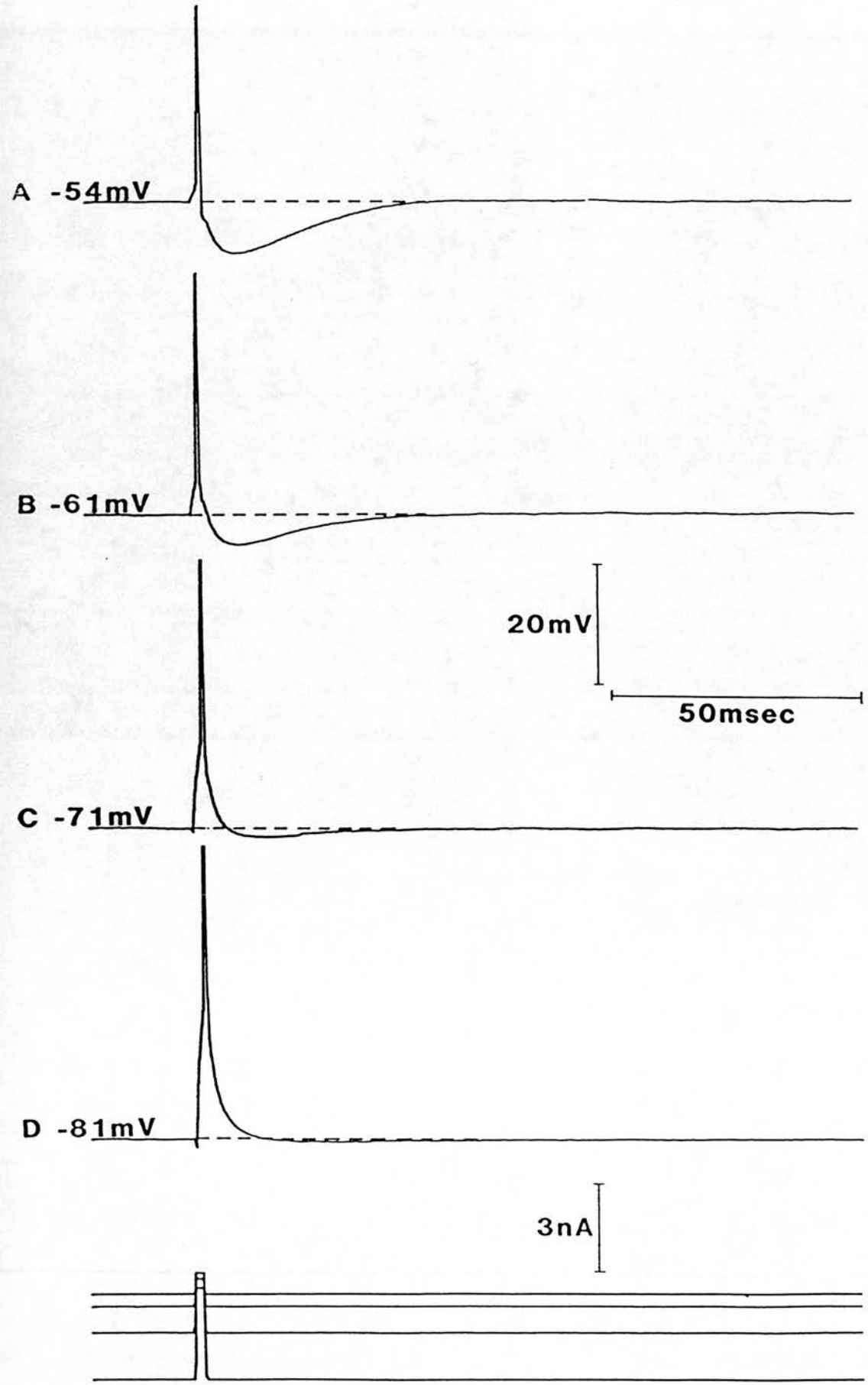

Figure 3.26

The effect of membrane potential hyperpolarisation on slow ahp amplitude

Averaged records of directly evoked spikes (current steps bottom trace) at different holding potentials. (AP amplitude is attenuated in all traces but regularly overshot by ~26mV). At -54mV (A) the ahp had a peak amplitude of -8.7mV and a duration of 48msec. Progressive hyperpolarisation to -61 (B), -71 (C) and -81mV (D) reduced ahp amplitude to -5.2, -1.4 and -0.4mV with durations of 60, 43 and 51msec. Note that the fast ahp only undershoots the holding potential at -54mV (A).

Fig. 3.27

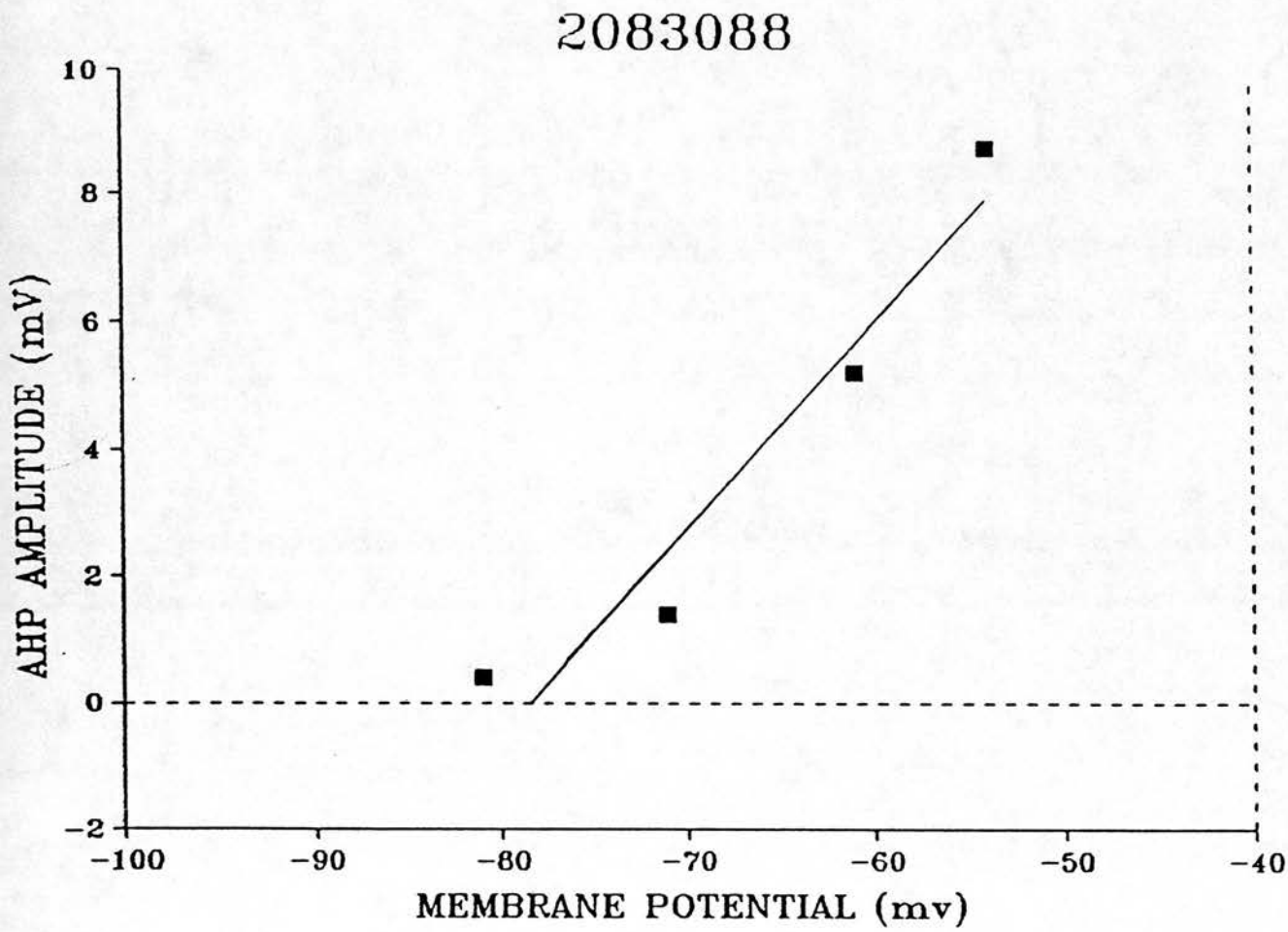
2083088
10
8
6
4
2
0
-2
AHP AMPLITUDE (mV)
-100
-90
-80
-70
-60
-50
-40
MEMBRANE POTENTIAL (mv)

Figure 3.27

Estimate of the reversal potential of the slow ahp
Linear regression on the plot of ahp amplitude against membrane potential for the neurone in Fig. 3.28 gives an apparent reversal potential of -79mV for the ahp ($y = 25.3 + 0.32X$; $r = -0.971$).

Fig. 3.28

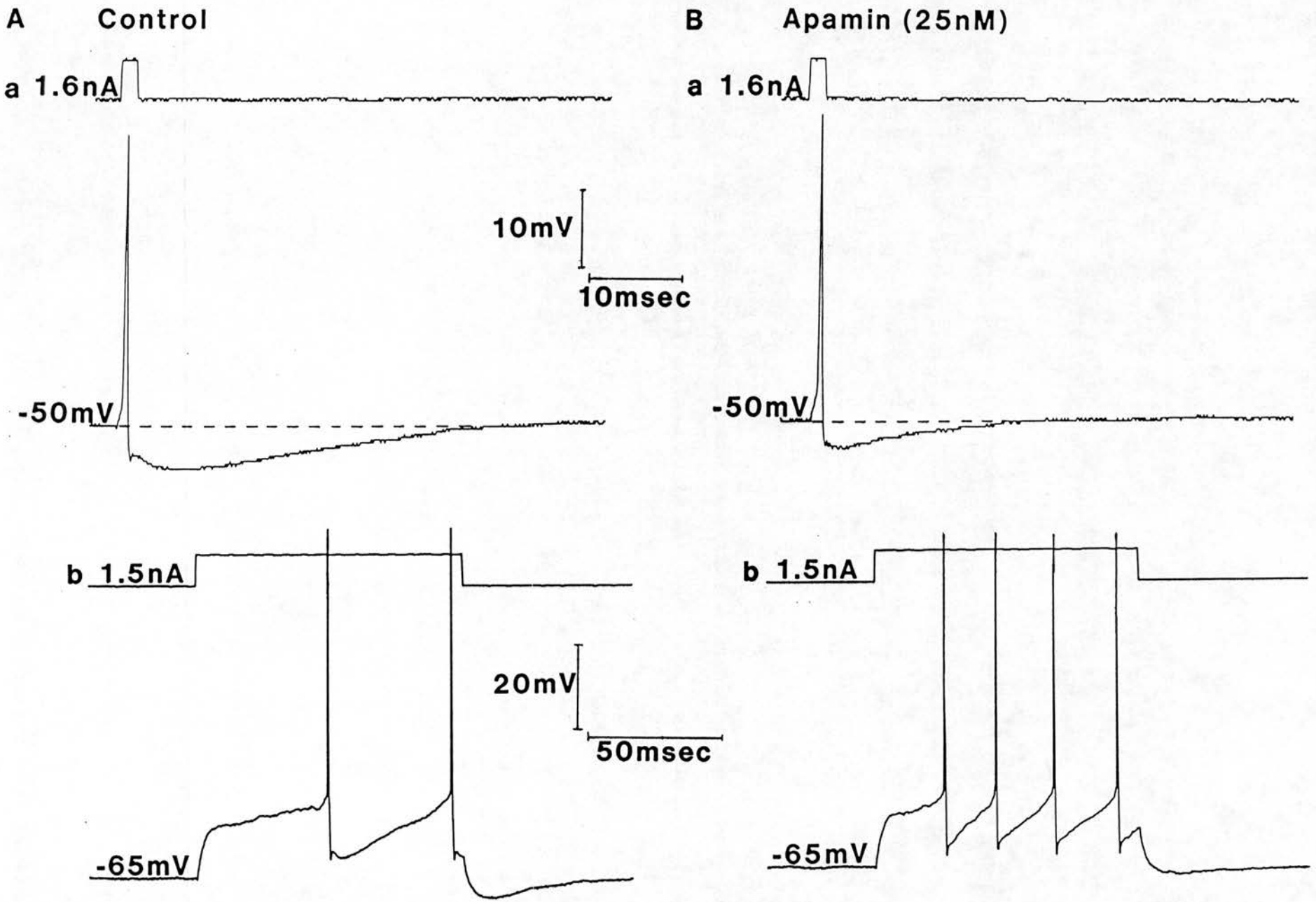
A Control
B Apamin (25nM)
a 1.6nA
a 1.6nA
10mV
10msec
-50mV
-50mV
b 1.5nA
b 1.5nA
20mV
50msec
-65mV
-65mV

Figure 3.28

The effects of Apamin on the ahp of facial motoneurones

Aa) An action potential evoked at -50mV by a +1.6nA, 2msec current pulse had an amplitude of 73mV and was followed by an ahp of -11.8mV and lasting 50msec.

Ab) A depolarising current pulse of +1.5nA, 100msec evoked two action potentials from a resting potential of -65mV. The AP's were separated by a pronounced ahp. $R_{m(pk)}$ was 10.6MΩ (not shown).

Ba) Superfusion of Apamin (25nM) for 30 mins reduced the amplitude of the ahp at -50mV to -7.7mV and also its duration to 21msec. AP amplitude was unchanged (78mV).

Bb) Apamin did not affect the resting potential or $R_{m(pk)}$ (-65mV; 10.1MΩ) however a +1.5nA current pulse now evoked four AP's with reduced intervals and steeply rising trajectories between them. The amplitude of the fast ahp appeared unaffected.

CHAPTER 4 DISCUSSION

Characterisation of the facial motoneurone

Characterisation of the facial motoneurone (FM)

Intracellular recordings from rat FM's *in vitro* demonstrated a characteristic profile of passive and active membrane properties which indicated a relatively homogeneous population of neurones throughout the FMN. Morphological studies in the rat and cat have suggested that the FMN contains few if any interneurones (Courville, 1966; McCall and Aghajanian, 1979a). In the cat recordings from neurones in which an antidromic spike could not be elicited by stimulation of the facial nerve have been made (Fanardjian et al, 1983b) but the frequency of these observations was not stated and thus difficult to compare with previous morphological data.

Values of peak input resistance for FM's *in vitro* are more than two fold greater than those measured *in vivo* in the rat and cat (VanderMaelen and Aghajanian, 1982; Fanardjian et al, 1983b). Higher input resistances appear to be a characteristic of *in vitro* slice preparations and have been attributed to a number of different factors. Reduced cell membrane damage due to finer electrode tips and subsequent improved "sealing" of membrane around the electrode have both been suggested. Additionally input resistance is related to soma size and the extent of dendritic branching. Facial motoneurones in the rat have been shown to have soma dimensions of on average 20 x 36μM in their shortest and longest diameters, with 5 to 11 primary dendrites (Friauf, 1986). Similar values were seen with HRP labelling in this study. Moreover, dendritic branching is extensive and can continue for up to 600μm. These values suggest that significant dendritic damage must take place in a coronal slice 350μm thick. This amputation of dendrites may also contribute to an increase in input resistance. Finally replacement of the normal

extracellular environment with an artificial medium and the severing of synaptic connections is also likely to play a part in altering cell input resistance.

The values we have obtained compare well with the values obtained for rat ocular and hypoglossal motoneurones by intrasomatic recordings (Gueritaud, 1988; Mosfeldt-Laursen and Rekling, 1989) in vitro, but are much lower than those of rat and guinea-pig vagal motoneurones which have considerably less dendritic branching and smaller cell bodies (Yarom et al, 1985; Fukuda et al, 1987). By day 9-11 in the neonatal rat spinal cord in vitro, lumbar motoneurones had lower input resistances than those of adult FM's even when measured at 20-22°C (Fulton and Walton, 1986). Presumably soma growth and dendritic expansion will lead to lower input resistances of rat spinal motoneurones in the adult. Consistent with differences in cell size and factors mentioned previously values of input resistance for adult cat spinal motoneurones in vivo are much lower than those measured here (Coombs et al, 1959; Ito and Oshima, 1965; Burke and Ten Bruggencate, 1971; Barrett and Crill, 1974). Similarly frog motoneurones at room temperature and below, both in situ (Magherini et al, 1976) and in vitro (Kubota and Brookhart, 1963) have lower input resistances than FM's. Interestingly despite being on average larger than FM's, motoneurones in the turtle spinal cord in vitro have greater input resistances (Hounsgaard, Kiehn and Mintz, 1988). The linearity of current voltage relations in FM's over a wide voltage range above and below resting potential contrasts with that seen in cat motoneurones by Ito and Oshima, (1965) although Barrett and Crill (1974) did show linearity between resting potential and threshold. Similar observations have been made in frog spinal

motoneurones (Magherini et al, 1976), whereas recent observations from rat ocular motoneurones in vitro have shown linearity over a narrower range (Gueritaud, 1988).

The time constants for membrane charging, despite higher cell input resistances, are comparable with those obtained from neonatal rat spinal motoneurones, adult rat ocular-motoneurones and adult cat spinal motoneurones (Coombs et al, 1959; Barrett and Crill, 1974; Fulton and Walton, 1986; Gueritaud, 1988) but are considerably less than those observed in frog and turtle spinal motoneurones (Magherini et al, 1976; Hounsgaard et al, 1988).

As described earlier FM's show a prominent time-dependent sag in membrane potential when a hyperpolarising current pulse is applied. Inward or "anomalous" rectification has been used to describe this decrease in membrane resistance recorded using current-clamp methods. In FM's, hyperpolarising step voltage commands elicit a slowly developing inward current which has a time course and voltage range similar to the sag seen in current clamp records. This suggests that this current underlies inward rectification (IR) in FM's.

IR activated by hyperpolarisation has been described in detail in both peripheral and central neurones as well as muscle and marine egg cells. Two different mechanisms have been identified. The first is mediated by K^+ ions and has a voltage range of activation dependent on the difference between the membrane potential and the potassium equilibrium potential. The second is a mixed Na^+/K^+ current which shows increased conductance in high $[K^+]_o$ but no shift in its activation curve. Both are blocked by extracellular Cs^+ but can be distinguished by the formers selective block with Ba^{++} and its rapid activation kinetics (Constanti and Galvan (1983) had to

reduce the temperature of their preparation to 23°C so that IR activation could be separated from the capacitative transient at the onset of voltage step commands). This Ba^{++} sensitive IR has been studied in frog skeletal muscle cells (Hestrin, 1981) starfish egg cells (Hagiwara et al, 1976) and neurones of the olfactory cortex (Constanti and Galvan, 1983). Inward rectifiers with similar properties appear to be modulated by Substance P and 5-HT leading to central neuronal depolarisation (Stanfield et al, 1985; North and Uchimura, 1989).

Non-linearity of the peak I/V plot at potentials more negative than -90mV seen in FM's may be a consequence of this form of inward rectification. The activation threshold for this current in olfactory cortex neurones was -100mV (Constanti and Galvan, 1983). One of the actions of Cs^{+} on FM's in vitro, seen in voltage clamp, was a linearising of the peak current-voltage relation at potentials more negative that -100mV. However, such rectification may also be explained by the increased activation of the time dependent IR seen in FM's at more hyperpolarised potentials. The effects of Ba^{++} in this region of the peak I/V curve may help to resolve this question.

The second slower Ba^{++} insensitive IR has been described in hippocampal pyramidal cells where it is termed Iq, (Halliwell and Adams, 1982), cerebellar Purkinje cells, I_h (Crepel and Penit-Soria, 1986), Betz cells of the somatosensory cortex (Spain et al, 1987), cultured sensory ganglion neurones, I_h, (Mayer and Westbrook, 1983) as well as cardiac Purkinje fibres, I_f, (DiFrancesco, 1981) and in the sino-atrial node (Brown and DiFrancesco, 1980). The time dependent responses observed in FM's have similarities to this second form of IR. The mixed Na^{+}/K^{+} permeability of the IR gives a reversal potential positive to the resting potential. For sensory

ganglion neurones and Betz cells values of -50mV and -34mV respectively were obtained (Spain et al, 1987; Mayer and Westbrook, 1983). The values obtained from FM's are also positive to the resting potential in agreement with these other studies. However, the involvement of Cl^- ions in IR of FM's cannot be excluded especially considering the use of KCl filled microelectrodes, which would be expected to move E_{Cl^-} to this same region of membrane potential. Impermeable anion substitutes did block IR in sensory ganglion neurones but this was suggested to be a non-specific action (Mayer and Westbrook, 1983). More decisively in cortical Betz neurones the reversal potential for IR was unaffected by the use of KCl or $K_2CH_3SO_4$ filled microelectrodes while the fast Cl^- mediated GABA responses changed from depolarising to hyperpolarising respectively.

Sag in hyperpolarising voltage responses first appears at around -70mV in cultured sensory ganglion neurones (Mayer and Westbrook, 1983) and similar observations were made in FM's. Detailed voltage clamp investigations have shown an activation range of between -55mV and -120mV in a variety of neuronal types with half maximal activation at around -80mV (Mayer and Westbrook, 1983; Spain et al, 1987; Bobker and Williams, 1989). This indicates that the inward rectifier plays an active role in determining the resting potential of these neurones. The divergence of peak and steady-state current-voltage plots with only small hyperpolarising current pulses indicates that this is also likely to be the case in FM's. When held at hyperpolarised potentials sensory ganglion neurones showed outward current relaxations in response to depolarising voltage commands. This was attributed to the time dependent closure of IR channels. Voltage sag in response to

depolarising current steps seen in some FM's at rest and especially when held at hyperpolarised potentials is likely to be a manifestation of this deactivation of IR channels, further supporting a role for IR at rest. A similar phenomenon seen in hypoglossal motoneurones in vitro is blocked by extracellular Cs^+ reinforcing the view that this sag is mediated by the closure of IR channels at these potentials. In contrast the IR mediated by Iq in hippocampal pyramidal cells appears not to be active at resting potential. It has a more negative activation range with a threshold at -80mV and half maximal activation at -95mV (Halliwell and Adams, 1982).

This form of inward rectification has been distinguished from that mediated by M-current inactivation on two counts. Primarily M-current evoked hyperpolarising inward rectification is associated with decreased conductance whereas comparison of instantaneous currents at the beginning and the end of a voltage step in sensory ganglion neurones, Betz cells and cerebellar Purkinje cells as well as FM's in this and two other recent studies show IR to be associated with an increase in conductance (Mayer and Westbrook, 1983; Spain et al, 1987; Crepel and Penit-Soria, 1986; Nishimura et al, 1989; Aghajanian and Rasmussen, 1989). Secondly, voltage sag or inward current, if due to M-current relaxation, would be lost with increasing hyperpolarisation of the membrane potential due to its more positive range of activation. This is clearly not the case in FM's or any of the previously mentioned cell types.

The onset of IR in voltage-clamp could be approximated to a single exponential in hippocampal pyramidal cells and cerebellar Purkinje neurones but was more complex in Betz cells and sensory ganglion neurones (Halliwell and Adams, 1982; Crepel and Penit-

Soria, 1986; Spain et al, 1987; Mayer and Westbrook, 1983). In all cells though onset became faster with increasing hyperpolarisation similar to that seen in FM's.

The reduction of both instantaneous and steady-state current amplitude by extracellular Cs^+ in FM's is consistent with its actions on other inward rectifiers. Some voltage dependence of this action has been demonstrated in sensory ganglion neurones, Betz cells and cerebellar Purkinje cells, being greater at potentials more negative than -80mV. In Purkinje cells the explanation for this may be that at more positive potentials than -80mV a tonically active Ca^{++} dependent K current, which inactivates on hyperpolarisation, contributes to the observed IR but is less sensitive to Cs^+ than I_h (Crepel and Penit-Soria, 1986). Cs^+ block was also shown to be dose-dependent which may explain the incomplete block seen in FM's. However, as suggested by Spain et al (1987) the block by a single ion suggests that it is a single channel with mixed ionic permeability which mediates IR. Consistent with other studies (Mayer and Westbrook, 1983; Spain et al, 1987) intracellular Cs^+ loading of FM's failed to block inward rectification.

The presence of time-dependent IR was described in cat spinal motoneurones by Ito and Oshima (1965) and subsequently studied by Nelson and Frank (1967). In fact prior to this Coombs et al (1955; 1959) had observed that values of cell input resistance were lower if measured after several seconds of current injection than when using short (15-20msec) current pulses. In these studies linearity of steady-state current voltage plots varied considerably between cells and often calculated slope resistances were different in the hyperpolarising and depolarising directions, similar to observations

made in FM's. Studies of IR in FM's in vivo have not been made though its presence has been referred to (VanderMaelen and Aghajanian, 1982). Barrett et al (1980) showed inward rectification in voltage clamped cat motoneurones in response to hyperpolarising steps, to be due to a slowly developing inward current reversing near the resting potential which in these cells was relatively depolarised probably due to impalement damage. Prominent IR has been recorded in rat ocular motoneurones (Gueritaud, 1988) rat hypoglossal motoneurones (Mosfeldt-Laursen and Rekling, 1989) and turtle spinal motoneurones (Hounsgaard et al, 1988) in vitro where the steady-state current voltage relation linearity is often affected. The presence of IR was not observed in neonatal rat spinal motoneurones or in cultured embryonic rat and chick motoneurones (Fulton and Walton, 1986; O'Brien and Fischbach, 1986; Fruns et al, 1987). Thus there appears to be a developmental difference supported by the observation that cells in rat dorsal root ganglia develop IR concurrent with axonal myelination during early neonatal development (Fulton, 1987).

Depolarising IR appears to be mediated by a different mechanism to that seen in the hyperpolarising direction. The presence of TTX in the aCSF seemed to reduce this phenomenon suggesting that it may be mediated by a Na^+ conductance. Recently guinea-pig FM's in vitro have been shown to display TTX sensitive depolarising IR responses (Nishimura et al, 1989). A slow persistent Na^+ conductance mediates this response and has similarities to those seen in cortical neurones (Stafstrom et al, 1985) and other central neurones (See Llinas, 1988). Depolarising IR has also been shown to be mediated by a low threshold Ca^{++} current which acts either directly or indirectly through interactions with Ca^{++} sensitive

conductances. Such conductances have been identified in cat and turtle spinal motoneurones (Barrett et al, 1980; Hounsgaard et al, 1988) and also recently in guinea-pig hypoglossal motoneurones (Mosfeldt-Laursen and Rekling, 1989) where they appear to underlie plateau potentials responsible for biphasic firing patterns seen in these neurones (Hounsgaard et al, 1986, 1988, 1989).

Depolarising rebound tail potentials occurring after hyperpolarising current steps at negative membrane potentials show a stimulus dependency which appears to be more directly related to the amount of sag seen in the previous voltage response. In addition the time to peak and time course reflects the sag seen in a depolarising voltage response to an inward current pulse. These facts suggest that the mechanism underlying these potentials is time dependent inactivation of IR channels. In voltage clamp a slowly relaxing inward tail current at the end of a hyperpolarising voltage step appears to mediate these potentials. In conditions where the IR is blocked by extracellular Cs^{+} the amplitude of the tail potentials is also suppressed. End of current pulse resting potential overshoots were also observed in cat motoneurones (Ito and Oshima, 1965) rat ocular motoneurones (Gueritaud, 1988) guinea-pig hypoglossal motoneurones (Mosfeldt-Laursen and Rekling, 1989) sensory ganglion neurones (Mayer and Westbrook, 1983) and cortical Betz neurones (Spain et al, 1987) but not in olfactory cortex neurones which display Ba^{++} sensitive IR (Constanti and Galvan, 1983). In hypoglossal motoneurones <u>in vitro</u>, the development of depolarising tail potentials was related to the duration of the preceding hyperpolarising pulse. Maximum amplitude of the tail

potential was only reached when the sag in the hyperpolarising voltage response had reached a steady-state (Mosfeldt-Laursen and Rekling, 1989).

Hyperpolarising tail potentials after sub-threshold depolarising voltage responses may also be explained in this way only it is IR activation, not inactivation, which is responsible. Threshold for IR activation lies in the range between rest and threshold for AP firing. Thus a maximum amplitude for the hyperpolarising tail potential is obtained which cannot be increased by further increasing the amplitude of the preceding depolarising electrotonic potential.

When FM's were held at more positive potentials close to threshold for AP's, depolarising tail potentials were suppressed or even lost altogether even though sag was present in the preceding voltage response. While such a reduction in amplitude would be expected as the holding potential approaches the reversal potential for IR it was clear that tail potentials were lost before this reversal level was reached. The observation that rebound depolarisations were more prominent in Cs^+ loaded cells suggests that under normal conditions a Cs^+ sensitive current or currents may oppose the tail potentials in this region of membrane potential. Such events are discussed later in relation to the delay seen before the first AP evoked by prolonged current pulses. It is clear though from figure 3.24 that in some cells it is the preceding amplitude of the hyperpolarisation which is essential for the development of these opposing outward currents seen on repolarisation at the end of the current pulse. In this respect

such potentials are similar to those mediated by the A-current (Connor and Stevens, 1971) which requires a preceding hyperpolarisation to allow for its deinactivation.

Action potentials evoked by pulses of constant depolarising current into the FM soma show a sequence of afterpotentials similar to those observed in adult rat, cat and frog motoneurones (Coombs et al, 1955; Granit et al, 1963; Barrett and Barrett, 1976). The action potential is of short duration and overshoots zero potential indicating a somatic location for the recording electrode. The amplitude of this overshoot varies and while it may be overestimated by the continued presence of depolarising current, action potentials evoked by very brief current pulses, which end before the action potential reaches a peak, also overshoot. The action potential is blocked by TTX inferring similarity to the Na^+ dependent inward current described in cat motoneurones (Barrett and Crill, 1980) and so far seen in all mammalian central neurones (Crill and Schwindt, 1983).

The action potential is followed by a fast and a slow ahp and a delayed depolarisation (DD). The peak amplitude of the fast and slow ahp's was strongly dependent on the resting potential. As described earlier the fast ahp was only clearly seen when cells were held at potentials depolarised to rest. Often, at resting potential, the fast ahp was not clearly observed. In cat, frog and neonatal rat spinal motoneurones the repolarising phase of the action potential is contributed to by an increase in a voltage dependent K^+ conductance which is said to be responsible for the fast ahp observed in these cells (Barrett and Barrett, 1976; Magherini et al, 1976; Barrett et al, 1980; Walton and Fulton, 1986). In common with these neurones, the fast ahp was shown to be

potassium ion mediated in FM's by its blockade in Cs^+ loaded cells. This was accompanied by a widening of the AP indicating that as in other neurones outward K^+ conductances are important in AP repolarisation.

The slow ahp seen in FM's peaks later, is of longer duration and can be equated to the medium duration ahp's seen in other central neurones (Llinas, 1988). Progressive hyperpolarisation of the membrane potential showed the slow ahp to gradually decrease in amplitude to a point at which it was nullified at about -80mV. The use of KCl filled electrodes excludes a Cl^- mediated event leaving the implication that K^+ is the mediating ion, however the apparent reversal potential is more positive than that predicted by the Nernst equation. This may be due to contamination of the slow ahp by the increased prominence of the DD at hyperpolarised levels. Alternatively increased activation of IR at these potentials may also occlude the slow ahp thus altering the predicted reversal level. An interaction between IR and post repetitive firing ahp's has been described in cortical Betz cells (Schwindt et al, 1988) and similar interactions have recently been described in guinea-pig FM's (Nishimura et al, 1989). Such an interaction with ahp's following single spikes is less clear and may only be important in the decaying phase of the ahp as IR slowly activates. This may explain the apparent reduction in duration of the slow ahp at hyperpolarised potentials. The duration of the slow ahp is comparable to those of adult rat spinal (Bradley and Somjen, 1961) ocular (Gueritaud, 1988) and hypoglossal (Mosfeldt-Laursen and Rekling, 1989) motoneurones *in vitro* and facial motoneurones *in vivo* (Fanardjian et al, 1983a) but shorter than those of neonatal rat spinal motoneurones *in vitro* (Fulton and Walton, 1986). Interestingly, the slow ahp observed in

cultured embryonic rat motoneurones is also of equivalent duration though they were not always observed and the temperature at which recordings were made was not given (Fruns et al, 1987), while the slow ahp in cultured embryonic chick motoneurones at 24°C was longer (O'Brien and Fischbach, 1986). Frog spinal motoneurones in situ have similar duration ahp's (Magherini et al, 1976) while in vitro they appear to be longer (Barrett and Barrett, 1976). Cat spinal motoneurones have longer slow ahp's than detailed here (Bradley and Somjen, 1961) as do turtle spinal motoneurones in vitro (Hounsgaard et al, 1988). Despite this variation the underlying current appears to be outward and calcium dependent to some extent (Barrett and Barrett, 1976; Barrett et al, 1980; Walton and Fulton, 1986; O'Brien and Fischbach, 1986; Hounsgaard et al, 1988). The sensitivity of the slow ahp of FM's to intracellular Cs^+ was not clear. While slow ahp amplitude was reduced it was not fully abolished even after prolonged impalement. A similar phenomenon has been observed in hypoglossal and neonatal rat spinal motoneurones where it is suggested that the slow ahp is insensitive to intracellular Cs^+ and that the reduction in amplitude is due to increased prominence of the DD (Mosfeldt-Laursen, 1989; Walton and Fulton, 1986). That a similar Ca^{++} sensitive K^+ conductance mediates the slow ahp in FM's is supported by its sensitivity to Apamin. This neurotoxin has been shown to selectively block the Ca^{++} activated K^+ conductance underlying the medium ahp's in several other central neurones including spinal motoneurones (Zhang and Krnjevic, 1987; Castle et al, 1989). However further work with Ca^{++} channel antagonists is required to confirm this. The medium duration ahp described in guinea-pig FM's has been shown to be blocked by Co^{++} indicating a role for Ca^{++} in its generation.

Burke and Rudomin (1977) suggested a correlation between short duration ahp's and innervation of fast-twitch type muscle. This has support here as rat facial muscles are predominantly of the fast-twitch type (Lindquist, 1973). AHP amplitude in rat spinal motoneurones has been shown to be smaller than in cat motoneurones (Bradley and Somjen, 1961) and said to be related to the faster repetitive firing properties of rat motoneurones.

The DD observed as a hump separating the fast and slow AHP's has been noted in about 50% of cat spinal motoneurones and more frequently in rat, frog and turtle spinal motoneurones (Granit et al, 1963; Nelson and Burke, 1967; Barrett and Barrett, 1976; Magherini et al, 1976; Hounsgaard et al, 1988). It was also prominent in neonatal rat spinal motoneurones, adult rat ocular, but not hypoglossal motoneurones in vitro and also rat and cat facial motoneurones in vivo (Fanardjian et al, 1983b; Walton and Fulton, 1986; Gueritaud, 1988; Iwata et al, 1972). Its presence has been attributed to passive or active passage of the soma action potential into the dendrites (Granit et al, 1963; Nelson and Burke, 1967) while Traub and Llinas (1977) in their model of neuronal conductivity suggested its root to be in a localised density of Na^{+} conductance in the dendrites. However, variation may occur as in neonatal rat motoneurones the DD is Ca^{++} dependent (Walton and Fulton, 1986) while in turtle spinal motoneurones it is insensitive to Ca^{++} antagonists (Hounsgaard et al, 1988).

Antidromically evoked AP's of FM's showed a clear separation between initial segment (IS) and soma-dendritic (SD) components using hyperpolarising or refractory techniques, as seen in cat and rat spinal motoneurones in vivo (Coombs et al, 1957a,b). The absence of an M component was probably due to the small spatial

separation of recording and stimulating electrodes because only a reduced length of axon remained in the slice. Antidromic action potentials on several occasions were followed by a prominent DD along with a slow ahp of similar amplitude and duration to that seen after directly-evoked AP's. In adult and neonatal rat spinal motoneurones these after potentials were only seen after SD invasion indicating that it is this part of the neuronal membrane which possesses the responsible channels (Coombs et al, 1957a,b; Fulton and Walton, 1986).

In other neurones the AP afterpotentials were obscured by additional synaptic potentials, which showed stimulus dependency and were able to evoke orthodromic AP's when of sufficient amplitude to reach threshold. The nature and origin of these potentials was not investigated. In the cat, in vivo studies have indicated that a recurrent collateral pathway does not exist (Fanardjian et al, 1983a). If a similar situation exists in the rat then it appears that the coronal slice retains some FM afferents which can be excited by the same stimulus used to antidromically invade the cell soma.

The use of long duration current pulses to evoke a single action potential often showed a delay to the generation of the AP. The depolarising electrotonic potential upon which the AP was evoked appeared to be biphasic. Depolarisation to just sub-threshold potentials was rapid and presumably due to the passive properties of the membrane. This rapid component of the depolarisation was followed by a more slowly rising component which was distinct from the Na^+ dependent IR described earlier because it was insensitive to TTX. It could be clearly seen on sub-threshold depolarising electrotonic potentials from hyperpolarised potentials. A similar

phenomenon was also observed on the repolarising phase after large amplitude hyperpolarising electrotonic potentials from depolarised membrane potentials. In this situation depolarizing rebound potentials were occluded by this biphasic repolarisation. The prominence of depolarising rebound potentials in Cs^+ loaded neurones even at depolarised holding potentials suggests that an outward potassium current or currents may mediate the slow depolarising component which delays AP generation. Preceding hyperpolarisation may act to deinactivate these conductances which are normally rapidly inactivated near threshold. In these respects there are similarities to the transient outward current I_A described first in molluscan neurones by Connor and Stevens (1971) and subsequently identified in several central neurones (Rogawski, 1985). However, a recent study reports that an I_A-like current could not be evoked in voltage-clamped rat FM's (Aghajanian and Rasmussen, 1989). In guinea-pigs a different picture has been compiled. Two 4-AP sensitive transient outward currents have been distinguished but only when evoked from negative holding potentials. Both undergo voltage dependent inactivation but occupy different ranges as well as one undergoing fast decay and the other being more sustained (Nishimura et al, 1989).

The firing properties of FMs <u>in vitro</u> appear to show rapid adaptation to a tonic firing frequency which was dependent on stimulus intensity and sustained for the length of the stimulus. The underlying mechanisms of this rapid adaptation were not studied however in adult cat spinal motoneurones these phenomena are controlled by the specific Ca^{++} mediated K^+ conductance underlying the ahp (Barrett and Barrett, 1976; Barrett, Barrett and Crill, 1980). Similar firing properties have also been studied in guinea-

pig FM's and both hypoglossal and ocular motoneurones of the rat, in vitro (Nishimura et al, 1989; Gueritaud, 1988; Mosfeldt-Laursen and Rekling, 1989).

In conclusion, the data obtained in this study suggests that despite the necessary dendritic amputation which occurs in the slice preparation facial motoneurones in vitro possess membrane properties comparable to other cranial and spinal motoneurones investigated both in vitro and in vivo. Recordings from neurones in the FMN provide a characteristic, uniform electrophysiological profile suggesting a homogeneous population. Investigations into the actions of 5-HT on these neurones in the second part of this study reinforce this view. The evidence thus supports the use of the FMN slice as a relevant model for the study of adult rat motoneurones.

PART II

The Ionic Mechanism and Pharmacological Characterisation of Serotonin (5-Hydroxytryptamine)-Evoked Depolarisation of Facial Motoneurones *in vitro*.

CHAPTER 5 INTRODUCTION

In the central nervous system, Serotonin (5-HT) has been shown to evoke inhibitory, excitatory and biphasic, inhibitory followed by excitatory, responses depending on cell type. Inhibition of spontaneous or evoked single unit activity with iontophoretic 5-HT has been shown to predominate in the dorsal raphe nucleus (DRN) (Aghajanian et al, 1972) hippocampus (Segal 1975, 1976) lateral septal nucleus (LSN) (Joels and Urban, 1985) cerebellum (Lee et al, 1986) cerebral cortex (Roberts and Straughan, 1967) and brainstem midline neurones (Davies et al, 1988a). Excitatory responses have also been described in the hippocampus (Jahnsen, 1980) cortex (Roberts and Straughan, 1967) facial motor nucleus (McCall and Aghajanian, 1979a) other brainstem neurones (Davies et al, 1988b), neonatal and adult spinal motoneurones (White and Neuman, 1980; Connell and Wallis, 1988) and sympathetic preganglionic neurones (SPN) (Yoshimura and Nishi, 1982). Intracellular electrophysiological studies have uncovered the mechanisms by which some of these effects are achieved and indicate that they appear to have several mechanistic and pharmacological features in common.

Inhibition of central neurones by 5-HT appears to operate through a common mechanism. Neurones of the DRN (Rainnie, 1988; Aghajanian and Lakoski, 1984; Williams et al, 1988), LSN (Joels et al, 1986; Joels and Gallagher, 1988) and hippocampus (Jahnsen, 1980; Segal, 1980; Andrade and Nicoll, 1987a; Colino and Halliwell, 1987; Ropert, 1988; Baskys et al, 1989) all show the primary effect of 5-HT application to be a hyperpolarization associated with a decrease in R_m and a reduction in τ through a post-synaptic site of action. Voltage clamp data indicates that this is mediated by an outward current associated with an appropriate increased conductance. The reversal potential ($E_{5\text{-}HT}$)

for this effect is dependent on $[K^+]_o$ and not affected by Cl^- loading of the cell indicating that activation of a K^+ conductance mediates the hyperpolarisation. In hippocampal pyramidal cells the outward current displays inward rectification and is blocked by intracellular Cs^+ and extracellular Ba^{++} (Colino and Halliwell, 1987) while in the DRN two components have been identified one which displays inward rectification and is Ba^{++} sensitive and another which is both voltage and Ba^{++} insensitive (Williams et al, 1988). 5-HT evoked hyperpolarisation can explain the suppression of extracellular activity from these neurones in vivo. In addition, the reduction in R_m and τ lowers the excitability of the neurone to incoming excitatory synaptic input. Paradoxically there is a simultaneous suppression of the current mediating the spike ahp (I_{AHP}) in the LSN and hippocampus. Thus an increase in firing frequency can occur in response to a suprathreshold excitatory input even under conditions of overall reduced excitability determined by intracellularly recorded events from the cell soma.

Based on the qualitative effectiveness of 5-HT_{1A} receptor ligands and the ineffectiveness of 5-HT_{1B} and 5-HT_2 ligands, a 5-HT_{1A} receptor can be proposed as the mediator of the increase in potassium conductance leading to hyperpolarisation in the DRN (Rainnie, 1988; Lakoski and Aghajanian, 1985; Williams et al, 1988), LSN (Joels et al, 1987) and hippocampus (Andrade and Nicoll, 1987a,b; Colino and Halliwell, 1987; Baskys et al, 1989; Beck, 1989; Segal et al, 1989). Buspirone and 8-OH-DPAT are potent agonists in the DRN and LSN and partial agonists in the hippocampus while spiperone at concentrations consistent with its affinity for the 5-HT_{1A} site is an effective antagonist. Given the low agonist

activity of 5-HT_{1A} ligands in the hippocampus a definitive classification of this receptor awaits development of a potent selective 5-HT_{1A} antagonist.

Intracellular recording techniques have uncovered three distinct mechanisms underlying depolarising excitatory effects of 5-HT on central and peripheral neurones. A slow depolarisation associated with increased R_m is evoked by 5-HT application to hippocampal pyramidal cells (Andrade and Nicoll, 1987a; Colino and Halliwell, 1987) nucleus accumbens neurones (North and Uchimura, 1989) cortical neurones (Davies et al, 1987), SPN's (Ma and Dun, 1986; Yoshimura and Nishi, 1982) and facial motoneurones in vivo (VanderMaelen and Aghajanian, 1980), while in the peripheral nervous system (PNS) coeliac ganglion (Dun et al, 1984; Wallis and Dun, 1988) myenteric ganglion (Wood and Mayer, 1979; Johnston et al, 1980) and sub-mucous ganglion neurones (Surprenant and Crist, 1988) of the guinea-pig all display a similar response. Suppression of a resting K^+ conductance has been identified as the mechanism mediating this depolarisation, though characterisation of the conductance has only been detailed in two studies. In nucleus accumbens neurones of the basal ganglia 5-HT acts primarily to reduce a Ba^{++} sensitive inwardly rectifying potassium conductance which contributes to the resting potential throughout the physiological range (North and Uchimura, 1989). It may in part be Ca^{++} sensitive but otherwise resembles that described in cultured nucleus basalis neurones which is similarly modulated by Substance P (Stanfield et al, 1985). The $E_{5\text{-}HT}$ was dependent on $[K^+]_o$ and the depolarisation could be seen to readily reverse polarity when the neurone was held at potentials below E_{K^+}.

In contrast the depolarisation and associated increase in R_m observed in hippocampal neurones was difficult to reverse. Decrease of a resting K^+ conductance was inferred by the blocking effects of extracellular Ba^{++} and intracellular Cs^+ as well as the maintenance of the response when the chloride gradient across the membrane was reversed. The associated inward current evoked by 5-HT comprised of two components, one strongly voltage sensitive at potentials above -55mV the other voltage insensitive. The voltage sensitivity is claimed to be due to a suppression by 5-HT of the M-current though the exact contribution of this to the inward current is contested (Colino and Halliwell, 1987; Andrade and Nicoll, 1987a). Clearly, the observation that 5-HT evoked a depolarisation outside the range of M-current activation implicates involvement of a second potassium conductance. This is unlikely to be a continuously activated calcium sensitive conductance as blockade of I_{AHP} (with high intracellular cAMP) did not suppress 5-HT evoked inward current.

The 5-HT evoked depolarisation of rat SPN's (Ma and Dun, 1986) showed some attenuation in low Ca^{++} high Mg^{++} or TTX containing aCSF suggesting some presynaptic or Na^+/Ca^{++} dependent component to depolarisation. The depolarisation could be nullified at the presumed E_{K+}, as judged by the potential at which the spike ahp was eliminated, however, its polarity could not be reversed. Similar voltage sensitivity has been seen in guinea-pig sub-mucous plexus neurones where the 5-HT evoked inward current shows a conductance decrease in the range -45 to -80mV but failed to produce a clear point of intersection of control and 5-HT I/V plots even though similar currents evoked by SP and muscarine clearly reversed at E_{K+} (Surprenant and Crist, 1988). Depolarisation of coeliac ganglion

cells could not be reversed and indeed displayed an increase in amplitude as E_{K+} was approached leading the authors to suggest an additional Na^+ and/or Ca^{++} conductance increase to be involved (Wallis and Dun, 1988).

Excitatory actions of 5-HT through suppression of a resting K^+ conductance have also been reported in invertebrates. Sensory neurons of the molluscs Aplysia and Helix depolarise in association with increased R_m in response to 5-HT, and this event has a reversal potential dependent on E_{K+} (Gerschenfeld and Paupardin-Tritsh, 1974). A depolarising synaptic potential with the same properties as the 5-HT evoked depolarisation is mediated by a suppression of the S-current, a non-inactivating K^+ current which displays strong outward rectification. Reversal of the 5-HT synaptic event is prevented by this rectification in low $[K^+]_o$ but can be observed in high $[K^+]_o$ when the ionic gradient is sufficient to generate a current which can be measured (Pollock et al, 1985). The S-current can be blocked by intracellular Cs^+ but is unaffected by Co^{++} and Ni^{++} indicating that it is not Ca^{++} sensitive (Klein and Kandel, 1980).

Cell attached and excised patch studies have shown single channel events which possess all the properties of the S-current with an average single channel conductance of 55 ± 6pS (slope conductance at 0mv). The S-channel has two probability of open states but the action of 5-HT is to close the channels for periods much longer than either of the two closed times, an action consistent with depolarisation and increased R_m (Siegelbaum et al, 1982). In molluscs these effects of 5-HT in both whole cell and

membrane patch preparations can be mimicked by cAMP, forskolin and the catalytic sub-unit of cAMP-PK suggesting mediation by the adenylate cyclase/cAMP second messenger cascade.

Three recent studies have reported a novel depolarising action of 5-HT. Neurones of the adult rat nucleus prepositus hypoglossi (PrH) (Bobker and Williams, 1989) guinea-pig and cat medial and dorsal lateral geniculate nucleus (LGNd/m) (Pape and McCormick, 1989) and neonatal rat spinal motoneurones (Takahashi and Berger, 1990) show a depolarisation in response to 5-HT which is associated with a decrease in membrane resistance. Unlike 5-HT_3 responses it shows no desensitisation and is insensitive to 5-HT_3 antagonists. Voltage-clamp studies show 5-HT to augment the time and voltage dependent inward current relaxation evoked by hyperpolarising voltage step commands without any effect on the instantaneous current response in PrH and LGNd neurones. This inwardly rectifying relaxation termed I_h is active at rest in these neurones and further activated by hyperpolarisation. It is mediated by a mixed Na^+/K^+ conductance with an extrapolated reversal potential lying between the K^+ and Na^+ equilibrium potentials and positive to rest. Whether the action of 5-HT is through a shifting of the voltage dependence of activation or just an enhancement of I_h at a given potential (or both) is not clear though in the PrH it appears that 5-HT can increase this conductance even at potentials where I_h is fully activated by hyperpolarisation. In neonatal rat motoneurones the depolarisation was shown to be mediated by an inward current associated with increased membrane conductance, especially in the hyperpolarising direction using ramp voltage commands. In all three cases the 5-HT effect was dependent on both

$[K^+]_o$ and $[Na^+]_o$ but not $[Cl^-]_o$, and, consistent with the properties of I_h, it could be blocked by extracellular Cs^+ but not by extracellular Ba^{++}, TEA, 4-AP or apamin.

Pharmacological investigations into the receptors mediating these depolarisations do not present the clear picture seen with 5-HT induced neuronal hyperpolarisation though some conformity of receptor type to ionic mechanism is apparent.

Two studies put a definite classification on the receptor mediating neuronal depolarisation associated with increased R_m though it must be pointed out that one is not comprehensive. The most detailed is on neurones of the rat nucleus accumbens in vitro (North and Uchimura, 1989) which shows 5-HT depolarisation to be antagonised by ketanserin, mianserin and long applications of low concentrations of spiperone. Antagonism appears to be competitive as it can be overcome by increasing 5-HT concentrations. The agonists 5-CT, 8-OH-DPAT, mCPP and 2-CH_3-5-HT were all inactive as was the 5-HT_3 antagonist ICS 205-930. The depolarisation of guinea-pig cortical neurones can be antagonised by ritanserin (1μM) and cinanserin (10μM) (Davies et al, 1987). Both studies implicate a 5-HT_2 receptor.

The receptor mediating the depolarisation in the hippocampus is unclear. While the frequently preceding hyperpolarisation is blocked by micromolar concentrations of spiperone, the depolarization remains suggesting that neither a 5-HT_{1A} or 5-HT_2 receptor is responsible (Andrade and Nicoll, 1987a). Application of 5-HT_{1A} agonists evoke only monophasic hyperpolarising responses (Andrade and Nicoll, 1987a; Beck, 1989). Ketanserin, mianserin and methysergide are all ineffective as antagonists while ICS 205 930 has been claimed to be ineffective in one study (5μM) but

effective in another (10μM) (Andrade and Nicoll, 1987a; Colino and Halliwell, 1987). Equally conflicting results with 5-HT_{1B} ligands have been reported which suggested that RU24969 (200-400nM) can show antagonistic effects (Colino and Halliwell, 1987) or that the agonist TFMPP (10μM) is inactive (Andrade and Nicoll, 1987a). The agonists 5-MeODMT and 5-MeOT both mimic 5-HT evoked depolarisations but the difference in potency between the two suggests that the receptor is different from that mediating hyperpolarisation.

The depolarisation associated with decreased resistance seen in PrH neurones was antagonised by high concentrations of spiperone but not by ketanserin, mianserin or ICS 205 930. However, while 5-CT was an agonist, 8-OH-DPAT, TFMPP and 2-CH_3-5-HT were all without effect. In the LGNd this response could be antagonised with methysergide but was insensitive to 8-OH-DPAT, ipsapirone and ketanserin. Both sets of data suggest an as yet undefined 5-HT_1-like receptor may be responsible (Bobker and Williams, 1989; Pape and McCormick, 1989). In neonatal rat motoneurones (Takahaski and Berger, 1990) this depolarisation is spiperone sensitive but is also, surprisingly in relation to the work of Connell and Wallis (1988), mimicked by 8-OH-DPAT (10μM). Given the potency of 5-HT in this system (EC_{50}~100nM) it is possible that this action of 8-OH-DPAT is through a site other than the 5-HT receptor (e.g. Crist and Surprenant, 1987). Of direct relevance here is the work by Connell and Wallis (1988, 1989) who have looked at the pharmacology of the receptor mediating 5-HT evoked depolarising ventral root potentials in neonatal rat hemisected spinal cord. The 5-HT response is mimicked by 5-CT, α-CH_3-5-HT and 5-MeOT while 8-OH-DPAT, RU 24969 and 2-CH_3-5-HT are ineffective. The relative agonist potency was 5-HT = 5-CT = α-CH_2-5-HT > 5-MeOT >> tryptamine while in the

presence of citalopram, a 5-HT uptake inhibitor, 5-HT was the most potent agonist. Methiothepin, ICS 205-930 and MDL 72222 had no antagonist activity. Spiperone, mesulergine, metergoline, cyproheptadine and methysergide were potent antagonists while ketanserin but not ritanserin could depress a maximal depolarisation but did not abolish it. The authors propose an as yet unclassified 5-HT_1-like receptor to mediate this response. In addition, 5-HT evoked depolarisation of cultured spinal cord neurones has been found to be blocked by spiperone but not ketanserin, methiothepin or cocaine (Legendre et al, 1989).

A transient depolarisation in response to iontophoretic or pressure ejected 5-HT has been demonstrated in cells of the guinea-pig submucous plexus (Surprenant and Crist, 1988) coeliac ganglion (Wallis and Dun, 1988) and rabbit superior cervical ganglion (Wallis and North, 1978). This response is similar to those evoked by acetylcholine, acting through a nicotinic receptor, in that it is due to increased cation conductance (mainly Na^+), desensitises quickly and is blocked by tubocurarine. Sensitivity to 5-HT_3 receptor antagonists such as ICS 205 930, MDL 72222 and GR 38032F distinguishes this response from nicotinic receptor mediated responses. Similar rapid inward currents mediated through 5-HT_3 receptors have been observed in a small proportion of cultured mouse hippocampal and striatal neurones (Yakel et al, 1988). These responses are indistinguishable from those seen more readily in the clonal cell line NG108-15 which possess the same biophysical and pharmacological properties seen in peripheral neurones (Yakel and Jackson, 1988). Although binding sites for 5-HT_3 receptor ligands have been demonstrated in the CNS (Kilpatrick et al, 1987) and administration of different peripherally defined antagonists have

been shown to evoke antipsychotic, anxiolytic and anti-emetic effects, demonstration of a functional central 5-HT_3 receptor at the cellular level is still awaited.

Recent evidence suggests the 5-HT_3 receptor is an integral receptor-ionophore complex of the nicotinic ACh, excitatory amino acid and $GABA_A$ super family type (Derkach et al, 1989). Whole cell recordings from isolated guinea-pig submucous plexus neurones show transient 5-HT depolarisations to be mimicked by 2-CH_3-5-HT and antagonised by ICS 205 930 and GR 38032F. 5-HT evoked single channel openings in outside out patches from the same cells show the same cation sensitivity and the probability of opening to be reduced by ICS 205 930 and GR 38032F. The evidence thus points to the possibility that 5-HT, as well as having slow post-synaptic actions, may also function as a "fast" neurotransmitter in a manner similar to the actions of ACh, EAA's and GABA.

In addition to these depolarising actions, 5-HT also suppresses the ahp following single or trains of spikes in hippocampal pyramidal and dentate granule neurones (Andrade and Nicoll, 1987a; Colino and Halliwell, 1987; Baskys et al, 1989), LSN neurones (Joels and Gallagher, 1987) and spinal inter- and motor-neurones of the cat (Hounsgaard et al, 1986), turtle (Hounsgaard and Kiehn, 1989) and lamprey (Wallen et al, 1989). The ahp is mediated by an outward Ca^{++} dependent K^+ current, I_{AHP}, and is responsible for accommodation of spike firing. In the hippocampus and LSN this effect occurs simultaneously with, but independently of, actions on membrane potential. In turtle motoneurones a small depolarisation accompanies this action while in the lamprey motoneurones suppression of I_{AHP} occurs in isolation. The effect of 5-HT does not appear to be through a reduction in Ca^{++} entry during the spike

as the durations of Na^+ spikes in the presence of TEA or Ca^{++} spikes in the presence of TTX and TEA are unaltered. This action of 5-HT in reducing spike frequency adaptation is proposed to increase firing in response to depolarising stimuli and thus alter the importance of incoming signals over the normal activity of the neurone, a concept loosely described as altering the "signal to noise" ratio (McCormick, 1989).

Spinal motoneurones of the cat in vivo and turtle in vitro have been shown to express biphasic firing patterns which are controlled by an underlying voltage plateau (Hounsgaard and Mintz, 1988; Hounsgaard et al, 1988; Hounsgaard and Kiehn, 1989). This plateau potential can be regarded as being generated by a nifedipine sensitive calcium, or calcium-dependent, inward current which is suppressed under normal conditions by steady-state outward currents. 5-HT, through a methysergide sensitive post-synaptic site of action, and the potassium channel antagonists 4-AP, Cs^+, TEA and apamin all promote expression of this calcium dependent plateau potential. This action of 5-HT leads to sustained high frequency firing in response to brief depolarising stimuli. As the ahp following an action potential is suppressed by 5-HT and a small depolarisation of membrane potential is also evoked by 5-HT it is suggested that this excitation is associated with the suppression of a Ca^{++}-activated K^+ current, possibly I_{AHP}, which is tonically active at rest.

Pharmacological studies using extracellular recording techniques in vivo have shown FM's to be potently excited by the amino acids, glutamate, aspartate and N-methyl-D-aspartate (NMDA), while γ-amino-butyric acid (GABA) and glycine act to depress excitatory amino acid (e.a.a.) evoked firing (Martin et al, 1977). Additionally the rat FMN has been shown to be innervated by 5-

hydroxytryptamine (5-HT) and catecholamine containing fibres (McCall and Aghajanian, 1979a). Four weeks after intracisternal injection of [^{3}H]-5-HT, dense labelling was noted in the ventral half of the FMN. Other studies using immunohistochemistry specific for 5-HT show 5-HT positive fibres to arise in the medial part of the nucleus and continue ventrally, but decreasing in density rapidly at more caudal regions. In the transverse plane variation in innervation showed a very high density of fibres in the intermediate region with lower levels in the medial and lateral aspects (Steinbusch, 1981). The density of 5-HT innervation in the rat FMN is greater than in any of the other cranial motor nuclei (Takeuchi et al, 1983). At the electron microscopic level both axosomatic but predominantly axodendritic (81%) synaptic contacts were observed. It was estimated that 2% of synaptic contacts in the FMN were serotonergic a figure which compares favourably with other densely serotonergic innervated nuclei (Aghajanian and McCall, 1980).

The source of these serotonergic connections in the rat is uncertain. The presence of discrete groups of 5-HT containing cell bodies in the rat CNS has been well documented. The majority of these neurones are clustered in the Raphe nuclei, designated areas B1-B9 however other serotonergic neurones are distributed outwith these locations (Steinbusch, 1981). Projections from the midline medullary raphe nuclei to the FMN in the rat have been demonstrated to be mainly ipsilateral to the medial subdivision (Isokawa-Akesson and Komisaruk, 1987). This connection is supported by the observation that after lesioning with 5,7-dihydroxytryptamine regenerating 5-HT fibres approaching the medial aspects of the FMN could be traced back to damaged axons in the region of the raphe magnus (McCall and Aghajanian, 1979b). In the cat projections to

the dorsal/lateral subdivisions from the medullary raphe were reported (Takada et al, 1984). Another study in the cat also demonstrated major raphe nuclei innervation of the intermediate and dorsal subdivisions, projections to the ventromedial region from the raphe's magnus and pallidus and another raphe pallidus projection to the dorsomedial region (Pogosyan and Fanardjian, 1986). A study using ^{3}H-leucine as a tracer suggested a direct link from the dorsal raphe nucleus to the lateral and ventrolateral subnuclei of the FMN in the cat (Holstege et al, 1984).

It has recently been reported that the serotonergic input to the locus coeruleus appears to be through serotonergic neurones found in the nucleus paragigantocellularis close to, but distinct from the B3 cell group of the raphe magnus (Aston-Jones et al, 1986; Pieribone et al, 1989). A projection from this region to the FMN in the rat has been proposed suggesting that a non-raphe site may supply some serotonergic innervation to the FMN (Isokawa-Akesson and Komisaruk, 1987). In vivo, iontophoresis of 5-HT facilitated e.a.a. or afferent nerve stimulation evoked excitation of FM's by inducing a slow subthreshold depolarisation associated with an increase in cell input resistance (McCall and Aghajanian, 1979a; VanderMaelen and Aghajanian, 1980; 1982). Using intracellular current clamp and voltage clamp techniques the mechanism and pharmacology of this 5-HT evoked depolarisation has been investigated in detail and compared with a similar action evoked by noradrenaline. The results are compared with the actions of 5-HT and NAd on other central neurones. Some of this data has been presented in abstract form (Larkman & Kelly, 1988; Larkman et al, 1988, 1989a,b; Kelly et al, 1988).

CHAPTER 6 RESULTS

The action of 5-HT on Facial Motoneurones in vitro

The action of NAd on Facial Motoneurones in vitro

The effects of increasing the aCSF potassium concentration on the 5-HT evoked depolarisation

The effects of altering $[K^+]_o$ on the Noradrenaline evoked depolarisation

A comparison of the effects of 5-HT and NAd on Facial Motoneurones

Voltage clamp studies of the action of 5-HT and NAd on Facial Motoneurones

Depolarisation of Facial Motoneurones is unaffected by TTX

5-HT does not suppress the ahp of FM's

The dose-dependency of the 5-HT evoked depolarisation

The dose-dependency of the NAd evoked depolarisation

The Pharmacology of the 5-HT Evoked Depolarisation of FM's

Methysergide

LY 53857

Ketanserin

Spiperone

Methiothepin

8-Hydroxy-2-(diN-propylamino)-tetralin (8-OH-DPAT)

Dipropyl-5-carboxamidotryptamine (DP-5-CT)

5-HT_3 Ligands : ICS 205 930 and 2-methyl-5-HT

Figures 6.1 - 6.48

Tables 6.1 - 6.2

THE ACTION OF 5-HT ON FACIAL MOTONEURONES IN VITRO

In intracellular current clamp experiments bath application of 5-HT (100 to 250μM) produced a slow monophasic depolarisation of 120 facial motoneurones which displayed the characteristic membrane properties described in Part I. Only 6 failed to respond in this way. A preceding hyperpolarisation was never observed.

A typical response of a facial motoneurone to superfusion with 5-HT is illustrated in Figures 6.1 to 6.4, and similar responses can be seen in further figures. The continuous chart record of Fig.6.1 illustrates the time course of 5-HT (200μM) action on facial motoneurones. Prior to 5-HT application the neurone had a resting potential of -71mV. Input resistance (R_m) was monitored by the voltage responses to a step current pulse of -1nA amplitude and 120msec duration injected through the intracellular microelectrode at a frequency of 0.25Hz. Addition of 5-HT to the superfusing aCSF for 10 minutes evoked a depolarisation of 6mV to a new membrane potential of -65mV. This depolarisation was associated with an increase in the R_m of the cell as shown by the increased voltage deflection in response to the test current pulse. On switching back to 5-HT free aCSF both the membrane potential and R_m recovered to control levels after about 20 minutes.

At the points marked a, b, c and d (Fig.6.1) voltage deflections in response to hyperpolarising and depolarising current pulses of varying amplitude were obtained. These electrotonic potentials are illustrated in expanded form in Fig.6.2 and were used to construct the current-voltage relations shown in subsequent figures 6.3 to 6.4. As seen in the previous section hyperpolarising potentials show the characteristic sag as a result of time dependent inward rectification. In the control condition,

measurement of the input resistance over the linear range at the peak of the voltage deflection ($R_{m(pk)}$) gave a value of 8.9MΩ (Figs.6.2a & 6.3A). The steady-state current-voltage relation showed non-linearity throughout most of the range measured (Fig.6.4A) [An estimate of $R_{m(ss)}$ measured over the range ± 0.5nA (3 data points) was 7.6MΩ]. An ohmic response was obtained from a 0.5nA depolarising current pulse. The charging curve approximated to a single exponential giving a membrane time constant (τ) of 2.6msec (Fig.6.4B). Increasing the amplitude of the depolarising step to 1.5nA/120msec evoked a single action potential from an approximate threshold of -55 mV. (An absolute value for threshold was difficult to obtain as the spike appeared to ride on a small depolarising prepotential as described previously).

The depolarisation evoked by superfusion with 5-HT (200μM) was associated with a 56% increase in $R_{m(pk)}$ to 13.9MΩ and τ, measured from a 0.2nA depolarising current step, also increased to 5.3 msec. Together these effects led to increased excitability of the neurone, a train of three spikes being evoked by the previously sub-threshold 0.5nA, 120msec depolarising current pulse. However, the threshold for spike generation appears to be unaffected by 5-HT. The depolarising tail potentials observed after the cessation of hyperpolarising current pulses were increased in amplitude and duration in the presence of 5-HT probably reflecting the effects on R_m and τ. Indeed an action potential was evoked by the tail potential evoked after a 3nA hyperpolarising current pulse (Fig.6.2b).

Given the prominence of the time and voltage dependent inward rectifier in these neurones, it was important to assess how much of this increase in R_m can be attributed to 5-HT and how much is a

result of voltage dependent membrane rectification which occurs with membrane depolarisation. Manual clamping of the membrane potential back to -71mV at the peak of the 5-HT response by passing 0.65nA continuous hyperpolarising DC through the microelectrode gives a new value of $R_{m(pk)}$ over its linear range of 12MΩ. This represents a 5-HT induced change in $R_{m(pk)}$ of 36% (Fig.6.2c & 6.3B). Measurement of the change in $R_{m(ss)}$ is difficult to quantify as a result of non-linearity of the current-voltage relations, however a small increase over the narrow range above and below the resting potential can be seen in Figure 6.4A. At more negative potentials the current-voltage plots converge. Under these conditions the value of τ was 4.1msec from a 0.5nA depolarising current pulse (Fig.6.4B). Increased excitability was maintained such that a depolarising current pulse of 1nA, 120msec evoked 4 action potentials. The depolarising tail potentials were also of greater amplitude than in control conditions. Washing with drug-free aCSF led to a recovery of membrane potential (-71mV) and $R_{m(pk)}$ (9.9MΩ) (Figs.6.2d, 6.3A).

Figure 6.3A,B shows the current-voltage relationships obtained by measuring the peak voltage deflections from the electrotonic potentials shown in Figure 6.2a,b,c,d. The control (a) and wash (d) peak deflection current voltage plots show linearity in the range -60 to -86mV. At more negative potentials than this considerable rectification occurred. The current-voltage relationship in 5-HT is linear over a similar range and almost up to the point of intersection with the control and wash plots. The estimated reversal potentials for the depolarisation evoked by 5-HT taken from the point of intersection of the extrapolated linear lines of regression are -82.6mV and -86mV against control and wash

plots respectively. These values approximate to the observed point of intersection on the non-linear portion of the current-voltage plots. It is interesting to note that the current-voltage plots after this point of intersection appear to converge. Similar observations have been made in other cells where the linear portions of the current-voltage plots intersect and thereafter the non-linear portions become parallel (e.g. Fig.6.8C). It should also be pointed out that in some cases peak deflection current-voltage plots failed to intersect in the range examined. In these cases the estimated reversal potential was obtained by extrapolation of linear lines of regression fitted by the same least squares analysis program used in the above example. This observation will be returned to later, in this and the discussion sections. Estimates of the reversal potential from steady-state current voltage relations were difficult to obtain due to the inability to pass large enough currents through the recording electrode to reach a point of intersection. As can also be seen in Figure 6.4A non-linearity of the steady-state current-voltage relationships prevented an estimation of the reversal potential by linear regression analysis.

Evidence that an accompanying change in membrane resistance is linked causally to a putative neurotransmitter (PNt) evoked depolarisation can be determined by comparing the change in membrane potential (δV) and the change in membrane resistance $1-(R^*/R)$ according to the relationship (rearranged from Ginsborg 1967, 1973; Ginsborg et al, 1974; Brown and Constanti, 1980)

$$\delta V = (E_{PNt} - Vm)\ (1 - R^*_m/R_m) \qquad \text{Eqn.1}$$

where δV is the depolarisation evoked by PNt, E_{PNt} is the reversal potential of PNt, Vm and R_m are the resting potential and membrane resistance in the absence of PNt and R^*_m is the membrane resistance during PNt application.

If the responses to 5-HT can be described by this equation the change in potential at any point during FM depolarisation should be linearly related to the ratio $1-(R^*_m/R_m)$ and the slope of the line through such measurements should be equivalent to the difference between $E_{5\text{-}HT}$ and the resting potential. In Figure 6.5A the membrane resistance of a FM resting at -77mV was tested at two second intervals, during superfusion with 5-HT (200μM), by injecting a 1nA hyperpolarising current pulse 120msec in duration. The expanded records of figure 6.5A show that the voltage responses displayed time dependent sag allowing measurement of both peak and steady-state voltage deflections. The ratio $1-(R^*_m/R_m)$ has been plotted against δV at 10 second intervals for both the peak (open circles) and steady-state (closed circles) responses (Figure 6.5B). Linear regression analysis of these relationships gave slopes of -9.8 and -9.2mV for the peak and steady-state responses with respective correlation coefficients of 0.98 and 0.95. These values agree closely with the reversal potential obtained from peak deflection current-voltage plots obtained at the peak of the 5-HT response and after recovery (-73mV; Fig.6.5C,D). The I/V relationships of figure 6.5D show a -1nA current step to evoke voltage deflections which lie on the linear portion of both control and 5-HT plots indicating that the peak membrane resistance at both rest and in the presence of 5-HT is independent of membrane potential.

Despite the correlation of $E_{5\text{-}HT}$ obtained by these two methods, the slope of the plots in figure 6.5B does show some reduction as the amplitude of the depolarisation increases, i.e. $1-(R^*_m/R_m)$ becomes proportionally larger as δV increases. It is likely that this is due to a contribution to the overall resistance increase by voltage dependent inactivation of the inward rectifier described in the next paragraph.

The above estimates of reversal potential for the 5-HT evoked depolarisation will be subject to an error introduced by the contribution made by voltage dependent rectification to the overall resistance change associated with the depolarisation. Based on the assumption that 5-HT does not affect the inward rectifier responsible for this rectification a value of the reversal potential for the 5-HT evoked depolarisation which is not subject to this error can be obtained from the change in $R_{m(pk)}$ measured when the membrane potential is offset back to the control level while still in 5-HT. Using the offset current to calculate a new value for the point of intercept of the regression line with the y-axis a new value for the point of intersection of control and 5-HT current voltage plots can be obtained (Fig.6.3B). It can be seen that the current voltage relations measured in this way do not intersect in the range shown, however, extrapolation of the linear portions of the respective plots gives a reversal potential of -93.9mV. This value is more negative than previously estimated but can be regarded as a more accurate assessment of the reversal potential for the 5-HT evoked depolarisation as the contribution of IR to the neuronal R_m is the same in both conditions.

This approach can be verified using the method of Brown and Constanti (1980) who advanced the model described in Eqn.1 to calculate the extra current (δI) induced to flow across the cell membrane by a neurotransmitter. Thus:

$$\delta I = (V' - E_{PNt}) \quad (R_m - R^*_m/R^*_m R_m) \qquad \text{Eqn.2}$$

where V' is an arbitrary level of membrane potential and δI the extra current required to maintain V' in the presence of agonist. The remaining component in the equation is the change in conductance evoked by the transmitter expressed in terms of resistance changes (Kelly, 1982). For the FM illustrated in Figs.6.1 to 6.4 manual clamping to the resting potential of -71mV (V') at the peak of the 5-HT response requires -0.65nA (δI). Membrane resistance at -71mV in the absence of 5-HT (R_m) was 8.9MΩ and in the presence of 5-HT (R^*_m) was 12MΩ. Thus the value of $E_{5\text{-}HT}$ obtained by this method is -93.4mV virtually identical to that achieved by the current-voltage plot method.

Coupled with the use of a microelectrode filled with 3M KCl which can be expected to shift the equilibrium potential for Cl^- ions to more positive potentials, this value of the reversal potential for the 5-HT response suggests that a reduction in a K^+ conductance is the mechanism underlying depolarisation. The Nernst equation predicts that, with an extracellular K^+ ion concentration of 5mM and assuming an intracellular K^+ ion concentration of 150mM, the reversal potential for a K^+ mediated event should be -91mV. The values obtained experimentally and shown in Figure 6.3B are close to this theoretically predicted value.

In 21 further neurones where conditions throughout the course of the experiment were unchanged 5-HT (200μM) evoked a depolarisation of 6.95 ± 3.6mV (range 2 to 14mV) from a mean resting potential of -73.8 ± 5.4mV (range -64 to -85mV). This was associated with an increase in $R_{m(pk)}$ of 54 ± 32% from a control level of 9.8 ± 5.1MΩ (range 4.6 to 25.7MΩ) to 14.5 ± 6.8 MΩ (range 5.1 to 32.2MΩ). Where measured τ increased from 3 ± 1.2msec to 4.2 ± 1.3msec (n = 13). Recovery of membrane potential to -72.9 ± 5.3mV and $R_{m(pk)}$ to 10.5 ± 5.3MΩ occurred on removal of 5-HT from the aCSF. The uncorrected mean reversal potentials estimated from peak deflection current-voltage plots were -89.2 ± 12mV and -94.5 ± 15.8mV against control and wash conditions respectively.

The response evoked by 5-HT did not show any desensitisation or tachyphylaxis with repeated application. Thus a depolarisation of 5.3 ± 1.5mV (n = 8) evoked by a first application of 5-HT from a resting potential of -70.9 ± 6.2mV was followed by a depolarisation of 5 ± 1.3mV from a recovery resting potential of -72.5 ± 7.4mV on a second 5-HT application. The changes in $R_{m(pk)}$ accompanying these depolarisations were also similar being 10.1 ± 4.1 to 13.9 ± 5.1MΩ (42 ± 32%) for the first application of 5-HT and 10 ± 4.9 to 13.3 ± 6.1MΩ (36 ± 21%) for the second. The estimated reversal potential was unchanged being -87 ± 5.8mV and -90.1 ± 3.8mV for first and second applications respectively. Further evidence for the maintained effect of 5-HT on repeated application can be seen in later figures involving the use of TTX and other pharmacological agents.

That the depolarisation is sustained in the continued presence of 5-HT was observed in experiments where different doses of 5-HT were applied continuously and will be discussed in a later section.

While no attempt was made to determine the maximum length that a depolarisation could be sustained, on several occasions no diminution of the depolarisation or increase in R_m was observed for periods of 5-HT application up to 30 minutes in duration.

While being close to what would be predicted for a pure K^+ ion mediated event these values do not take into account the influence of voltage dependent rectification illustrated in Figs.6.2 and 6.3. Where the manual clamping technique was used to obtain a new value for the reversal potential a value more negative than would be predicted by the Nernst equation was obtained. In this situation the mean resting potential and $R_{m(pk)}$ were -72.3 ± 4.2 and 8.1 ± 2.5MΩ respectively. 5-HT depolarised the cells by 6 ± 2.2mV associated with an increase in $R_{m(pk)}$ to 11.8 ± 2MΩ (54 ± 38%). The uncorrected reversal potential was estimated at -88.3 ± 8.2mV (n = 12). When offset back to the control resting potential the value of $R_{m(pk)}$ was 10.5 ± 2.3MΩ representing a 5-HT evoked increase of 34 ± 25%. The τ also showed an increase in duration measuring 3.4 ± 1msec compared to 2.6 ± 0.7msec (n = 8) prior to 5-HT application. Using these new values the reversal potential was recalculated at -107.5 ± 18.4mV (n = 12).

An alternative method for correcting for membrane rectification is to manually depolarise the neurone to the membrane potential reached during exposure to 5-HT after recovery has been achieved, thereby equating the contribution of voltage-dependent rectification in both conditions. Using this method similar results to above were obtained. A mean 5-HT evoked depolarisation of 7.7 ± 4.6mV from a membrane potential of -74 ± 8.9mV was associated with an increase in $R_{m(pk)}$ from 9.3 ± 2.5 to 15 ± 7.3MΩ (56 ± 43%, n = 5) and gave an estimated reversal potential of -90.2 ± 6.7mV. Manual

depolarisation was accompanied by an increase in $R_{m(pk)}$ to 11.1 ± 3.9MΩ (14 ± 9%). Corrected values for the reversal potential gave a mean estimate of -115.7 ± 8.3mV. In one neurone where both procedures were performed values of -103 and -115mV for hyperpolarising and depolarising manoeuvres respectively were obtained.

THE ACTION OF NORADRENALINE ON FACIAL MOTONEURONES

It has been reported *in vivo* that the excitability of facial motoneurones can be facilitated not only by 5-HT but also by iontophoretic application of noradrenaline (NAd) (McCall and Aghajanian, 1979a). This was investigated *in vitro* in the following experiments with the aim of using the noradrenaline response as a control when using serotonergic antagonists to characterise the 5-HT receptor mediating the depolarisation of facial motoneurones.

Intracellular recordings in current-clamp experiments demonstrated that superfusion of facial motoneurones with noradrenaline (10 to 100μM) led to depolarisation associated with an increase in input resistance (n = 21). These neurones all possessed the membrane properties characterised in the previous chapter and where tested (n = 20) all responded in the manner previously described to superfusion with 5-HT (150 to 200μM) (see later). Figure 6.6 illustrates the characteristic response of a facial motoneurone to noradrenaline. The neurone had a resting potential of -77mV and measurements of input resistance obtained from the linear ranges of the current-voltage plots at the peak and steady-state voltage levels, seen in Figure 6.6Ba, were 7.04 and 3.82MΩ, respectively. τ measured 1.92msec. Addition of noradrenaline (50μM) to the perfusing aCSF depolarised the neurone

to a plateau at -74mV which was sustained as long as noradrenaline was in the bathing aCSF (Fig.6.6A). $R_{m(pk)}$ and $R_{m(ss)}$ increased to 9.09 and 4.16MΩ, while τ lengthened to 2.73msec (Fig.6.6Bb). Removal of noradrenaline from the aCSF allowed recovery back to -77mV and a fall in peak and steady-state input resistances to control levels (6.42 and 3.36MΩ) (Fig.6.6Bd). τ recovered to 1.99msec.

Plotting the current-voltage relationships obtained from peak voltage deflections in response to intracellular current pulse injection in the control, noradrenaline and wash conditions gave reversal potentials of -83.1 and -84.7mV (Figure 6.7A). Extrapolation of the linear portions of the steady-state current voltage plots on the noradrenaline and wash conditions gave a similar value of -88.4mV (not shown).

The increase in input resistance was shown to be comprised of two components, a noradrenaline sensitive component and one due to voltage dependent membrane rectification as has been demonstrated for 5-HT. At the peak of the noradrenaline depolarisation manual clamping of the membrane potential back to -77mV by injecting -0.6nA DC continuously through the microelectrode, showed the peak and steady-state input resistances to be 8.29 and 3.86MΩ respectively (Fig.6.6Bc). These represent increases of 29 and 15% over recovery levels and also illustrate that depolarisation does not appear to involve a direct action on the time-dependent inward rectifier of these neurones. When the DC offset is taken into account (as described earlier) the point of intersection of peak voltage deflection current voltage plots was -97.7mV against control and -94.2mV against wash conditions (Figure 6.7B).

This manoeuvre was performed on three neurones treated with noradrenaline (50μM). The neurones depolarised by 5.7 ± 3.8mV from a resting potential of -72.3 ± 4.2mV (n = 3). $R_{m(pk)}$ increased from 9.5 ± 2.7MΩ to 14.6 ± 6.2MΩ, a 52 ± 34% change. When offset back to control resting potential levels $R_{m(pk)}$ measured 12.7 ± 4.4MΩ an increase of 33 ± 17%. The reversal potential obtained from the intersection of peak deflection current voltage plots before the membrane potential was offset was -81.1 ± 3.2mV compared with -94.2 ± 3.6mV after being offset. These values indicate that a noradrenaline evoked reduction in a K^+ conductance is likely to be the cause of depolarisation as the corrected value agrees closely with that predicted by the Nernst equation for K^+ mediated event. (Assuming an intracellular $[K^+]$ of 150mM at 37°C, the predicted E_{NAd} is -91mV).

THE EFFECT OF INCREASING THE aCSF POTASSIUM CONCENTRATION ON THE 5-HT EVOKED DEPOLARISATION

The evidence presented in the previous section suggest that 5-HT and NAd evoke a depolarisation by closing potassium channels. To investigate this further a series of experiments was performed in which the K^+ ion concentration of the superfusing aCSF ($[K^+]_o$) was altered as described in the methods section. When the $[K^+]_o$ was raised to 10 or 15mM the estimated reversal potential for the 5-HT evoked depolarisation increased in accordance with the changes predicted by the Nernst equation for a potassium conductance (Fig.6.13).

$$E_{5\text{-HT}} = E_K = \frac{RT}{ZF} \ln \frac{[K^+]_o}{[K^+]_i}$$

where	R	= $8.314\ VCK^{-1}mol^{-1}$	GAS CONSTANT
	T	= 310.15	TEMPERATURE ^oK
	Z	= 1	VALENCY OF PERMEANT ION
	F	= $9.645 \times 10^4 Cmol^{-1}$	FARADAY CONSTANT

However, when the $[K^+]_o$ was lowered from the standard 5mM to 2.5mM a less clear correlation with the predicted potential was observed. In two experiments the reversal potential was lowered (but not to the value predicted by the Nernst equation) while two other cells showed little change in the reversal potential obtained in 2.5 and 5mM $[K^+]_o$. This was despite an increase in cell input resistance in 2.5mM $[K^+]_o$.

In Figures 6.8A,Ba the motoneurone in normal 5mM K^+ containing aCSF had a resting potential of -76mV, $R_{m(pk)}$ of 8.2MΩ and a τ of 2.4msec. When superfused with 5-HT (200μM) it depolarised by 6mV to -70mV (Fig.6.8A) the $R_{m(pk)}$ increased by 85% over control to 15.3MΩ and τ lengthened to 4msec (Fig.6.8Bb). On washing with 5-HT free aCSF the membrane potential recovered to -77mV and $R_{m(pk)}$ to 9.3MΩ (Fig.6.8Bc). The estimated reversal potentials obtained from the peak deflection current voltage plots in figure 6.8C were -84mV against control and -89mV against recovery levels.

The neurone was then superfused with aCSF containing 10mM K^+ (Fig.6.9A) which evoked a depolarisation of 6mV to a new resting potential of -71mV. In the control condition (in this case the wash/recovery state, Fig.6.9Bb) the peak current voltage plot showed linearity over the range of 15mV negative to the resting potential of -71mV. Over this range the $R_{m(pk)}$ was 5.5MΩ (Fig.6.9Bb). The steady state current-voltage plot showed linearity over the same range of injected current pulses and gave an $R_{m(ss)}$ of 4.8MΩ (not

shown). In the presence of 5-HT (200μM) the cell had a resting potential of -69mV representing a depolarisation of 2mV (Fig.6.9A). The $R_{m(pk)}$ was 8.6MΩ an increase of 36% over the wash/control condition (Fig.6.9Ba) and $R_{m(ss)}$ increased to 7.3MΩ. The point of intersection of the peak deflection current-voltage plots shown in Figure 6.9C gives a reversal potential of -74mV. Steady-state I/V plots also intersect at -74mV (not shown).

In all 5 cells were treated in this way. In normal 5mM K^+ aCSF the motoneurones depolarised by 4.6 ± 2.1mV from a resting potential of -73.4 ± 6.7mV in response to 5-HT (150/200μM) superfusion. This was associated with an increase in $R_{m(pk)}$ of 37 ± 30% from 6.7 ± 1.3 to 9.6 ± 3.8MΩ. The mean reversal potential for this response was -92 ± 8.5mV. On switching to 10mM $[K^+]_o$ the neurones depolarised to -65 ± 6.6mV and $R_{m(pk)}$ fell to 6.2 ± 1.9MΩ. Superfusion of 5-HT (equivalent concentrations) evoked a 2.8 ± 2.2mV depolarisation and $R_{m(pk)}$ increased to 8.3 ± 2mΩ a 32 ± 13% increase. The mean reversal potential was -72 ± 1.9mV (Figure 6.13).

A second motoneurone shown in Figures 6.10 to 6.12 was superfused with aCSF containing 2.5, 5 and 15mM K^+. This neurone had previously been used to evaluate ketanserin as an antagonist of the 5-HT response and is illustrated further in Figure 6.39. As such it had been exposed to 5-HT twice previously in 5mM$[K^+]_o$ with reversal potentials of -95 and -99mV. A third response in 5mM $[K]_o$ is illustrated in Figure 6.10. The neurone was resting at -82mV and had an $R_{m(pk)}$ of 6.8MΩ (Fig.6.10Ba). 5-HT (200μM) depolarised the neurone by 3mV associated with a 24% increase in $R_{m(pk)}$ to 8.5MΩ (Fig.6.10A, Bb). Washing with aCSF led to a recovery to -80mV and an $R_{m(pk)}$ of 5.9MΩ (Fig.6.10Bc). These figures give two values for

the reversal potential of this event of -94.5mV against control and -83mV against recovery conditions (Fig.6.10C). The neurone was then superfused with 2.5mM K^+ containing aCSF (Fig.6.11). The resting membrane potential was unchanged by this procedure (-79mV) while the $R_{m(pk)}$ increased to 9.3MΩ from 7.9MΩ (Fig.6.11Ba).

Application of 5-HT (200μM) depolarised the neurone by 4mV to -75mV and the $R_{m(pk)}$ increased to 13.2MΩ (42%) (Fig.6.11A,Bb). Washing with 5-HT free 2.5mMK^+ aCSF led to a recovery of membrane potential to -80mV and $R_{m(pk)}$ to 10.7MΩ (Fig.6.11Bc). When measured against control and recovery current-voltage plots the estimated reversal potentials were -88 and -102mV respectively (Fig.6.11C). These values are on average slightly lower than those obtained in 5mM $[K]_o$ but the difference is not as large as would be predicted by the Nernst equation.

This lack of effect of reducing $[K^+]_o$ on the reversal potential was observed in 4 cells. The mean resting potential and $R_{m(pk)}$ in 5mM $[K^+]_o$ were -81.3 ± 5mV and 7.9 ± 1.4MΩ (n = 4). 5-HT (200μM) evoked a depolarisation of 4 ± 1.2mV and increase in $R_{m(pk)}$ to 11 ± 2.3MΩ (36 ± 9%). The reversal potential was -92.1 ± 3.7mV. When superfused with 2.5mM K^+ containing aCSF the mean resting potential was -77 ± 8.3mV and the $R_{m(pk)}$ was 12 ± 2.2MΩ. The change in membrane potential observed here is a result of changes in the stability of the electrode resistance in two of the cells. Where conditions were unchanged during this transition from 5 to 2.5mM $[K^+]_o$ the membrane potential was unaffected while an increase in $R_{m(pk)}$ from 8.9 ± 1.4 to 11 ± 2.4MΩ (n = 2) was measured. Superfusion with 5-HT evoked a depolarisation of 3.5 ± 1mV (n = 4) and an increase in $R_{m(pk)}$ of 28 ± 11% to 15.3 ± 2MΩ. The reversal

potential for the response in 2.5mM $[K^+]_o$ was -93.1 ± 5.8mV which was not significantly different from that obtained in 5mM$[K^+]_o$ (Fig.6.13).

The same neurone was then superfused with 15mM$[K^+]_o$ (Fig.6.12). This led to a depolarisation to -61mV. The peak deflection current voltage plot (Fig.6.12C) was only linear in a narrow range around the resting potential giving a measure of $R_{m(pk)}$ of 8.7MΩ (Fig.6.12Bb). Additionally there was very little sign of the time dependent sag in hyperpolarising electrotonic potentials. When 5-HT (200μM) was added to the superfusing aCSF an increase in R_m of 27% to 11MΩ was observed (Fig.6.12Ba) however this was not accompanied by a change in membrane potential (Fig.6.12A). Thus it appears that the neurone is resting at the reversal potential for the 5-HT response (Fig.6.12C) in agreement with the predicted reversal potential, i.e. -61mV.

The results from these experiments are plotted in Figure 6.13. The dashed line represents the values of the reversal potential for the different $[K^+]_o$ predicted from the Nernst equation assuming an intracellular K^+ ion concentration of 150mM. It includes additional data from 13 neurones which were superfused with aCSF containing 6.25mM K^+. A mean value of -87.3 ± 14.3mV was obtained for $E_{5\text{-}HT}$ under these conditions. It can be seen that the experimentally determined values in higher K^+ ion concentrations fit the predicted values well with little variation. At lower $[K^+]_o$ a wider variation in experimentally determined values is obtained along with deviation from the theoretically predicted values.

These mean values for reversal potentials obtained in 5mM K^+ containing aCSF are a consequence of a wide range of experimentally observed values. Thus values obtained from the point of

intersection of peak deflection I/V plots show a range of -125 to -73mV (n = 107) while the values from similar plots obtained during manual clamping range from -83 to -146mV (n = 17). These results can still be regarded as being in agreement with the suggestion that 5-HT evokes a depolarisation by decreasing a leak potassium conductance. The wide variation in reversal potentials observed will be discussed later.

THE EFFECTS OF ALTERING $[K^+]_o$ ON THE NORADRENALINE-EVOKED DEPOLARISATION

The dependence of the NAd evoked depolarisation on $[K^+]_o$ was further suggested in two experiments where the $[K^+]_o$ was raised to 10mM. In 5mM K^+ containing aCSF, noradrenaline (50μM) evoked a depolarisation of 4.5mV from a resting potential of -76mV and was associated with an increase in $R_{m(pk)}$ of 73% (8.2 to 14.2MΩ) (Fig.6.14A,B). The estimated reversal potential taken from peak deflection current voltage plots was -84mV (Fig.6.14C). Superfusion with 10mM K^+ depolarised the neurone by 6mV to a new resting potential of -70mV. Associated with this depolarisation was a fall in $R_{m(pk)}$ from 9.9MΩ in 5mM $[K^+]_o$ to 9.2MΩ in 10mM $[K^+]_o$. When retested in 10mM $[K^+]_o$ noradrenaline (50μM) evoked a 2mV depolarisation associated with an increase in $R_{m(pk)}$ of 70% (9.2 to 15.6MΩ) (Fig.6.15A,B). The reversal potential obtained by the same method in these conditions was -72.6mV (Figure 6.15C).

Combining the data from the two cells treated in this way the reversal potential in 5mM $[K^+]_o$ was -81 ± 4.7mV and in 10mM $[K^+]_o$, -72 ± 0.9mV. While the reversal potentials estimated by this method are more positive (especially in 5mM $[K^+]_o$) than those predicted by the Nernst equation, a phenomenon which may be a result of the influence of voltage-dependent rectification, altering the K^+

ion concentration of the aCSF changes the measured reversal potential of the noradrenaline evoked depolarisation in a way which would be predicted through an action on a K^+ conductance.

The experimentally determined reversal potentials obtained for 5-HT (diamonds) and NAd (circles) from each of the FM's exposed to more than one aCSF K^+ concentration are plotted in Figure 6.16 against the predicted value obtained from the Nernst equation. Points relating to the same neurone have been joined up. The theoretically predicted relationship should be linear, running through the origin with a slope of 1. As can be seen a good correlation between predicted and experimental values for both 5-HT and NAd is obtained in 10 (and 15)mM K^+aCSF. In control, 5mM K^+ aCSF, experimental reversal potentials for 5-HT show a wide variation around the predicted value while NAd reversal potentials are more positive than both the predicted and 5-HT figures (see later). In 2.5mM K^+ aCSF the experimental reversal potentials for both 5-HT and NAd are clearly more positive than predicted.

A COMPARISON OF THE EFFECTS OF 5-HT AND NORADRENALINE ON FACIAL MOTONEURONES

As mentioned earlier, where tested on the same facial motoneurones, the response to both 5-HT and noradrenaline application was a depolarisation associated with an increase in neuronal input resistance. The actions of the two neurotransmitters were, however, not identical. There was a significant difference in the concentration of the respective transmitters required to evoke a depolarisation of similar amplitude. Thus concentrations of 5-HT, 2 to 6 times higher than noradrenaline were required to evoked responses of similar

amplitude. On average a concentration of 5-HT of 200 ± 47μM was required to evoke the same depolarisation evoked by 61.9 ± 1μM noradrenaline (n = 9).

Of greater interest however was the observation that the associated increase in $R_{m(pk)}$ evoked by noradrenaline for a given depolarisation was greater than that evoked by 5-HT. This is reflected in the reversal potential for the noradrenaline evoked depolarisation being less negative than that obtained for 5-HT. In a sample of 20 motoneurones exposed to both 5-HT and noradrenaline the reversal potential for the former was more negative in 17 cases, less negative in 2 and the same in one.

Where conditions of the experiment remained constant over the period of applications of both 5-HT and noradrenaline reversal potentials of -95.4 ± 10.6 and -86.9 ± 4.8mV (n = 9) respectively were obtained (Fig.6.17). The mean depolarisation evoked by 5-HT was 4.1 ± 1.7mV and this was associated with an increase in $R_{m(pk)}$ from 8.5 ± 3.3 to 11 ± 4.2MΩ (29 ± 15%). Noradrenaline evoked a depolarisation of similar amplitude, 4.1 ± 1.1mV, but this was associated with an increase in $R_{m(pk)}$ from 8.7 ± 3.2 to 13 ± 5.1MΩ (50 ± 17%). The control resting potential for both effects was -76.8 ± 5.4mV, indicating that this difference could not be accounted for as a result of voltage dependent rectification.

The bar chart in figure 6.18 illustrates the difference in estimated reversal potentials for all FM's tested with 5-HT (200μM) and NAd (50 - 100μM). The predicted reversal potential of -91mV is illustrated by the left hand bar. The estimated reversal potentials for the actions of NAd and 5-HT in the absence of any correction for voltage dependent rectification were -85 ± 9mV (n = 21) and -93.2 ± 12.4mV (n = 107) respectively. Under conditions

where voltage dependent membrane rectification was attempted to be excluded from these measurements using manual or voltage clamp techniques this difference was maintained. NAd responses reversed close to the predicted value with a mean value of -94 ± 5.2mV (n = 5) while the 5-HT response reversed at a more negative value of -109 ± 17.3mV (n = 19).

VOLTAGE CLAMP STUDIES OF THE ACTION OF 5-HT AND NAd ON FACIAL MOTONEURONES

When FM's were voltage clamped at or near resting potential superfusion of 5-HT and NAd evoked a slowly developing inward current, with a time course similar to the depolarisation seen in current-clamp. The inward current was associated with a decrease in conductance. For example, the chart record in figure 6.19 shows a FM clamped at its resting potential of -67mV. Addition of 5-HT (200μM) and subsequently NAd (50μM) to the bathing aCSF evoked a slow inward current with a steady-state peak amplitude, in both cases, of -0.5nA. Input conductance was tested with a voltage step command -20mV in amplitude and 250msec duration at a frequency of 0.2Hz. Both 5-HT and NAd evoked inward currents were associated with a decrease in conductance which was greater for the NAd evoked response, an observation consistent with the current-clamp studies reported earlier.

Figure 6.20Aa-e show the currents evoked by step voltage commands of varying amplitude taken at the equivalently labelled times in figure 6.19a-e. Currents evoked by 250msec voltage step commands demonstrated the time dependent slow inward relaxation characteristic of inward rectification in FM's described earlier. In the presence of 5-HT and NAd these evoked currents were smaller than control currents when measured at both the instantaneous and

steady-state levels confirming the decrease in conductance seen on the chart record (Fig.6.19). Current voltage plots taken from the records in figure 6.20Aa-e are illustrated in figure 6.20B,C. Control instantaneous and steady-state I/V relationships both displayed non-linearity as the membrane was hyperpolarised. In the presence of 5-HT the instantaneous and steady-state current voltage plots intersected with the control curves at the same potential, but this was more negative than the crossover point obtained for instantaneous and steady-state NAd plots.

The reversal potentials were more clearly observed by obtaining plots of the net inward current evoked by 5-HT and NAd at different potentials by subtracting currents evoked in control and 5-HT and NAd treated conditions (Fig.6.21). The reversal potentials thus obtained were -117mV of both inst. and ss 5-HT evoked current (Fig.6.21A,B), and -100mV for inst. NAd current (Fig.6.21C) and -96mV for ss NAd evoked current (Fig.6.21D). In all cases the net currents appeared to be linear despite the rectification of the whole cell membrane currents. Voltage-clamp of the transmitter evoked responses was obtained in three neurones for 5-HT and two neurones for NAd. Inward currents were evoked in all 5 cases. The mean reversal potentials for the two transmitters were -104.7 ± 19.7mV for 5-HT and -94.2 ± 8.3mV for NAd, agreeing with corresponding values obtained using current clamp techniques.

DEPOLARISATION OF FACIAL MOTONEURONES BY 5-HT IS UNAFFECTED BY TTX

The depolarisation evoked by 5-HT was shown to be a direct post-synaptic action on the motoneurone as the response was essentially unaffected by superfusion with Tetrodotoxin (TTX; 1μM) which prevents synaptic transmission through an inhibition of Na^+ dependent action potentials.

Superfusion of 5-HT (200μM) evoked a 9mV depolarisation from a resting potential of -83mV associated with an increase in $R_{m(pk)}$ from 3.2 to 6MΩ (Fig.6.22Aa,b). Recovery to -81mV was obtained and after rebalancing of the electrode $R_{m(pk)}$ was 4.5MΩ (not shown). TTX (1μM) was then added to the superfusing aCSF leading to abolition of Na^+ dependent action potentials (Fig.6.22Ac). The resting potential and $R_{m(pk)}$ were not altered by the presence of TTX being -81mV and 4.6MΩ respectively. Subsequent application of 5-HT (200μM) evoked a 7mV depolarisation and an increase in $R_{m(pk)}$ to 6.7MΩ (Fig.6.22Ad) values similar to those obtained when TTX was absent. The reversal potential estimated from the peak deflection current voltage relationships were -92.5 and -95mV in the absence and present of TTX respectively (Fig.6.22B,C).

The mean response to 5-HT in the presence of TTX was a depolarisation of 8.7 ± 3.8mV from a resting potential of -80.7 ± 1.5mV (n = 3). The associated increase in $R_{m(pk)}$ was from 10.4 ± 5MΩ to 13.2 ± 5.7MΩ and the estimated reversal potential was -90.7 ± 6.7mV. This response is the same as the control 5-HT response of a 9.3 ± 6.5mV depolarisation from a resting potential of -83.3 ± 2.9mV associated with an increase in $R_{m(pk)}$ from 9.7 ± 5.8MΩ to 15.2 ± 8.7MΩ and a reversal potential of -96.3 ± 8.6mV (n = 3).

It should be pointed out that two neurones with higher control resting potentials (-67 and -69mV) showed a different response to 5-HT in the presence of TTX which is illustrated for one cell in Fig.6.23. The motoneurone, resting at -69mV, was depolarised by 11mV when exposed to 5-HT (200μM) (Fig.6.23Aa,b). The control peak deflection I/V relation was linear throughout the tested range giving a $R_{m(pk)}$ of 13.2MΩ. In the presence of 5-HT (200μM) the I/V plot was linear over a narrower range giving a $R_{m(pk)}$ of 17.8MΩ.

Thereafter it showed pronounced rectification such that no point of intersection with the control I/V curve was observed. Extrapolation of the linear portions of I/V plots gave an estimated reversal potential of -102mV (Fig.6.23B). Addition of TTX (1μM) did not alter the resting membrane potential or the responses to hyperpolarising current pulses. Thus $R_{m(pk)}$ in the hyperpolarising direction was maintained (Fig.6.23Ca). However, electrotonic responses to depolarising current pulses exhibited strong outward rectification such that the peak and steady state current voltage relationships in this direction were non-linear, a phenomenon not seen in neurones with more negative resting potentials (Fig.6.23Ca).

When 5-HT was applied a depolarisation of 9mV, similar in magnitude to that seen in the absence of TTX was obtained, however, the associated increase in $R_{m(pk)}$ estimated over the hyperpolarising linear portion of the current-voltage plot was greatly reduced to only 7% (14.7 to 15.8MΩ) (Fig.6.23Cb). Thus the I/V plots do not cross in the range tested and an extrapolated value for the point of intersection was estimated at -193mV (Fig.6.23D). The prominence of the outward rectification observed in the depolarising range of electrotonic potentials appears to have masked the normal increase in $R_{m(pk)}$ observed in the presence of 5-HT. Unfortunately, the inability of the microelectrode to pass sufficient current to return the neurone to the resting level prevented evaluation of a change in $R_{m(pk)}$ evoked by 5-HT at more hyperpolarised levels.

5-HT DOES NOT SUPPRESS THE AHP OF FM'S

In addition to a direct depolarising action of 5-HT on the post-synaptic membrane a second excitatory effect of 5-HT has been observed in hippocampal CA_1 neurones, (Colino and Halliwell, 1987) lateral septal neurones (Joels et al, 1987) and spinal motoneurones

(Hounsgaard et al, 1989; Wallen et al, 1989). It involves a suppression of the afterhyperpolarisation (ahp) following spike firing which normally prevents prolonged neuronal discharge, producing accommodation of action potential firing. This action of 5-HT prolongs firing in response to depolarising stimuli. It was of interest to see whether the direct excitatory effects of 5-HT on facial motoneurones were accompanied by an effect on the spike ahp.

Figure 6.24 shows averaged traces of single spikes evoked by a current pulse 1msec in duration from the neurone shown in Figures 4.1 to 4.4. In the presence of 200μM 5-HT the neurone was resting at the depolarised level of -67mV. A depolarising current pulse of 2.2nA evoked a single spike which had a peak amplitude of 94mV (not fully reproduced). It was followed by the series of after potentials described previously, a fast ahp, a DD and a slow longer lasting ahp. The DD had a peak 11.1mV above resting potential. The slow ahp had a maximum amplitude of -1.7mV and a duration of 46msec measured from the extrapolated point where the downstroke of the action potential crosses the resting potential (Fig.6.24B). When the neurone had recovered from the depolarisation evoked by 5-HT (to -71mV) it was manually depolarised to -67mV by passing +0.5nA D.C. through the intracellular electrode. A step current pulse of +2.5nA (1msec) was then required to evoke a single spike. It again overshot zero mV with an amplitude of 94mV (not shown). The following DD had an amplitude of 10.5mV while the ahp undershot resting potential by 1.7mV with a duration of 37msec (Fig.6.24A).

When superimposed (Fig.6.24C) the averaged records show clearly that there is little difference between the amplitude and duration of the ahp in the presence and absence of 5-HT. The threshold for action potential generation was also unaffected by the presence of

5-HT. It is equally apparent that the DD shows an increase in amplitude and duration in the presence of 5-HT. It is likely that this is a consequence of the increased input resistance and lengthening of the time constant induced by 5-HT as well as a contribution by the underlying electrotonic potential and not a direct effect on events mediating the DD.

The same results were obtained in a second motoneurone where the membrane potential at the peak of the hyperpolarisation evoked by 5-HT was offset back to the control level (-71mV). The ahp showed no change in amplitude (-2.6mV control against -2.6mV in 5-HT) while the DD was again larger in 5-HT (9.8mV control against 11.9mV in 5-HT).

Further evidence against an effect of 5-HT on the ahp seen after spikes in facial motoneurones can be gained from the observation that when evoked by a sustained depolarising current pulse the ahp seen in the presence of 5-HT was often the same amplitude if not slightly larger than that seen in control conditions (e.g. Figs.6.2, 6.25). Thus, increased excitability of FM's in the presence of 5-HT can be attributed to depolarisation associated with increased R_m and a lengthening of τ and not a reduction in accommodation via a suppression of the spike ahp.

THE DOSE DEPENDENCY OF THE 5-HT EVOKED DEPOLARISATION

The amplitude of the depolarisation in response to 5-HT (200μM) varied considerably. On one occasion no effect of this concentration of 5-HT was observed on either membrane potential or R_m while the range of depolarisation obtained excluding this observation was 2 to 16mV (n = 70). From a mean resting potential of -73.8 ± 6mV the average depolarisation was 6.4 ± 3.6mV. This was associated with a change in $R_{m(pk)}$ of 44 ± 32% from 9 ± 4MΩ to

12.7 ± 5.5MΩ (Range 7 to 131%). Where measurements uncontaminated by IR were made a lengthening of τ from 2.9 ± 1.3 to 3.7 ± 1.5msec was detected (n = 38). The mean reversal potential estimated from peak deflection current voltage plots was -94.2 ± 12.4mV (n = 70).

The mean depolarisation evoked by 5-HT (150μM) was 5.96 ± 3.6mV (range 0 to 17mV) from a resting potential of -71.2 ± 5mV (n = 23). The $R_{m(pk)}$ increased from 11.4 ± 4.2MΩ to 15.3 ± 6MΩ an increase of 35 ± 31% while the reversal potential was estimated at -93.4 ± 12.7mV. 5-HT (100μM) was applied to 13 neurones of which 4 (31%) failed to respond with a depolarisation. The mean depolarisation obtained was 4.1 ± 3.5mV (range 0 to 10mV) from a resting potential of -70.9 ± 3.3mV (n = 13). $R_{m(pk)}$ increased from 8.9 ± 4 to 10.7 ± 3.8MΩ (28 ± 38%) and where calculated the reversal potential was -92.8 ± 8.9mV (n = 9).

Given the wide variation in responses obtained to single dose applications of 5-HT (100 to 200μM) onto motoneurones it was decided to be of importance to assess more accurately the dose response relationship for the 5-HT evoked depolarisation so that a suitable test concentration of 5-HT could be chosen for future pharmacological experiments. Thus a series of experiments in which different concentrations of 5-HT were applied to the same neurone were performed. Results were similar using either a continuous or discontinuous 5-HT application protocol. In the former increasing concentrations of 5-HT were superfused without allowing baseline recovery in between doses while in the latter the neurone was allowed to recover from each 5-HT application before a subsequent application was made. Figures 6.25 to 6.28 illustrate that the amplitude of the depolarisation is indeed related to the 5-HT concentration.

The motoneurone in Figure 6.25a had a resting potential of -76mV and $R_{m(pk)}$ was 6.7MΩ. Addition of 150μM 5-HT to the superfusing aCSF led to a 5mV depolarisation and increase in $R_{m(pk)}$ to 8.6MΩ (27%) (Fig.6.25b). Increasing the 5-HT concentration to 200μM led to further depolarisation to a plateau 9mV above control levels and $R_{m(pk)}$ also increased to 10MΩ (49%) (Fig.6.25c). Raising the 5-HT level to 250μM increased the depolarisation to -64mV, 12mV above the control level. This was associated with a further increase in $R_{m(pk)}$ to 10.9MΩ, 63% higher than the control level (Fig.6.25d). Fig. 6.26 shows the peak deflection current-voltage plots for the control and each concentration of 5-HT. The estimated reversal potential can be seen to be constant at each level of depolarisation, being -95.7mV, -95.9mV and -95.4mV for 150, 200 and 250μM 5-HT respectively. The cell subsequently recovered to -73mV with an $R_{m(pk)}$ of 7.1MΩ on washing with 5-HT free aCSF (Fig.6.25e). A second cell shown in Figure 6.27 shows a similar dose response relationship obtained by applying three different 5-HT concentrations in a discontinuous protocol. A first application of 5-HT (150μM) depolarised the cell by 6mV from a resting potential of -71mV (Fg.6.27Ba,b). $R_{m(pk)}$ increased by 20% from 9.7 to 11.6MΩ and the estimated reversal potential was -100.7mV (Fig.6.28B). After recovery of Vm (-70mV) and $R_{m(pk)}$ (11.2MΩ) the neurone was superfused with 100μM 5-HT. The cell depolarised to a plateau 3mV above the new control level and $R_{m(pk)}$ increased to 12.3MΩ (10%) with an estimated reversal potential of -98mV (Fig.6.27Aa,b; 6.28A). After a second period of recovery to -70mV ($R_{m(pk)}$ = 11MΩ) application of 200μM 5-HT evoked a depolarisation of 10mV with a 32% increase in $R_{m(pk)}$ to 14.6MΩ (Fig.6.27Ca,b). The reversal potential was estimated by extrapolation of the linear portions of

the current voltage plots because they did not intersect in the range shown. The value obtained was -101.9mV (Fig.6.28C).

Two or three applications of 5-HT at different concentrations (100 to 250μM) were made on 11 motoneurones. Each neurone displayed an increased depolarisation in response to a raised concentration of 5-HT. However, while the relative amplitude to a particular dose of 5-HT remained fairly constant the absolute value of the depolarisation varied considerably, as seen earlier. The mean depolarisation values for the dose-response relationship are shown in Fig.6.29. 5-HT (100μM) evoked a depolarisation of 3.2 ± 1.9mV (range 0 to 6mV; n = 5); 5-HT (150μM) evoked a depolarisation of 4.5 ± 3.2mV (range 0 to 9mV; n = 10); 5-HT (200μM) evoked a depolarisation of 6 ± 3.9mV (range 1 to 13mV; n = 8) and 5-HT (250μm) evoked a depolarisation of 7.3 ± 3.4mV (range 4 to 12mV; n = 3). For each group the control resting potential was similar (-71.3 ± 7.3mV; 250μM; -71.1 ± 4.9mV; 200μM; -70.2 ± 4.7mV; 150μM; -70.6 ± 1.6mV; 100μM 5-HT).

A clear D/R relationship between the change in $R_{m(pk)}$ and the concentration of 5-HT was not established. The control $R_{m(pk)}$ values showed some variation between the groups (12 ± 3.8MΩ, 250μM; 9.8 ± 3.9MΩ, 200μM; 12.2 ± 5MΩ, 150μM; 13.9 ± 5.8MΩ, 100μM) such that the change in $R_{m(pk)}$ could not be compared directly. Even when expressed as a percentage change a clear correlation to dose was not established. Thus 100μM 5-HT evoked a 24 ± 16% increase in $R_{m(pk)}$, 150μM a 25 ± 18% increase 200μM a 32 ± 22% increase and 250μM a 31 ± 22% increase. The reasons for this poor correlation are not clear as in the two examples shown an increase in the amplitude of the depolarisation was quite definitely accompanied by increases in the $R_{m(pk)}$. One possible explanation may be related

to the variation in reversal potentials observed previously, such that there is an unequal distribution of neurones with more negative reversal potentials in the higher concentration groups (i.e. larger depolarisations are generated with smaller changes in input resistance).

The data indicates that the dose response relationship for the 5-HT response lies over the range tested. Maximal responses were not evaluated in any individual case though the mean D/R curve indicates that the steep rising phase is over the range 100 to 200μm and that a levelling off is likely to occur after the 250μM maximum dose used in this study. It was therefore decided that the use of 150 to 200μM 5-HT as a test dose in pharmacological experiments would on balance provide the just sub-maximal response optimal for these studies. Given the variation in amplitude of the response and possibly the dose-response curve it was thought that these doses would never be so supra-maximal as to obscure pharmacological antagonism. Thus any potential antagonists of the 5-HT response would not have to shift the dose-response relationship very far to the left before antagonistic effects on the test dose of 5-HT would be observed.

THE DOSE-DEPENDENCY OF THE NAD EVOKED DEPOLARISATION

The sensitivity of motoneurones to noradrenaline varied as was seen with 5-HT. The mean response to 100μM noradrenaline (n = 8) was a depolarisation of 5.13 ± 2.7mV from a resting potential of -75.6 ± 7.2mV associated with an increase in $R_{m(pk)}$ from 12.4 ± 8.6 to 18 ± 12.1MΩ (n = 8) and a lengthening of τ from 4.1 ± 2.8 to 5.6 ± 3.2msec (n = 6). Noradrenaline (50μM; n = 11) evoked a depolarisation of 4.7 ± 2.1mV from a resting potential of -71.5 ± 4.3mV an increase in $R_{m(pk)}$ from 9.6 ± 3.9 to 14.1 ± 4.5MΩ and a

lengthening of τ from 2.5 ± 0.3 to 3.5 ± 1.1msec (n = 7). 25μM noradrenaline (n = 2) evoked a depolarisation of 4.5 ± 2.1mV from a resting potential of -72 ± 9mV a change in $R_{m(pk)}$ from 9.6 ± 3.1 to 15.1 ± 3.6MΩ and an increase in τ from 2.5 ± 0.6 to 4.3 ± 0.5msec. The reversal potentials obtained from all these experiments, estimated from the point of intersection of peak deflection current-voltage plots, were pooled (given the similarity in amplitude of response and resting potential) giving a value of -85 ± 9mV (n = 21).

The dose-dependency of the noradrenaline induced depolarisation and increase in input resistance is illustrated in Figure 6.30. Noradrenaline concentrations of 10, 25, 50 and 75μM evoked depolarisation of 1, 3, 4.5 and 5mV associated with increases in $R_{m(pk)}$ of 24, 43, 73 and 79% respectively (Figs.6.30B,C). The estimated reversal potential remained constant being -82.3, -84.1, -83.2 and -84.7mV for each concentration respectively.

PHARMACOLOGY OF THE 5-HT EVOKED DEPOLARISATION OF FACIAL MOTONEURONES

Methysergide

Methysergide is a non-selective antagonist of 5-HT_1 and 5-HT_2 receptor subtypes with only low affinity for 5-HT_3 sites (Bradley et al, 1986; Fozard and Gray, 1989). A partial agonist action has also been demonstrated in some peripheral target tissues (Bradley et al, 1986) and possibly also on hippocampal CA_1 neurones (Andrade and Nicoll, 1987a). In vivo the facilitation of excitability and depolarisation evoked by 5-HT of facial motoneurones could be antagonised by iontophoretic and intravenous administration of methysergide (VanderMaelen and Aghajanian, 1980). In the following

series of experiments methysergide has been demonstrated to selectively antagonise 5-HT evoked depolarisation of facial motoneurones but not that evoked by noradrenaline, in vitro.

Figures 6.31 to 6.35 illustrate the effects of methysergide on 5-HT and noradrenaline evoked depolarisations recorded from the same motoneurone using the current clamp technique. The continuous chart record (Fig.6.31) shows the effects of the various treatments on the membrane potential (V_m) and input resistance (R_m) of the neurone as indicated by voltage responses to a 1nA hyperpolarising current pulse, 120msec in duration, injected through the microelectrode at a frequency of 1Hz. At the points marked a-j current-voltage relationships were established by injecting hyperpolarising and depolarising current pulses of various amplitude into the neurone through the microelectrode. These are illustrated in Figs.6.32, 6.33 and will be referred to later. Superfusion of 5-HT (150μM) for 8.5 minutes evoked a depolarisation of 5mV from a resting potential of -78mV. After washing with normal aCSF for 9 minutes recovery to -78mV was obtained. Subsequent superfusion of noradrenaline (25μM) for 9 minutes evoked a depolarisation of 3mV. After recovery back to -78mV, methysergide (50μM) was added to the aCSF. Twenty minutes superfusion with 50μM methysergide did not alter resting membrane potential or R_m. Subsequent co-application of 5-HT (150μM) and methysergide (50μM) for 10 minutes led to only a small change in Vm (about 1mV) and no change in R_m. After a period of washing with methysergide-containing aCSF to remove 5-HT from the chamber the neurone was superfused with noradrenaline (25μM) and methysergide containing aCSF. Despite the continued presence of methysergide for 40 minutes noradrenaline still evoked a depolarisation of 3.5mV, the same as seen in the control response.

The superimposed voltage responses obtained by injection of current pulses through the intracellular microelectrode and the current voltage relationships taken from measurements of the peak voltage-deflection at points a-f throughout the experiment illustrate more clearly the effects of methysergide on 5-HT and noradrenaline evoked depolarisations (Figs.6.32, 6.33). The depolarisation of 5mV evoked by 5-HT was accompanied by an increase in $R_{m(pk)}$ from 7.5 to 11MΩ (47%) recovering to 7.4MΩ after washing with drug-free aCSF (Fig.6.32A). A reversal potential of -89.6mV was determined from the point of intersection of peak deflection current-voltage plots (Fig.6.32B). After superfusion with methysergide, $R_{m(pk)}$ was 7.8MΩ. Co-application of 5-HT (150μM) evoked a small depolarisation of 1.5mV with only a small increase in $R_{m(pk)}$ to 8.2MΩ indicated by the small parallel shift in the current-voltage plots (Fig.6.32C,D). Washing with methysergide only, led to a 1mV recovery in Vm to -77mV while $R_{m(pk)}$ remained at 8.2MΩ. This suggests that the changes in Vm and R_m were not a direct effect of 5-HT.

Application of noradrenaline (25μM) prior to methysergide exposure evoked a depolarisation of 3mV associated with an increase in $R_{m(pk)}$ from 7.4 to 12.6MΩ (70%) and recovering to 7.8MΩ after washing with normal aCSF (Fig.6.33A). The current voltage plot of peak voltage deflections shows a point of intersection at -83.4mV (Fig.6.33B). Application of methysergide (50μM) for 40 minutes did not effectively alter the noradrenaline response. A 3.5mV depolarisation was accompanied by an increase in $R_{m(pk)}$ from 8.2 to 11.6MΩ (41%) with recovery to 7.8MΩ (Fig.6.33C). The estimated reversal remained unchanged at -83.9mV (Fig.6.33D).

A second neurone superfused with methysergide (100μM) also showed the response to noradrenaline to be unaffected. A control depolarisation of 4mV associated with an increase in $R_{m(pk)}$ of 38% in response to noradrenaline (50μM) had a reversal potential of -84.9mV. After application of methysergide (100μM) for 20 minutes noradrenaline again evoked a 4mV depolarisation associated with a 23% increase in $R_{m(pk)}$ and giving a reversal potential -85.9mV.

The antagonism of the 5-HT response was very long-lasting. A challenge with 5-HT (150μM) 90 minutes after switching back to methysergide-free aCSF still failed to evoke a depolarisation of the FM in figure 4.30. However, in another neurone (not shown) methysergide induced antagonism of the 5-HT evoked depolarisation was surmounted by raising the concentration of 5-HT from a test dose of 100μM to 200μM, however, this still required a wash period of 100 minutes. In this case the control response to 5-HT (100μM) had been a depolarisation of 3mV and an increase in $R_{m(pk)}$ of 34% reversing at -82.4mV. Methysergide (100μM) for 25 minutes completely blocked this response. After 100 minutes in drug-free aCSF, 5-HT (100μM) still failed to evoke a response, while increasing the concentration to 200μM evoked a 4mV depolarisation with a 23% increase in $R_{m(pk)}$ and a reversal potential of -89.5mV.

Methysergide, in concentrations ranging from 10 to 200μM had no effect on the passive membrane properties of facial motoneurones (n = 10). The mean resting Vm and $R_{m(pk)}$ being -74 ± 4.2mV and 8.9 ± 2.7MΩ before methysergide application and -73 ± 3.6mV and 9.2 ± 2.3MΩ after it. Values for each tested concentration are shown in table 6.1. Nine of these neurones had previously been depolarised

by 5-HT (100 to 200μM) amplitudes ranging from 2 to 14mV and associated with increases in $R_{m(pk)}$ of between 14 and 119%. The mean reversal potential was -91.6 ± 9.6mV (n = 9).

Six of these neurones were subsequently retested with 5-HT in the presence of methysergide. Methysergide (100μM, n = 2) virtually completely abolished the 5-HT response reducing the depolarisation from 8.5 ± 5.5mV to 1 ± 1mV and the increase in $R_{m(pk)}$ from 77 ± 43% to 14 ± 14%. As seen in Figures 6.31 to 6.33 50μM methysergide was also effective at blocking the 5-HT response. Methysergide at a concentration of 10μM was only partially effective at blocking 5-HT responses. The 5-HT response of one neurone was completely blocked at this concentration whereas in two others 5-HT evoked a smaller response after methysergide superfusion (Fig.6.34). The control response in these 2 neurones to 5-HT was a depolarisation of 6.5 ± 2.5mV associated with an increase in $R_{m(pk)}$ from 9.8 ± 3MΩ to 14.1 ± 3MΩ and a reversal potential of -95 ± 6mV. After methysergide (10μM) the depolarisation was reduced to 3 ± 2mV associated with an increase in R_m from 7.9 ± 1MΩ to 11 ± 0.5MΩ and a reversal potential of -83 ± 5mV.

LY-53857 [4-isopropyl-7-methyl-9-(2-hydroxy-1-methylpropoxycarbonyl)4,6,6A,7,8,9,10,10A-octahydroindolo(4,3-FG)quinoline maleate]

LY-53857 has been shown to be a potent antagonist of central and peripheral 5-HT_2 receptors with approximately 300,000-fold lower affinity for α-adrenergic receptors (Cohen et al, 1983). Of added advantage for this study is its free-solubility in aqueous media. When tested against the 5-HT evoked depolarisation of facial motoneurones it was found to effectively antagonise this response at concentrations of 50 and 100μM.

The motoneurone in Fig.6.35 had a resting potential of -72mV, and a $R_{m(pk)}$ of 16.3MΩ. In response to bath-applied 5-HT (150μM), a depolarisation to a plateau 5mV above resting Vm associated with an increase in $R_{m(pk)}$ of 23% was obtained (Fig.6.35Aa to Ac). The current-voltage plots were found not to intersect but extrapolation of the linear portions gave an estimated reversal potential of -95mV (Fig.6.35B). LY-53857 (50μM) was then added to the superfusing aCSF for 20 minutes. At the end of this period the resting potential had depolarised by 2mV with a small (0.4MΩ/2%) increase in $R_{m(pk)}$. This is unlikely to be due to an agonistic action through the 5-HT receptor as the estimated reversal potential was -112mV much more -ve than that for the 5-HT evoked depolarisation. (A second cell also depolarised by 2mV in response to LY-53857 (50μM) superfusion though this was without any change in $R_{m(pk)}$). Retesting with 5-HT (150μM) was found to evoke a reduced depolarisation of 2mV associated with an increase in $R_{m(pk)}$ of 7% (1.1MΩ), responses which were 40% and 30% of control changes in V_m and $R_{m(pk)}$ respectively (Fig.6.35Ad,Ae). A reversal potential of -98mV was directly obtained from the point of intersection of I/V plots in their non-linear regions (Fig.6.35C).

In an attempt to obtain data which confirms the antagonist activity of LY-53857 without any changes in control membrane potential, the ability of 50μM LY-53857 to suppress an ongoing 5-HT depolarisation was tested. A sustained depolarisation of +4mV from a resting Vm of -72mV associated with an increase in $R_{m(pk)}$ of 1.42MΩ (22%) was evoked by 5-HT (200μM). Co-application of LY-53857 50μM for 25 mins reduced this to a depolarisation of +2mV and a change in $R_{m(pk)}$ of 1MΩ (16%) without altering the estimated reversal potential (-89mV 5-HT only; -84mV 5-HT and LY-53857).

Increasing LY-53857 to 100μM for a further 20 minutes virtually completely abolished the 5-HT response reducing it to a depolarisation of 1mV and an increase in $R_{m(pk)}$ of 0.4MΩ.

Taken together LY-53857 (50μM; n = 3) reduced the 5-HT evoked depolarisation of 4.7 ± 0.6mV and associated increase in $R_{m(pk)}$ of 2.5 ± 1.1MΩ to 2 ± 0mV and 0.9 ± 0.3MΩ respectively. The histogram of figure 6.36 illustrates the antagonism of the 5-HT evoked increase in $R_{m(pk)}$, expressed as a percentage of control $R_{m(pk)}$, by LY-53857 for each of the three FM's tested.

Ketanserin

Ketanserin has been demonstrated to bind with high affinity to 5-HT_2 sites in both the peripheral and central nervous systems (Leysen et al, 1981). A recent autoradiographic study demonstrated that there was a moderate density of ^{3}H-ketanserin binding in the rat facial motor nucleus (Fischette et al, 1987) thus it was necessary to see whether this binding site correlates to the functional receptor mediating depolarisation of facial motoneurones.

Ketanserin was superfused at concentrations of 1 to 100μM on three different facial motoneurones in vitro. In all cases, even after exposure times of over 60 minutes, the response to 5-HT appeared to be depressed but not completely abolished unlike the effects seen previously with methysergide. The actions of ketanserin on the 5-HT evoked depolarisation are illustrated in figures 6.37 to 6.40 and summarised in the histogram of Fig.6.41 and Table 6.2. Superfusion of 1uM ketanserin for 20 minutes appeared to reduce the test 5-HT evoked depolarisation from a control of 10mV to 7mV and the associated change in $R_{m(pk)}$ from 75% (4.3MΩ) to 49% (3.2MΩ) (Fig.6.37a-e). The estimated reversal potential for the 5-HT effect was similar in both cases, -94mV before and -93mV after

ketanserin application (Fig.6.38A,B). Increasing the ketanserin concentration to 10μM for a further 20 minutes led to a reduction in the 5-HT evoked depolarisation to 5mV and associated increase in $R_{m(pk)}$ to 38% (2.9MΩ) (Fig.6.37f,g). During the course of the experiment the baseline Vm fell by 1mV to -81mV. Additionally there was an increase in control $R_{m(pk)}$ from an initial value of 5.8MΩ to 7.7MΩ at the end. This did not appear to be a result of the presence of ketanserin as only part of the increase (6.5 to 7.7MΩ) occurred during its presence.

In an attempt to obtain more positive evidence for antagonism of the 5-HT evoked depolarisation higher concentrations of ketanserin, combined with longer exposure times, were employed. Figures 6.39 and 6.40 show the actions of 100μM ketanserin on a different motoneurone. After 20 minutes the depolarisation and increase in $R_{m(pk)}$ in response to a test 5-HT (200μM) application had been reduced from 8 to 5mV and 74% (4MΩ) to 32% (2.2MΩ) respectively (Fig.6.39a-d), with little change in the reversal potentials of -95 and -99.5mV (Figs.6.40A,B). In case penetration of the slice by ketanserin was a problem, and hence the incomplete block is a result of a failure to allow full equilibration, ketanserin application was maintained for one hour. After this time 5-HT (200μM) was still able to evoke a depolarisation of 3mV associated with an increase in $R_{m(pk)}$ of 25% (1.7MΩ) (Fig.6.39e,f) and a reversal potential of -94.5mV (Fig.6.40C). Again the $R_{m(pk)}$ increased over the course of the experiment from 5.4 to 6.8MΩ without any associated change in Vm.

Thus sustained application of high concentrations of ketanserin appears to show a partial block of the 5-HT response though confirmation of this by recovery of the control response could not

be obtained. However, given the high affinity ketanserin shows for 5-HT_2 binding sites (Leysen et al, 1981) its inability to completely block the 5-HT evoked response even at very high concentrations suggests a lack of affinity for the receptor mediating this response.

Spiperone

Radioligand binding studies have shown the neuroleptic, Spiperone to selectively distinguish between 5-HT binding site subtypes, labelling with high affinity 5-HT_2 and 5-HT_{1A} sites but having low affinity for other 5-HT sites (Peroutka and Snyder, 1979; Pedigo et al, 1981). The relative affinity of the 5-HT_{1A} and 5-HT_2 sites for [^{3}H]-5-HT can be used in conjunction with spiperone to differentiate between these sites. Study of the effect of this compound on 5-HT responses of FM's was pursued in an attempt to further elucidate the receptor subtype responsible for depolarisation. No effective antagonism of the 5-HT evoked depolarisation was obtained using concentrations of Spiperone regarded as supramaximal for actions at both 5-HT_{1A} and 5-HT_2 sites (Figs.6.42 and 6.43). The high lipophilicity of this compound has been claimed to be responsible for slow equilibration in the test system thus long preincubation periods are necessary (Andrade & Nicoll, 1987a). In both the DR and hippocampal slice preparations these incubation periods have been demonstrated to be effective at antagonising 5-HT evoked hyperpolarisation (Andrade and Nicoll, 1987a; Rainnie, 1988). Spiperone (10 or 100μM) was superfused on 6 FM's for periods lasting from 30 to 110 minutes. All neurones had previously been shown to respond to 5-HT with a depolarisation of 5.7 ± 3.8mV and increase in $R_{m(pk)}$ of 3 ± 2.8MΩ. The mean resting potential, -71 ± 3 (n = 6) and $R_{m(pk)}$, 9.4 ± 6.3MΩ (n = 4),

before Spiperone application were similar to those obtained after superfusion, -71 ± 4mV and 9.6 ± 5.2MΩ, respectively, indicating that passive membrane properties are unaffected by prolonged application of spiperone. The motoneurone shown in Figure 6.42 illustrates the poor antagonistic effects of Spiperone on the 5-HT evoked depolarisation. The neurone had a resting potential of -69mV and a $R_{m(pk)}$ of 7.7MΩ measured from the slope of the I/V plot in Fig.6.43A, constructed from peak deflections of graded hyperpolarising and depolarising electrotonic potentials shown in Fig.6.42a. Application of 200μM 5-HT evoked a depolarisation which plateaued at a level 13mV above rest and was associated with an increase in $R_{m(pk)}$ of 93% (7.12MΩ) (Fig.6.42b). The estimated reversal potential for this effect obtained from the current voltage plot (Fig.6.43A) was -84mV. The neurone was then superfused with 10μM spiperone for 75 minutes. During this time the resting membrane potential fell to -74mV and $R_{m(pk)}$ rose to 8.7MΩ suggesting further "sealing" of the electrode within the neuronal membrane. After this period of spiperone superfusion, 5-HT (200μM) was co-applied. A depolarisation of 8mV associated with an increase in $R_{m(pk)}$ of 83% (7.2MΩ) and an apparent reversal potential of -84mV was obtained (Fig.6.42c,d, 6.43B). The difference in amplitude of the depolarisation but not the change in $R_{m(pk)}$ compared with the control 5-HT response suggests that no antagonism has occurred and that the depolarisation is smaller due to the settling of the resting potential closer to the equilibrium potential for the 5-HT response.

In an attempt to obtain antagonism of this response the spiperone concentration was increased to 100μM and applied for a further 30 minutes before being rechallenged with 100μM 5-HT. The

subsequent depolarisation measured 7mV and was associated with an increase in $R_{m(pk)}$ of 85% (7.04MΩ), the estimated reversal potential being unchanged at -84mV (Figs.6.42e,f; 6.43C).

A second neurone which was depolarised by 2mV with an increase of $R_{m(pk)}$ of 0.5MΩ by 5-HT (200μM) was still depolarised by 2mV with an increase in $R_{m(pk)}$ of 0.45MΩ after superfusion of 100μM spiperone for 30 minutes. The resting membrane potential remained at -72mV throughout the experiment and the reversal potential was -90mV for the control response and -95mV for the spiperone treated response. It is interesting to note that on two occasions motoneurones impaled after the slice had previously been exposed to spiperone (10μM) for up to one hour responded reversibly to 5-HT (150μM) with depolarisations of 9 and 6mV. Both were associated with increases in $R_{m(pk)}$ though the former could not be measured accurately due to the firing of action potentials at the peak of the response while the latter showed a change of 5.4MΩ.

The results indicate that spiperone, at concentrations and exposure times shown previously to antagonise the 5-HT evoked hyperpolarisation of DR and hippocampal CA_1 neurones, is ineffective against 5-HT evoked depolarisation of FM's.

Methiothepin

Methiothepin is a non-selective 5-HT_1 receptor antagonist shown to be active against 5-HT hyperpolarisations of CA_1 pyramidal cells (Andrade and Nicoll, 1987a). In our studies great care was taken to ensure that methiothepin reached the preparation in the concentrations indicated by using plastic reservoirs in place of the normal glass ones to prevent adhesion. Methiothepin at concentrations of 1, 10 and 100μM failed to antagonise 5-HT evoked depolarisations of facial motoneurones (Fig.6.44). 5-HT (200μM)

evoked a depolarisation of 5mV from a resting potential of -71mV in the neurone shown in Fig.6.44Aa,b. This was accompanied by an increase in $R_{m(pk)}$ of 1.9MΩ (23%) and extrapolation of the current-voltage plots shown in Fig.6.44B, gave an estimated reversal potential of -94mV. Superfusion of Methiothepin (10μM) for twenty minutes did not significantly alter the resting membrane potential (-72mV) or $R_{m(pk)}$ (8.2MΩ). Co-application of 5-HT (200μM) for a further 10 minutes evoked a depolarisation of 8mV associated with an increase in $R_{m(pk)}$ of 3.28MΩ (40%) (Fig.6.44Ac,d) with an estimated reversal potential of -96mV (Fig.6.44C). This apparent potentiation of the 5-HT response was not observed in two other neurones exposed to 1, 10 and 100μM methiothepin. Even prolonged application failed to suppress the 5-HT response. Thus a depolarisation of 5mV associated with an increase in $R_{m(pk)}$ of 3.2MΩ (44%) evoked by 5-HT (200μM) after exposure to Methiothepin (10μM) for thirty minutes was unaffected by a further sixty minutes exposure to 100μM methiothepin (δV = 5mV; $\delta R_{m(pk)}$ = 1.7MΩ (21%)) (not shown). Interestingly when this latter neurone was then exposed to 100μM methysergide for 15 minutes the 5-HT response was completely abolished further suggesting the ineffectiveness of methiothepin as an antagonist at this site.

8-hydroxy-2-(di-N-propylamino)-tetralin (8-OH-DPAT)

8-OH-DPAT has been demonstrated to bind selectively and with high affinity to 5-HT_{1A} binding sites in the rodent CNS (Middlemiss and Fozard, 1983). Electrophysiological experiments have shown it to mimic 5-HT evoked hyperpolarisation of serotonergic dorsal raphe and lateral septal neurones, while it acts as a partial agonist of the same response in hippocampal CA_1 pyramidal neurones.

8-OH-DPAT (10μM) was shown to have no effects either on FM's alone or on the 5-HT evoked depolarisation (Fig.6.45). This concentration has been shown to be active in both the DR and hippocampal slice preparations. The neurone in Fig.6.45Aa had a resting potential of -78mV and the electrotonic potentials evoked by hyperpolarising and depolarising current pulses showed the peak input resistance to be 8.4MΩ. Superfusion of 8-OH-DPAT did not alter the membrane potential or $R_{m(pk)}$ significantly (-78mV; 9.3MΩ) (Fig.6.45Ab). Bearing in mind the partial agonist action of 8-OH-DPAT in the hippocampus it was necessary to check for any antagonistic actions on 5-HT responses. Subsequent co-application of 5-HT (200μM) evoked a depolarisation of 5mV associated with an increase in peak input resistance of 4.4MΩ (Fig.6.45Ac). The current-voltage relationship (Fig.6.45B) shows the estimated reversal potential to be -85mV. This response was similar to the control 5-HT (200μM) evoked depolarisation (6mV) and increase in $R_{m(pk)}$ (5.3MΩ) obtained prior to 8-OH-DPAT application (not shown).

The mean resting potential and peak input resistance of four neurones were unaffected by exposure to 8-OH-DPAT (10μM). The values being -73.8 $\pm$ 5.8mV and 12.9 $\pm$ 4.9MΩ before and -73.8 $\pm$ 8.1mV and 13.4 $\pm$ 6MΩ after 8-OH-DPAT superfusion. Three of these neurones with a membrane potential of -77 $\pm$ 2mV before and -78 $\pm$ 2mV after 8-OH-DPAT application had previously depolarised by 4.7 $\pm$ 0.9mV in response to 5-HT (200μM). A depolarisation of 5 $\pm$ 1mV evoked by 5-HT (200μM; n = 2) was associated with an increase in $R_{m(pk)}$ of 2.8 $\pm$ 0.4MΩ and gave an estimated E_{rev} of -97 $\pm$ 3mV.

The results thus indicate that 8-OH-DPAT (10μM) is unable to mimic or antagonise the 5-HT evoked depolarisation of facial motoneurones.

Dipropyl-5-carboxamidotryptamine (DP-5-CT)

Based on experiments using the guinea-pig ileum as a model for peripheral 5-HT_{1A} receptors (Hagenbach et al, 1986) DP-5-CT was demonstrated to be a highly selective and potent agonist at this site, results confirmed by its potent action in hyperpolarising DR neurones (Rainnie, 1988). In accordance with the data obtained using 8-OH-DPAT, DP-5-CT was found to be unable to mimic the actions of 5-HT on facial motoneurones.

DP-5-CT (10μM) superfused for 15 mins had no effect on one FM which had previously responded to 5-HT (200μM), by depolarising to a plateau 4mV above rest associated with an increase in $R_{m(pk)}$ of 4.1MΩ (36%) and having an extrapolated reversal potential of -95mV. Fig.6.46 shows the effects of a higher concentration of DP-5-CT on a second FM. The motoneurone had a resting potential of -77mV, $R_{m(pk)}$ of 4.8MΩ and responded to 15 minutes superfusion of 5-HT (200μM) with a depolarisation of 5mV and an increase in $R_{m(pk)}$ of 3.9MΩ (81%) (Fig.6.46Aa to Ac). 5-HT and control I/V plots intersected at -83mV (Fig.6.46B). On recovery the cell was superfused with DP-5-CT (100μM) for 15 minutes (not shown). No effects on Vm (-76mV) or $R_{m(pk)}$ (4.9MΩ) were observed. During the wash off period of this application it was found necessary to alter the bridge balance compensating for the microelectrode resistance from 15MΩ to 13.3MΩ. This did not alter the resting potential (-76mV) but the values for $R_{m(pk)}$ and $R_{m(ss)}$ increased to 6 and 3.7MΩ in their linear ranges respectively. DP-5-CT (200μM) was then added to the aCSF for a further 15 minutes. A small reversible increase in membrane potential of about 1mV was observed along with a small increase in $R_{m(pk)}$ between 0.5 and 1MΩ (Fig.6.46Ad to Af) (against wash and control values respectively). This may represent

a small agonist action as the points of intersection of control/DP-5-CT and DP-5-CT/ wash peak I/V plots were -83 and -89mV respectively (Fig.6.46C). Nevertheless an action of 5-HT through a 5-HT_{1A} receptor can be discounted by the poor potency of this drug.

<u>5-HT_3 receptor ligands: ICS 205 930 and 2-methyl-5-HT</u>

The depolarisation associated with increased R_m evoked by 5-HT in facial motoneurones does not resemble the characteristic depolarisation caused by increased cation conductance associated with 5-HT_3 receptor activation in the peripheral nervous system (Wallis and North, 1978). Experiments utilizing the 5-HT_3 receptor ligands ICS 205 930 and 2-methyl-5-HT support the idea that a 5-HT_3 receptor does not mediate the depolarisation seen in facial motoneurones.

Addition of 100μM ICS 205 930, a putative 5-HT_3 receptor antagonist, to the superfusing aCSF for 30 minutes had no effect on resting membrane potential (-84mV) or $R_{m(pk)}$ (9.2MΩ). Subsequent co-application of 5-HT (200μM) evoked a depolarisation of 4mV associated with a 63% increase in $R_{m(pk)}$ to 15MΩ (Fig.6.47). The estimated reversal potential was -91.5mV (Fig.6.47C). This response was similar to the control 5-HT response, evoked prior to ICS 205 930 application, which comprised of a 4mV depolarisation associated with a 28% increase in $R_{m(pk)}$ and an estimated reversal potential of -100mV (Fig.6.47Aa,Ab,B).

Application of the 5-HT_3 receptor agonist 2-methyl-5-HT failed to mimic the response evoked by 5-HT (Fig.6.48). Superfusion with 2-methyl-5-HT (200μM) for 15 minutes had little effect on the resting potential or input resistance of the neurone in Figure 6.48Aa,Ab. A resting potential of -67mV during 2-methyl-5-HT application compared with -68mV after washing with drug-free aCSF

for 25 minutes. The $R_{m(pk)}$ in 2-methyl-5-HT was 8.9MΩ and this increased during wash to 9.9MΩ. Prior to 2-methyl-5-HT application $R_{m(pk)}$ was 7.9MΩ suggesting that this gradual increase was not drug-related. The neurone had previously depolarised by 5mV associated with an increase in input resistance in response to 5-HT (200μM) (not shown). A second application of 5-HT (200μM) after exposure to 2-methyl-5-HT evoked a depolarisation of 5mV and an increase in $R_{m(pk)}$ to 13.7MΩ (Fig.6.48Ac,Ad). The current-voltage relationships in Figure 6.48B showed the estimated reversal potential to be -81mV. Subsequent recovery to a resting potential of -67mV was obtained on changing back to control aCSF.

Application of 2-methyl-5-HT (200μM) to a second motoneurone which had previously depolarised in response to both 5-HT (200μM; δV = +3mV, E_{rev} -92mV) and noradrenaline (100μM; δVm = +3mV; E_{rev} = -92mV), also failed to evoke any change in membrane potential or $R_{m(pk)}$.

Fig. 6.1

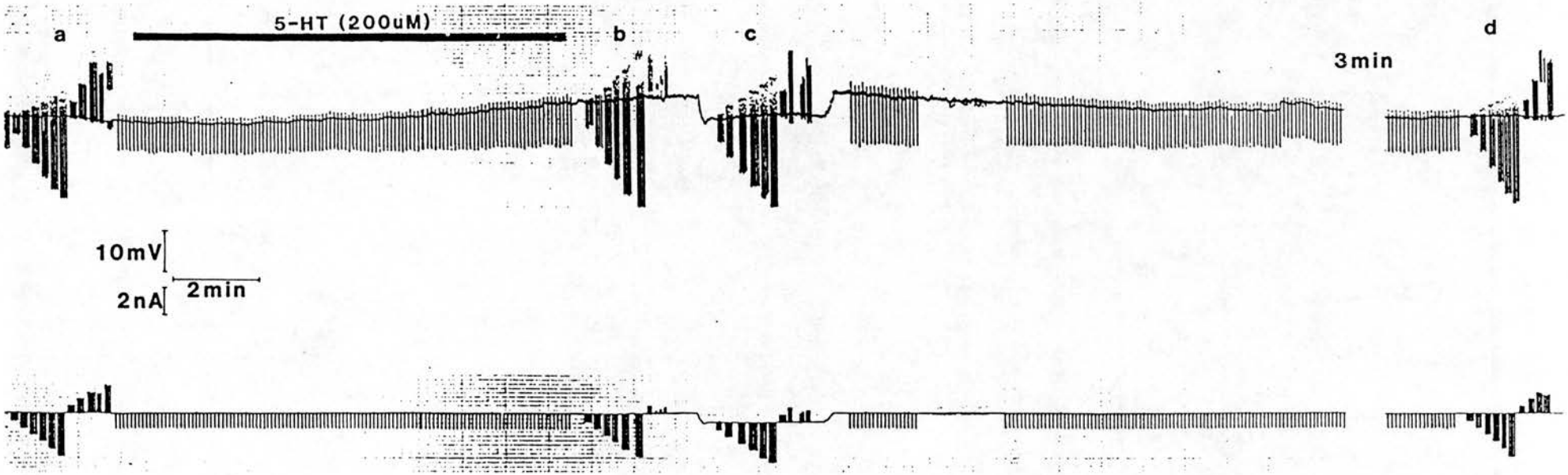

Figure 6.1

Intracellular current clamp response of a FM to superfusion with 5-HT in vitro

A continuous chart record of membrane potential and responses to hyperpolarising current pulses (-1nA, 0.2Hz) showing a slow depolarisation associated with increased input resistance during superfusion with 5-HT (200μM). The cell depolarised by 6mV from a resting potential of -71mV and the effect was fully reversed when 5-HT was removed from the aCSF. Voltage responses to current pulses of varying amplitude were obtained at points a, b, c and d and are illustrated in figure 6.2. Voltage, upper trace, current, lower trace.

Fig. 6.2

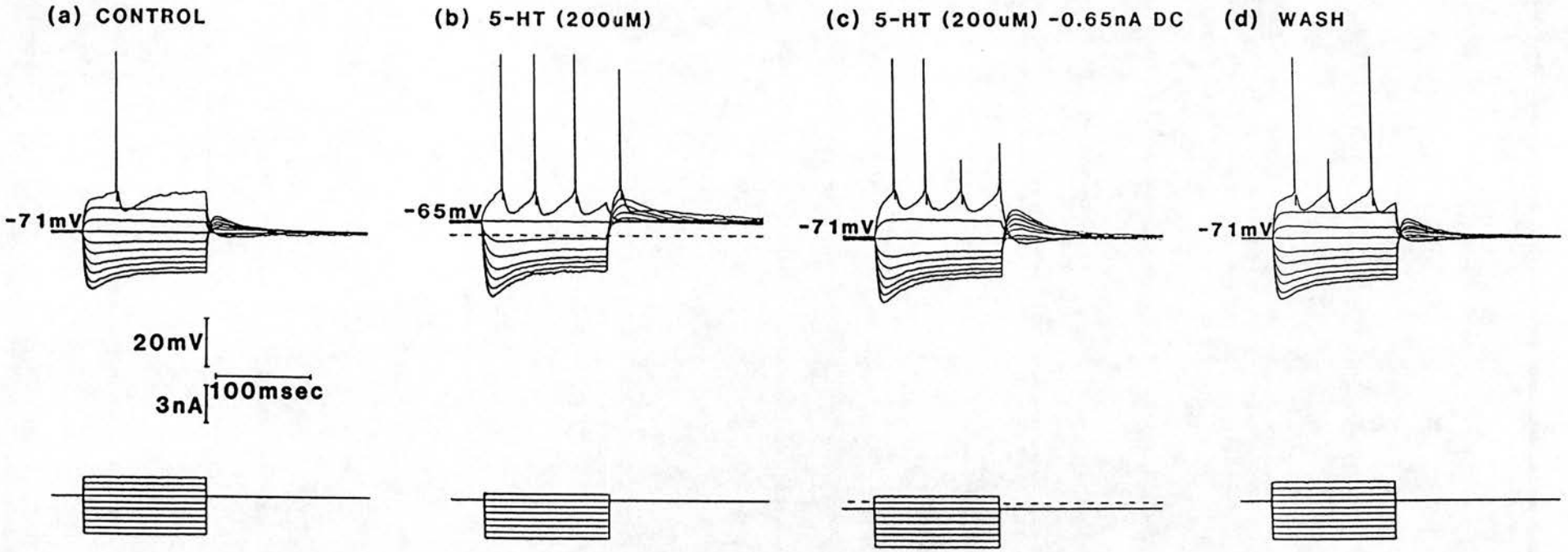
(a) CONTROL
(b) 5-HT (200uM)
(c) 5-HT (200uM) -0.65nA DC
(d) WASH
-71mV
-65mV
-71mV
-71mV
20mV
3nA
100msec

Figure 6.2

Electrotonic potential from a FM before, during and after 5-HT superfusion

Voltage responses (upper traces) obtained by intracellular injection of current steps (lower traces) 120msec in duration taken at the corresponding times (a-d) in Fig.6.1. Rm measured over the linear portion of the current voltage relation at the peak of the voltage deflection increased from 8.9MΩ in control (a) to 13.9MΩ in 5-HT (b). When the membrane potential was manually clamped to the resting level, at the peak of the 5-HT response, (c) $R_{m(pk)}$ was 12MΩ indicating that voltage dependent membrane rectification contributes to the overall resistance increase. $R_{m(pk)}$ recovered to 9.9MΩ on washing with 5-HT-free aCSF (d). Note the increased action potential firing in response to previously sub-threshold current steps during 5-HT application (b,c). Rebound depolarising tail potentials show increased amplitude and duration in the presence of 5-HT and can even lead to AP generation after large hyperpolarising current steps (b). (AP amplitude has been attenuated by the slow sampling speed used during data analysis in this and all later figures unless otherwise stated. Faster sampling rates show AP in this FM to overshoot by about 20mV).

Fig. 6.3

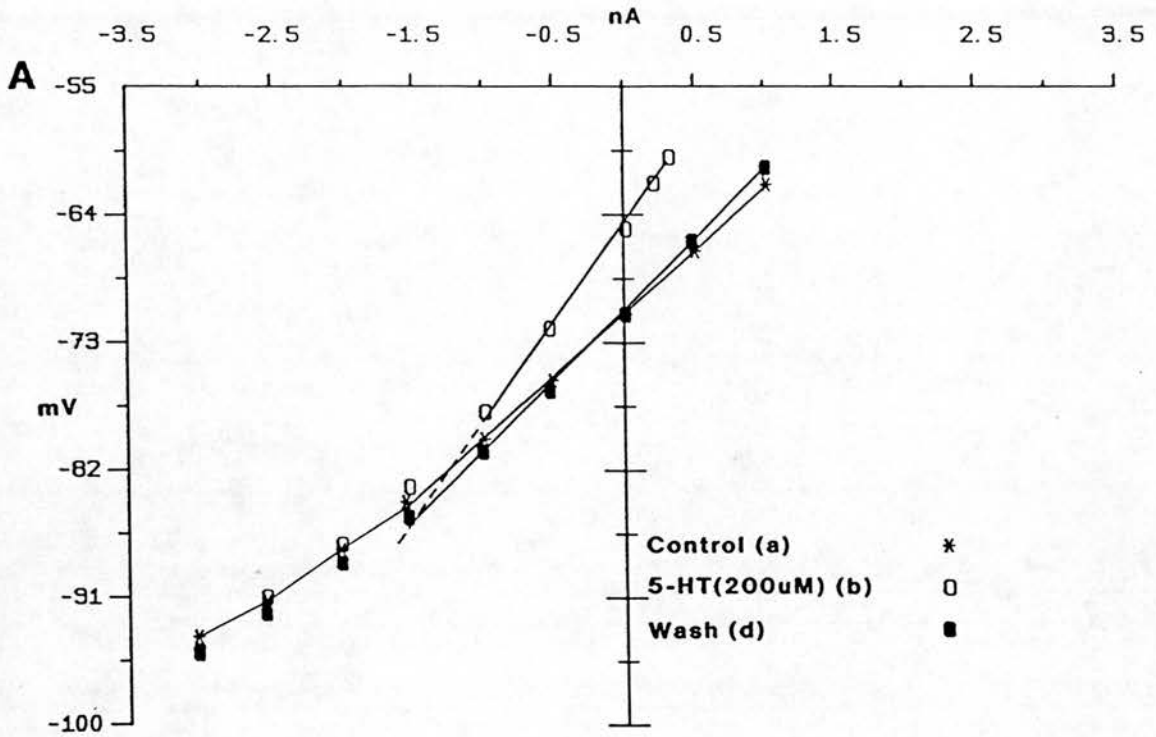
A
nA
-3.5
-2.5
-1.5
-0.5
0.5
1.5
2.5
3.5
-55
-64
-73
mV
-82
-91
-100
Control (a)
5-HT(200uM) (b)
Wash (d)

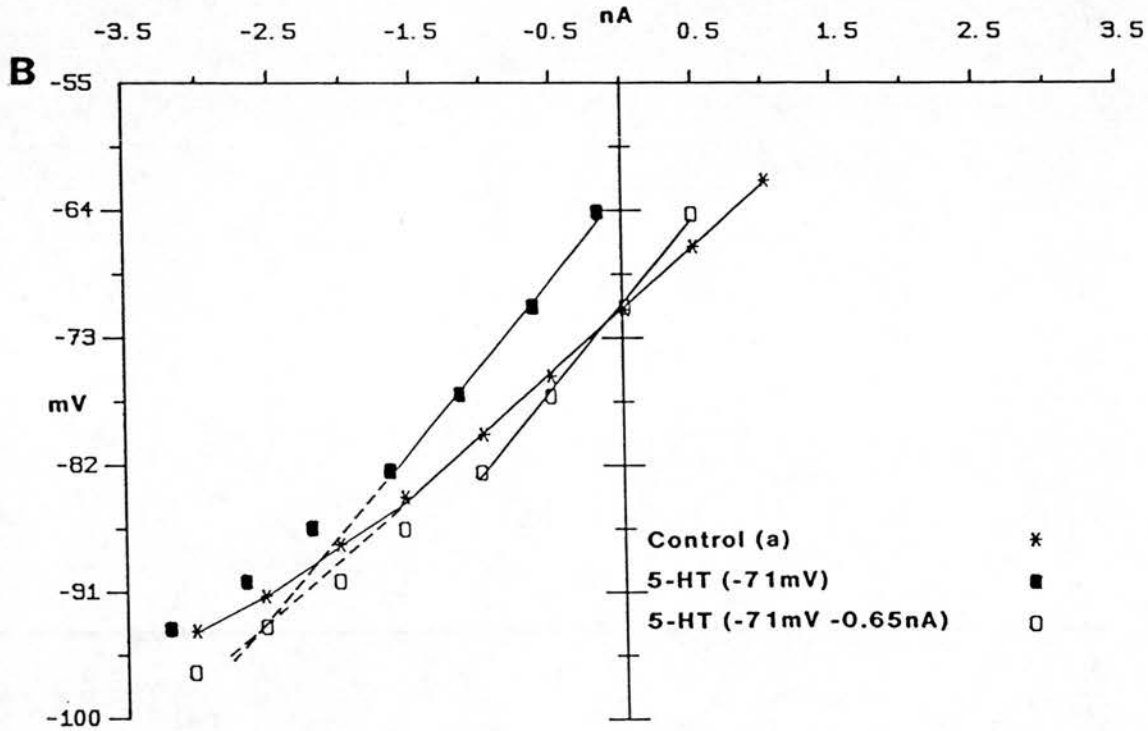
B
nA
-3.5
-2.5
-1.5
-0.5
0.5
1.5
2.5
3.5
-55
-64
-73
mV
-82
-91
-100
Control (a)
5-HT (-71mV)
5-HT (-71mV -0.65nA)

Figure 6.3

Peak deflection current voltage plots taken from the electrotonic potentials shown in Fig.6.2a-d

A) Control (asterisks), 5-HT (open squares) and wash (closed squares) I/V plots each show some rectification at hyperpolarised potentials. The reversal potential for the 5-HT evoked depolarisation taken from the extrapolated point of intersection of the linear portions of the respective I/V plots was -83mV against control and -86mV against wash. These values were close to the observed points of intersection on the non-linear portions of the I/V curves. The linear portions of the I/V curves were represented by the equation $y = a + bx$ where $a = -70.9, -64.5, -70.7$, and $b = 8.9, 13.9, 9.9$, for control, 5-HT and wash respectively.

B) Peak deflection I/V plots during control (asterisks) and manual clamping of the 5-HT response (see fig. 6.2c). Open squares represent the 5-HT response at -71mV without the offset current, illustrating a 5-HT evoked change in slope resistance. The linear portion of the I/V plot is described by the equation $Y = -71 + 12X$. When the offset current is taken into account (closed squares), ($Y = -62.9 + 12X$) the 5-HT and control I/V plots converge but do not intersect in the tested range. Extrapolation of the linear portions of the two I/V plots gives an estimated reversal potential of -93.9mV.

Fig. 6.4

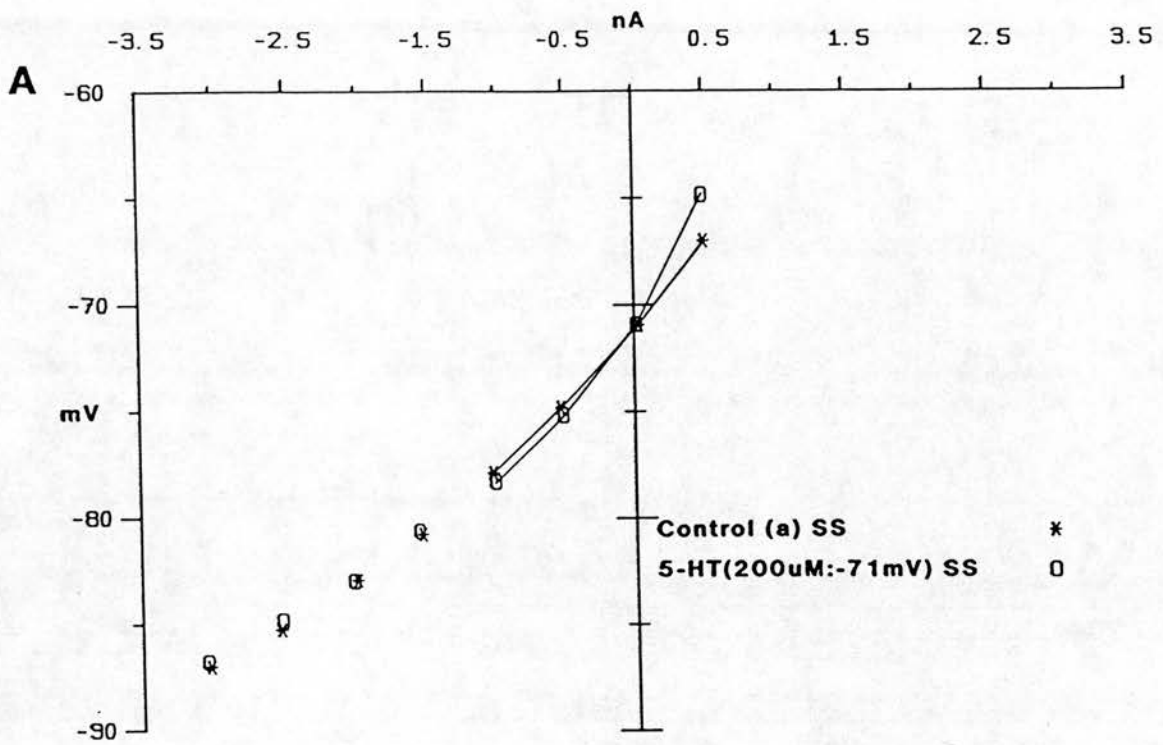
A
nA
-3.5
-2.5
-1.5
-0.5
0.5
1.5
2.5
3.5
-60
-70
-80
-90
mV
Control (a) SS
5-HT(200uM:-71mV) SS

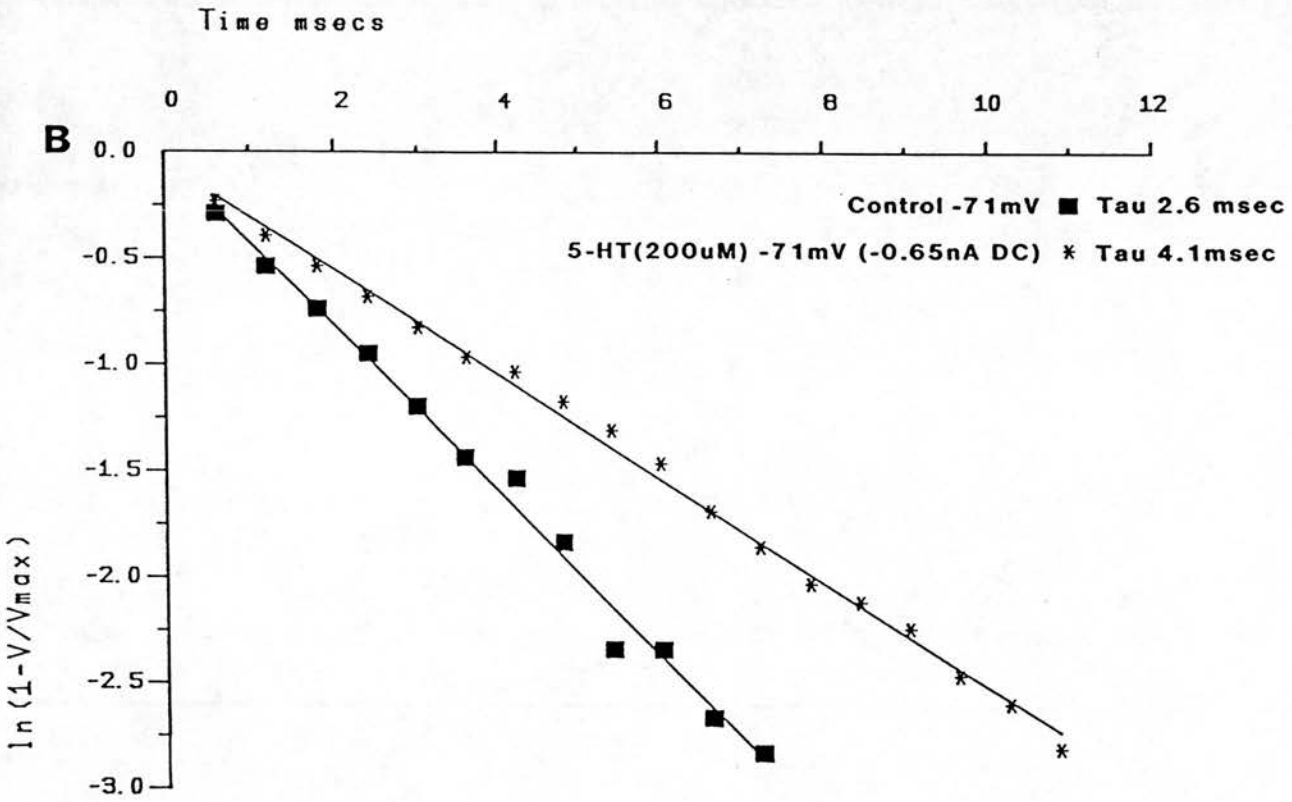
Time msecs
B
0
2
4
6
8
10
12
0.0
-0.5
-1.0
-1.5
-2.0
-2.5
-3.0
ln(1-V/Vmax)
Control -71mV ■ Tau 2.6 msec
5-HT(200uM) -71mV (-0.65nA DC) * Tau 4.1msec

Figure 6.4

Steady state I/V plots and measurement of the membrane time constant in the absence and presence of 5-HT

A) Control (asterisks) and manually clamped 5-HT (open squares; no current offset). I/V plots taken at the end of the electrotonic potentials shown in Fig.6.2a,c, when a steady state (ss) potential has been reached. Plots are non-linear throughout the tested range and only a small increase in input resistance ($R_{m(ss)}$) is observed in the presence of 5-HT. B) A semilogarithmic plot of ln(1-V/Vmax) against time showing the single exponential nature of the membrane charging curves taken from small ohmic depolarising voltage responses in the presence (asterisk) and absence of (closed squares) of 5-HT at a membrane potential of -71mV. The time constant for membrane charging, τ, increased from 2.6ms in control to 4.1ms in 5-HT (200μM).

Fig. 6.5

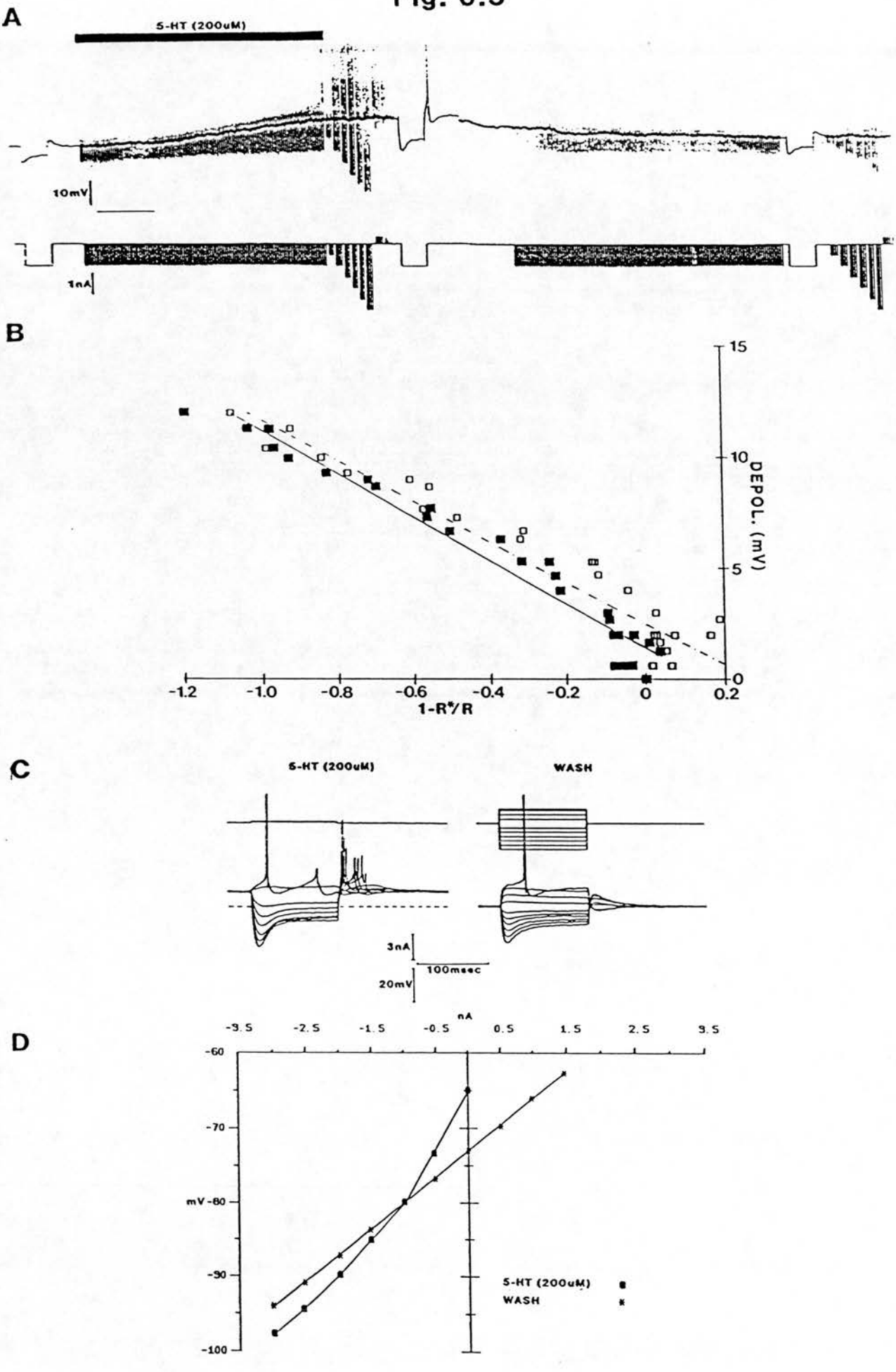
A
5-HT (200uM)
10mV
1nA
B
DEPOL. (mV)
15
10
5
0
-1.2
-1.0
-0.8
-0.6
-0.4
-0.2
0
0.2
1-R*/R
C
5-HT (200uM)
WASH
3nA
100msec
20mV
D
nA
-3.5
-2.5
-1.5
-0.5
0.5
1.5
2.5
3.5
-60
-70
-80
-90
-100
mV
5-HT (200uM)
WASH

Figure 6.5

The relationship between the 5-HT-evoked depolarisation and the associated increase in membrane resistance

A) A continuous chart record showing superfusion of 5-HT (200μM) to evoke a 12mV depolarisation from the resting potential of -77mV. Input resistance, tested with a 1nA hyperpolarising test current pulse (120ms duration, 0.5Hz) increased in the presence of 5-HT (see expanded inset). Full recovery of resting potential and input resistance was obtained on removal of 5-HT from the aCSF. Voltage, upper record; current lower record. Time calibration is 1 min except when records are expanded where the same bar represents 250ms.

B) The relationship between depolarisation amplitude and 1-(R*/R) were R and R* are the input resistances in the absence and presence of 5-HT, respectively. Measurements were taken every 10 seconds from the neurone depicted in A. The relationships were linear for both peak (closed squares/solid line) and steady-state (open squares/broken line) resistance measurements. The regression lines were represented by $y = a + bX$ where $a = 1.4$ and 2.5 and $b = -9.8$ and -9.2 for peak and steady-state values respectively. The values for E_{5HT} according to equation 1 (see text) were -82.8 and -82.2mV respectively.

C) Averaged electrotonic potentials obtained by injecting current pulses of varying amplitude at the peak of the 5-HT response and after recovery clearly indicate the depolarisation, increase in Rm and increase in excitability. This is the same FM as in A and B. Action potentials evoked on depolarising tail potentials in the presence of 5-HT have been distorted by the averaging procedure.

D) Peak deflection current-voltage plots taken from the electrotonic potentials in C give a value of $E_{5\text{-}HT}$ of -80mV in close agreement with those obtained from the method of B. Note that the voltage deflections to -1nA current pulses used in A and B lie on the linear portions of both control and 5-HT relationships.

Fig. 6.6

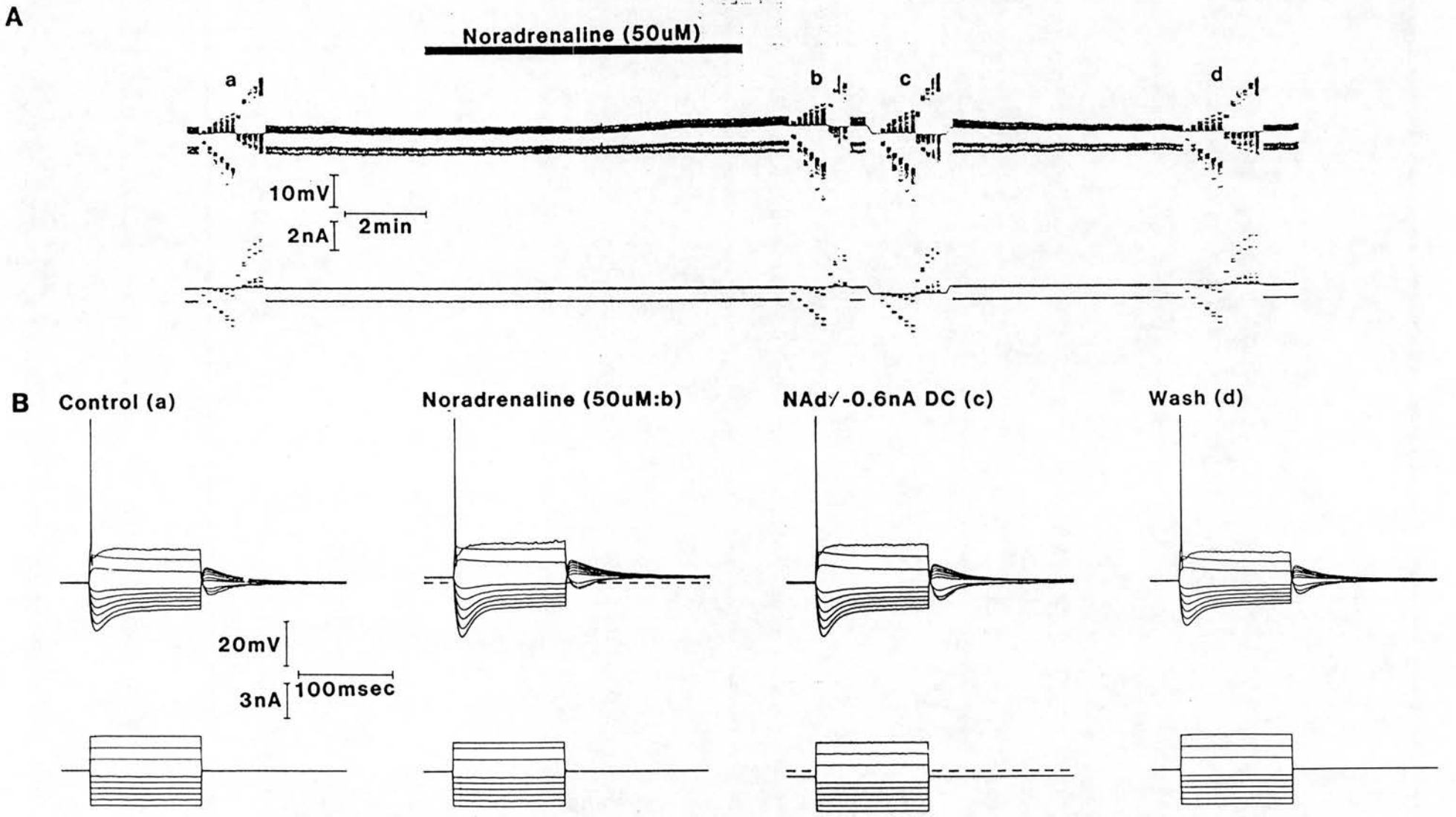
A
Noradrenaline (50uM)
a
b
c
d
10mV
2nA
2min
B
Control (a)
Noradrenaline (50uM:b)
NAd⁄-0.6nA DC (c)
Wash (d)
20mV
3nA
100msec

Figure 6.6

Intracellular current clamp recordings of the action of Noradrenaline (NAd) on FM's in vitro

A) A continuous chart record of membrane potential and responses to hyperpolarising current pulses (-1nA, 120msec, 1Hz) illustrating the slow depolarisation and associated increase in input resistance during superfusion with Noradrenaline (50μM). The FM reversibly depolarised by 3mV from a resting potential of -77mV. Current voltage relationships were established at the points a-d by injection of current steps of varying amplitude. Voltage, upper trace; current, lower trace.

B) Electrotonic potentials (upper traces) obtained by intracellular injection of current steps (lower traces) at the corresponding times in A. $R_{m(pk)}$ and $R_{m(ss)}$ increased from 7.04 and 3.82MΩ in control conditions (Aa, Ba) to 9.09 and 4.16MΩ respectively in NAd (Ab, Bb). Manual clamping of the NAd evoked depolarisation to -77mV (Ac, Bc) required -0.6nA DC and showed $R_{m(pk)}$ and (ss) to be 8.29 and 3.86 respectively. Washing with NAd-free aCSF led to recovery of Vm (-77mV), $R_{m(pk)}$ (6.42MΩ) and $R_{m(ss)}$ (3.36MΩ). In control conditions a single overshooting action potential (amplitude attenuated) was evoked by a + 3nA current step (Bb). In NAd threshold was attained with a + 2.4nA step (Bb) and this increased excitability was maintained during manual clamping (Bc) where the net current required to evoke an action potential was +2.5nA.

Fig. 6.7

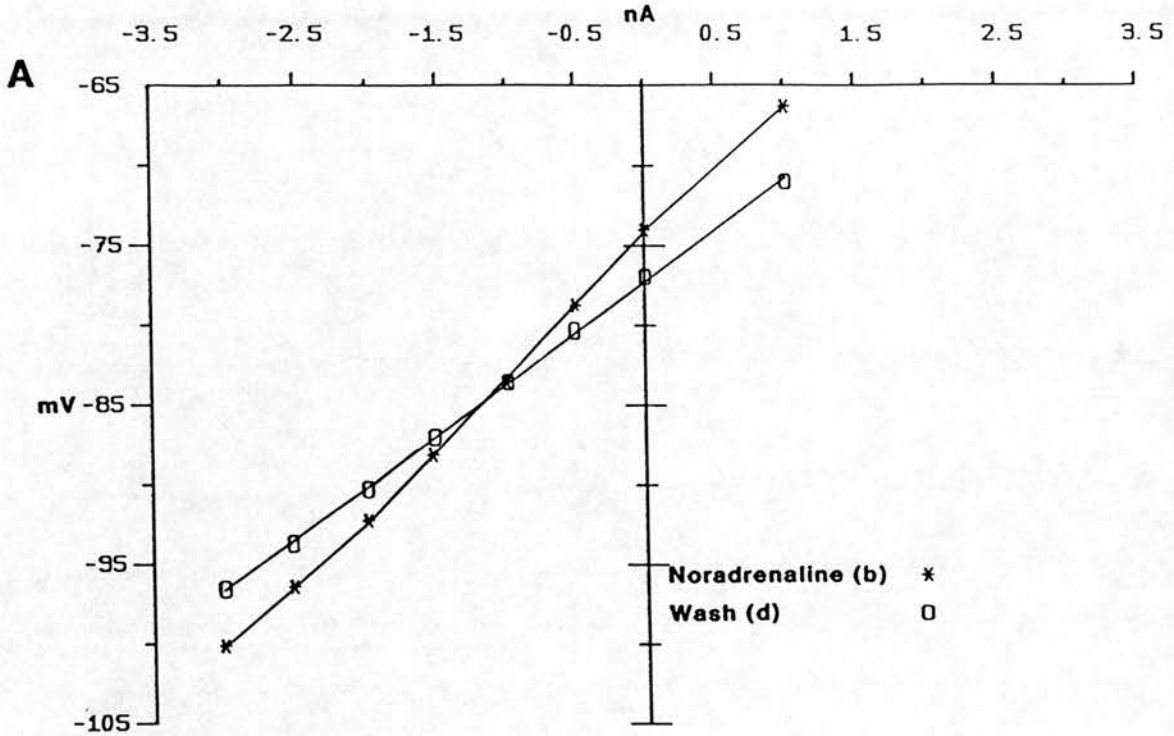
A
nA
-3.5
-2.5
-1.5
-0.5
0.5
1.5
2.5
3.5
-65
-75
mV -85
-95
-105
Noradrenaline (b)
Wash (d)

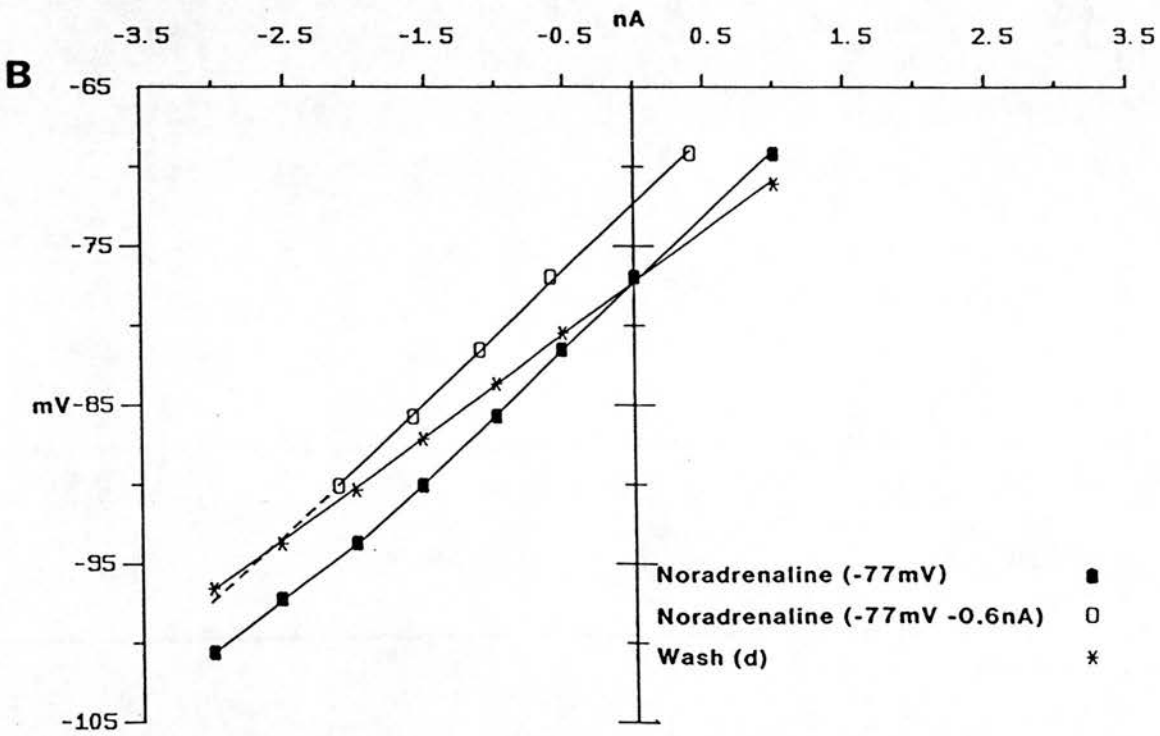
B
nA
-3.5
-2.5
-1.5
-0.5
0.5
1.5
2.5
3.5
-65
-75
mV-85
-95
-105
Noradrenaline (-77mV)
Noradrenaline (-77mV -0.6nA)
Wash (d)

Figure 6.7

Peak deflection current voltage plots taken from the electrotonic potentials seen in Fig.6.6B

A. The wash I/V relation (open squares) shows linearity throughout the tested voltage range whereas in the presence of NAd (asterisks) some rectification is seen at potentials more negative than -90mV. The point of intersection occurs within the linear ranges of the respective curves and gives a value of -85mV for the reversal potential of the NAd evoked depolarisation.

B. Manual clamping of the membrane potential to -77mV during the NAd evoked depolarisation shows a drug induced increase in slope resistance (closed squares) over wash (asterisks). When plotted with the offset DC current (open squares) the extrapolated point of intersection of the NAd and wash I/V plots was -94mV which closely agrees with the observed point of convergence or the non-linear portion of the NAd I/V plot.

Fig. 6.8

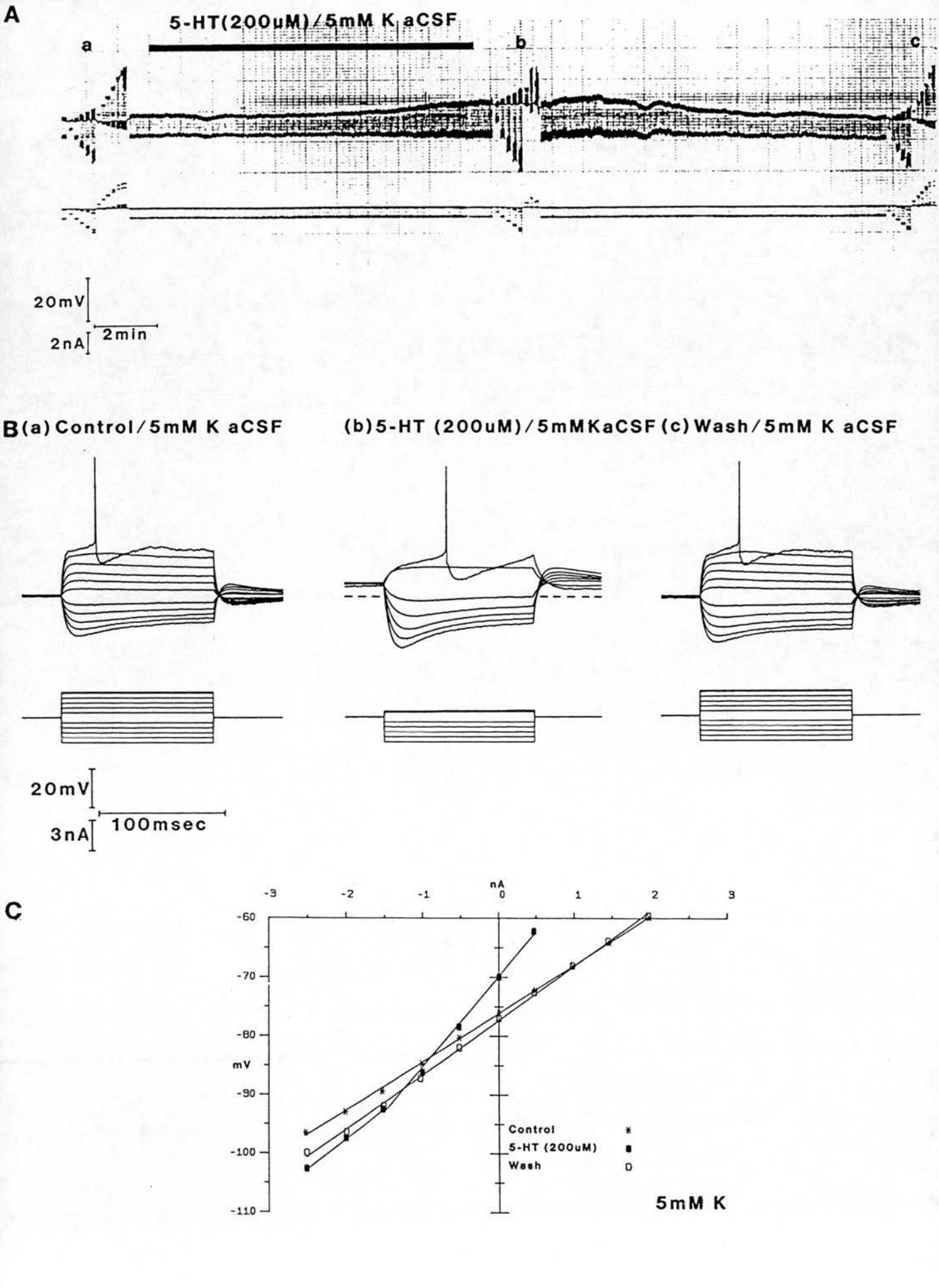
A
5-HT(200uM)/5mM K aCSF
a
b
c
20mV
2nA
2min
B(a) Control/5mM K aCSF
(b) 5-HT (200uM)/5mM KaCSF
(c) Wash/5mM K aCSF
20mV
3nA
100msec
C
nA
-3
-2
-1
0
1
2
3
-60
-70
-80
mV
-90
-100
-110
Control
5-HT (200uM)
Wash
5mM K

Figure 6.8

The action of 5-HT (200μM) in aCSF containing 5mM K^+ (I)
(A) A chart record showing 5-HT (200μM) evoked depolarisation of 6mV from a resting potential of -76mV and the associated increase in $R_{m(pk)}$ when tested with a hyperpolarising current test pulse (-1nA, 120msec, 1Hz).
(B) Electrotonic potentials (upper traces) evoked by current pulses of varying amplitude (lower traces) taken at the corresponding times in A. Control $R_{m(pk)}$ (Ba) was 8.2MΩ and increased to 15.3MΩ in the presence of 5-HT (200μM) (Bb). Recovery (Bc) to -77mV was associated with a reduction in $R_{m(pk)}$ to 9.3MΩ.
(C) Peak deflection I/V plots were linear in control (asterisks; $y = 76.1 + 8.2X$) and wash (open squares; $y = -77.3 + 9.3X$) conditions. In the presence of 5-HT (closed squares) the linear portion of the I/V plot ($y = -69.9 + 15.3X$) intersected with control at -84mV and wash at -89mV. Thereafter it showed marked rectification running parallel with control and wash I/V relations.

Fig. 6.9

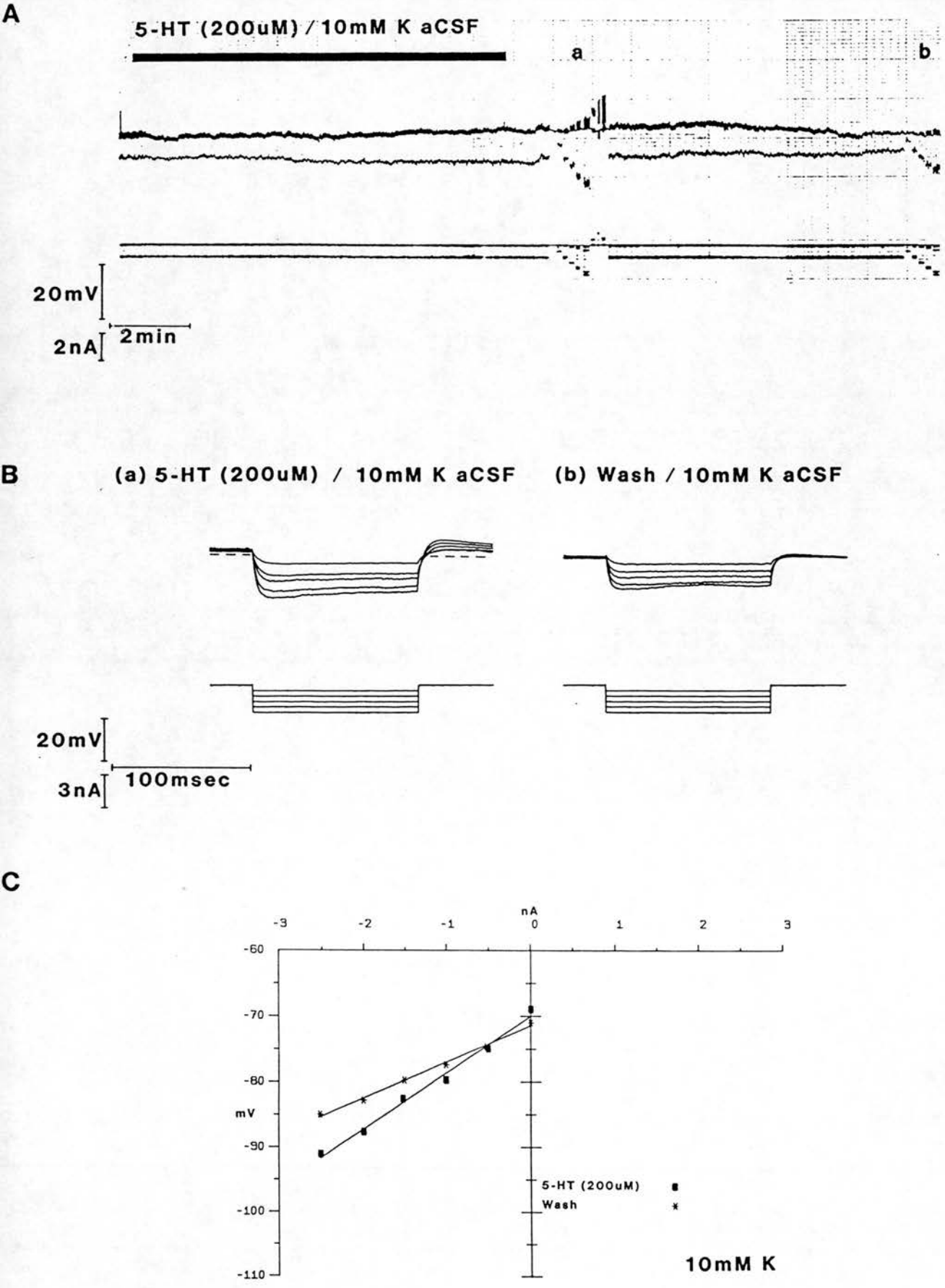
A
5-HT (200uM) / 10mM K aCSF
a
b
20mV
2nA
2min
B
(a) 5-HT (200uM) / 10mM K aCSF
(b) Wash / 10mM K aCSF
20mV
3nA
100msec
C
nA
-3
-2
-1
0
1
2
3
-60
-70
-80
mV
-90
-100
-110
5-HT (200uM)
Wash
10mM K

Figure 6.9

The action of 5-HT (200μM) in aCSF containing 10mM K^+ (I) (same neurone as in Fig. 6.8)

(A) A continuous chart record showing 5-HT (200μM) to evoke a 2mV depolarisation from a resting potential of -71mV. Voltage responses (upper traces) to test hyperpolarising current commands (-1nA, 120msec, 1Hz) indicate an associated increase in Rm.

(B) Electrotonic potentials obtained at the peak of the 5-HT response, (Ba), gave a $R_{m(pk)}$ of 8.6MΩ and $R_{m(ss)}$ of 7.3MΩ which recovered on removal of the 5-HT to 5.5MΩ and 4.8MΩ respectively (Bb).

(C) Peak deflection current-voltage relationships were linear for both 5-HT (closed squares; $y = -70 + 8.6X$) and wash (asterisks; $y = -71.4 + 5.5X$) conditions giving a point of intersection at -74mV.

Fig. 6.10

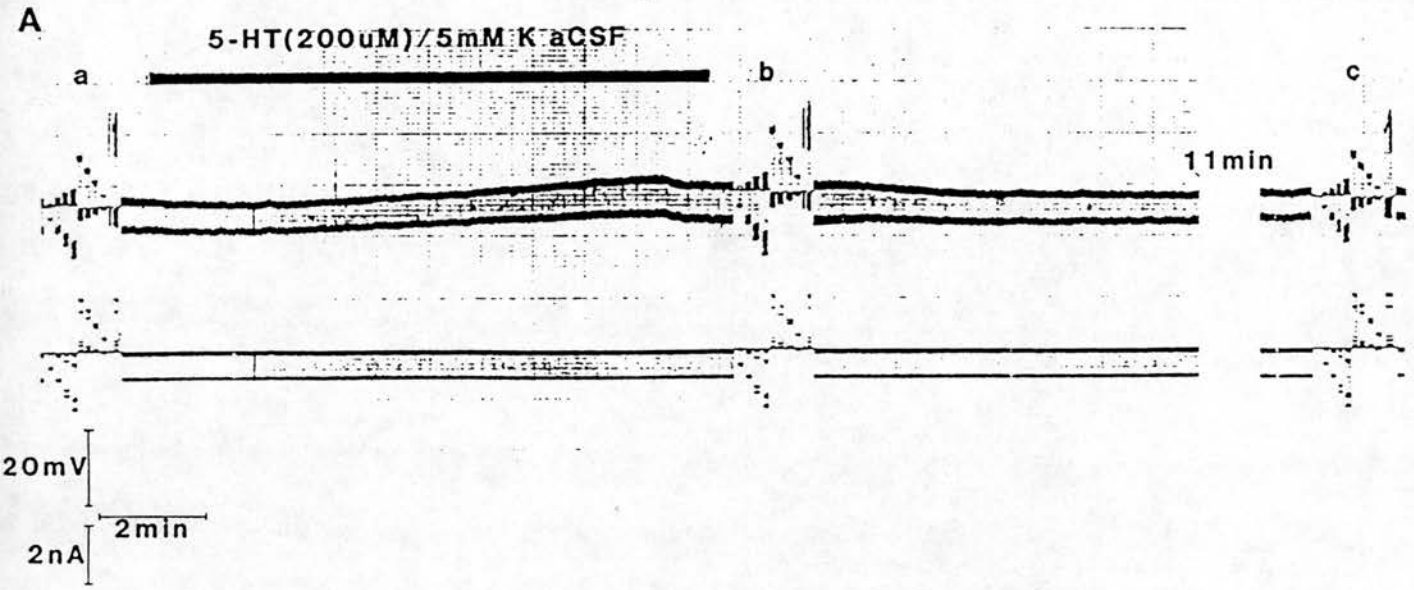
A
5-HT(200uM)/5mM K aCSF
a
b
c
11min
20mV
2min
2nA

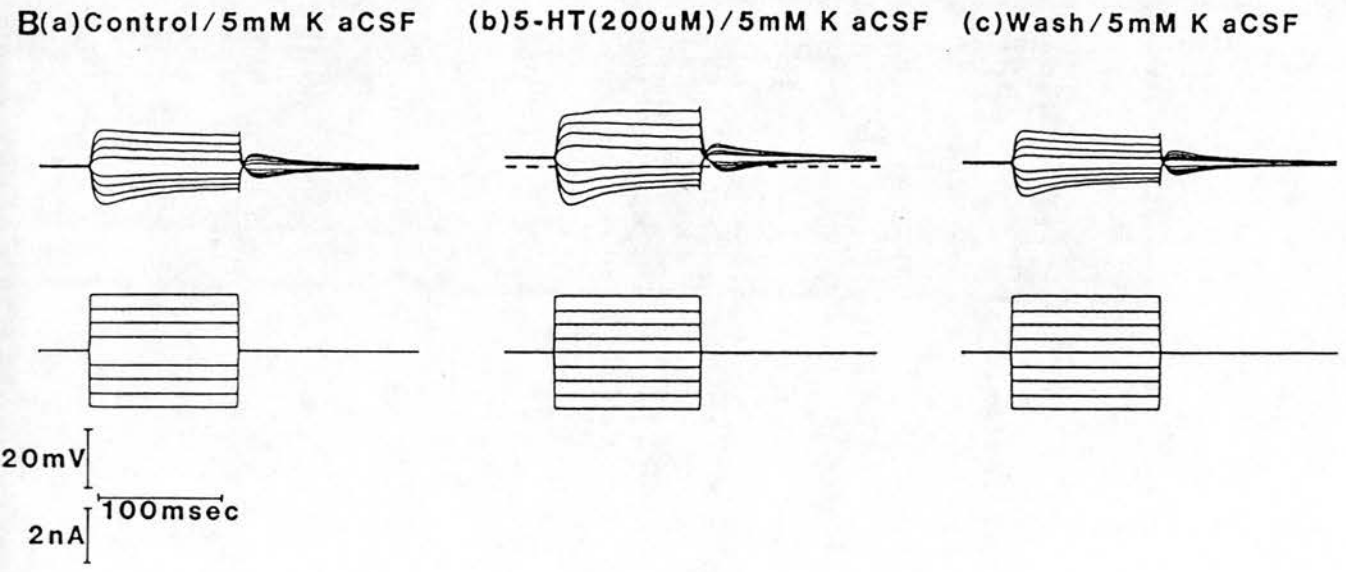
B(a)Control/5mM K aCSF
(b)5-HT(200uM)/5mM K aCSF
(c)Wash/5mM K aCSF
20mV
100msec
2nA

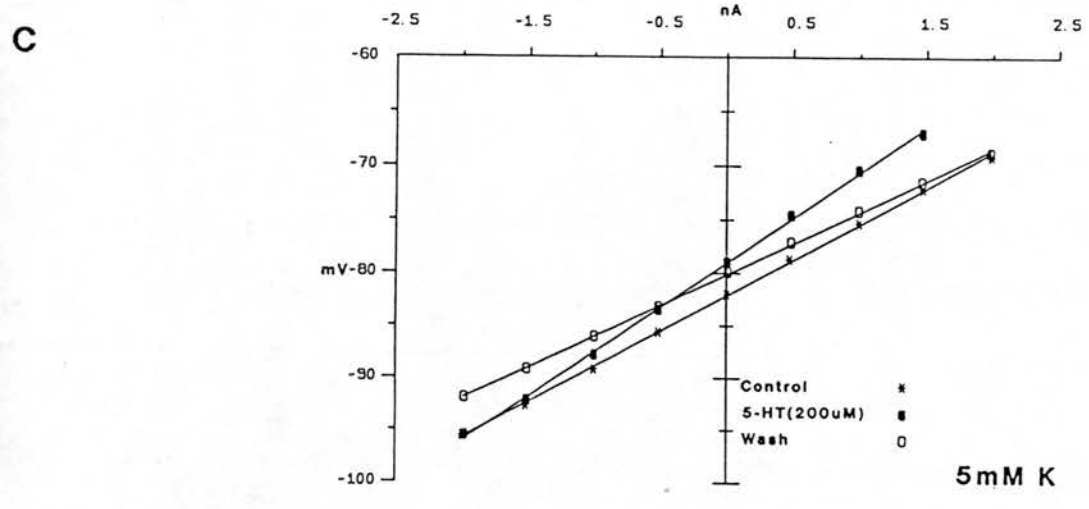
C
nA
-2.5
-1.5
-0.5
0.5
1.5
2.5
-60
-70
mV-80
-90
-100
Control
5-HT(200uM)
Wash
5mM K

Figure 6.10

The actions of 5-HT (200μM) in aCSF containing 5mM K^+ (II) (same cell as in Figs.6.11, 6.12)

(A) The 5-HT (200μM) evoked depolarisation plateaus at a potential of -79mV and is associated with an increase in R_m as indicated by voltage responses to test current pulses (-1nA, 120msec, 1Hz). Control resting potential was -82mV. Despite full recovery of control Rm, the recovery resting potential was -80mV.

(B) Membrane voltage responses to current steps of varying amplitude taken at the corresponding times in A. $R_{m(pk)}$ increased from a control value of 6.8MΩ (Ba) to 8.5MΩ in 5-HT (Bb). Subsequent recovery in 5-HT-free aCSF to 5.9MΩ was obtained.

(C) Peak deflection I/V relations were linear throughout the tested range in each condition. The I/V plot in the presence of 5-HT (closed squares; $y = -79 + 8.5X$) intersected with the control plot (asterisks; $y = -82.1 + 6.8X$) at -94.5mV and with the wash plot (open squares; $y = -80.1 + 5.9X$) at -83mV.

Fig. 6.11

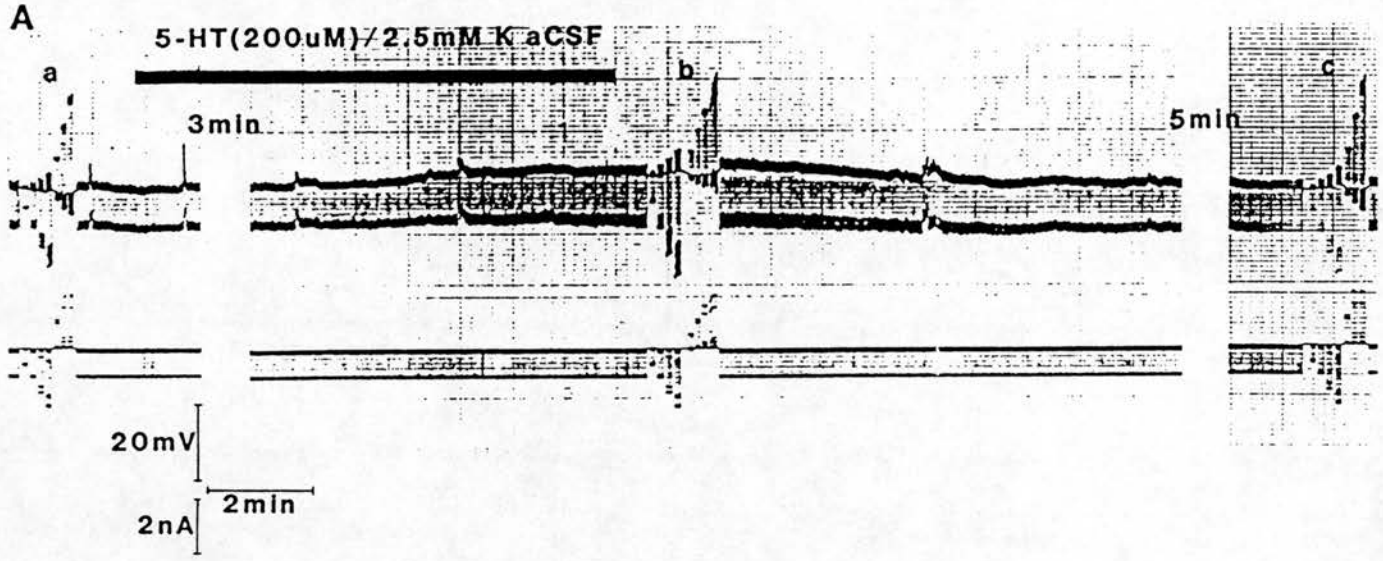
A
5-HT(200uM)/2.5mM K aCSF
a
b
c
3min
5min
20mV
2min
2nA

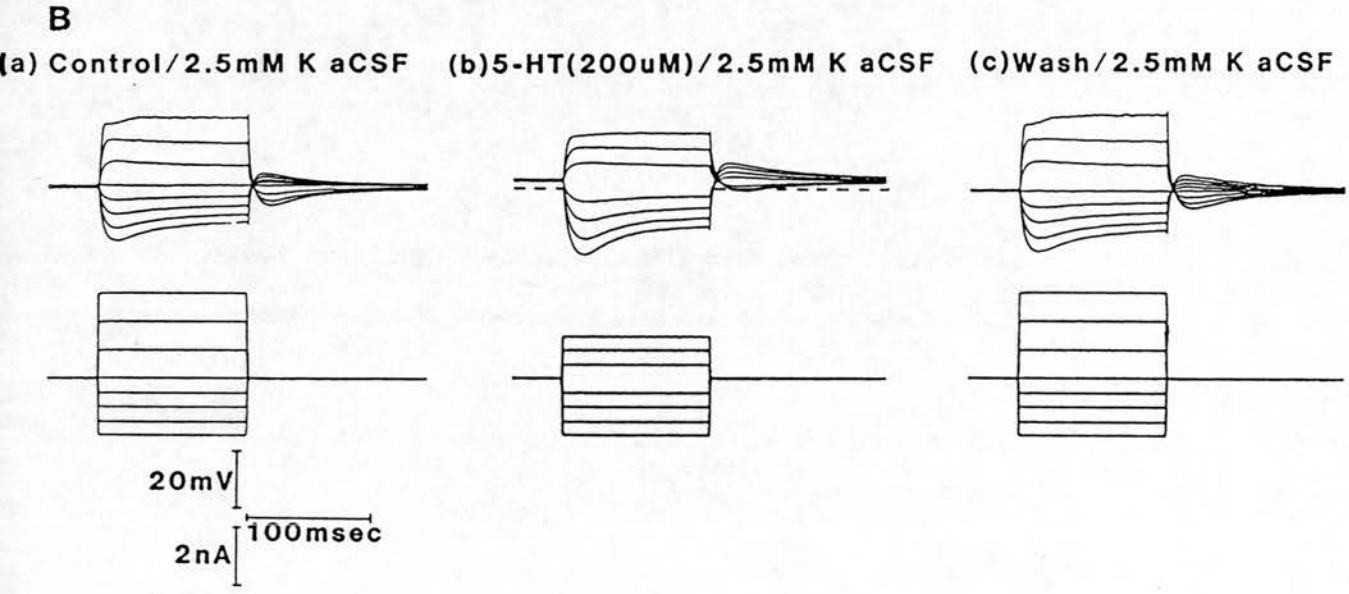
B
(a) Control/2.5mM K aCSF
(b)5-HT(200uM)/2.5mM K aCSF
(c)Wash/2.5mM K aCSF
20mV
100msec
2nA

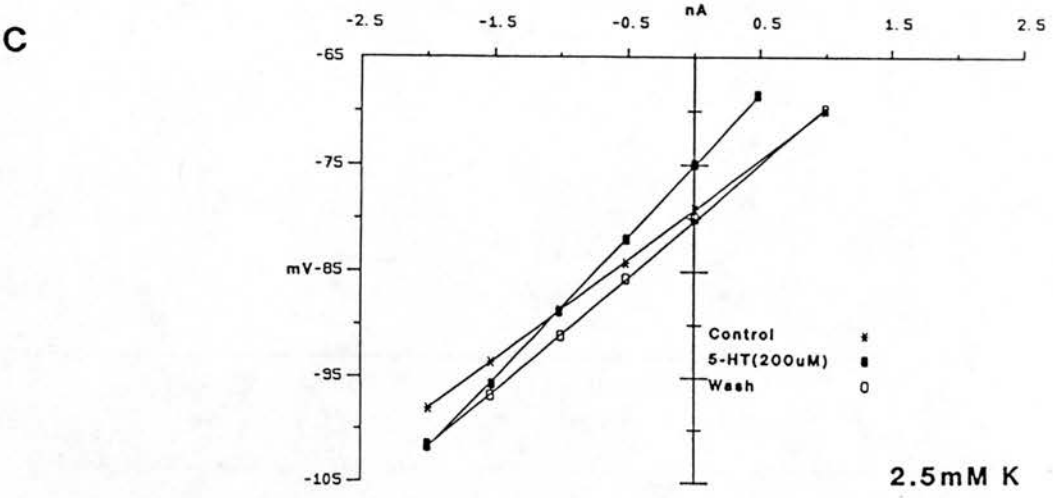
C
nA
-2.5
-1.5
-0.5
0.5
1.5
2.5
-65
-75
mV-85
-95
-105
Control
5-HT(200uM)
Wash
2.5mM K

Figure 6.11

The action of 5-HT (200μM) in aCSF containing 2.5mM K^+ (II) (same neurone as in Figs.6.10, 6.12)

(A) Chart record showing superfusion of (200μM) 5-HT evokes a reversible 4mV depolarisation from a resting potential of -79mV associated with an increase in Rm.

(B) In the presence of 2.5mM K^+ containing aCSF $R_{m(pk)}$ increased to 9.3MΩ (Ba) (cf. Fig.6.10Bc). 5-HT evoked an increase in $R_{m(pk)}$ to 13.2MΩ (Bb) which recovered to 10.7MΩ on washing with 5-HT free aCSF (Bc).

(C) As in 5mM K^+ aCSF (Fig. 6.10) peak deflection I/V plots were linear up to the point of intersection. Reversal potentials obtained from control (asterisks; $y = -79.2 + 9.3X$) and 5-HT (closed squares; $y = -75.1 + 13.2X$) and 5-HT and wash (open squares; $y = -80 + 10.7X$) I/V plots were -88mV and -102mV respectively.

Fig. 6.12

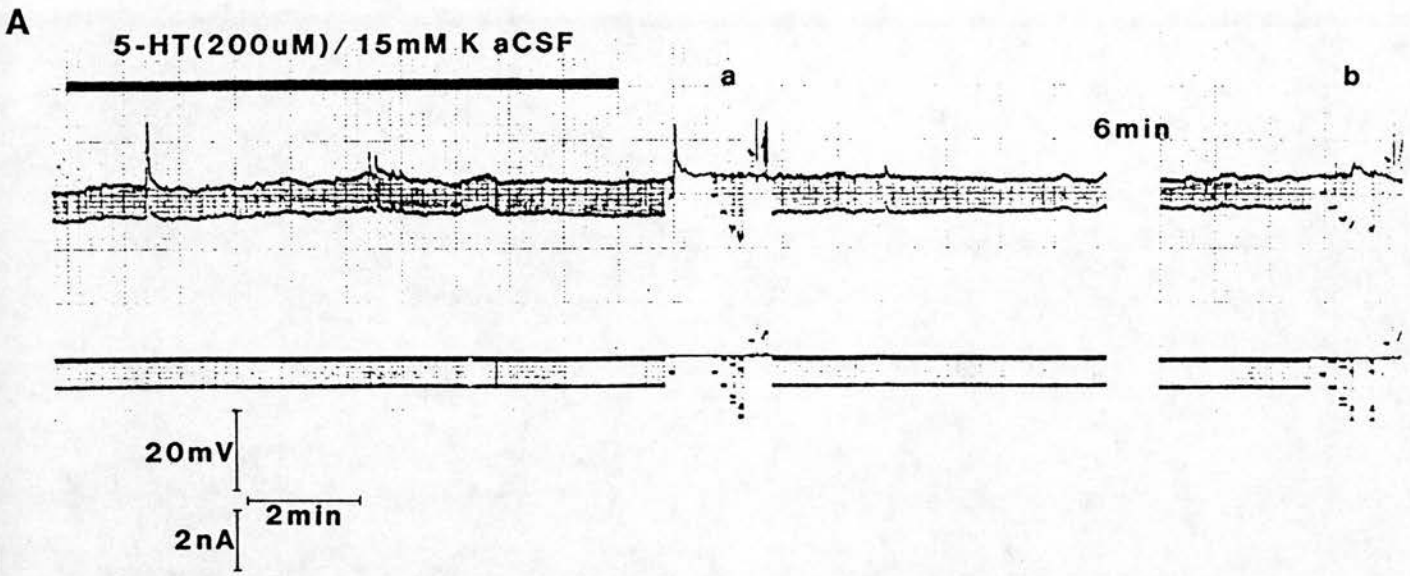
A
5-HT(200uM)/15mM K aCSF
a
b
6min
20mV
2min
2nA

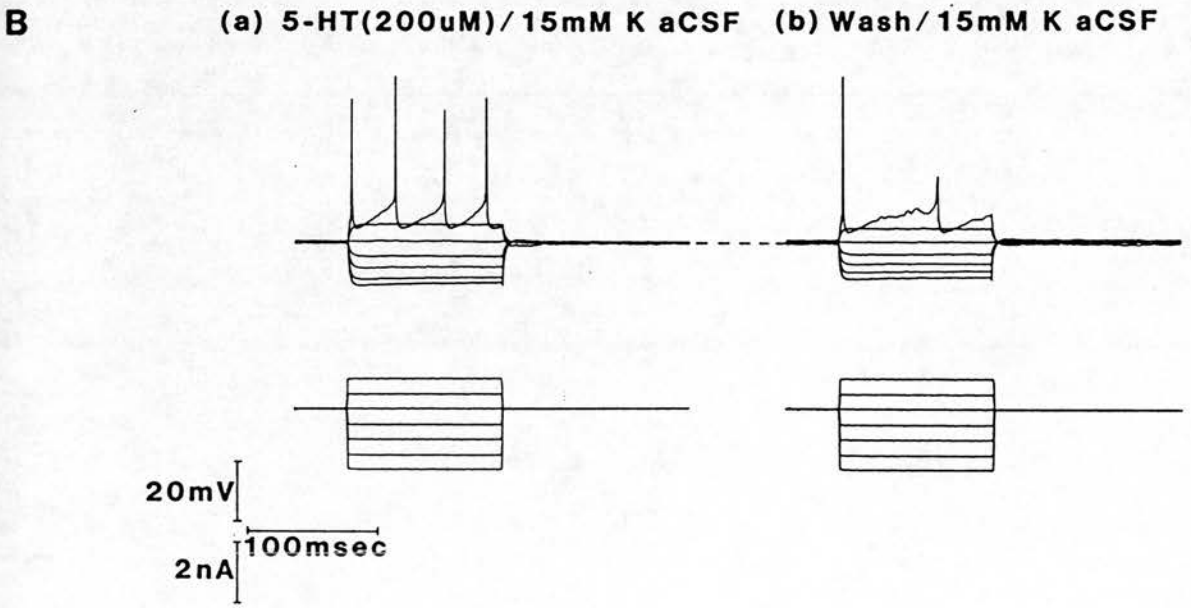
B
(a) 5-HT(200uM)/15mM K aCSF
(b) Wash/15mM K aCSF
20mV
100msec
2nA

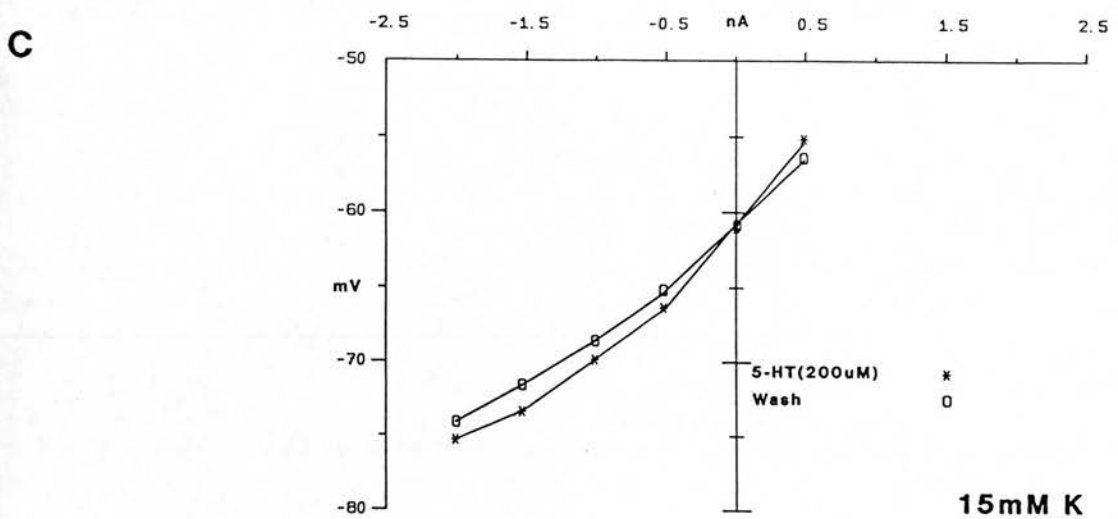
C
-2.5
-1.5
-0.5
nA
0.5
1.5
2.5
-50
-60
mV
-70
-80
5-HT(200uM)
Wash
15mM K

Figure 6.12

The action of 5-HT (200μM) in aCSF containing 15mM K^+ (II) (same cell as in Figs. 6.10, 6.11)

(A) Superfusion with 15mM K^+ aCSF led to depolarisation of the FM to a new resting potential of -61mV. 5-HT (200μM) superfusion did not evoke a change in membrane potential but an increase in Rm was observed.

(B) In the presence of 5-HT (200μM) $R_{m(pk)}$ measured over a narrow voltage range around Vm was 11MΩ (Ba). Washing with 5-HT free aCSF led to a recovery of $R_{m(pk)}$ to 8.7MΩ (Bb). Notice the absence of time dependent IR under these conditions and also the increase excitability in the presence of 5-HT (Ba).

(C) I/V plots in the absence of any depolarisation intersect at -61mV and linearity is observed only in the region ±5mV around resting potential. Thereafter both wash (open squares) and 5-HT (asterisks) curves show rectification, though in the presence of 5-HT increased Rm is maintained over this region of non-linearity.

Fig. 6.13

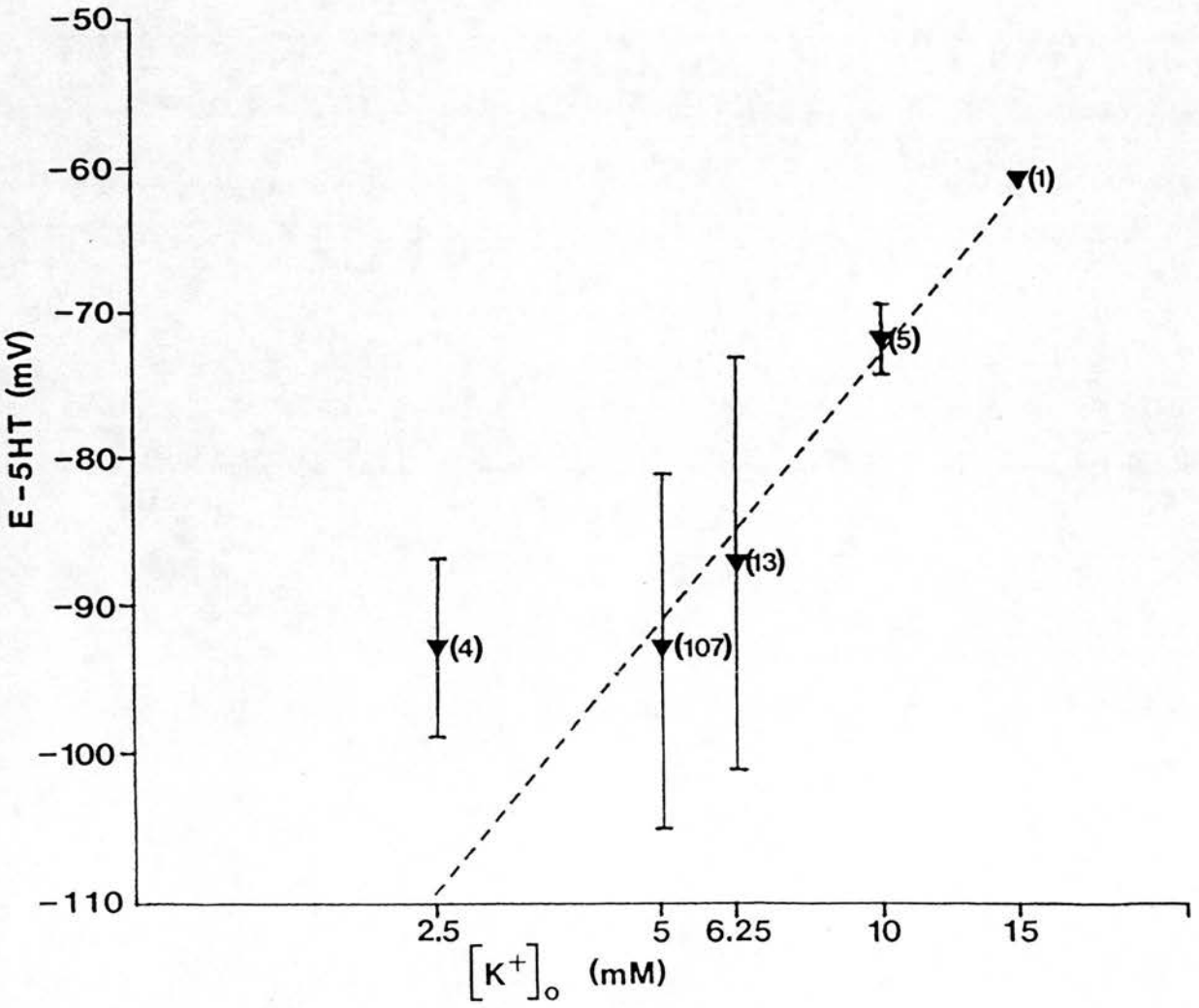

Figure 6.13

The reversal potential for the 5-HT evoked depolarisation of FM's in varying extracellular K^+ concentrations

The reversal potential for the 5-HT evoked depolarisation ($E_{5\text{-HT}}$ (mean ± SD for the number of observations in parentheses) is plotted against the $\log_{10}$ of the extracellular K^+ concentration. The dashed line represents the predicted values obtained from the Nernst equation for a conductance solely mediated by K^+. At higher $[K^+]_o$ (10 and 15mM), predicted and experimental values of $E_{5\text{-HT}}$ conform. In 6.25 and 5mM K^+, the mean values still conform to the predicted value but a wider variation is observed. In 2.5mM K^+ aCSF the experimental values for $E_{5\text{-HT}}$ are greatly different from the predicted value.

Fig. 6.14

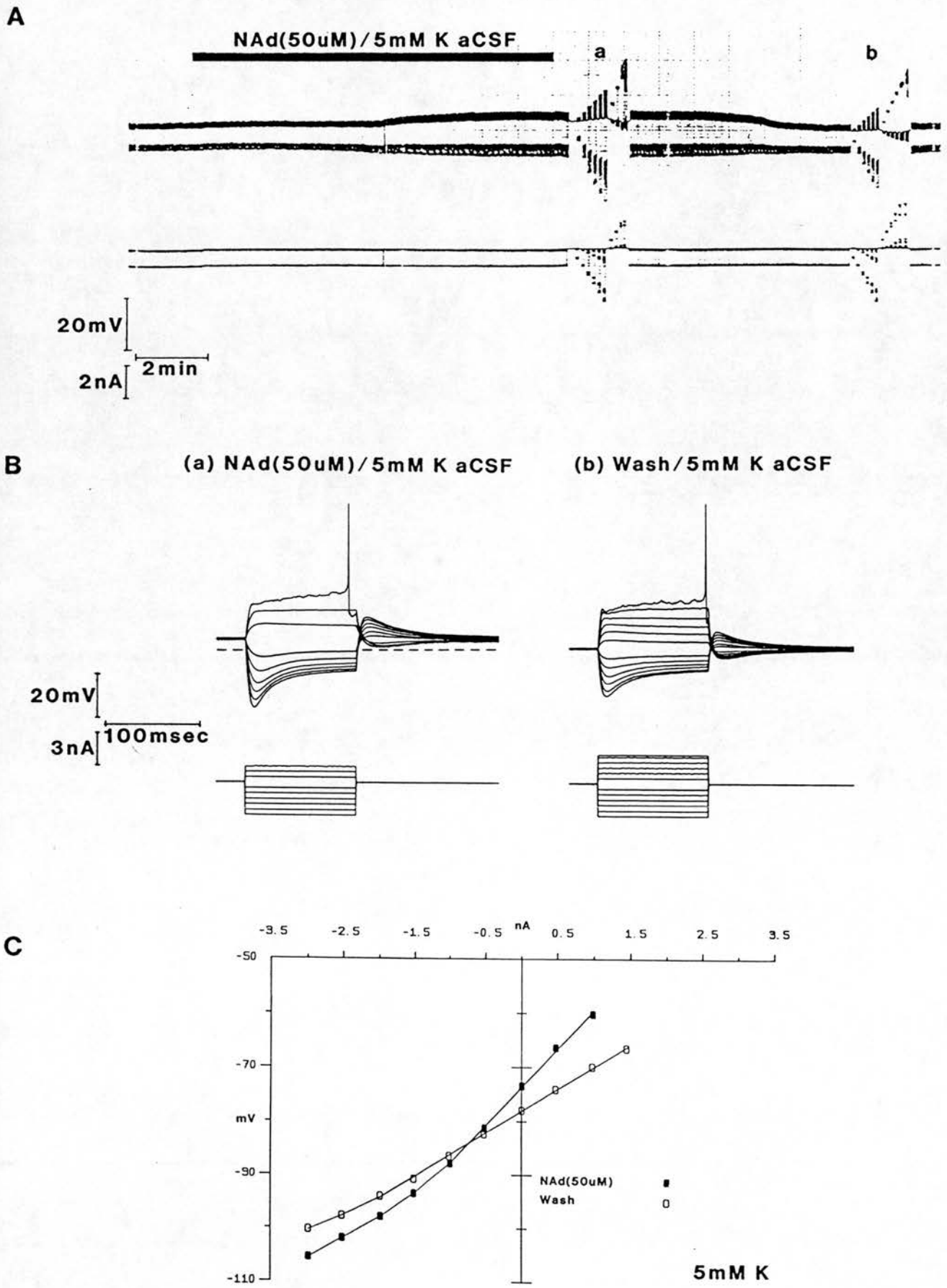
A
NAd(50uM)/5mM K aCSF
a
b
20mV
2nA
2min
B
(a) NAd(50uM)/5mM K aCSF
(b) Wash/5mM K aCSF
20mV
3nA
100msec
C
-3.5
-2.5
-1.5
-0.5
nA
0.5
1.5
2.5
3.5
-50
-70
mV
-90
-110
NAd(50uM)
Wash
5mM K

Figure 6.14

The action of NAd (50μM) in aCSF containing 5mM K^+ (I) (same cell as in Fig.6.15)

(A) Superfusion of NAd (50μM) evoked a depolarisation of 4.5mV from a resting potential of -76mV (upper trace). An associated increase in Rm was seen in response to test hyperpolarising current pulses (-1nA, 120msec, 1Hz; lower trace).

(B) Electrotonic potentials evoked by current steps of varying amplitude at the points marked in A showed the $R_{m(pk)}$ in NAd to be 14.2MΩ (Ba) and on recovery to be 8.2MΩ (Bb).

(C) Current voltage plots in NAd (closed squares) and after washing with drug-free aCSF (open squares) were linear up to the point of intersection at -84mV. (NAd, y = -71.5 + 14.2X; wash, y = -76 + 8.2X). Thereafter both relationships showed rectification though the slope in NAd remained steeper than in recovery conditions.

Fig. 6.15

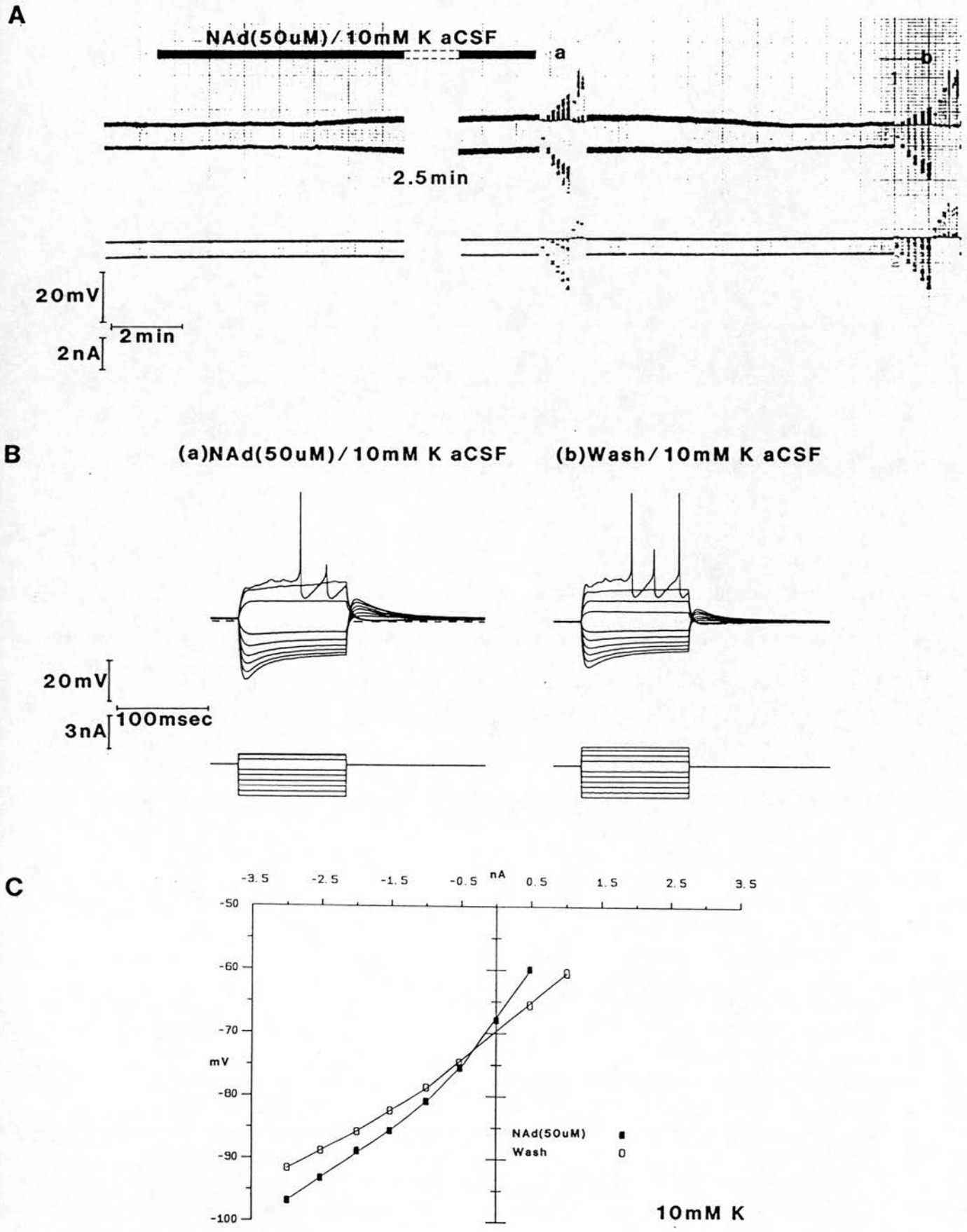
A
NAd(50uM)/10mM K aCSF
a
b
2.5min
20mV
2min
2nA
B
(a)NAd(50uM)/10mM K aCSF
(b)Wash/10mM K aCSF
20mV
100msec
3nA
C
-3.5
-2.5
-1.5
-0.5
nA
0.5
1.5
2.5
3.5
-50
-60
-70
mV
-80
-90
-100
NAd(50uM)
Wash
10mM K

Figure 6.15

The action of NAd (50μM) in aCSF containing 10mM K^+ (I) (same cell as in Fig.6.14)

(A) Superfusion with 10mM K^+ aCSF depolarised the FM to a new resting potential of -70mV. NAd (50μM) depolarised the neurone by 2mV associated with an increase in Rm, both of which were reversed by washing with drug-free aCSF.

(B) Values for $R_{m(pk)}$ of 15.6MΩ in NAd (Ba) and 9.2MΩ after washing (Bb) were obtained from electrotonic potentials evoked by a series of current pulses of different amplitude at the times labelled in A.

(C) The peak deflection current voltage plots were linear over a narrower range than seen in 5mM K^+ but intersected at -72.6mV (NAd, $y = -68 + 15.6X$; wash, $y = -70 + 9.2X$). Rectification occurred at potentials more negative than -80mV though NAd and wash I/V curves continued to diverge after this point.

Fig. 6.16

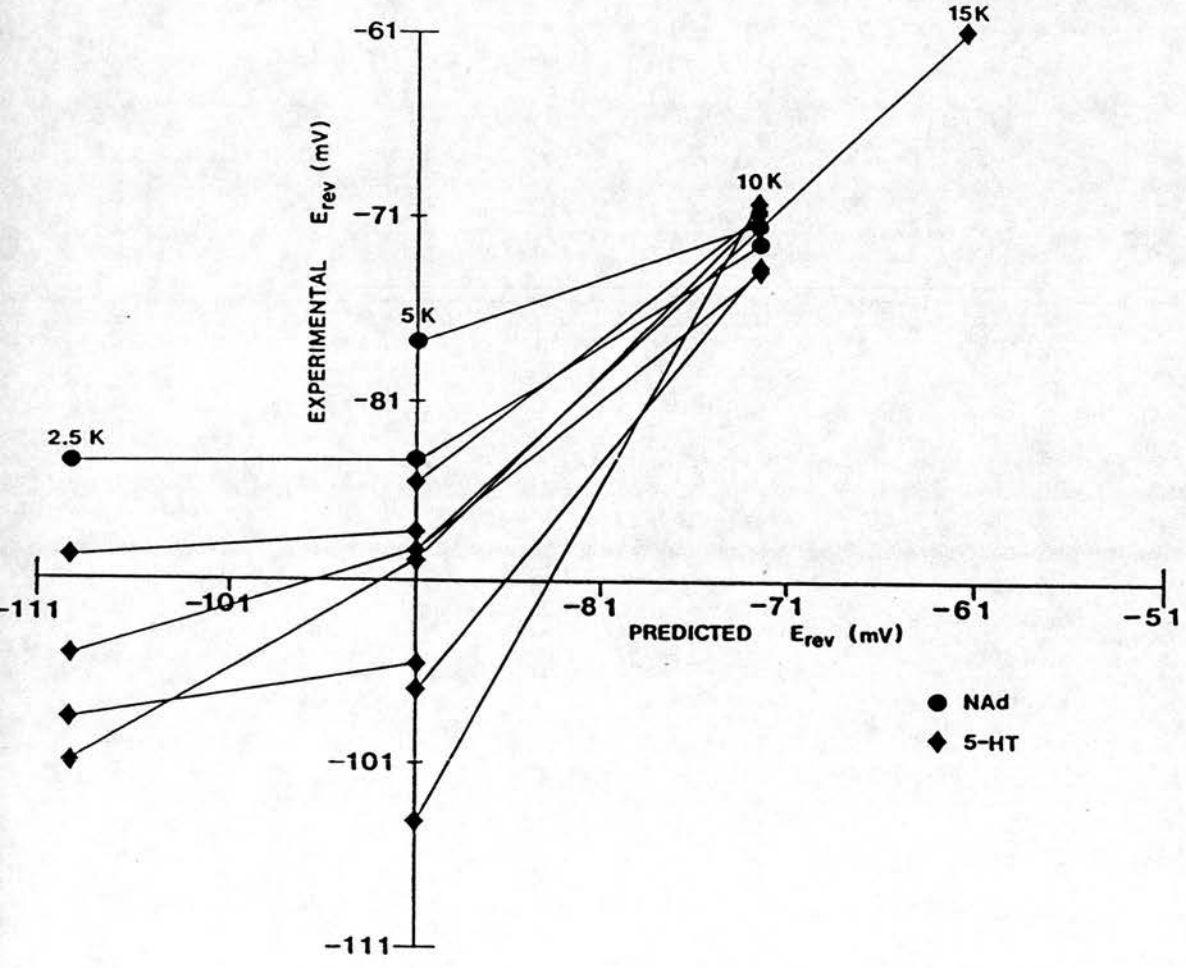
15K
-61
10K
-71
5K
-81
2.5 K
EXPERIMENTAL E_{rev} (mV)
-111
-101
-81
-71
-61
-51
PREDICTED E_{rev} (mV)
-101
-111
NAd
5-HT

Figure 6.16

Relationships between experimental and predicted $E_{5\text{-}HT}$ and E_{NAd}
Experimentally obtained reversal potentials for the actions of 5-HT and NAd on FM's plotted against values predicted from the Nernst equation, when superfusing with aCSF containing the concentration of K^+ indicated above each group of points (5-HT, diamonds, NAd, circles). Lines join points obtained from the same neurones.

Fig. 6.17

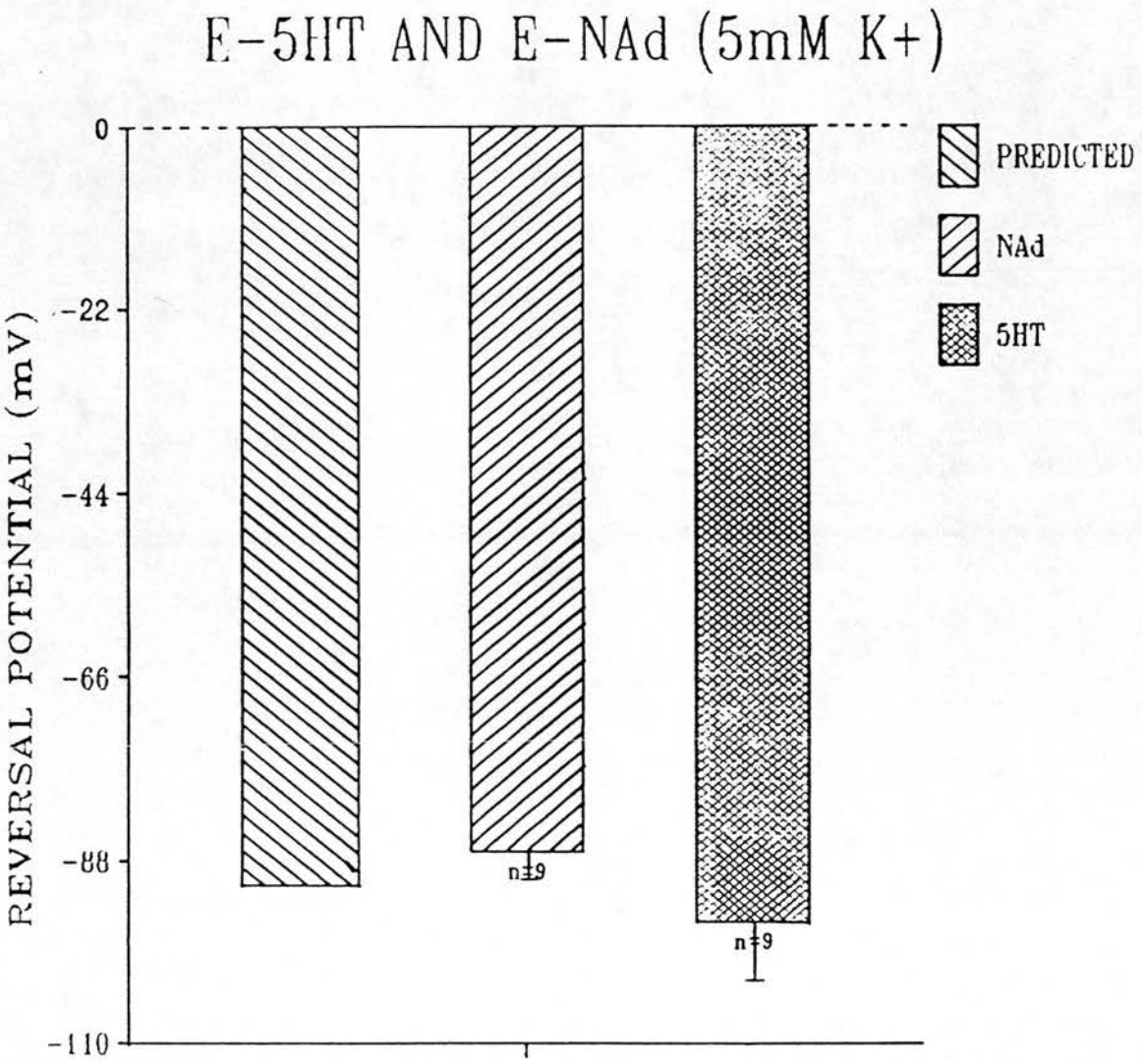
E-5HT AND E-NAd (5mM K+)
REVERSAL POTENTIAL (mV)
0
-22
-44
-66
-88
-110
n=9
n=9
PREDICTED
NAd
5HT

Figure 6.17

$E_{5\text{-}HT}$ and E_{NAd} obtained from the same FM's

Bar plot showing the difference between the reversal potentials obtained for NAd (-86.9 ± 4.8mV) and 5-HT (-95.4 ± 10.6mV) evoked depolarisation of similar magnitude on the same FM's (n = 9). The left hand bar represents the theoretically predicted value of -91mV (values are mean ± population SD).

Fig. 6.18

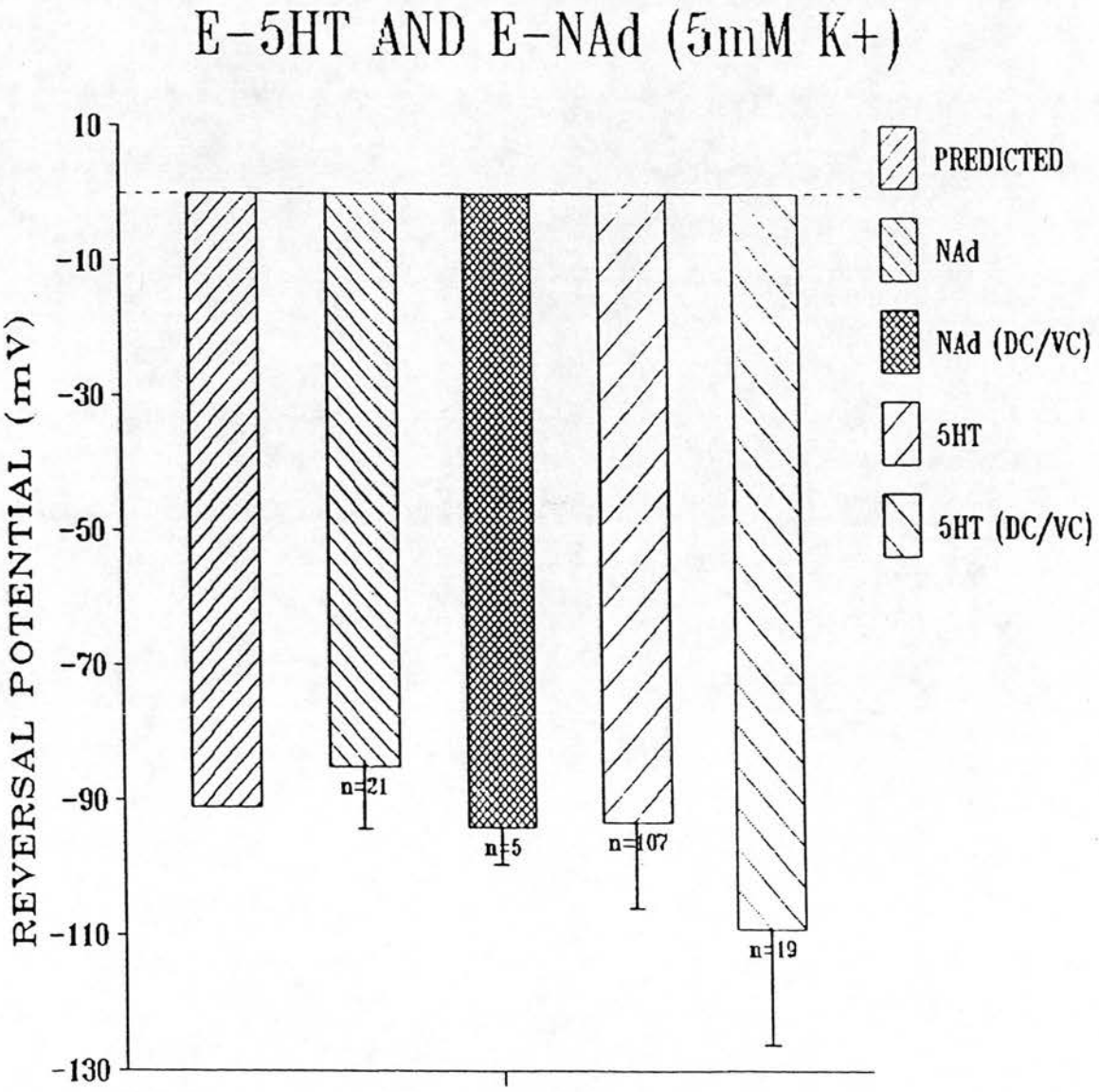
E-5HT AND E-NAd (5mM K+)
REVERSAL POTENTIAL (mV)
10
-10
-30
-50
-70
-90
-110
-130
n=21
n=5
n=107
n=19
PREDICTED
NAd
NAd (DC/VC)
5HT
5HT (DC/VC)

Figure 6.18

The effects of clamping the membrane potential on $E_{5\text{-}HT}$ and E_{NAd}
A bar chart summarising the reversal potentials obtained from all FM's tested with 5-HT and NAd both with and without manual or voltage clamping aimed at eliminating the effects of voltage dependent rectification. (See text for details) (mean ± SD for n observations).

Fig. 6.19

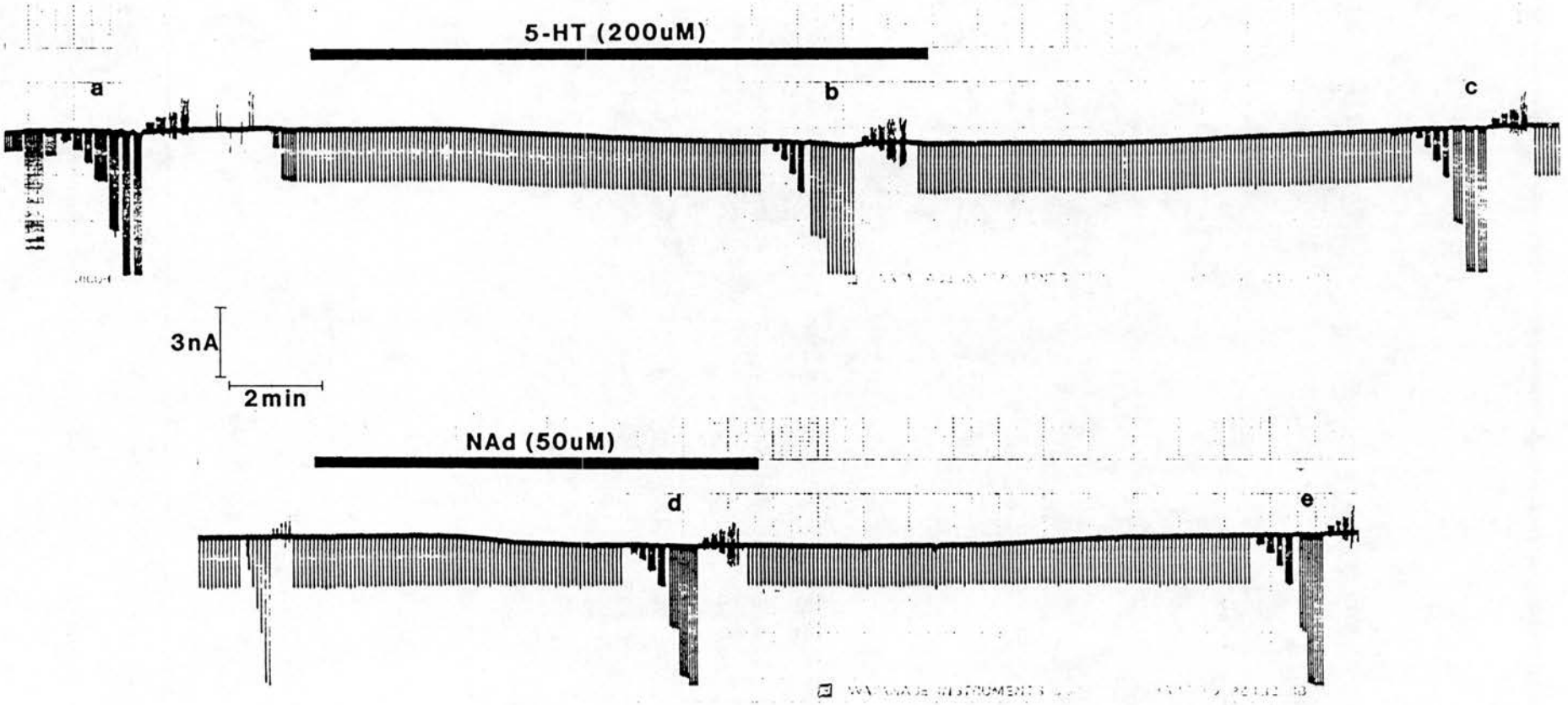

Figure 6.19

The effects of 5-HT (200μM) and NAd (50μM) on the same FM studied in dSEVC

A continuous chart record of membrane current responses to superfusion with 5-HT and NAd. The neurone was voltage clamped at its resting potential of -67mV. 5-HT (200μM) and NAd (50μM) both reversibly evoked inward currents -0.5nA in amplitude. Input conductance was monitored using a step hyperpolarising test voltage command (-20mV, 250msec, 0.2Hz) (voltage trace not shown). Both 5-HT and NAd inward currents were associated with a decrease in input conductance. Voltage-current relationships were constructed from current responses to voltage commands of varying amplitude at the points labelled a to e (see fig.6.20).

Fig. 6.20

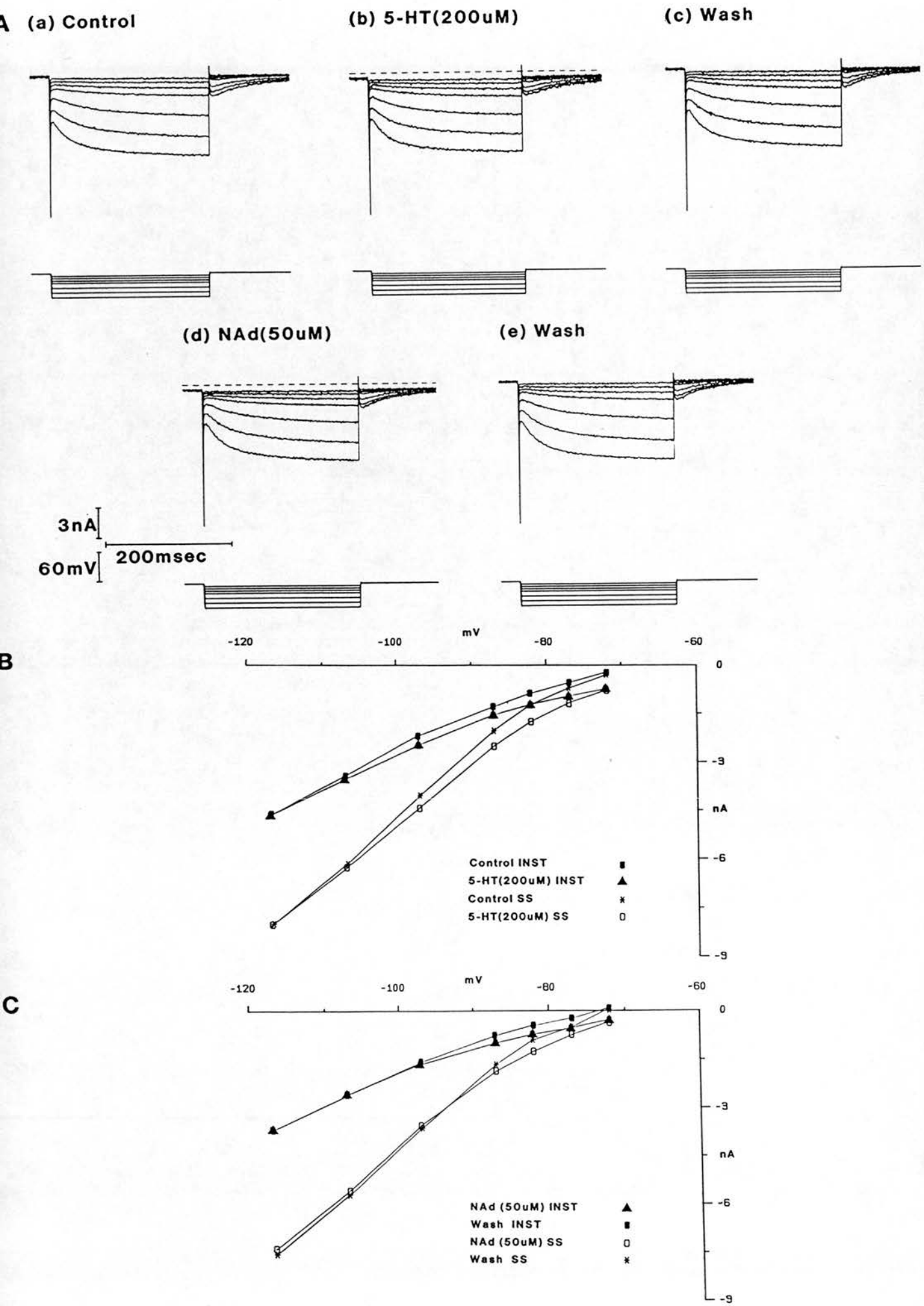
A
(a) Control
(b) 5-HT(200uM)
(c) Wash
(d) NAd(50uM)
(e) Wash
3nA
200msec
60mV
B
mV
-120
-100
-80
-60
0
-3
nA
-6
-9
Control INST
5-HT(200uM) INST
Control SS
5-HT(200uM) SS
C
mV
-120
-100
-80
-60
0
-3
nA
-6
-9
NAd (50uM) INST
Wash INST
NAd (50uM) SS
Wash SS

Figure 6.20

Step currents and voltage current relationships obtained from a FM superfused with 5-HT and NAd

A) Step currents (upper traces) evoked by step voltage commands (lower traces) at the corresponding times in Fig.6.19. Hyperpolarising voltage commands evoke a time and voltage dependent inward current (Aa) followed by a slowly relaxing inward tail current at the end of the voltage step. 5-HT (Ab) and NAd (Ad) reversibly evoke an inward current which is associated with a reduction in the amplitude of evoked currents measured both at the beginning (inst.) and the end (steady-state) of the pulse.

B) Voltage-current curves obtained in the absence and presence of 5-HT (Aa, Ab) measured at the start (inst; closed squares and triangles) and at the steady-state (asterisks and open squares) of the evoked current steps. Both sets of curves intersect at -117mV.

C) Voltage-current curves obtained in the absence and presence of NAd (50μM) measured at the start (inst; triangle and closed squares) and steady-state (open squares and asterisks) of the evoked current steps. Instantaneous curves intersect at -100mV and steady state curves at -96mV.

Fig. 6.21

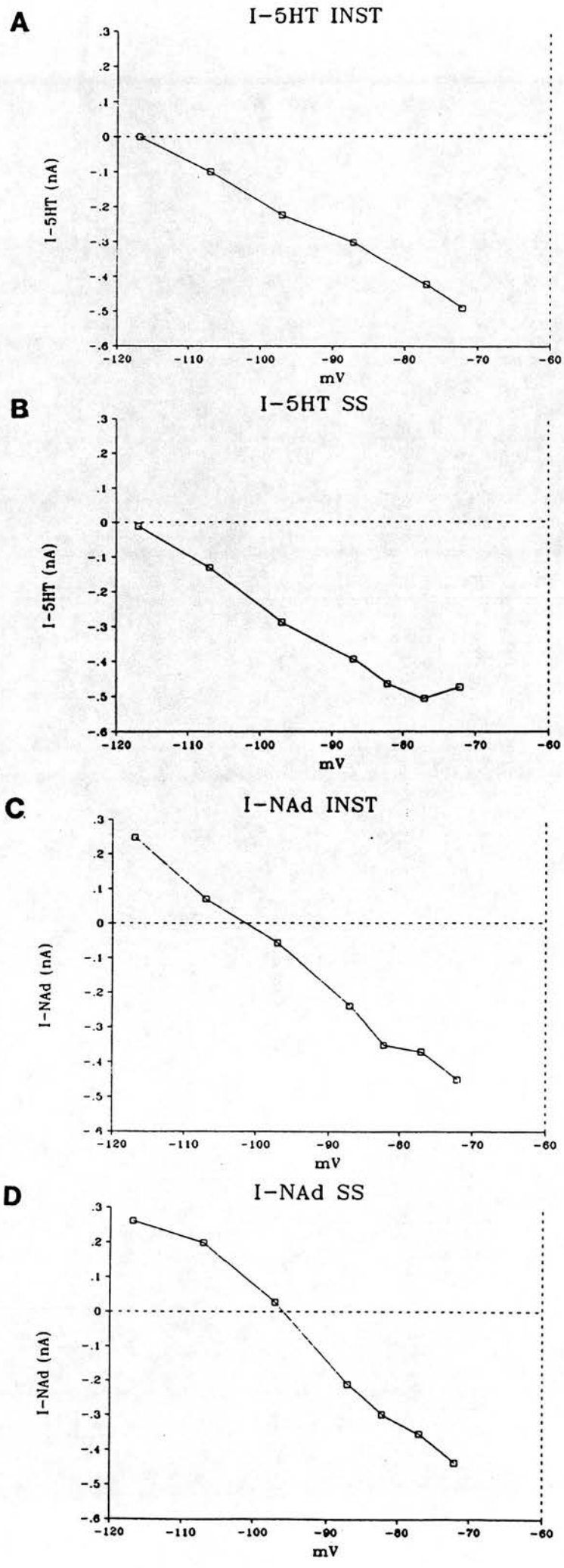
A
I-5HT INST
I-5HT (nA)
.3
.2
.1
0
-.1
-.2
-.3
-.4
-.5
-.6
-120
-110
-100
-90
-80
-70
-60
mV
B
I-5HT SS
I-5HT (nA)
mV
C
I-NAd INST
I-NAd (nA)
mV
D
I-NAd SS
I-NAd (nA)
mV

Figure 6.21

Inward currents evoked by 5-HT and NAd

5-HT and NAd evoked currents obtained by subtraction of step currents evoked in the absence of neurotransmitter from those evoked in its presence. The reversal potentials for the two transmitters are clearly shown to be different from the points of intersection with zero evoked current. Both 5-HT and NAd evoked currents are linear and the same whether measured at the start (I-5-HT INST/I-NAd INST) or the steady-state (I-5-HT SS; I-NAd SS) of the step current, indicating that time dependent IR appears not to be affected by either transmitter.

Fig. 6.22

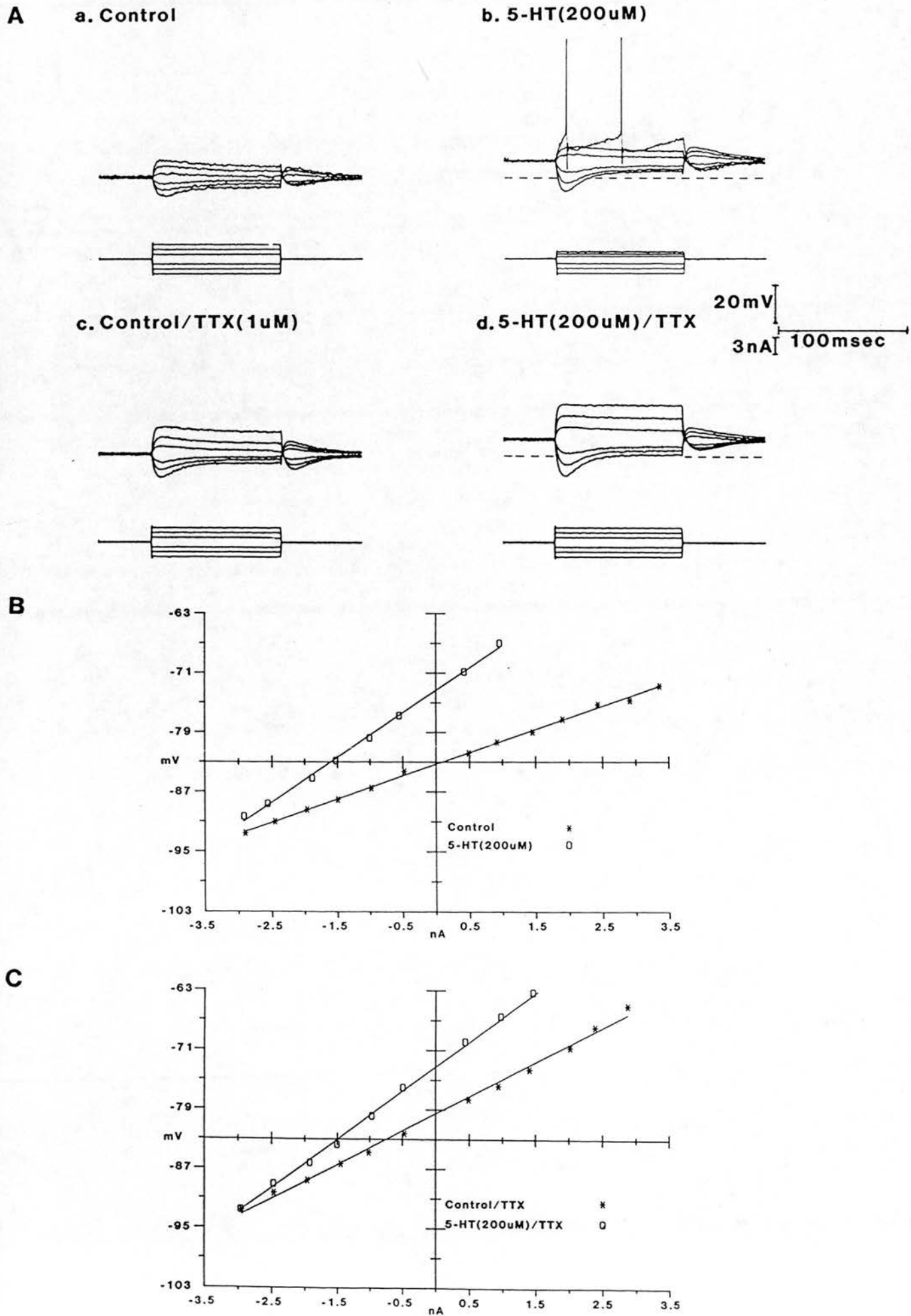
A
a. Control
b. 5-HT(200uM)
20mV
3nA
100msec
c. Control/TTX(1uM)
d. 5-HT(200uM)/TTX
B
-63
-71
-79
mV
-87
-95
-103
-3.5
-2.5
-1.5
-0.5
nA
0.5
1.5
2.5
3.5
Control
5-HT(200uM)
C
Control/TTX
5-HT(200uM)/TTX

Figure 6.22

The action of 5-HT (200μM) on a FM in the presence of Tetrodotoxin (1μM) (I)

A) Electrotonic potentials (upper trace) evoked by current steps (lower traces) show 5-HT (200μM) to evoke a depolarisation to -74mV from a resting potential of -83mV associated with an increase in $R_{m(pk)}$ from 3.2 to 6MΩ (Aa, Ab). Recovery to -81mV with a $R_{m(pk)}$ of 4.5MΩ was obtained (not shown). TTX (1μM) abolished Na^+ dependent action potentials but did not affect resting potential (-81mV) or $R_{m(pk)}$ (4.6MΩ) (Ac). Superfusion of 5-HT (200μM) evoked a depolarisation again to -74mV with an increase in $R_{m(pk)}$ to 6.7MΩ (Ad).

B) Peak deflection current-voltage plots obtained in control (asterisks) and 5-HT (open squares) conditions were linear and had an extrapolated crossover point at -92.5mV.

C) In the presence of TTX current voltage plots remained linear and intersected at -95mV.

Fig. 6.23

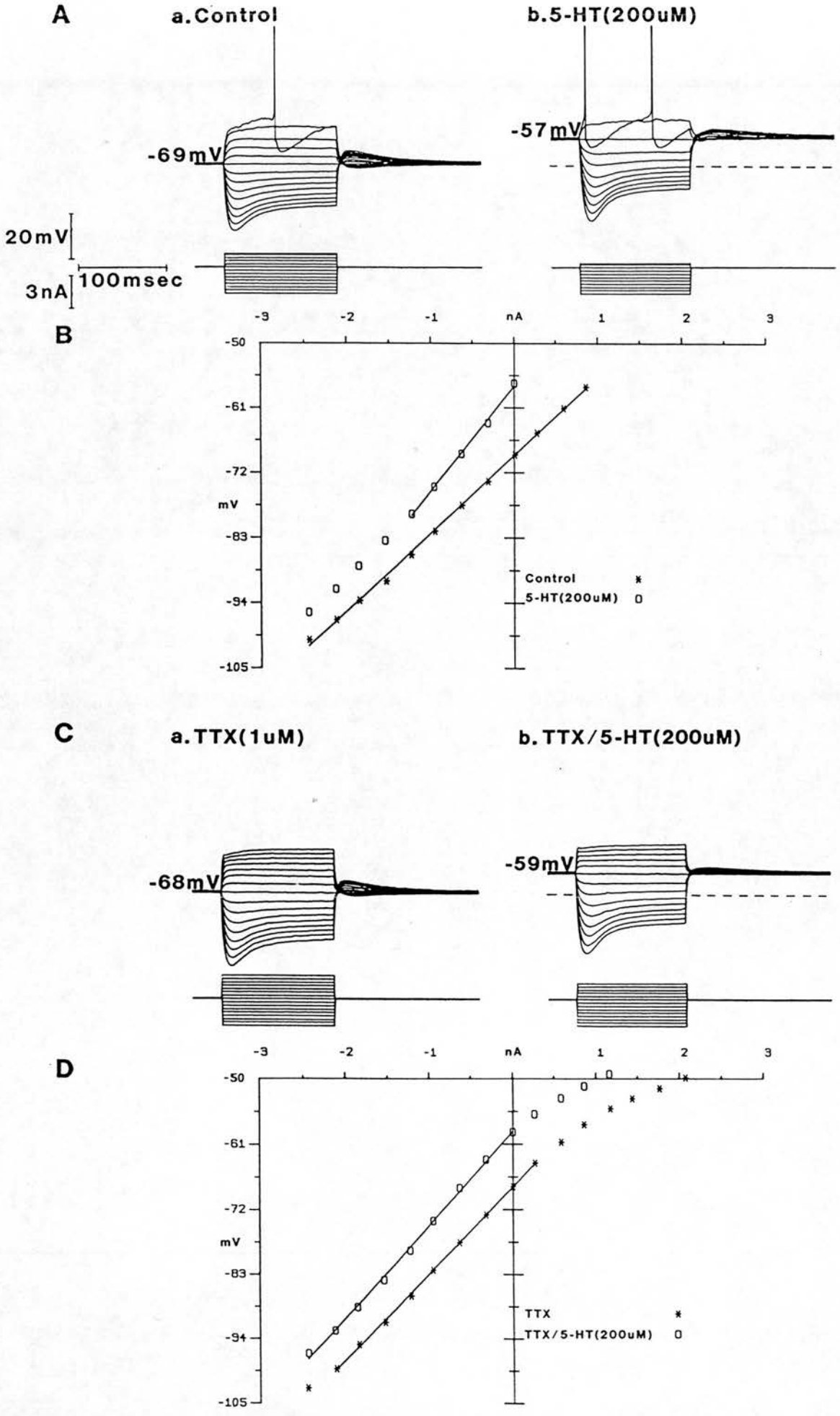
A
a.Control
b.5-HT(200uM)
-69mV
-57mV
20mV
3nA
100msec
B
-3
-2
-1
nA
1
2
3
-50
-61
-72
mV
-83
-94
-105
Control
5-HT(200uM)
C
a.TTX(1uM)
b.TTX/5-HT(200uM)
-68mV
-59mV
D
TTX
TTX/5-HT(200uM)

Figure 6.23

The action of 5-HT (200μM) on a FM in the presence of TTX (1μM) (II)
A) The FM was resting at -69mV and $R_{m(pk)}$ over its linear range measured from the electrotonic potentials in Aa, was 13.2MΩ. Addition of 5-HT (200μM) evoked a depolarisation of 11mV (Ab). $R_{m(pk)}$ was linear over a smaller voltage range but increased to 17.8MΩ (Ab). Note the suppression of the depolarising tail potential after large amplitude hyperpolarising potentials (Ab).
B) Current voltage plots in the absence (asterisks) and presence of 5-HT (open squares) did not intersect and at more negative potentials tended to become parallel. An estimated reversal potential of -102mV was obtained from the extrapolated point of intersection of the linear components of the I/V plots.
C) Addition of TTX (1μM) did not affect the resting potential or $R_{m(pk)}$ in the hyperpolarizing direction (14.7MΩ) (Ca). However pronounced outward rectification was seen in the depolarising portion of the control I/V relation (Ca, D). 5-HT (200μM) in the presence of TTX, evoked a similar amplitude depolarization as control (9mV) (Cb). $R_{m(pk)}$ was this time linear over the same voltage range as control but showed only a small increase to 15.8MΩ.
D) Control (asterisks) and 5-HT (open squares) current voltage relations in the presence of TTX fail to intersect.

Fig. 6.24

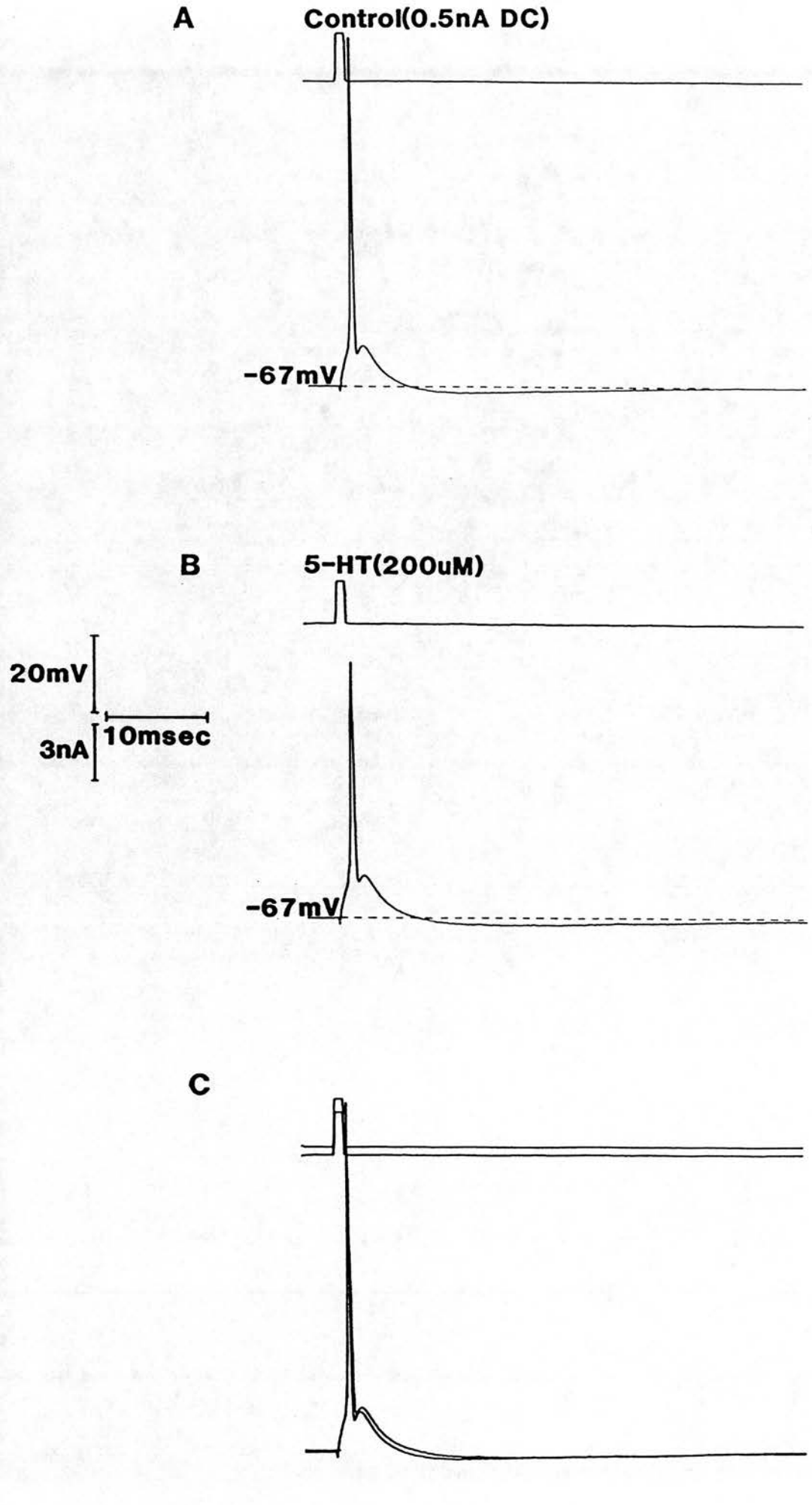

Figure 6.24

Effects of 5-HT on the delayed depolarisation (DD) and slow afterhyperpolarisation (s ahp) following the FM action potential (AP)

A and B show averaged records of AP's evoked by 1ms duration depolarising current pulses. Action potential amplitude is attenuated due to the slow sampling rate used to observe the slower post-AP events. At the peak of the 5-HT evoked depolarisation (-67mV) a single spike evoked by a +2.2nA current pulse was followed by a DD 11.1mV in amplitude and a s ahp of -1.7mV and 46ms in duration (B). After recovery from the 5-HT evoked depolarisation the neurone was manually depolarised to -67mV with +0.5nA DC and an AP evoked with a +2.5nA current pulse. The amplitude of the DD was reduced to 10.5mV while the s ahp remained constant at -1.7mV, 37msec (A). When superimposed as in C, the difference in amplitude and duration of the DD is clearly seen.

Fig. 6.25

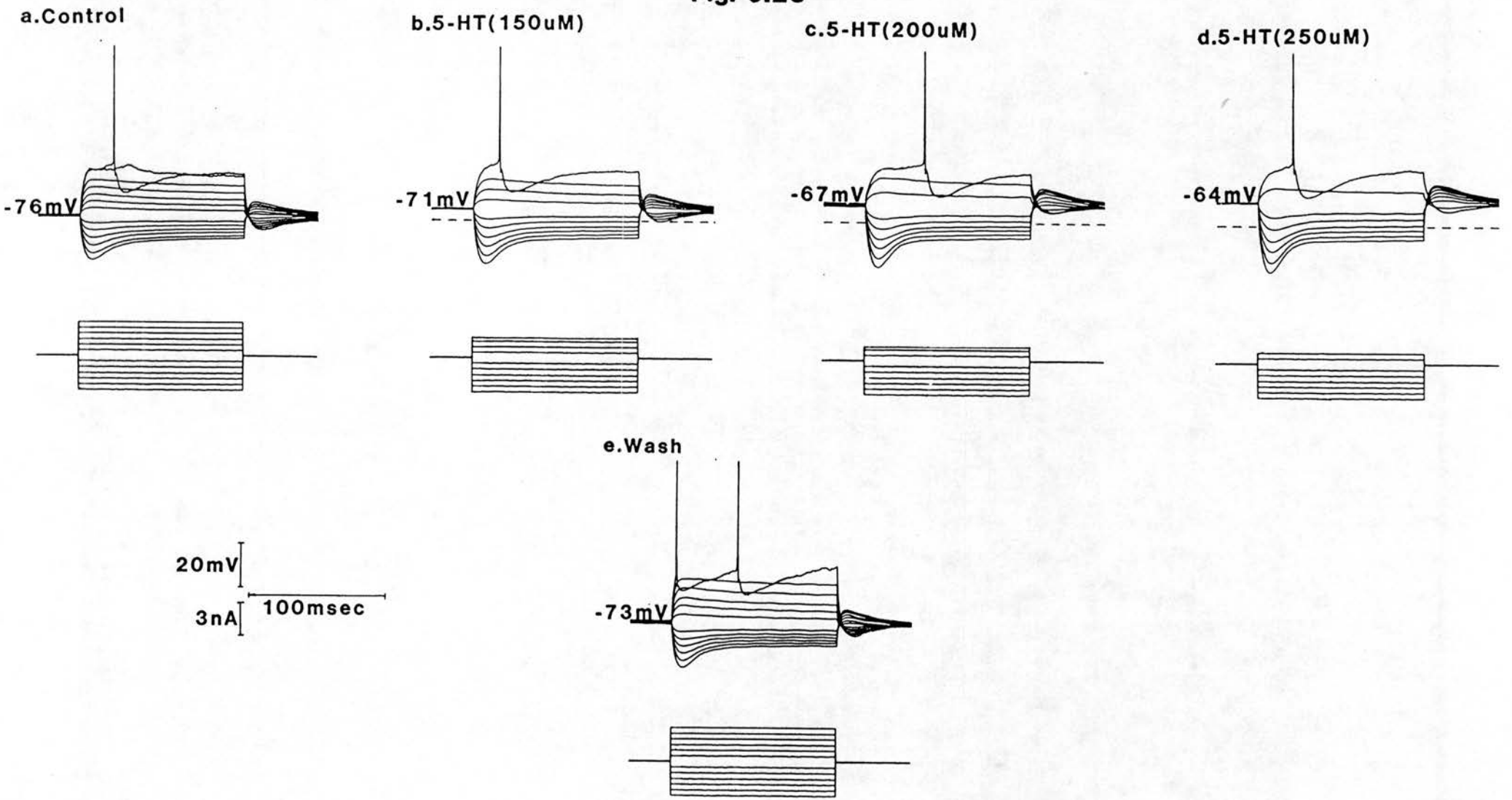
a.Control
b.5-HT(150uM)
c.5-HT(200uM)
d.5-HT(250uM)
-76mV
-71mV
-67mV
-64mV
e.Wash
-73mV
20mV
3nA
100msec

Figure 6.25

5-HT dose response relationship of a single FM using a continuous application protocol

Averaged membrane voltage responses (upper traces) evoked by current pulses of varying amplitude (lower traces) show that prior to 5-HT application the FM had a $R_{m(pk)}$ of 6.7MΩ and was resting at -76mV. A single AP was evoked by a +3nA, 120msec current pulse (a). Addition of 5-HT (150μM) to the superfusing aCSF evoked a depolarisation of 5mV to a new steady-state potential of -71mV. This was associated with an increase in $R_{m(pk)}$ to 8.6MΩ and a single AP could be evoked by a +1.9nA, 120msec current pulse (b). Without allowing baseline membrane potential recovery the concentration of 5-HT in the aCSF was raised to 200μM (c). Depolarisation to a new plateau at -67mV followed associated with an increase in $R_{m(pk)}$ to 10MΩ. A +1.2nA, 120msec current pulse was now sufficient to evoke a single AP. Raising of the 5-HT concentration to 250μM depolarised the neurone a further 3mV to -64mV and $R_{m(pk)}$ increased to 10.9MΩ (d). A single AP was now evoked by a +1nA, 120msec current pulse. Subsequent washing with 5-HT-free aCSF led to a recovery of membrane potential to -73mV and $R_{m(pk)}$ to 7.1MΩ (e).

Fig. 6.26

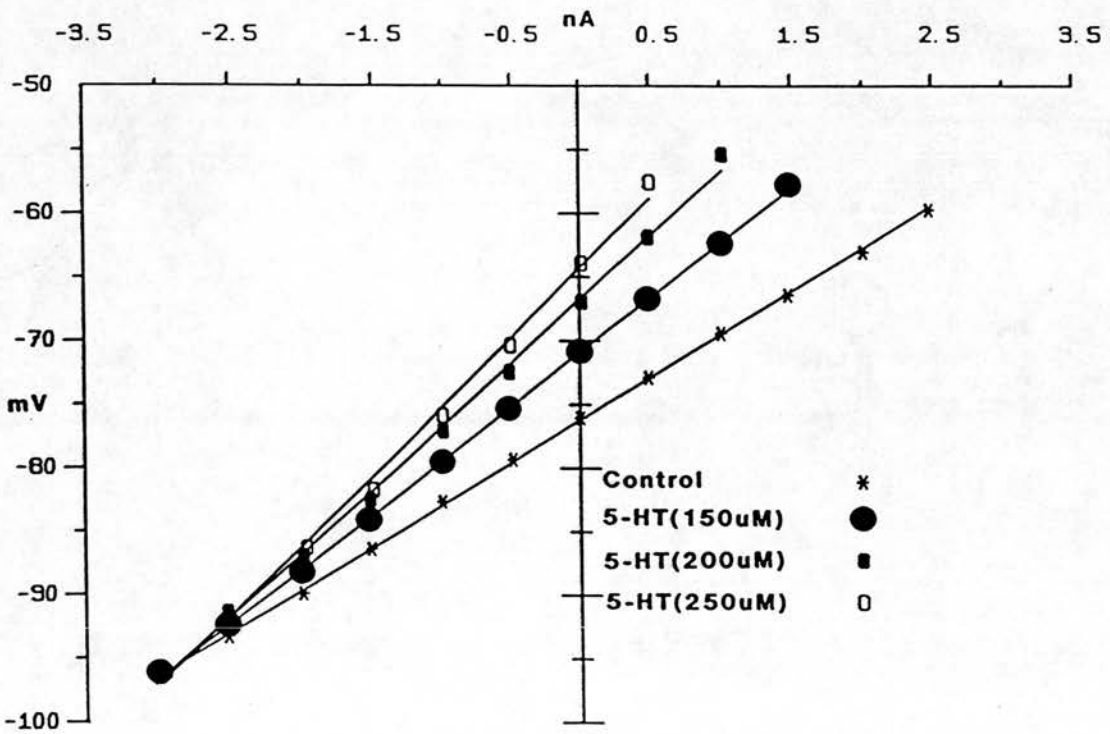
-3.5
-2.5
-1.5
-0.5
nA
0.5
1.5
2.5
3.5
-50
-60
-70
mV
-80
-90
-100
Control
5-HT(150uM)
5-HT(200uM)
5-HT(250uM)

Figure 6.26

Current voltage plots for the FM in Fig.6.25
Peak deflection current-voltage plots taken from the records in figure 6.25a-d were linear in control conditions and each concentration of 5-HT tested. The reversal potential for the 5-HT evoked depolarisation taken from the point of intersection of these I/V plots was independent of 5-HT concentration and had a value of around -96mV.

Fig. 6.27

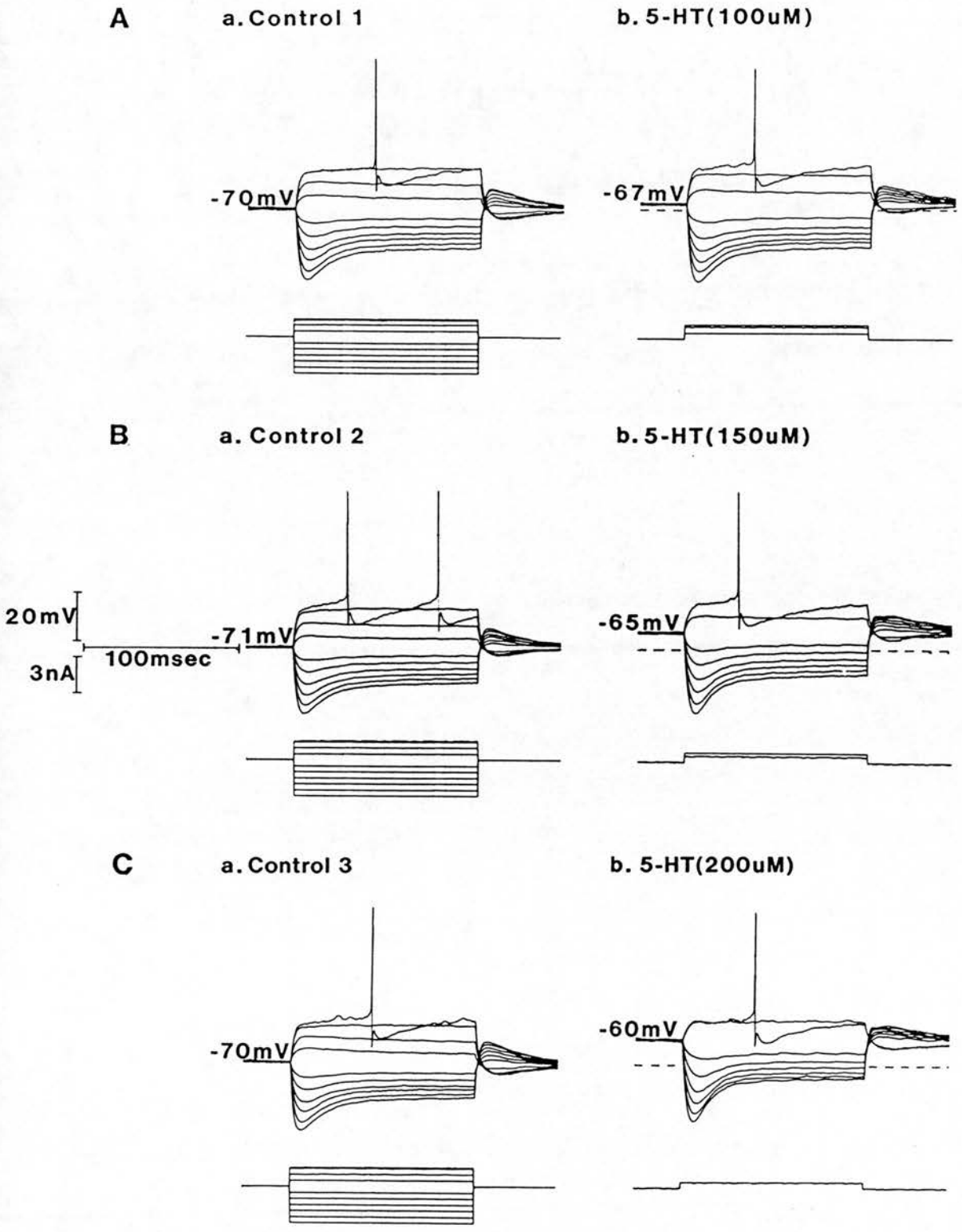
A
a. Control 1
b. 5-HT(100uM)
-70mV
-67mV
B
a. Control 2
b. 5-HT(150uM)
20mV
100msec
3nA
-71mV
-65mV
C
a. Control 3
b. 5-HT(200uM)
-70mV
-60mV

Figure 6.27

5-HT dose-response relationship of a single FM using a discontinuous application protocol

5-HT (100μM) evoked a 3mV depolarisation from a resting potential of -70mV and was associated with an increase in $R_{m(pk)}$ from 11.2 to 12.3MΩ (Aa,b). Full recovery from 5-HT evoked effects was obtained before the next dose of 5-HT was applied.

5-HT (150μM) evoked a larger depolarisation (6mV) and increase in $R_{m(pk)}$ (9.7 to 11.6MΩ) (Ba,b).

5-HT (200μM) further increased the amplitude of the depolarisation (10mV) and change in $R_{m(pk)}$ (11 to 14.6MΩ) (Ca,b). In each case AP threshold remained constant but the current step required to reach this level was reduced from a control value of +1.6nA to +1.2, +0.8, and +0.6nA in 100, 150 and 200μM 5-HT respectively. Hyperpolarising current steps seen under control records also apply to the corresponding 5-HT records.

Fig. 6.28

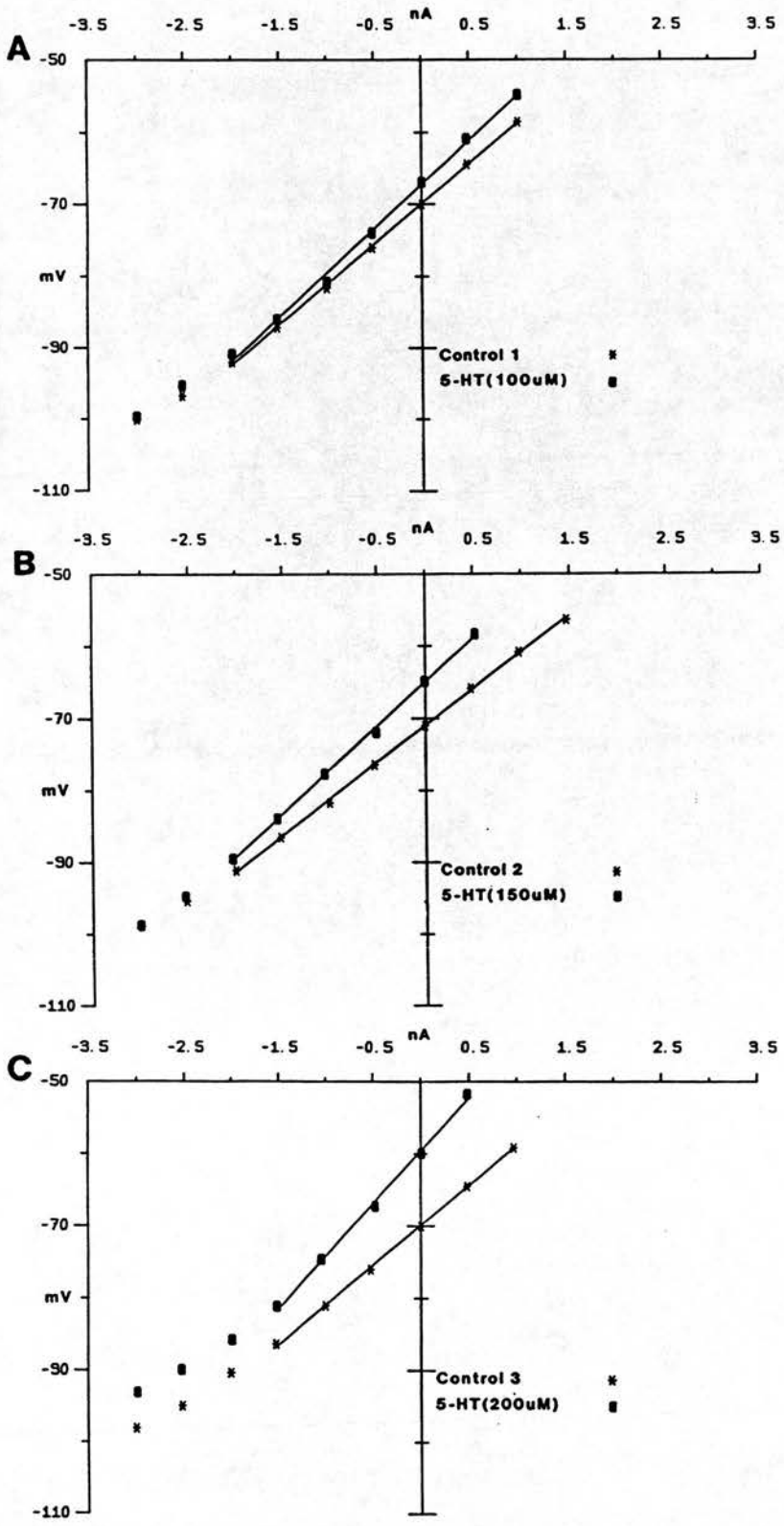
A
B
C
nA
-3.5
-2.5
-1.5
-0.5
0.5
1.5
2.5
3.5
-50
-70
-90
-110
mV
Control 1
5-HT(100uM)
Control 2
5-HT(150uM)
Control 3
5-HT(200uM)

Figure 6.28

Peak deflection current-voltage relationships for the electrotonic potentials shown in figure 6.27

In each case control and 5-HT plots show some non-linearity at more negative potentials.

A) Control 1 and 5-HT (100μM) plots show a point of intersection at about -100mV on the non-linear region of the curves which is close the extrapolated value of -98mV taken from the linear regions.

B) Control 2 and 5-HT (150μM) relationships also intersect at about -100mV in their non-linear region while extrapolation of the linear regions gives a value of -101mV.

C) Control 3 and 5-HT (200μM) relationships do not intersect in the tested range. Non linearity in the 5-HT curve occurs at less negative potentials than seen previously (compare C with A and B) and appears to then run parallel with the control 3 plot (cf fig.6.23B). The extrapolated point of intersection from the linear regions is similar to the values obtained for lower concentrations of 5-HT at -102mV.

Fig. 6.29

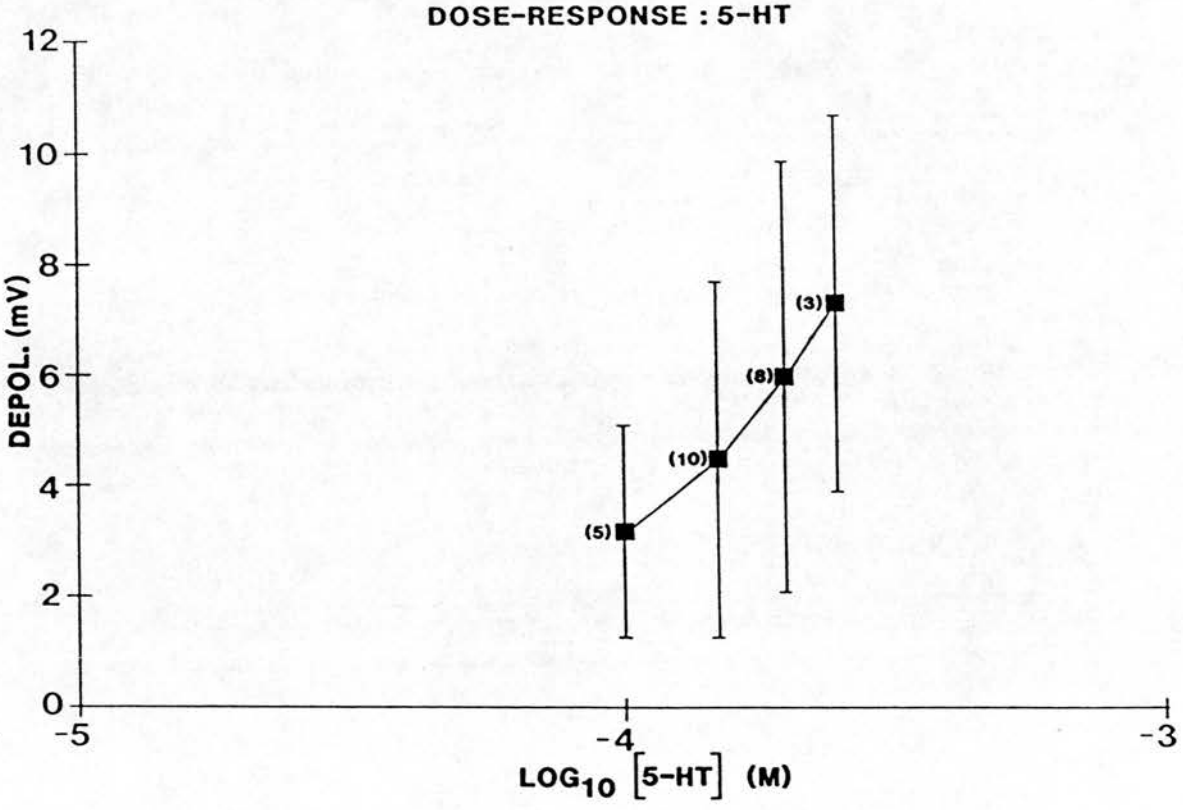

Figure 6.29

Dose-response curve for 5-HT-evoked depolarisation of FM's

The effects of 5-HT concentration on the amplitude of the evoked depolarisation from a population of FM's. Values are mean ± SD for the number of observations in brackets.

Fig. 6.30

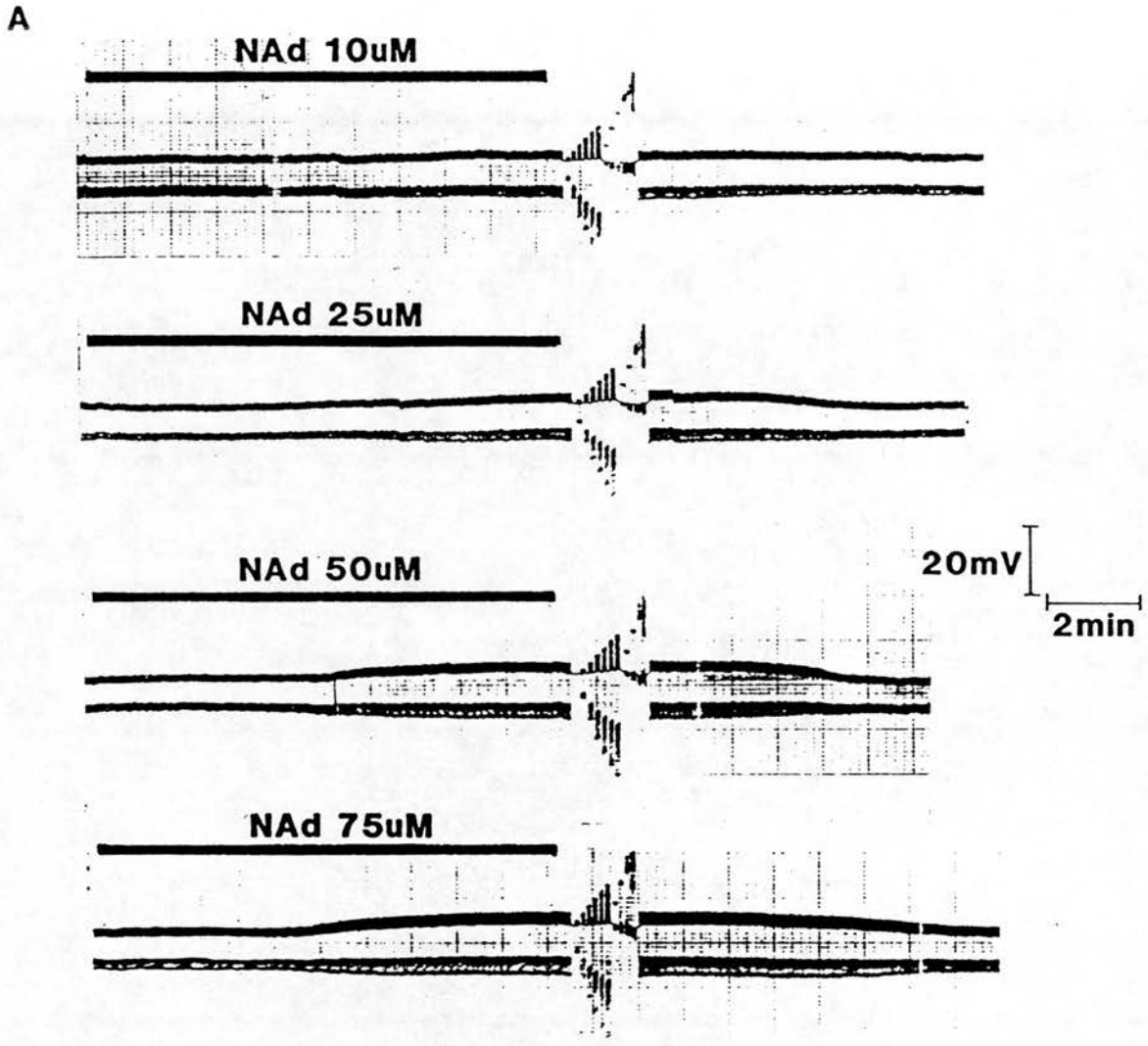
A
NAd 10uM
NAd 25uM
NAd 50uM
NAd 75uM
20mV
2min

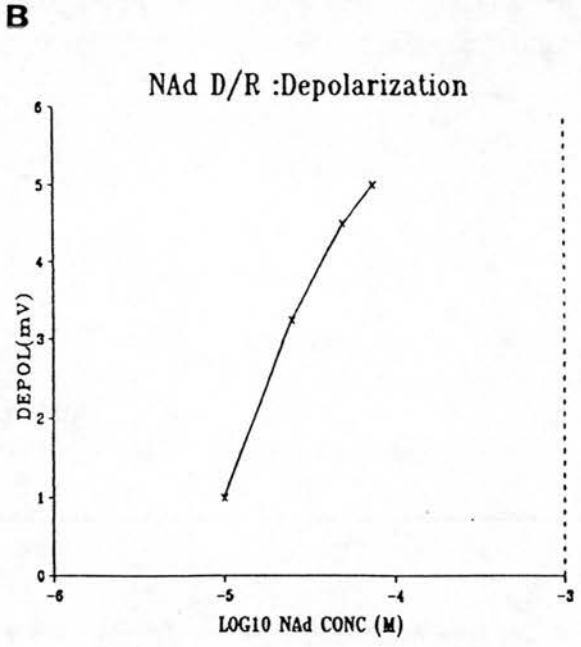
B
NAd D/R :Depolarization
DEPOL(mV)
LOG10 NAd CONC (M)

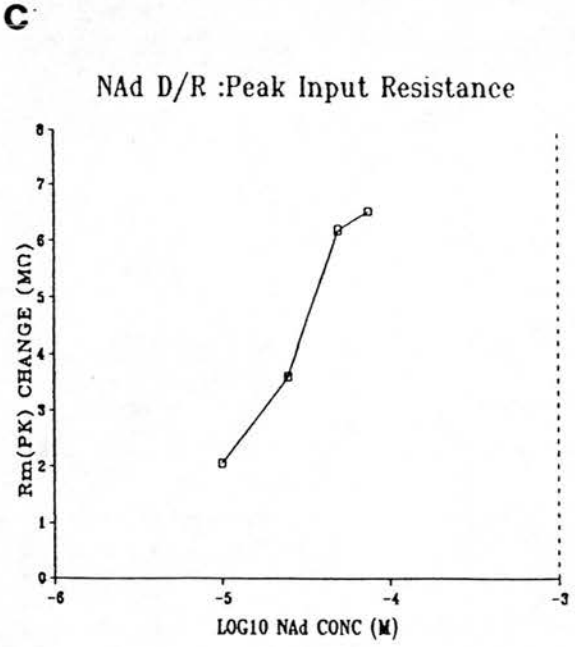
C
NAd D/R :Peak Input Resistance
Rm(PK) CHANGE (MΩ)
LOG10 NAd CONC (M)

Figure 6.30

D/R relationship for the effect of NAd on a FM

A) The continuous chart records illustrate the dose dependency of the NAd evoked depolarisation and associated increase in input resistance as a result of membrane voltage responses to -1nA, 120msec current pulses at a frequency of 1Hz (not shown). The relationship between depolarisation amplitude and NAd concentration and change in $R_{m(pk)}$ and NAd concentration are illustrated in B and C respectively. 10μM NAd evoked a 1mV depolarisation associated with a change in $R_{m(pk)}$ from 8.9 to 10.9MΩ. Responses for 25, 50 and 75μM NAd were depolarisations of 3, 4.5 and 5mV associated with increases in $R_{m(pk)}$ of 8.2 to 11.6MΩ, 8.2 to 14.2MΩ and 8.9 to 15.8MΩ respectively.

Fig. 6.31

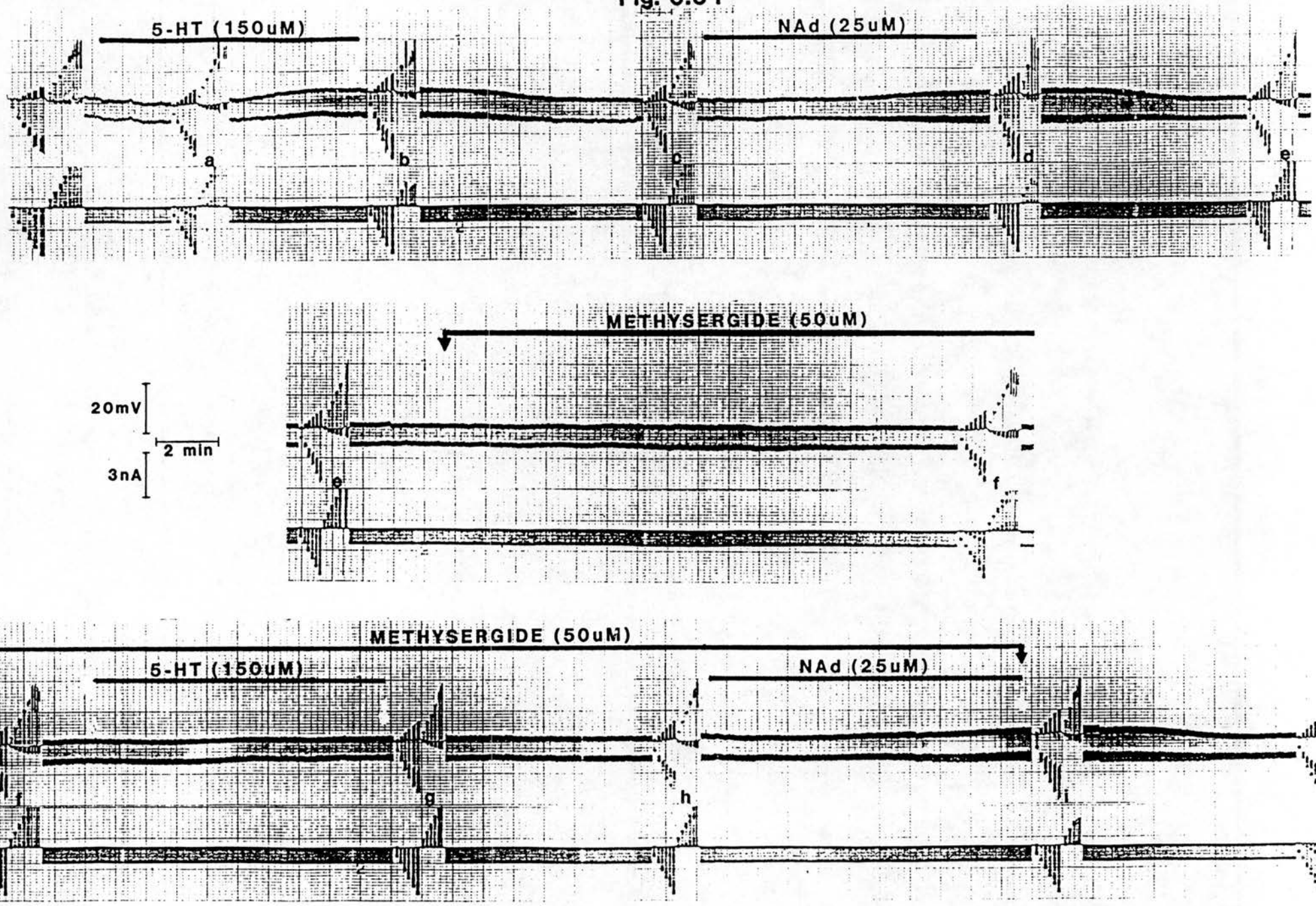
5-HT (150uM)
NAd (25uM)
a
b
c
d
e
METHYSERGIDE (50uM)
20mV
2 min
3nA
e
f
METHYSERGIDE (50uM)
5-HT (150uM)
NAd (25uM)
g
h
i
j

Figure 6.31

Antagonism of the 5-HT but not the NAd-evoked depolarisation by superfusion with methysergide

Continuous chart records to show the effects of methysergide (50μM) on 5-HT (150μM) and NAd (25μM) evoked changes in membrane potential (upper trace) and input resistance determined from voltage responses to a hyperpolarising current test pulse (-1nA, 120msec, 1Hz) (lower trace). 5-HT (150μM) evoked a 5mV depolarisation from the resting potential of -78mV while NAd (25μM) evoked a 3mV depolarisation. Both responses were associated with an increase in R_m. Subsequent coapplication of 5-HT (150μM) with methysergide (50μM) led to only a small 1mV depolarisation with little change in R_m. The action of NAd (25μM) was unaffected by the presence of methysergide, evoking a 3.5mV depolarisation associated with an increase in R_m. At points a to j current pulses of various amplitudes were used to evoke the membrane voltage responses shown in expanded form in figures 6.32 and 6.33 from which measures of R_m and the reversal potential of the actions of 5-HT and NAd were evaluated.

Fig. 6.32

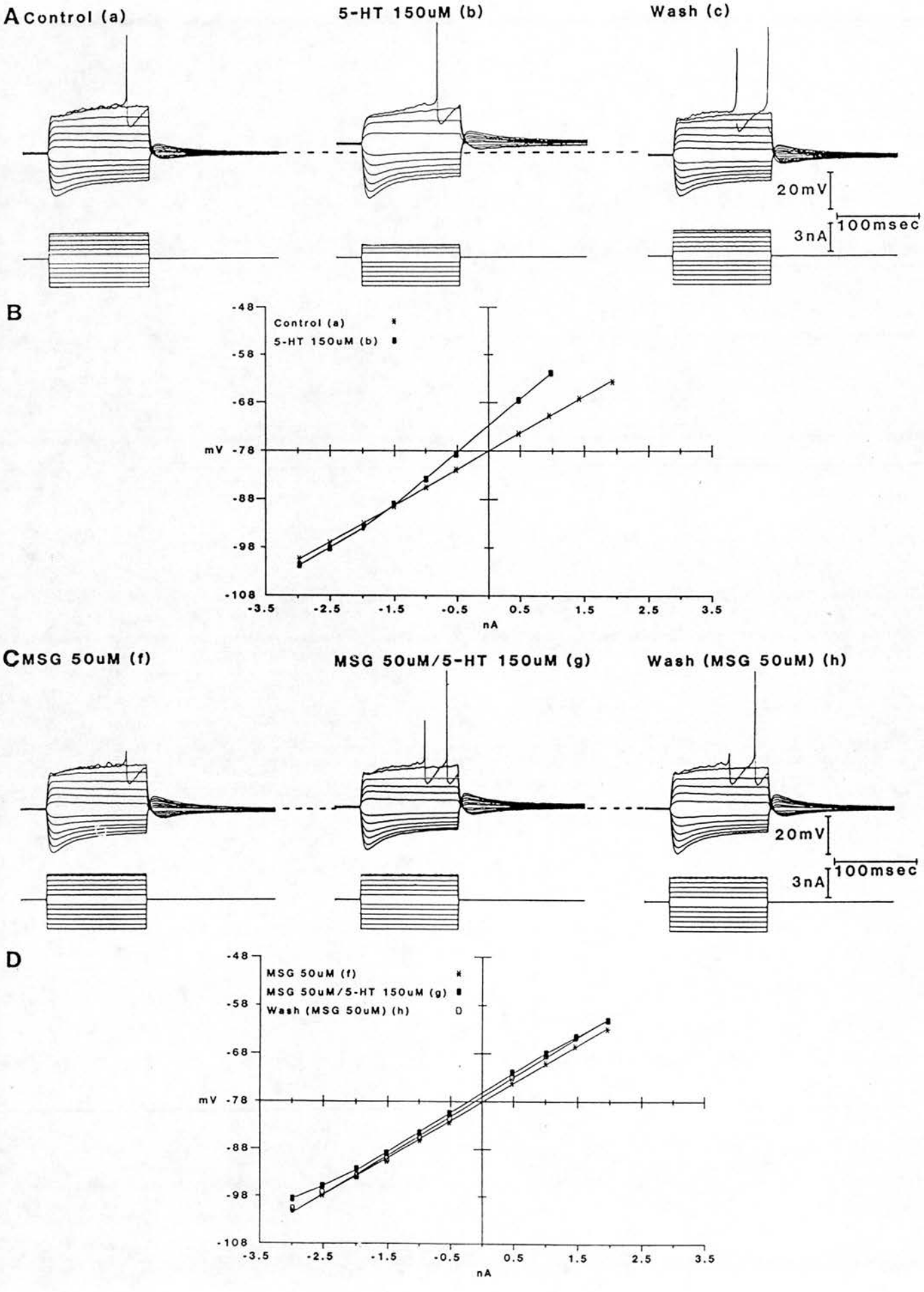
A
Control (a)
5-HT 150uM (b)
Wash (c)
20mV
100msec
3nA
B
Control (a)
5-HT 150uM (b)
-48
-58
-68
mV -78
-88
-98
-108
-3.5
-2.5
-1.5
-0.5
0.5
1.5
2.5
3.5
nA
C
MSG 50uM (f)
MSG 50uM/5-HT 150uM (g)
Wash (MSG 50uM) (h)
20mV
100msec
3nA
D
MSG 50uM (f)
MSG 50uM/5-HT 150uM (g)
Wash (MSG 50uM) (h)
-48
-58
-68
mV -78
-88
-98
-108
-3.5
-2.5
-1.5
-0.5
0.5
1.5
2.5
3.5
nA

Figure 6.32

Electrotonic potentials and I/V plots showing antagonism of the 5-HT-evoked depolarisation by methysergide

A) In control conditions the FM had a $R_{m(pk)}$ of 7.5MΩ and was resting at -78mV. 5-HT (150μM) depolarised the neurone by 5mV and this was associated with an increase in $R_{m(pk)}$ to 11MΩ. Recovery to -78mV, 7.4MΩ was obtained on washing with 5-HT free aCSF.

B) The control (asterisks) peak deflection current-voltage plot was linear throughout the tested range. The 5-HT (closed squares) relationship was linear up to the point of intersection with the control plot at -89.6mV. Thereafter it showed non-linearity and eventually ran virtually parallel to the control curve.

C) Superfusion with methysergide (MSG; 50μM) for twenty minutes did not affect V_m (-78mV) or $R_{m(pk)}$ (7.8MΩ). Application of 5-HT (150μM) in the presence of MSG led to a 1.5mV rise in V_m with only a small change in $R_{m(pk)}$ (8.2MΩ). Removal of 5-HT led to a recovery of V_m to -77mV while $R_{m(pk)}$ remained at 8.2MΩ.

D) Current-voltage plots taken from the electrotonic potentials in C are almost parallel showing no point of intersection. Interestingly, in the presence of MSG, control (asterisks) and wash (open squares) relationships are linear while in the presence of 5-HT (closed squares) some rectification is seen at more negative potentials.

Fig. 6.33

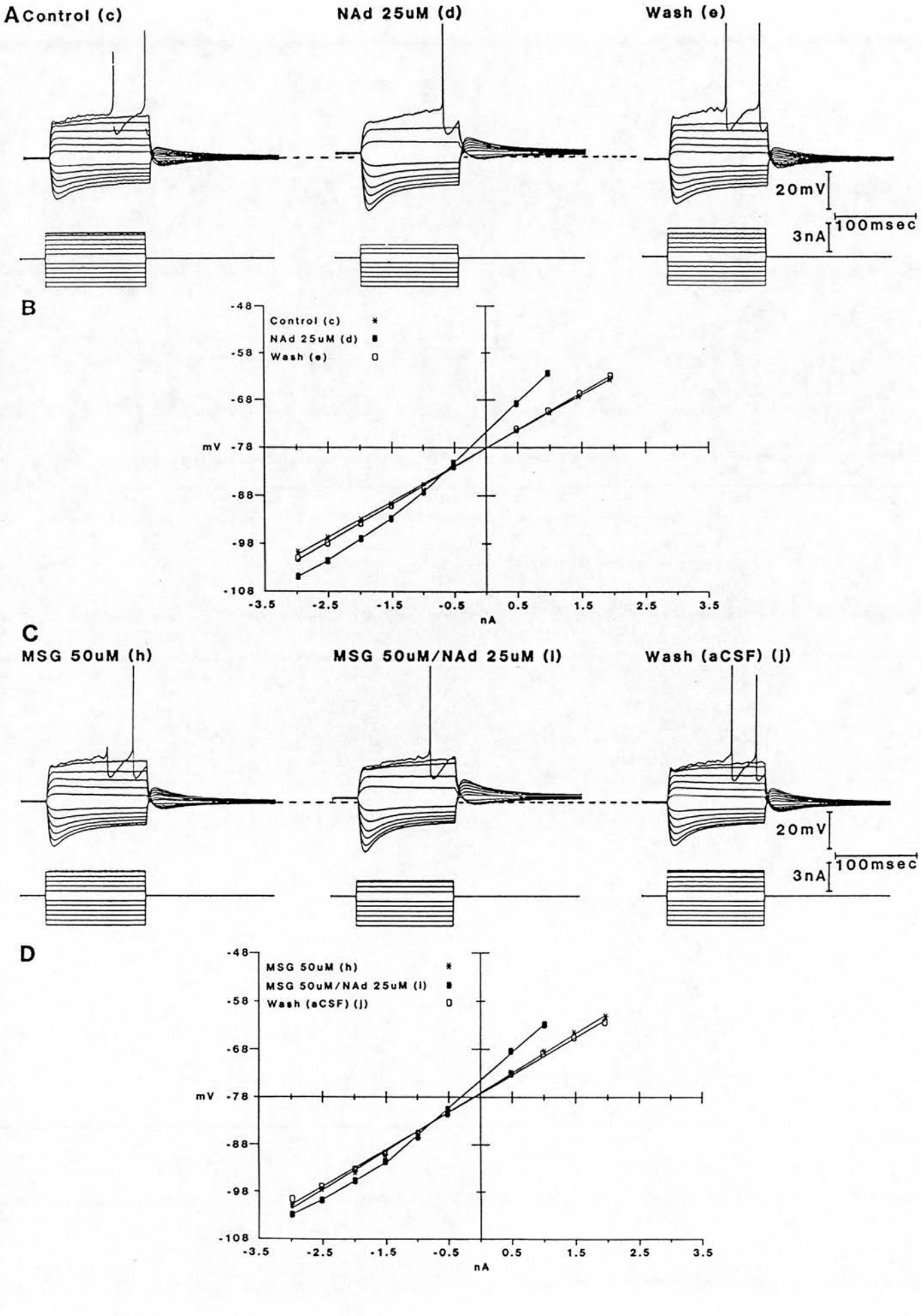
A
Control (c)
NAd 25uM (d)
Wash (e)
20mV
100msec
3nA
B
Control (c)
NAd 25uM (d)
Wash (e)
mV
-48
-58
-68
-78
-88
-98
-108
-3.5
-2.5
-1.5
-0.5
0.5
1.5
2.5
3.5
nA
C
MSG 50uM (h)
MSG 50uM/NAd 25uM (I)
Wash (aCSF) (J)
20mV
100msec
3nA
D
MSG 50uM (h)
MSG 50uM/NAd 25uM (I)
Wash (aCSF) (J)
mV
-48
-58
-68
-78
-88
-98
-108
-3.5
-2.5
-1.5
-0.5
0.5
1.5
2.5
3.5
nA

Figure 6.33

Electrotonic potential and I/V plots showing the NAd evoked depolarisation to be unaffected by methysergide

A) The control response to NAd (25μM) comprised of a reversible 3mV depolarisation from the resting potential of -78mV associated with an increase $R_{m(pk)}$ from 7.4 to 12.6MΩ which recovered to 7.8MΩ on washing with NAd-free aCSF.

B) Control (asterisks) and wash (open squares) peak deflection I/V relationships were linear throughout the tested range. The NAd (closed squares) relationship was linear up to the point of intersection at -83.4mV a value more positive than obtained for 5-HT. As with the 5-HT curve (fig.6.32B) after the point of intersection the NAd I/V relationship rectified tending towards running parallel with the control plots.

C) Coapplication of NAd (25μM) with MSG, after its continued presence for 40 minutes, evoked a 3.5mV depolarisation associated with an increase in $R_{m(pk)}$ from 8.2 to 11.6MΩ. Resting membrane potential (-77mV) and $R_{m(pk)}$ (7.8MΩ) were regained on washing with NAd-free aCSF.

D) Peak deflection current voltage plots show the same properties as for the control NAd response and gave a reversal potential of -83.9mV.

Fig. 6.34

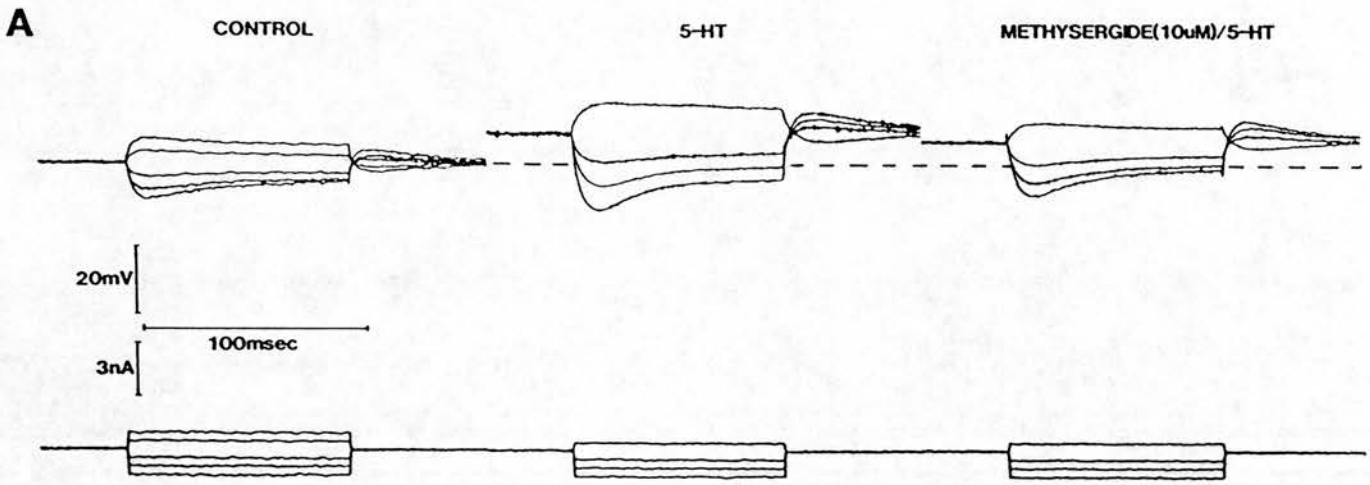
A
CONTROL
5-HT
METHYSERGIDE(10uM)/5-HT
20mV
100msec
3nA

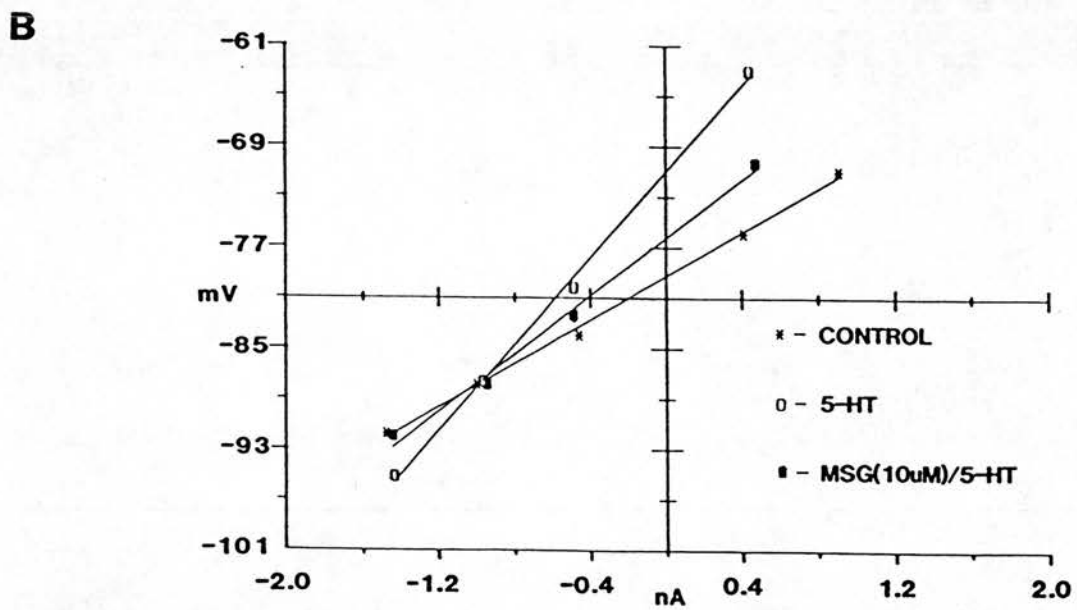
B
-61
-69
-77
mV
-85
-93
-101
-2.0
-1.2
-0.4
nA
0.4
1.2
2.0
* - CONTROL
0 - 5-HT
■ - MSG(10uM)/5-HT

Figure 6.34

Partial antagonism of the 5-HT-evoked depolarisation by methysergide (10μM)

A) Superimposed membrane potential traces show 5-HT (200μM) to evoke an 8mV depolarisation from a resting potential of -79mV associated with an increase in $R_{m(pk)}$ from 8.7 to 17.1MΩ. This was fully reversible and the subsequent application of 10μM MSG for twenty minutes did not alter resting potential or $R_{m(pk)}$ (not shown). Subsequent coapplication of 5-HT (200μM) with MSG (10μM) evoked a 3mV depolarisation and $R_{m(pk)}$ increased to 11.5MΩ.

B) Peak deflection current-voltage plots from the records in A were linear and show that despite partial block of the 5-HT response by MSG the reversal potential is unaffected (-87.2mV and -88.3mV in the absence and presence of MSG respectively).

Fig. 6.35

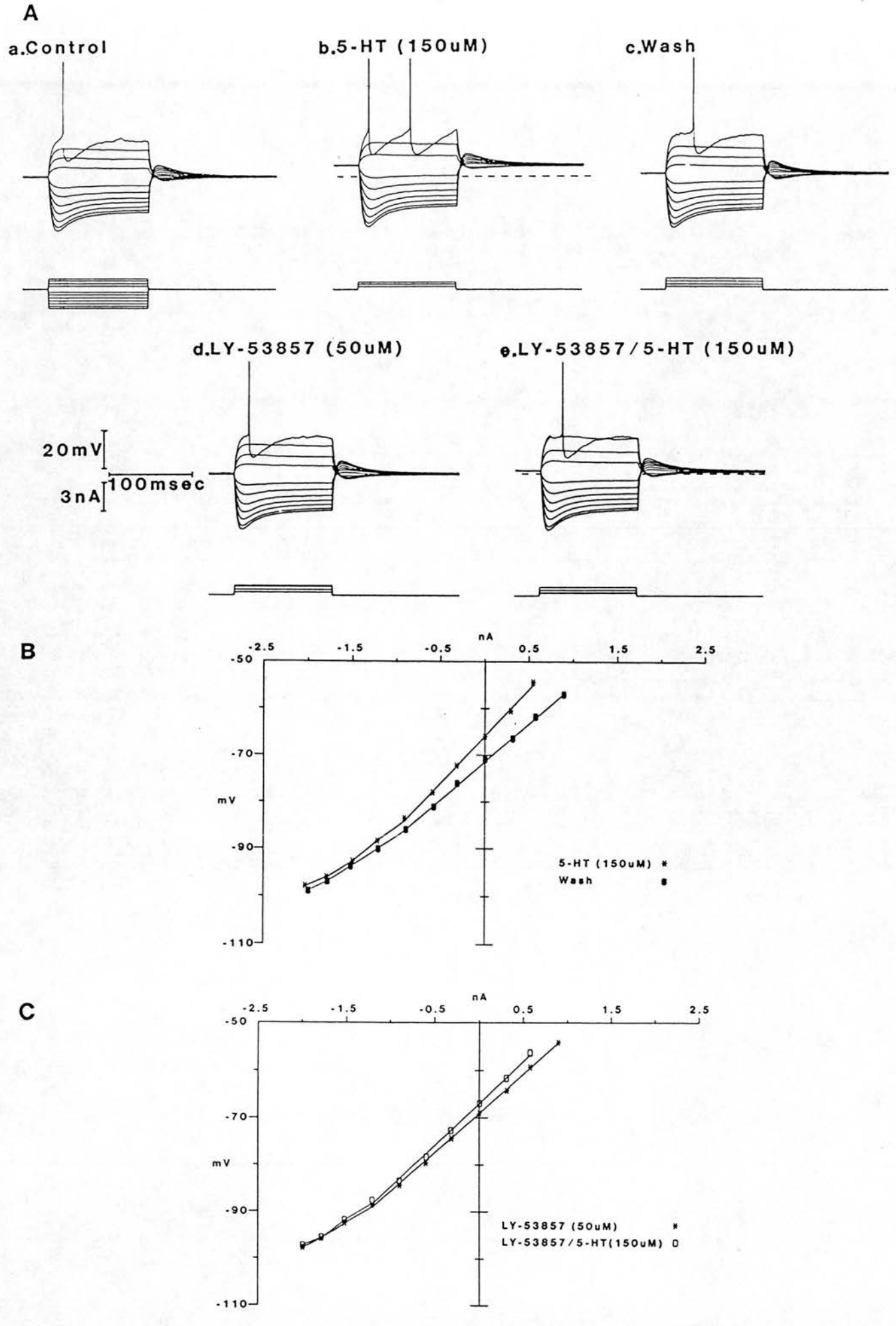
A
a.Control
b.5-HT (150uM)
c.Wash
d.LY-53857 (50uM)
e.LY-53857/5-HT (150uM)
20mV
3nA
100msec
B
nA
-2.5
-1.5
-0.5
0.5
1.5
2.5
-50
-70
-90
-110
mV
5-HT (150uM) *
Wash
C
nA
-2.5
-1.5
-0.5
0.5
1.5
2.5
-50
-70
-90
-110
mV
LY-53857 (50uM) *
LY-53857/5-HT(150uM) O

Figure 6.35

Antagonism of the 5-HT evoked depolarisation by LY-53857 (50μM)
A) The FM was resting at -72mV and $R_{m(pk)}$ over its linear range was 16.3MΩ (Aa). 5-HT (150μM) evoked a reversible 5mV depolarisation associated with an increase in $R_{m(pk)}$ to 20MΩ (Ab,c). LY-53857 (50μM) was superfused for 20 minutes during which time the membrane potential drifted to -70mV though $R_{m(pk)}$ remained constant at 16.7MΩ (Ad). Co-application of 5-HT (150μM) with LY-53857 evoked a depolarisation reduced in amplitude to 2mV and an associated increase in $R_{m(pk)}$ to 17.8MΩ. Hyperpolarising current records shown in Aa also apply to Ab to Ae.
B) Peak-deflection current-voltage plots showing wash (closed squares) and 5-HT (asterisks) relationships to converge but not intersect over their non-linear ranges. The reversal potential estimated by extrapolation of the linear ranges was -95mV.
C) In the presence of LY-53857 the slope of the 5-HT evoked response, in its linear range was reduced and gave an estimated point of intersection with the control plot at -100mV. This was close to the observed value on the non-linear portion of the respective I/V relationships.

Fig. 6.36

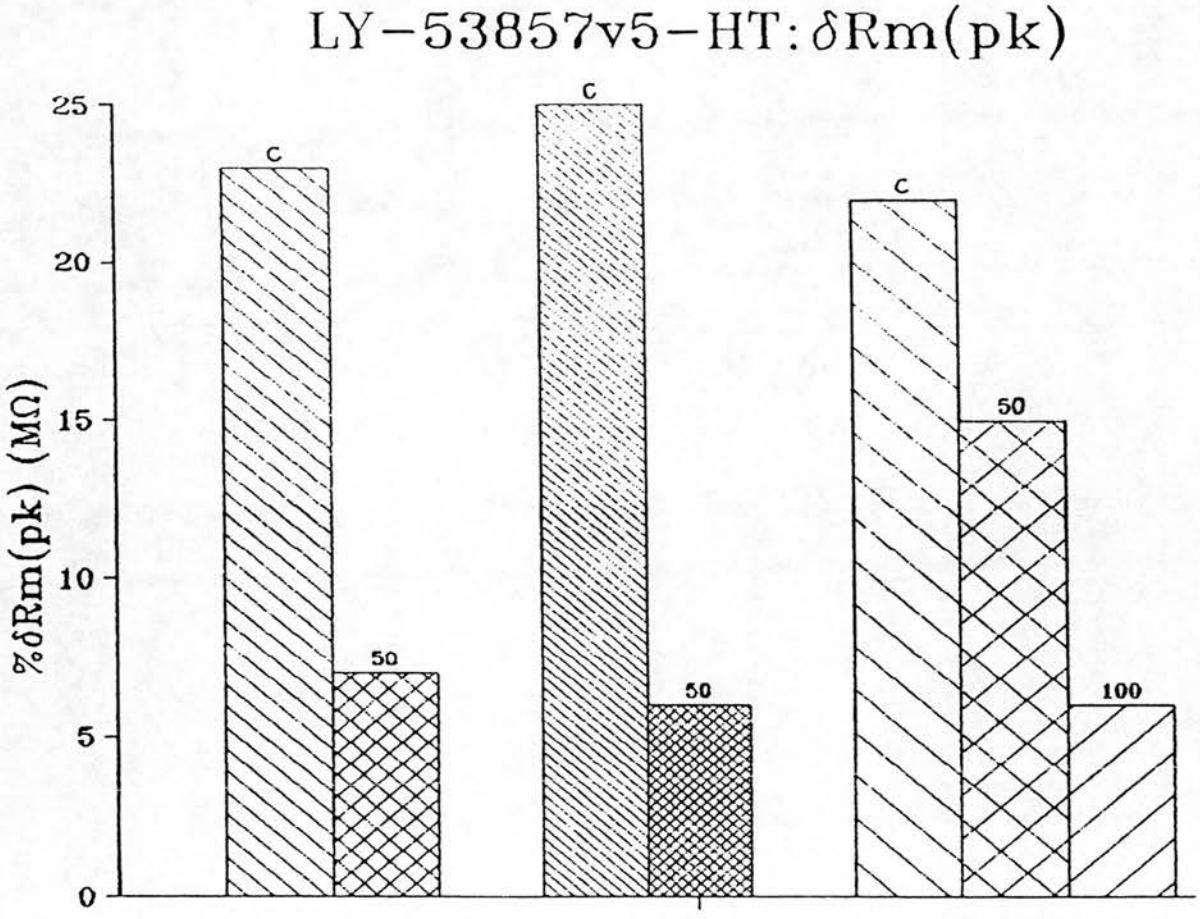

Figure 6.36

The effects of LY-53857 on 5-HT-evoked increase in R_m

A histogram showing the effects of LY-53857 on the 5-HT evoked increase in $R_{m(pk)}$ expressed as a percentage of the control value, for three different FM's C, control; 50, LY-53857 (50μM); 100, LY-53857 (100μM).

Fig. 6.37

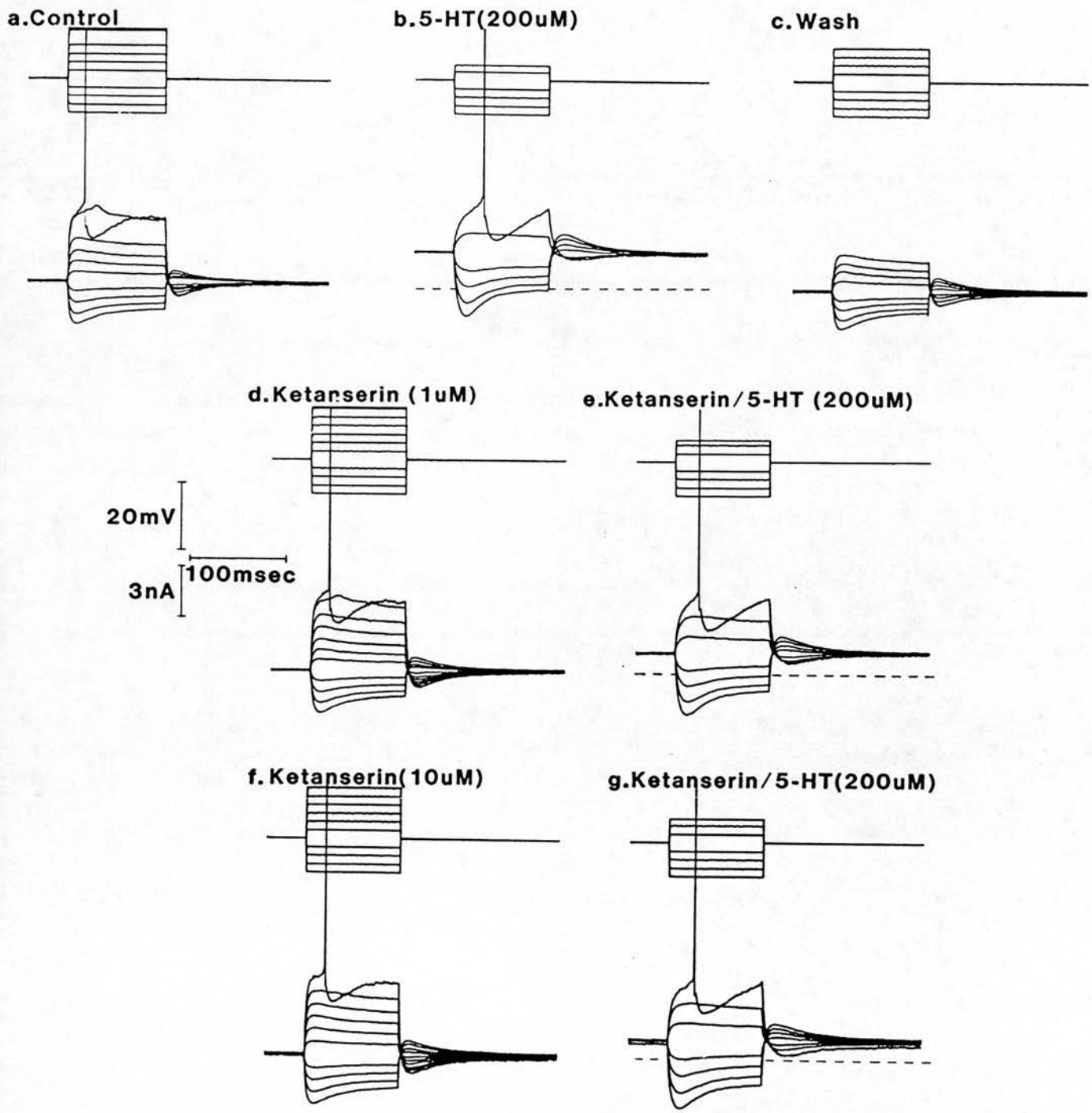
a.Control
b.5-HT(200uM)
c.Wash
d.Ketanserin (1uM)
e.Ketanserin/5-HT (200uM)
20mV
100msec
3nA
f.Ketanserin(10uM)
g.Ketanserin/5-HT(200uM)

Figure 6.37

The effects of ketanserin on 5-HT evoked responses of FM's
Prior to ketanserin application 5-HT (200μM) evoked a 10mV depolarisation from a resting potential of -80mV associated with an increase in $R_{m(pk)}$ from 5.8 to 10.1MΩ (75%) (a, b). This was fully reversed on washing with 5-HT-free aCSF (c). Superfusion with ketanserin (1μM) for 20 minutes did not alter the resting potential but $R_{m(pk)}$ increased slightly to 6.5MΩ (d). Co-application of 5-HT (200μM) evoked a 7mV depolarisation associated with an increase in $R_{m(pk)}$ to 9.7MΩ (49%) (e). After increasing the ketanserin concentration to 10μM for a further 20 minutes the resting potential was -81mV and $R_{m(pk)}$, 7.7MΩ (f). Superfusion of 5-HT evoked a 5mV depolarisation associated with an increase in $R_{m(pk)}$ to 10.6MΩ (38%) (g). Voltage, lower records; current, upper records.

Fig. 6.38

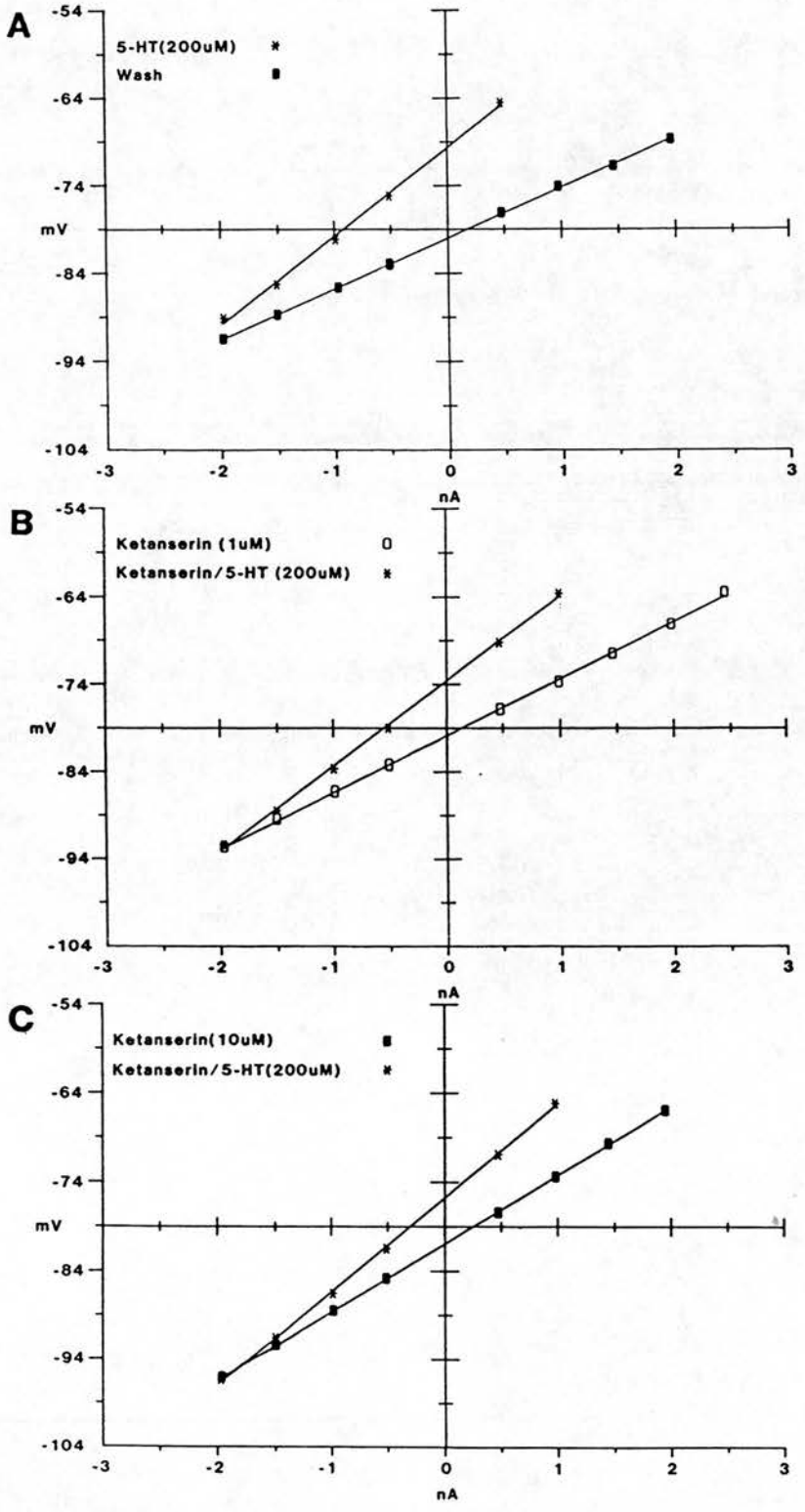
A
5-HT(200uM)
Wash
-54
-64
-74
mV
-84
-94
-104
-3
-2
-1
0
1
2
3
nA
B
Ketanserin (1uM)
Ketanserin/5-HT (200uM)
-54
-64
-74
mV
-84
-94
-104
-3
-2
-1
0
1
2
3
nA
C
Ketanserin(10uM)
Ketanserin/5-HT(200uM)
-54
-64
-74
mV
-84
-94
-104
-3
-2
-1
0
1
2
3
nA

Figure 6.38

Current voltage relationships in the presence of ketanserin
Peak deflection current voltage relationships taken from the records of Fig.6.37 in the presence (asterisks) and absence (closed squares) of 5-HT (200μM) while superfusing with zero (A), 1μM (B), and 10μM (C) ketanserin containing aCSF. Despite changes in the amplitude of the 5-HT effect the reversal potential, determined by the crossover of linear I/V plots, was unchanged by the presence of ketanserin, values of -94, -93 and -94mV were obtained from A, B and C respectively.

Fig. 6.39

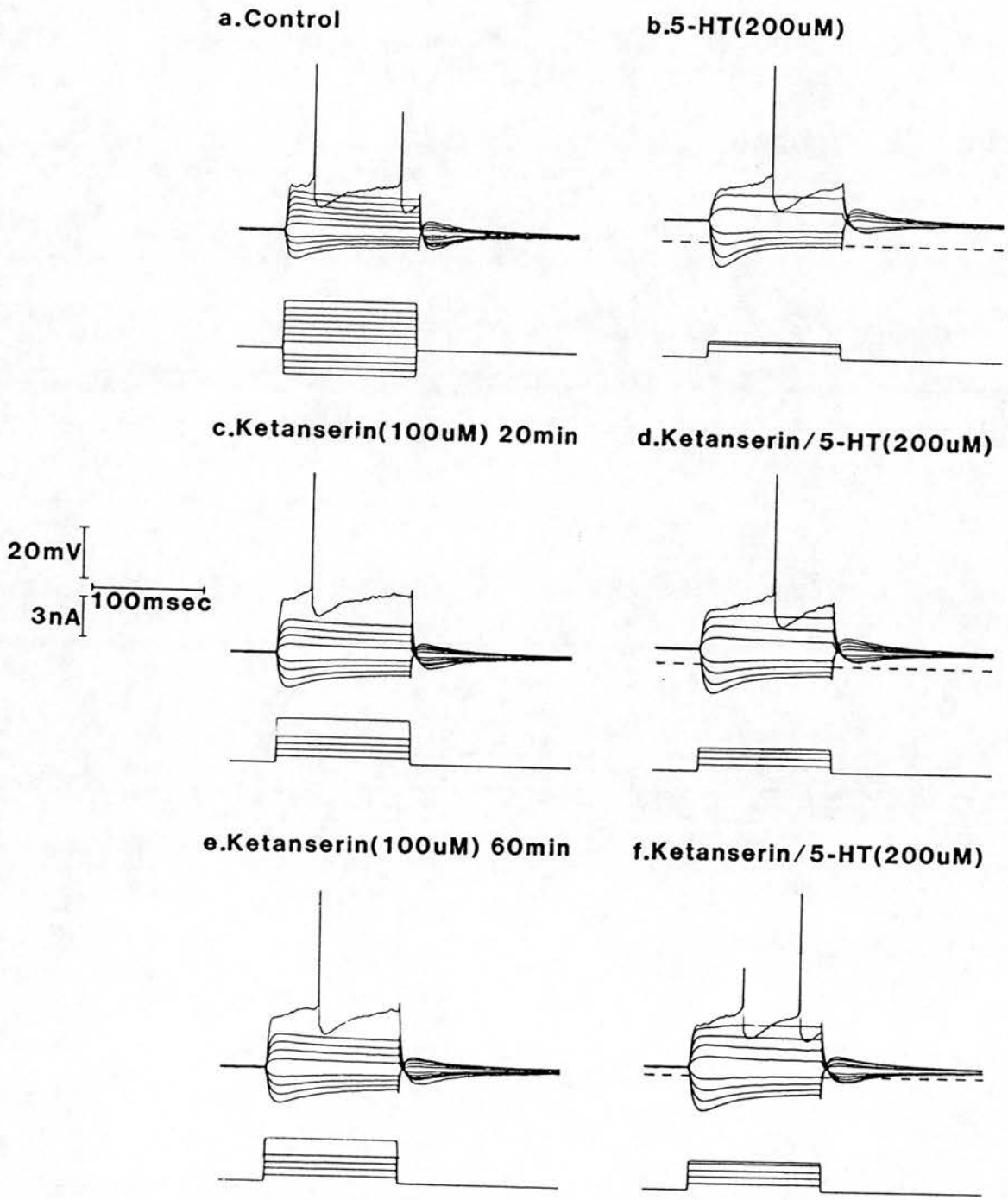
a.Control
b.5-HT(200uM)
c.Ketanserin(100uM) 20min
d.Ketanserin/5-HT(200uM)
20mV
3nA
100msec
e.Ketanserin(100uM) 60min
f.Ketanserin/5-HT(200uM)

Figure 6.39

The effects of prolonged application of ketanserin on 5-HT evoked depolarisation of FM's

A control 5-HT (200μM) evoked depolarisation of 8mV from a resting potential of -83mV was associated with an increase in $R_{m(pk)}$ from 5.4 to 9.4MΩ (74%) (a,b). After recovery (not shown) ketanserin (100μM) was superfused for twenty minutes. Resting potential remained at -83mV while $R_{m(pk)}$ increased to 6.8MΩ (c). Superfusion of 5-HT (200μM) in the presence of ketanserin evoked a 5mV depolarisation associated with an increase in $R_{m(pk)}$ to 8.9MΩ (32%) (d). 5-HT was then removed from the aCSF but ketanserin application was sustained for a total application time of 60 minutes. After this length of application resting potential was -79mV and $R_{m(pk)}$ 6.8MΩ (e). 5-HT (200μM) application evoked a 3mV depolarisation and $R_{m(pk)}$ increased 25% to 8.5MΩ (f). Hyperpolarising current steps in a, apply to all records.

Fig. 6.40

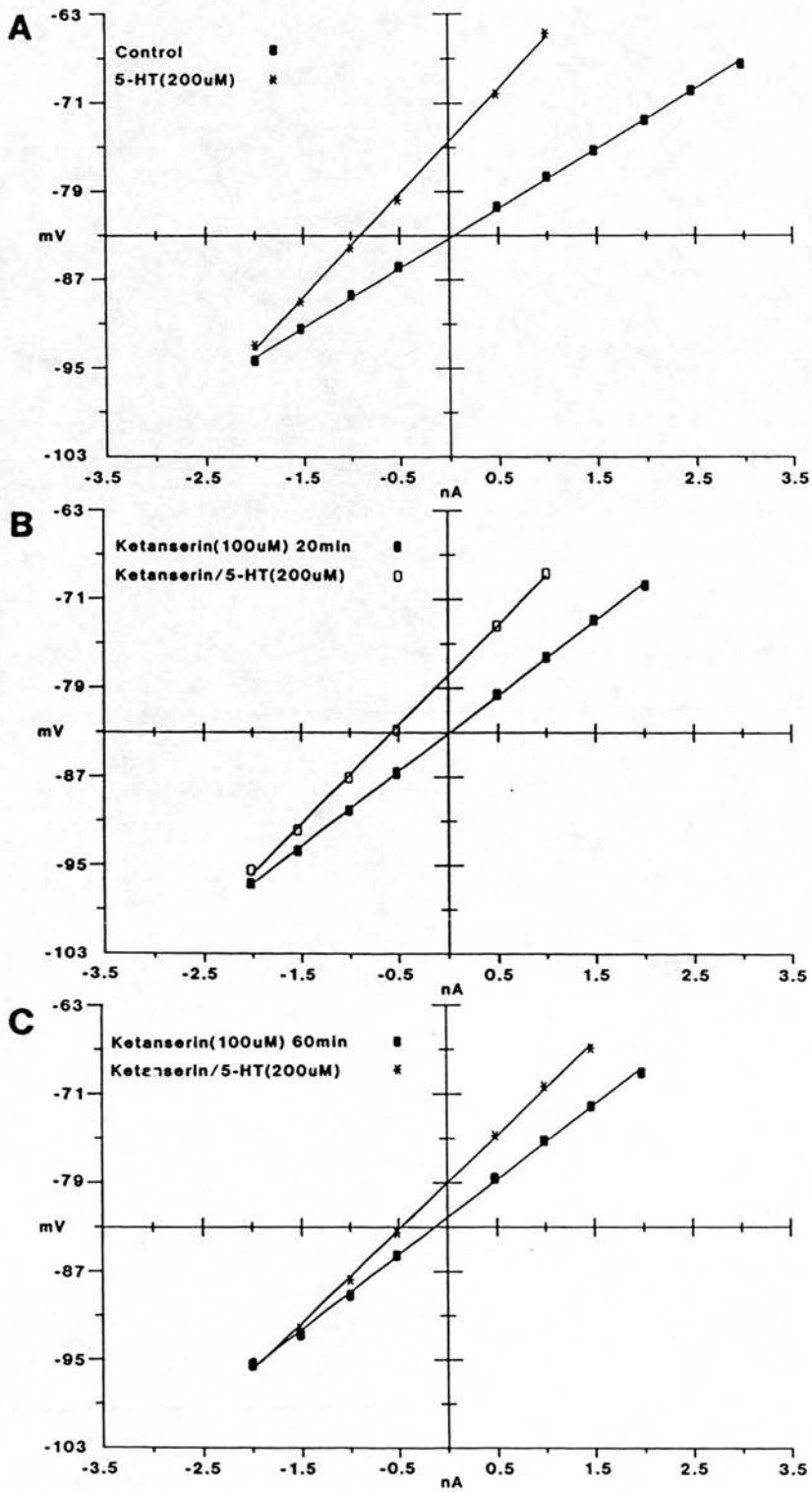
A
Control
5-HT(200uM)
-63
-71
-79
mV
-87
-95
-103
-3.5
-2.5
-1.5
-0.5
0.5
1.5
2.5
3.5
nA
B
Ketanserin(100uM) 20min
Ketanserin/5-HT(200uM)
C
Ketanserin(100uM) 60min
Ketanserin/5-HT(200uM)

Figure 6.40

Current voltage relationships before and after prolonged ketanserin application

Peak deflection current-voltage relationships from the records of Fig.6.39 in the presence (asterisks A and C, open squares B) and absence of 5-HT (200μM) (closed squares) after superfusion with ketanserin (100μM) for zero (A), 20 (B) and 60 minutes (C). Suppression of the 5-HT evoked depolarisation and change in $R_{m(pk)}$ is not associated with a change in the reversal potential as the point of intersection remains relatively constant at -95mV (A), -99.5mV (B) and -94.5mV (C).

Fig. 6.41

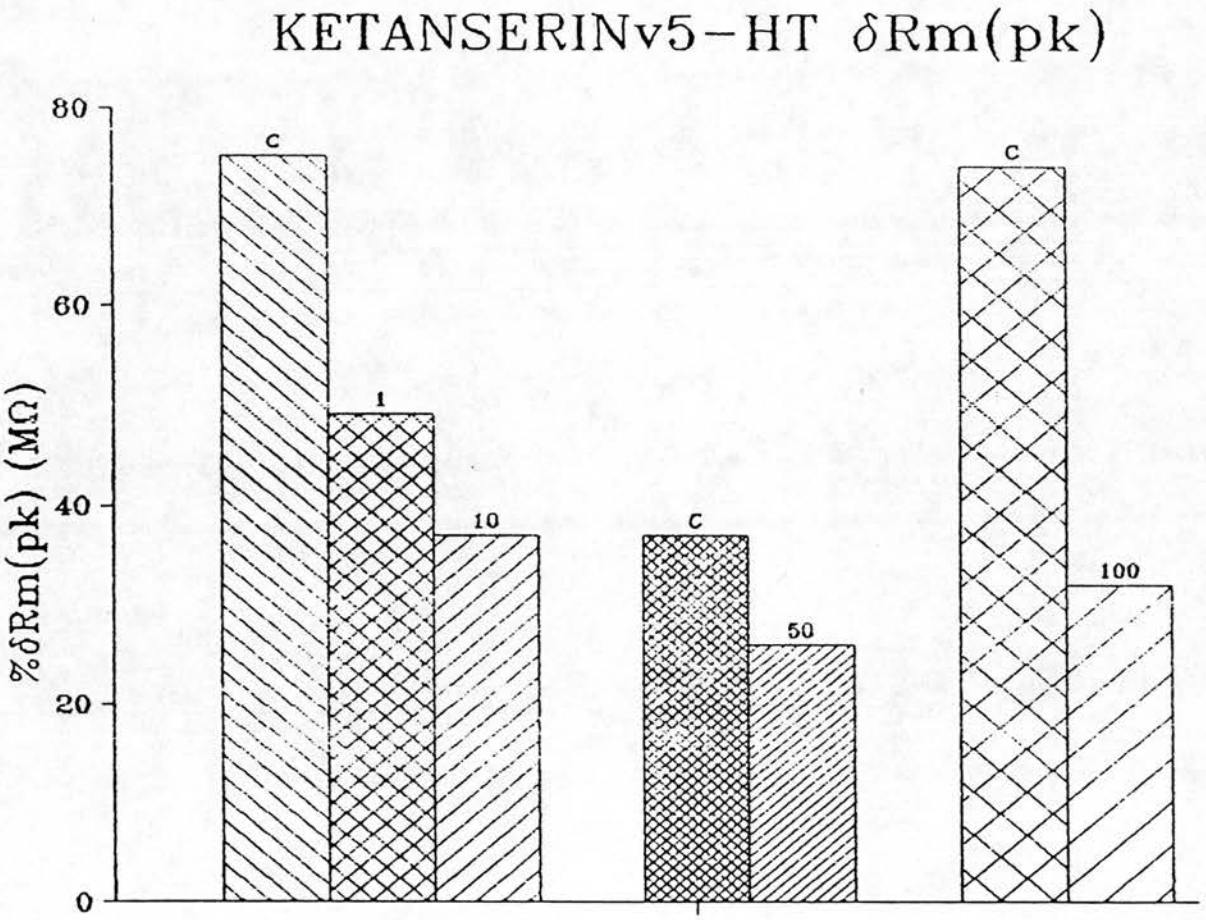

Figure 6.41

The effects of ketanserin of 5-HT-evoked increase in R_m

A histogram showing the action of ketanserin on the 5-HT evoked increase in $R_{m(pk)}$ expressed as a percentage of the control value for three different FM's. Ketanserin was superfused for 20 minutes at 1 and 10μM and for 16 minutes at 50 and 100μM prior to co-application of 5-HT. C, control; 1, 10, 50, 100, concentration of ketanserin (μM).

Fig. 6.42

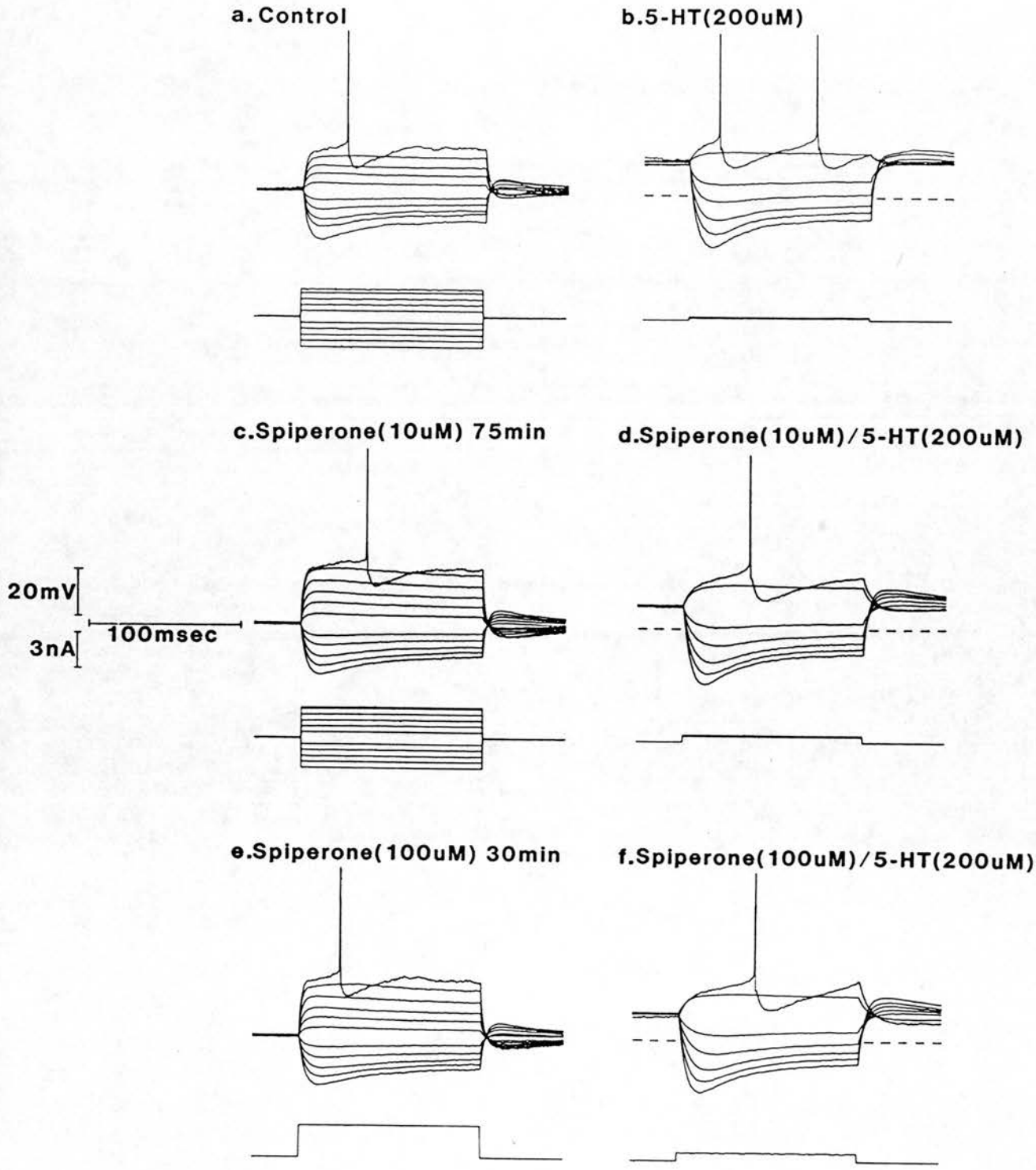
a. Control
b.5-HT(200uM)
c.Spiperone(10uM) 75min
d.Spiperone(10uM)/5-HT(200uM)
20mV
3nA
100msec
e.Spiperone(100uM) 30min
f.Spiperone(100uM)/5-HT(200uM)

Figure 6.42

Spiperone is an ineffective antagonist of 5-HT evoked depolarisation of FM's

5-HT (200μM) evoked a depolarisation of 13mV from resting potential of -69mV and an increase in $R_{m(pk)}$ over its linear range from 7.7 to 14.8 (93%) (a,b). Spiperone (10μM) was then superfused for 75 minutes during which period the resting potential fell to -74mV and $R_{m(pk)}$ rose to 8.7MΩ (c). Superfusion of 5-HT (200μM) evoked an 8mV depolarisation however $R_{m(pk)}$ rose by 83% to 15.9MΩ (d). The concentration of spiperone was the increased to 100μM for a further 30 minutes. Subsequent co-application of 5-HT (200μM) evoked a 7mV depolarisation from a resting potential of -75mV associated with an increase in $R_{m(pk)}$ from 8.2 to 15.3MΩ (86%) (e,f). Hyperpolarising current steps shown in a apply to b and those shown in c apply to d, e and f while the sub-threshold depolarising current steps shown in c also apply to e.

Fig. 6.43

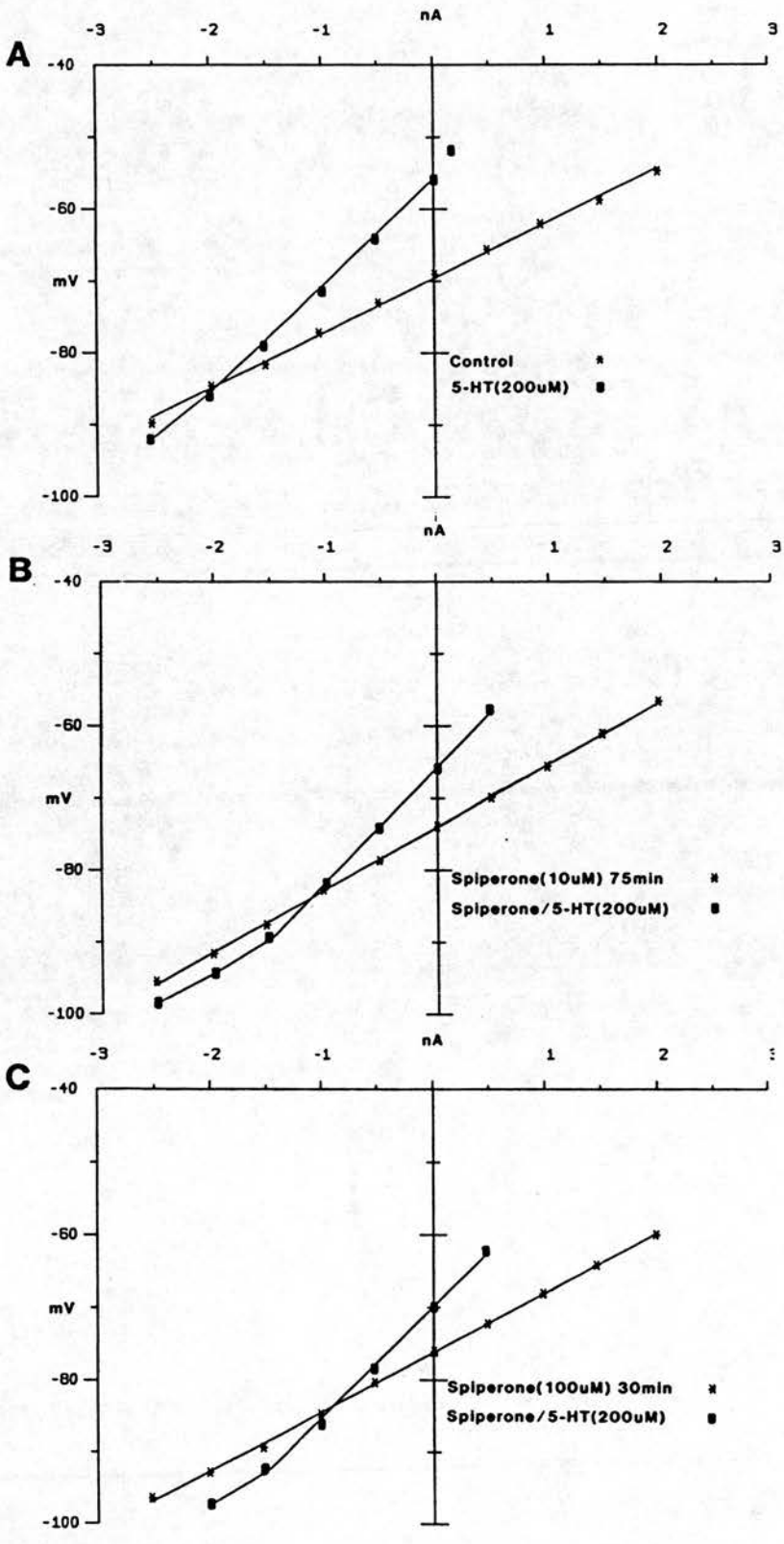
A
nA
-3
-2
-1
1
2
3
-40
-60
mV
-80
-100
Control
5-HT(200uM)
B
nA
-3
-2
-1
1
2
3
-40
-60
mV
-80
-100
Spiperone(10uM) 75min
Spiperone/5-HT(200uM)
C
nA
-3
-2
-1
1
2
-40
-60
mV
-80
-100
Spiperone(100uM) 30min
Spiperone/5-HT(200uM)

Figure 6.43

Peak deflection current voltage plots obtained from the records of figure 6.42

In each case control (i.e. absence of 5-HT, asterisks) plots are linear throughout the tested range. Plots in the presence of 5-HT (closed squares) are linear up to the point of intersection with control plots but thereafter show rectification. The point of intersection is unaffected by spiperone and was -84mV in control (zero spiperone) (A), 10μM spiperone (B) and 100μM spiperone (C).

Fig. 6.44

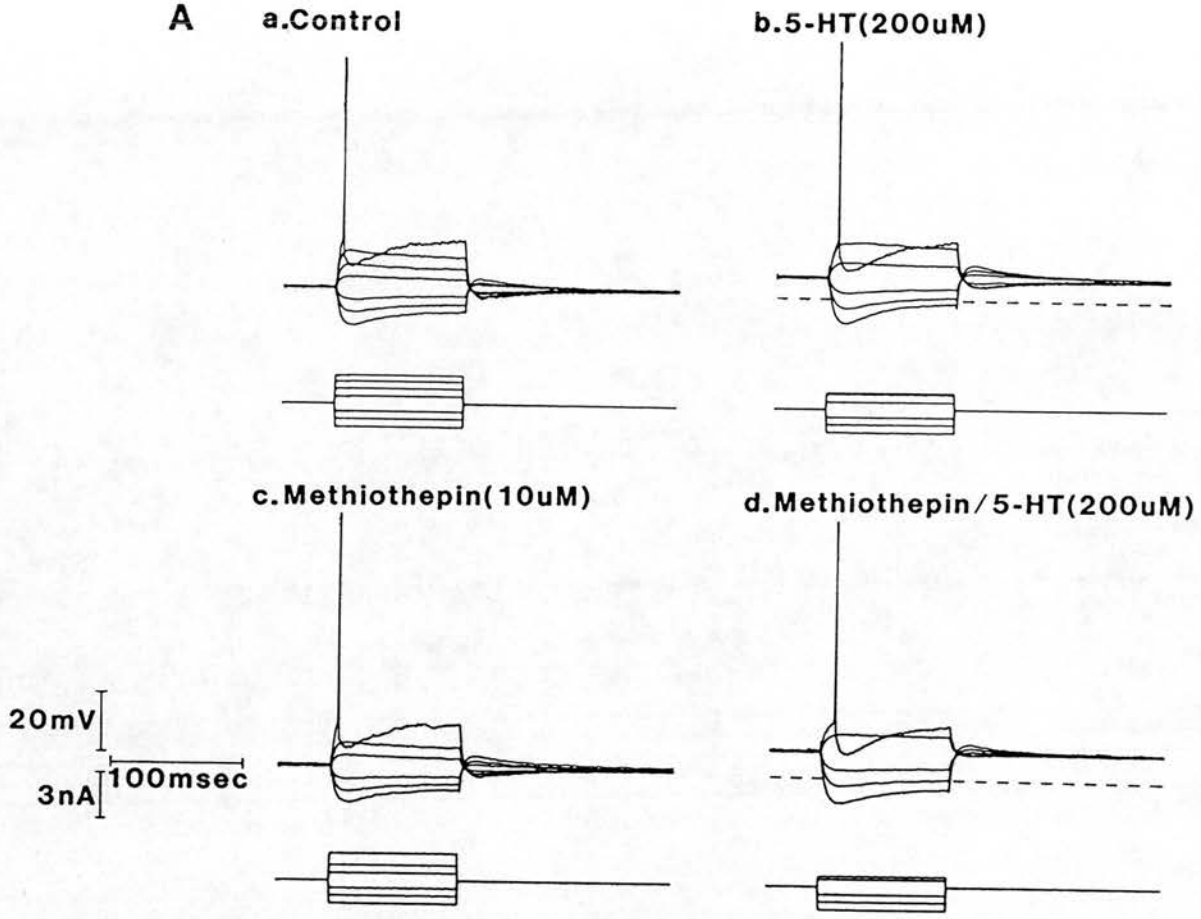
A
a.Control
b.5-HT(200uM)
c.Methiothepin(10uM)
d.Methiothepin/5-HT(200uM)
20mV
3nA
100msec

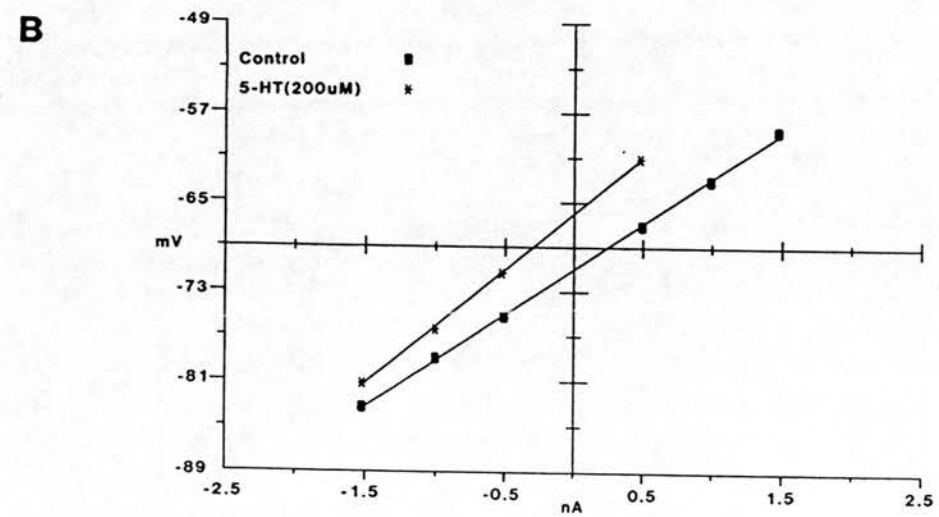
B
Control
5-HT(200uM)
-49
-57
-65
mV
-73
-81
-89
-2.5
-1.5
-0.5
nA
0.5
1.5
2.5

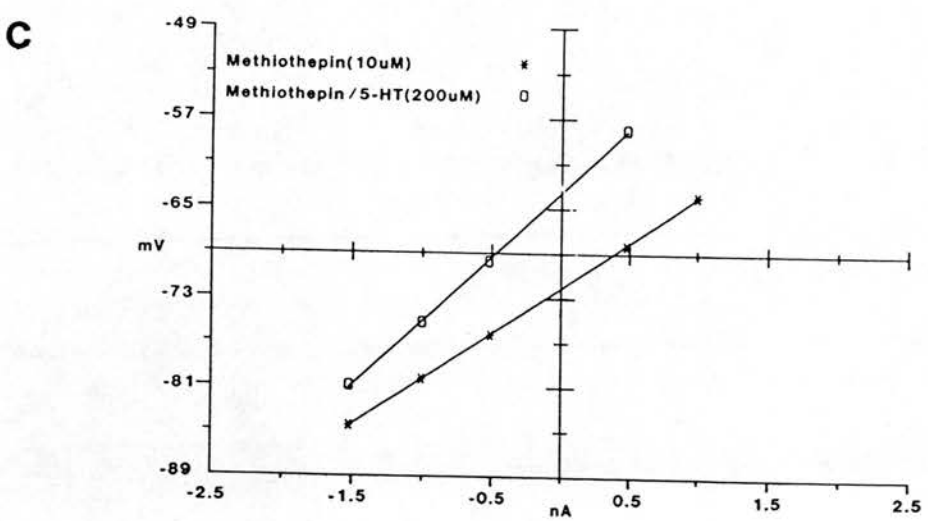
C
Methiothepin(10uM)
Methiothepin/5-HT(200uM)
-49
-57
-65
mV
-73
-81
-89
-2.5
-1.5
-0.5
nA
0.5
1.5
2.5

Figure 6.44

5-HT-evoked depolarisation is not blocked by Methiothepin

The electrotonic potentials (Aa-Ad) show that the 5-HT evoked depolarisation is unaffected by superfusion of methiothepin (10μM) for 20 minutes. 5-HT (200μM) evokes a 5mV depolarisation associated with an increase in $R_{m(pk)}$ from 8.2 to 10.1MΩ. Resting potential was -71mV (Aa, Ab). In the presence of methiothepin, 5-HT (200μM) evoked an 8mV depolarisation associated with an increase in $R_{m(pk)}$ from 8.2 to 11.5MΩ. Resting potential in methiothepin was -72mV (Ac, Ad). Peak deflection current voltage plots in the absence (B) and presence of Methiothepin gave extrapolated reversal potentials of -94 and -96mV respectively for the 5-HT evoked depolarisations.

Fig. 6.45

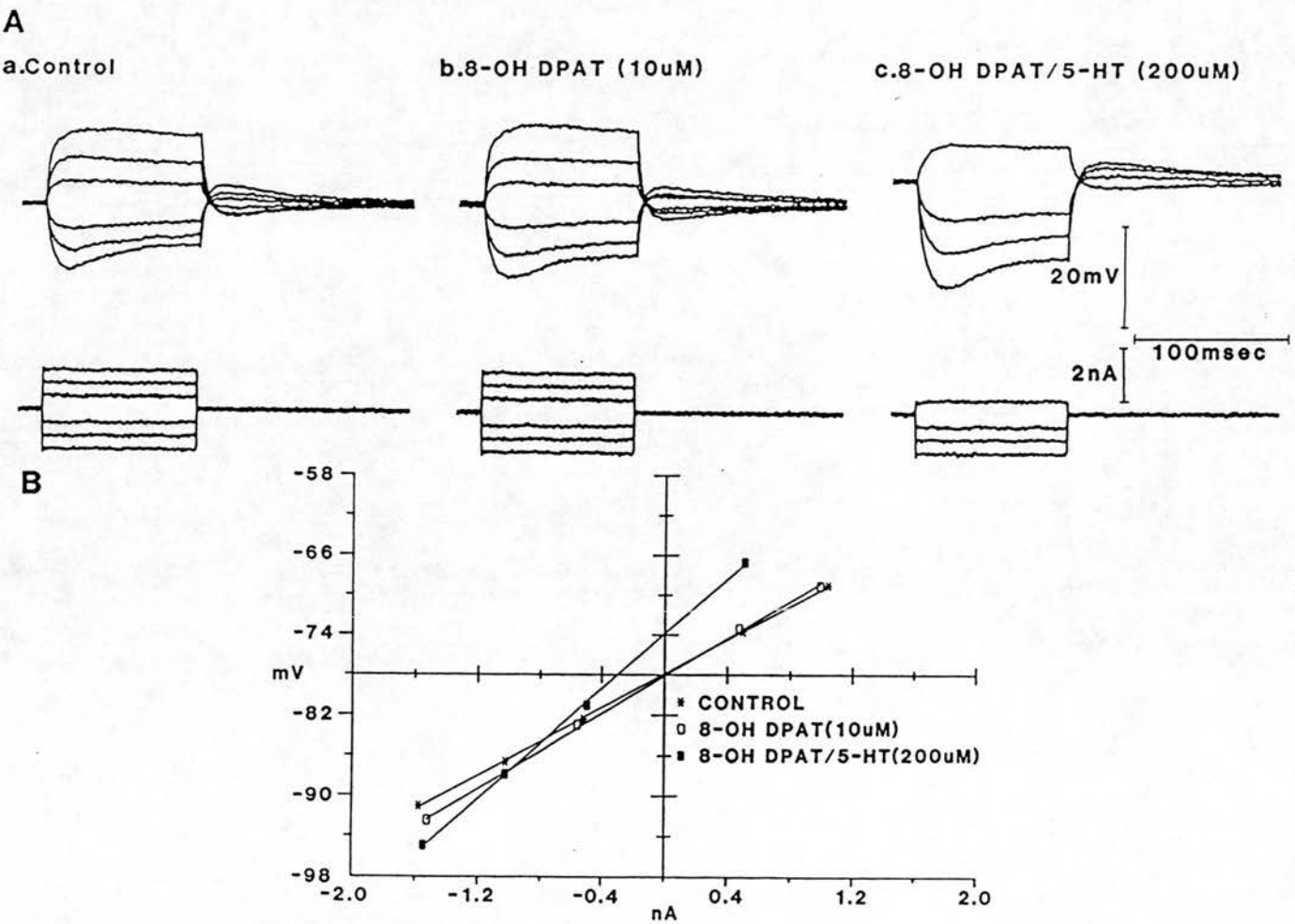
A
a.Control
b.8-OH DPAT (10uM)
c.8-OH DPAT/5-HT (200uM)
20mV
100msec
2nA
B
-58
-66
-74
mV
-82
-90
-98
-2.0
-1.2
-0.4
0.4
1.2
2.0
nA
CONTROL
8-OH DPAT(10uM)
8-OH DPAT/5-HT(200uM)

Figure 6.45

Electrotonic potentials showing the lack of agonist and antagonist effects of 8-OH-DPAT on 5-HT responses of a FM

Superfusion of 8-OH-DPAT (10μM) did not alter the resting potential (-78mV) or $R_{m(pk)}$ significantly (8.4MΩ control; 9.3MΩ 8-OH-DPAT) (Aa, Ab). Co-application of 5-HT (200μM) evoked a depolarisation of 5mV and an increase in $R_{m(pk)}$ to 13.7MΩ (Ac). (B) Peak deflection current-voltage plots show the reversal potential for the 5-HT effect in the presence of 8-OH-DPAT to be -85mV.

Fig. 6.46

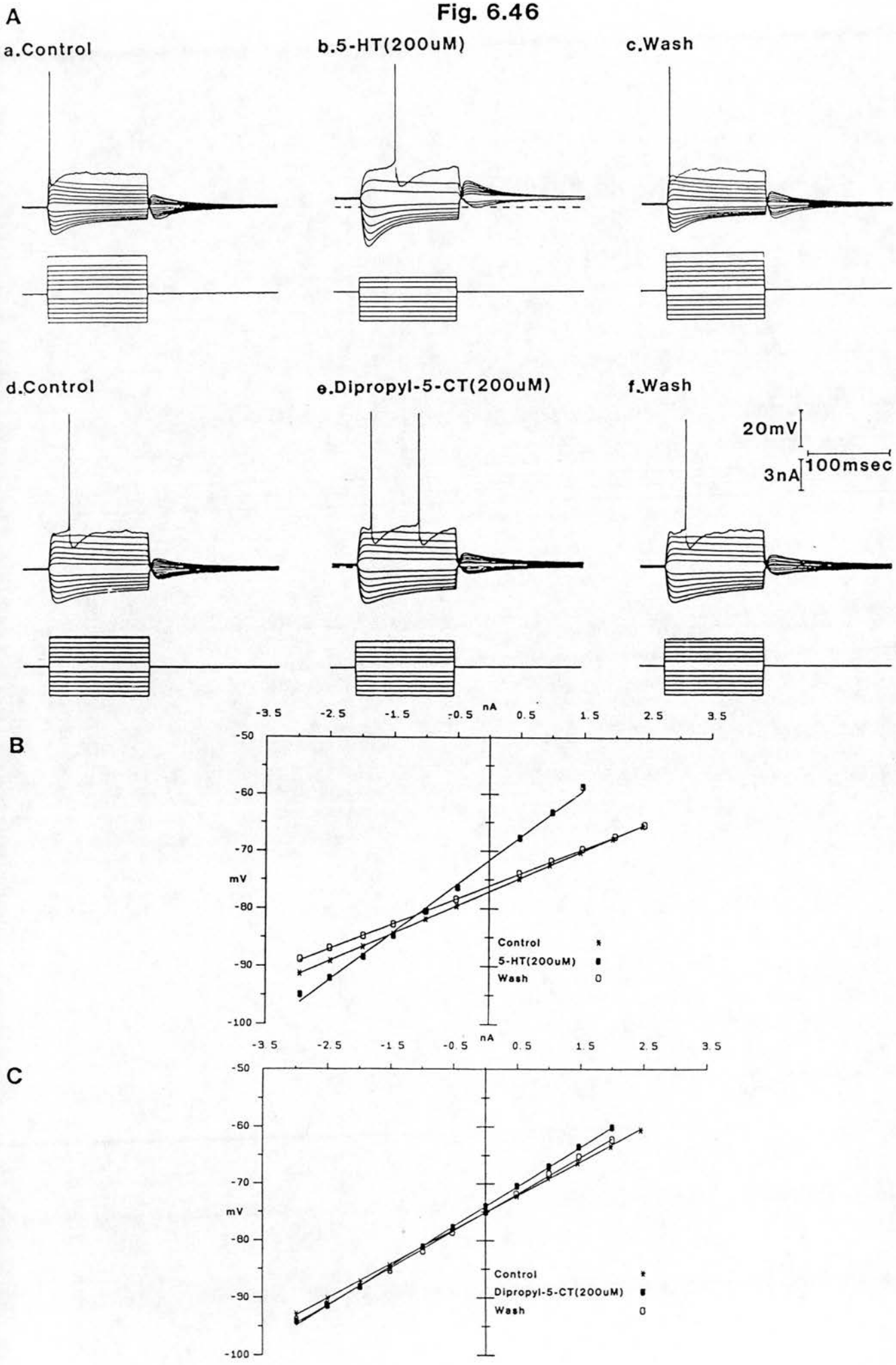
A
a.Control
b.5-HT(200uM)
c.Wash
d.Control
e.Dipropyl-5-CT(200uM)
f.Wash
20mV
3nA
100msec
B
-3.5
-2.5
-1.5
-0.5
nA
0.5
1.5
2.5
3.5
-50
-60
-70
mV
-80
-90
-100
Control
5-HT(200uM)
Wash
C
Control
Dipropyl-5-CT(200uM)
Wash

Figure 6.46

Electrotonic potentials showing the inability of dipropyl-5-CT to mimic the 5-HT evoked depolarisation

5-HT (200μM) evoked a 5mV depolarisation from a resting potential of -77mV and was accompanied by an increase in $R_{m(pk)}$ from 4.8 to 8.7MΩ (Aa, Ab). The effect was fully reversible (Ac) and a value for the reversal potential of -83mV was obtained from peak deflection current voltage plots (B). Superfusion of dipropyl-5-CT (200μM) for an equivalent length of time (15 minutes) showed a small 1mV rise in membrane potential while the $R_{m(pk)}$ was 6.7MΩ compared to a control value of 6MΩ (Ad to Ac). Current-voltage plots for the control, dipropyl-5-CT and wash conditions gave reversal potentials of -83 and -89mV respectively (C).

Fig. 6.47

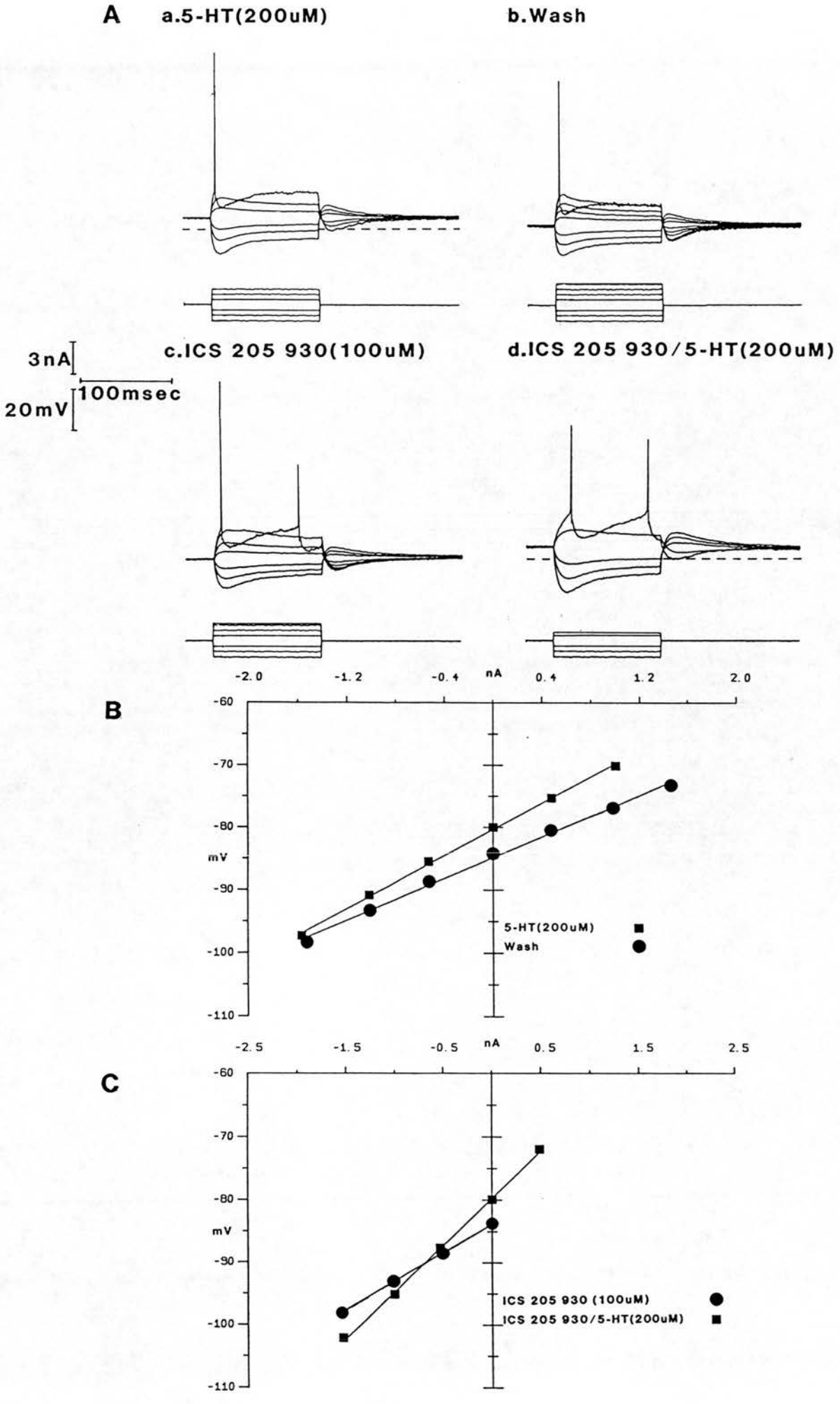
A
a.5-HT(200uM)
b.Wash
3nA
100msec
20mV
c.ICS 205 930(100uM)
d.ICS 205 930/5-HT(200uM)
-2.0
-1.2
-0.4
nA
0.4
1.2
2.0
B
-60
-70
-80
mV
-90
-100
-110
5-HT(200uM)
Wash
-2.5
-1.5
-0.5
nA
0.5
1.5
2.5
C
-60
-70
-80
mV
-90
-100
-110
ICS 205 930 (100uM)
ICS 205 930/5-HT(200uM)

Figure 6.47

ICS 205930, the 5-HT_3 antagonist does not block 5-HT-evoked depolarisation

Membrane voltage responses (upper records) elicited by current steps (lower records) show 5-HT (200μM) to evoke a 4mV depolarisation compared to the wash resting potential of -84mV. This was associated with an increase in $R_{m(pk)}$ of 28% (10.6MΩ in 5-HT to a recovery level of 8.3MΩ) (Aa, Ab). The reversal potential for this response was -100mV taken from the current voltage relationships in B. Superfusion with ICS 205 930 (100μM) for 30 minutes did not alter the resting potential but $R_{m(pk)}$ rose slightly to 9.2MΩ (Ac). Application of 5-HT (200μM) evoked a 4mV depolarisation and a rise in $R_{m(pk)}$ to 15MΩ (63%) (Ad). Under these conditions the reversal potential taken from the plot of intersection of the I/V plots in C was -91.5mV.

Fig. 6.48

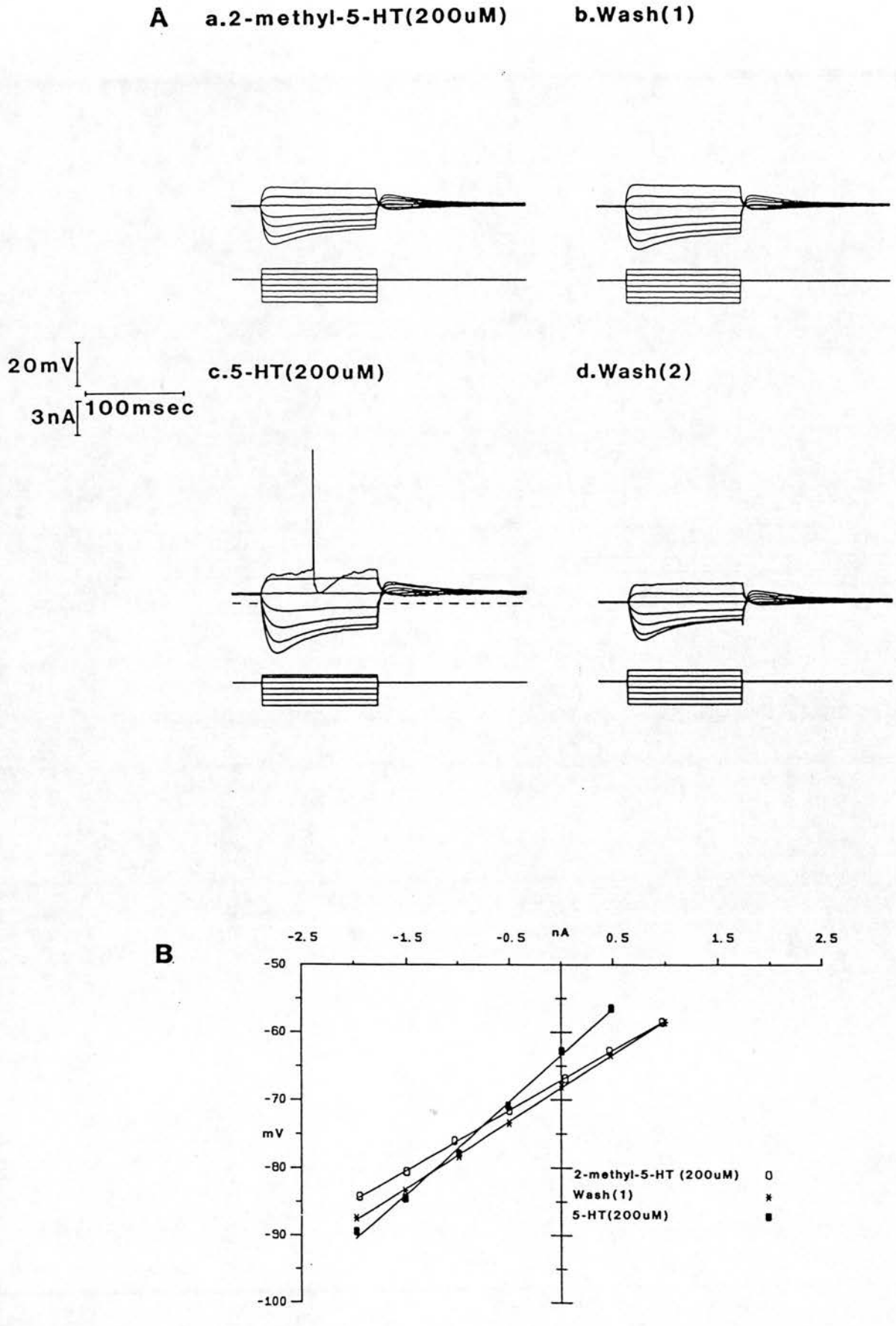
A
a.2-methyl-5-HT(200uM)
b.Wash(1)
20mV
3nA
100msec
c.5-HT(200uM)
d.Wash(2)
B
-2.5
-1.5
-0.5
nA
0.5
1.5
2.5
-50
-60
-70
mV
-80
-90
-100
2-methyl-5-HT (200uM)
Wash(1)
5-HT(200uM)

Figure 6.48

2-methyl-5-HT, a 5-HT_3 agonist, does not mimic 5-HT-evoked depolarisation of FM's

Superfusion of 2-methyl-5-HT (200μM) (Aa) did not significantly alter the resting potential or $R_{m(pk)}$ compared to recovery responses (Ab). Membrane potential in 2-methyl-5-HT was -67mV compared to -68mV in control while values for $R_{m(pk)}$ were 8.9 and 9.9MΩ respectively. Application of 5-HT (200μM) evoked a reversible depolarisation, 5mV in amplitude and associated with an increase in $R_{m(pk)}$ from 9.9 to 13.7MΩ (Ac, Ad).

B) Peak deflection current-voltage plots shows the point of intersection for the 5-HT and control (wash(1)) relationships to occur at -81mV.

TABLE 6.1 The effects of Methysergide on the resting potential and input resistance of facial motoneurones.

CONCN (μM) MSG		Vm (mV)		Rm pk (MΩ)	
	n	Control	Msg	Control	Msg
10	3	-74.5±4.7	-73±3.6	9.82±2.96	7.87±0.75
50	1	-78	-78	7.53	7.82
100	5	-74.8±3.7	-72±2	9.61±2.99	10.08±2.84
200	1	-67	-69	9.1	9.66

TABLE 6.2 The effects of ketanserin on the 5-HT evoked depolarisation and increase in input resistance of facial motoneurones.

CELL	KETANSERIN [μM]	DURATION (min)	δV(mV) Control	δV(mV) Ket.	δRI(MΩ) Control	δRI(MΩ) Ket.	Erev(mV) Control	Erev(mV) Ket.
2/181287	1	20	10	7	4.32	3.15	-94	-93
2/181287	10	20	10	5	4.32	2.87	-94	-95
1/181088	50	30	6	3	3.96	3.41	-86	-94
1/181088	50	60	6	3	3.96	3.6	-86	-90
3/200188	100	20	8	5	4	2.16	-95	-99.5
3/200188	100	60	8	3	4	1.68	-95	-94.5

CHAPTER 7 DISCUSSION

5-HT evokes a depolarisation of FM's associated with increased Rm

The reversal potential of the 5-HT evoked depolarisation: mediation by K+ channel closure

The reversal potential of the 5-HT depolarisation is dependent on the extracellular [K^+]

Noradrenaline evoked depolarisation of FM's also involves K^+ channel closure

Differences in the reversal potentials of 5-HT and NAd evoked depolarisations

The amplitude of the 5-HT evoked depolarisation is dose-dependent

Differences in the NAd and 5-HT D/R relationships

The receptor mediating 5-HT evoked depolarisations belongs to the 5-HT_2 family

Figures 7.1 - 7.3

Table 7.1

5-HT evokes a depolarisation of FM's associated with increased R_m

The data presented in this chapter indicates that superfusion of FM's with aCSF containing 5-HT evokes a dose-dependent depolarisation associated with an increase in cell input resistance. The depolarisations evoked by 5-HT are accompanied by a lengthening of τ which also suggests that, assuming there is no change in specific capacitance of the membrane, an increase in specific membrane resistance has occurred. A preceding hyperpolarisation was never evoked by 5-HT making this preparation useful for studying an uncontaminated 5-HT evoked depolarisation. It could be argued that because of the low input resistance of facial motoneurones a hyperpolarisation of the type mediated through 5-HT_{1A} receptor activation of a K^+ conductance and seen in the hippocampus, DRN and LSN (Andrade and Nicoll, 1987a; Joels et al, 1987; Rainnie, 1988; Williams et al, 1988; Aghajanian and Lakoski, 1984) may be small in amplitude and thus difficult to detect, especially if it occurred on distal dendrites. However, only depolarizing actions of 5-HT were observed in FM's of relatively high input resistance (15-20MΩ) which, since hyperpolarisations have been observed in hippocampal pyramidal cells of similar R_m, suggests this is not the case. That the depolarisation and associated increase in R_m is seen in neurones impaled with 3M KCl filled microelectrodes, which would be expected to lead to a reversed chloride gradient across the membrane, suggests it is mediated by a reduction in a K^+ conductance normally active at the resting potential. The reversal potential obtained from the point of intersection of current-voltage (I/V) plots was more negative than the resting potential and in the region of that predicted by the Nernst equation for a potassium mediated event.

It follows from equation 1 (page 78) that, provided the intracellular and extracellular ionic concentrations remain constant, the level of depolarisation (δV) evoked by 5-HT on each individual FM should also be linearly related to individual values of $1-(R^*_m/R_m)$. Figure 7.1 shows a plot of this relationship for the 107 FM's from which reversal potentials were obtained by the I/V relationship method. The correlation coefficient for the regression line which was forced through the origin was -0.71 with a slope of -12.4mV. When not forced through the origin the regression line was described by the equation $y = a + bX$ where $a = 3.1$, $b = -7.8$ and the correlation coefficient was -0.71. Thus the calculated regression line is little different to that forced through zero though it does suggest some non-linearity of the relationship. The mean resting potential for this population of FM's was -73 ± 5.7mV giving a value of $E_{5\text{-HT}}$ of about -85mV. This value supports the suggestion that decreased conductance to K^+ mediates the 5-HT evoked depolarisation despite being more positive than the value obtained from I/V plots or that predicted by the Nernst equation.

Voltage clamp studies show that superfusion of FM's with 5-HT evokes an inward current associated with a decrease in input conductance which possesses a similar time course to the depolarisation observed in current clamp studies. The magnitude of this inward current corresponds to the range of holding currents used in manual clamping experiments. Thus the evidence suggests that this current underlies 5-HT evoked depolarisation of FM's.

The reversal potential of the 5-HT evoked depolarisation : mediation by K^+ channel closure

Measurement of the reversal potential is complicated by the presence of a prominent time and voltage dependent inward rectifier which is active at the resting potential and further activated by hyperpolarisation. Direct measurement of the reversal potential by identifying the point of intersection of non-linear steady-state current voltage plots could not be achieved due to the inability of the microelectrodes to pass current steps of sufficient amplitude in the active bridge mode. Current voltage relationships at the peak of the voltage deflection were linear over a wider range of membrane potential, only showing rectification at hyperpolarised potentials in some cells. Peak I/V relationships before, during and after 5-HT application were in many cases linear up to the point of intersection giving an estimate of the reversal potential of the 5-HT evoked depolarisation. While this apparent reversal potential appears to agree with the predicted value taken from the Nernst equation it is clear from manual clamping data that a contribution to the measured resistance change is due to underlying changes in the steady-state activation of the "anomalous" inward rectifier. Changes in this inward rectifier were nullified by measuring the resistance change solely due to 5-HT using manual or voltage clamp methods. Along the same lines as argued for the relationship between δV and $1-(R^*_m/R_m)$, the relationship betwen δI and $R_m - R^*_m/R_m.R^*_m$ at a constant membrane potential, V', according to equation 2 should give a value of $E_{5\text{-}HT}$ independent of voltage dependent membrane rectification. Data obtained from manual clamping experiments is plotted in this way in figure 7.2. The regression line was forced through the origin and had a correlation

coefficient of 0.795 and a slope of 27.22mV. When not forced through zero the regression line was described by the equation y = a + bX where a = -0.22 and b = 21.76 with a correlation coefficient of 0.795 (Figure 7.2B). The mean resting potential and thus the mean value of V' was -72.3 ± 4.6mV giving a value of $E_{5\text{-}HT}$ (~ -99mV) considerably more negative than that obtained using the plot of δV against R_m^*/R_m and close to though more negative than the predicted value. In agreement with this value for $E_{5\text{-}HT}$ the mean reversal potential obtained from I/V relationships in control (5mM K^+) aCSF was also more negative than predicted by the Nernst equation. This reflects a wide range of values from close to the predicted reversal potential to considerably more negative. The latter were often extrapolated values taken from the linear regions of I/V plots which did not intersect in the tested voltage range. Despite this, in the majority of cells tested, the input resistance increased in response to 5-HT giving a reversal potential at or negative to the potassium equilibrium potential indicating that a K^+ conductance is the primary target of action.

The reasons for this difference between theoretical and experimental values can only be speculated at. Given the large size of the facial motoneurone soma and extensive dendritic field, events occurring distant to the site of the recording electrode may be subject to attenuation as a result of the electrotonic properties of the neuron. Based on a purely electrotonic model analysis of the hippocampal pyramidal neuron it was predicted that conductance changes measured at the soma, for events mediated on distal dendrites, may be attenuated by up to 30% (Johnston & Brown, 1983). Such an effect in current clamp mode would be reflected by a differential change in R_m which would be a direct cause of

overestimation of the reversal potential of the kind seen in FM's. Thus when manually clamped the current required to restore the resting potential at the site of the recording electrode is likely to generate a voltage across the dendritic resistance which may be insufficiently space clamped and will thus alter the measured reversal potential due to a lack of isopotentiality across the whole cell. This hypothesis is supported in voltage clamp experiments where reversal potentials obtained from the point of intersection of the 5-HT evoked current with the zero current level were more negative than predicted. Variations in the experimentally determined reversal potential from cell to cell may simply reflect differences in receptor/channel distribution and/or the relative electrotonic compactness of the individual motoneurone.

Histological and ultrastructural support for a distally dendritic localization of 5-HT receptors is not clear. Fluorescence histochemistry for 5-HT shows a dense network of 5-HT containing varicosities throughout the nucleus but with a perisomatic bias (McCall and Aghajanian, 1979a) while immunohistochemical analysis suggests this bias is not as pronounced in the rat as in the primate (Takeuchi et al, 1983). Further electron microscopic evidence in the rat identified 81% of [^{3}H]-5-HT labelled synaptic boutons to make axo-dendritic contacts the remainder being axo-somatic. That these contacts were made in regions devoid of dendritic spines could be interpreted as being indicative of a primary dendritic location (Aghajanian and McCall, 1980), this is in keeping with the finding that facial motoneurones have relatively few dendritic spines (Friauf, 1986) but misleading in the sense that the density of spines is a poor indicator of somatic versus dendritic location.

A second possible explanation for the difference in experimental and predicted values of $E_{5\text{-}HT}$ could be that the conductance change is not entirely selective for K^+ and may involve one or more other species of ion. This incorporates two possibilities, that either a single mixed ion conductance channel is closed or that two or more separate conductances including the K^+ conductance are modulated by 5-HT. An increase in a Na^+ and/or Ca^{++} conductance in addition to a decrease in the potassium conductance could account for the variation in reversal potentials, and may also explain the anomalous results obtained in two experiments with TTX where a depolarisation without any apparent increase in R_m was obtained.

Such a model has been proposed to account for the occurrence of non-crossing and even positively converging current-voltage relations seen as a result of carbachol evoked depolarisation of hippocampal pyramidal cells (Benson et al, 1988). The primary effect of carbachol (at potentials higher than threshold for I_M and not involving I_{AHP} effects) was suppression of an extracellular Ba^{++} sensitive and intracellular Cs^+ sensitive "leak" K^+ conductance, the reversal potential of which was controlled by $[K^+]_o$. In addition to this, activation of a dendritic Na^+ conductance is presumed to contribute to the depolarisation and effectively reduce the resistance increase obtained. Some voltage sensitivity of this conductance was inferred by the observation that the K^+ channel blockers were effective at blocking the whole depolarisation and not just the K^+ dependent part. Alternatively, a mixed Na^+/K^+ conductance with sensitivity to K^+ channel blockers may be the dendritic conductance that is activated.

It is of interest that 5-HT has recently been shown to augment a mixed cation conductance responsible for time and voltage dependent inward rectification in other neurones (Pape & McCormick, 1989; Bobker & Williams, 1989; Takahashi & Berger, 1990). Given the prominence of a similar inward rectifier in adult rat facial motoneurones 5-HT modulation of this conductance coupled with a closure of K^+ channels could enhance the depolarisation and also reduce the increase in R_m due to an effect on the K^+ conductance alone. Voltage clamp studies do not show any effect of 5-HT on the slow inward current relaxation underlying the inward rectifier such that the reversal potentials obtained from the instantaneous and steady-state I/V plots are the same. However, as discussed later with reference to NAd actions such effects may only be seen clearly in the presence of selective blockade of 5-HT mediated decrease of the K^+ conductance.

As mentioned earlier control peak I/V plots often showed some rectification at potentials more negative than -90mV. In many cases the peak I/V plot in the presence of 5-HT showed rectification at more positive potentials. This rectification commonly occurred after the point of intersection with the control plot, which it then tended to run parallel to. In other FM's intersection occurred on the non-linear portion of the I/V curves while cases where rectification of the 5-HT I/V curve prevented intersection with the control curve were also obtained. The latter cases were associated with large amplitude depolarisations into the range just sub-threshold for AP's. This behaviour is clearly illustrated in the dose response data shown in figures 6.27 and 6.28. Smaller amplitude depolarisations evoked by 100 and 150μM 5-HT showed intersections on the non-linear part of the I/V curves. A 10mV

depolarisation to -60mV evoked by 200μM 5-HT produced an I/V relationship which failed to intersect with, and ran parallel to, the control plot. However, in each case the reversal potential obtained by extrapolating the linear components of the I/V curves was constant and similar to the observed value with the smaller amplitude depolarisations. This could indicate either rectification of the response evoked by 5-HT or activation of a voltage dependent conductance which interferes with measurements of the 5-HT response at hyperpolarised potentials. A similar rectification of current-voltage curves was observed in guinea-pig sub-mucous plexus neurones (Suprenant & Crist, 1988) and the effects of NAd on guinea-pig LGNd neurones (McCormick & Prince, 1988). These observations suggest that true reversal of polarity of the depolarisation by holding at levels more negative to E_{K^+} would be difficult to obtain in FM's as is the case in hippocampal pyramidal cells (Colino & Halliwell, 1987) lateral horn SPN's (Ma & Dun, 1986) and guinea-pig myenteric plexus neurones (Surprenant & Crist, 1988). Indeed <u>in vivo</u> depolarisations of FM's evoked by iontophoretically applied 5-HT were not clearly reversed at hyperpolarised holding potentials (VanderMaelan & Aghajanian, 1982). 5-HT evoked depolarisation of coeliac ganglion neurones increased in amplitude at more hyperpolarised holding potentials without any apparent change in membrane resistance (Wallis & Dun, 1988). As has been suggested earlier for FM's a contribution to the depolarisation by an increased Na^+ and/or Ca^{++} conductance was proposed to explain this effect.

The reversal potential of the 5-HT depolarisation is dependent on the extracellular $[K^+]$

In order to further substantiate the idea that 5-HT acts to decrease a K^+ conductance in FM's, the effects of altering the extracellular K^+ ion concentration ($[K^+]_o$) on this action were evaluated. When the $[K^+]_o$ was increased the estimated reversal potentials were shifted in a positive direction and were close to the predicted values from the Nernst equation. In addition less variation of the reversal potential between cells was seen in 10mM $[K^+]_o$ compared to lower concentrations (Figs.6.13,6.15). The crossover point of current voltage plots could be measured directly in all cases without the use of extrapolation techniques. One neurone tested in 15mM $[K^+]_o$ clearly shows the K^+ dependence of the 5-HT evoked depolarisation. The neurone was resting at the theoretically predicted value for E_{K^+} and when 5-HT was applied a clear change in input resistance was measured but no depolarisation was observed. Two factors may contribute to the greater correlation observed between $E_{5\text{-}HT}$ and E_{K^+} in higher $[K^+]_o$. The resting potential (Vm) of neurones is determined by a resting permeability to a range of ions but notably K^+ and Na^+ and is represented by the Goldman equation. High permeability to K^+ indicates that as $[K^+]_o$ is raised it plays a greater role in determining V_m such that at concentrations greater than 10mM the resting potential is closely predicted by the Nernst equation for a K^+ conductance. This has been illustrated recently for neonatal rat spinal motoneurones (Forsythe & Redman, 1988). In the experiments reported here the resting potential was allowed to move to its new value in the presence of higher $[K^+]_o$ therefore settling at potentials close to the new E_{K^+}. This had the effect of

reducing the amplitude of the 5-HT evoked depolarisation and thus reducing effects of the underlying inward rectifier on reversal potentials estimated from peak deflection I/V plots. Additionally, in high potassium, cell input resistance decreases, therefore changes in dendritic resistance evoked by 5-HT will contribute less to measurements taken at the soma and would thus reduce any effect of electrotonic changes and/or changes due to an additional dendritic conductance increase on the measured R_m change.

Reducing $[K^+]_o$ to 2.5mM did not show a concomitant change in $E_{5\text{-HT}}$. It is not clear why this should be the case but it can be speculated that the prominent rectification seen at hyperpolarised membrane potentials may be the cause of this deviation from the Nernst equation.

The data is in agreement with and furthers earlier studies on FM's <u>in vivo</u> (VanderMaelen and Aghajanian, 1980, 1982). 5-HT increases facial motoneurone excitability primarily by depolarizing the membrane closer to the threshold for action potential generation thereby enhancing the effects of other excitatory synaptic inputs. In addition to this direct effect on membrane potential the associated increase in R_m and τ will serve to increase the amplitude and duration of synaptic potentials which may enhance both temporal and spatial integration in different areas of the soma-dendritic field. These actions underlie the facilitation provided by 5-HT of nerve-evoked or glutamate evoked firing of FM's <u>in vivo</u> (McCall & Aghajanian, 1979a). Subsequent intracellular studies <u>in vivo</u> indicated that suppression of a K^+ conductance may be responsible for the 5-HT depolarisation as use of KCl filled electrodes did not alter the 5-HT response but iontophoretically applied GABA evoked a depolarisation with a reversal potential much more positive than the

$E_{5\text{-HT}}$ (VanderMaelen and Aghajanian, 1982). The in vitro data presented here confirm the primary action of 5-HT is on a resting potassium conductance and show that altering the extracellular K^+ concentration alters the 5-HT depolarisation in the predicted way. However, it is clear that at physiological potassium concentrations the 5-HT response is modified by the action of voltage dependent membrane rectification which enhances the resistance increase at more depolarised potentials. In addition, factors such as the dendritic location of 5-HT receptors mediating the depolarisation and other effects on a variety of conductances may modify the actions of 5-HT on FM's.

Noradrenaline evoked depolarisation of FM's also involves K^+ channel closure

In addition to 5-HT, FM's were also depolarised by noradrenaline (NAd). An associated increase in R_m and a lengthening of τ suggests a suppression of a K^+ conductance similar to that evoked by 5-HT. Preliminary voltage clamp data show NAd to evoke an inward current associated with a decrease in conductance which is maintained in the presence of TTX indicating a direct post-synaptic action. The reversal potential obtained from the point of intersection of peak current-voltage plots in control (5mMK^+) aCSF was more positive than that predicted by the Nernst equation. Applying the same rationale as for the 5-HT analysis the relationship between the NAd evoked depolarisation and the ratio of the resistance change $1-(R^*m/R_m)$ is shown in figure 7.3. When forced through the origin the slope of the regression line was -7mV with a correlation coefficient of -0.46. When not forced through zero the regression line was described by $y = a + bX$ where $a = 2.7$ and $b = -3$ the correlation coefficient being unchanged. Mean

resting potential was -73.1 ± 5.9mV giving and estimate of E_{NAd} at around -80mV. However, when voltage dependent rectification was separated from the NAd induced resistance change by manual or voltage clamping the neurone, the reversal potential was very close to the theoretical value for a change in K^+ conductance. Non-crossing current-voltage plots were not seen with NAd evoked depolarisations though parallel current voltage curves at more negative potentials after the point of intersection similar to those seen in the presence of 5-HT were common. When the external K^+ ion concentration was raised the reversal potential was shifted to more positive values in agreement with the Nernst equation, while lowering the K^+ concentration, again, did not significantly alter the reversal potential.

Differences in the reversal potentials of 5-HT and NAd evoked depolarisations

The data highlights two differences in the actions of 5-HT and NAd on FM's. Firstly, lower NAd concentrations were needed to evoke similar size depolarisations. Secondly, the mean reversal potential for the NAd depolarisation was lower than that for the 5-HT evoked response. These differences were retained and thus reinforced when 5-HT and NAd were tested on the same neurone. For the same depolarisation amplitude NAd evoked a greater change in R_m which led to a more positive point of intersection of control and NAd current-voltage plots than was obtained with 5-HT. The reasons for these differences may be speculated upon along the same lines as previously argued above for the 5-HT reversal potential. The apparent difference in reversal potential may be the result of a differential localisation of NAd and 5-HT receptors on the soma-dendritic membrane. If receptors mediating the NAd-evoked

depolarisation are to be found on the soma and primary dendrites close to the site of the recording electrode the measured potential and resistance changes would accurately reflect those at the site of receptor/channel interaction. The space-clamp imposed either manually or by voltage-clamp would thus maintain isopentiality of the soma and active membrane region allowing accurate measurement of the reversal potential in the absence of effects of voltage-dependent IR. Little evidence for or against this proposal exists. Diffuse histofluorescence for NAd is seen in the FMN but of lower intensity than is seen for 5-HT (McCall and Aghajanian, 1979a) though other studies claim a dense innervation of the FMN by noradrenergic terminals especially in the anteroventral aspect (Swanson and Hartman, 1975). Ultrastructural evidence for the location of NAd containing synaptic contacts similar to that detailed for 5-HT is not available. Differences in the reversal potentials for Adenosine and 5-HT mediated hyperpolarisation of hippocampal pyramidal cells have been reported. Both responses are mediated through a partially shared pool of pertussis toxin (PTX) sensitive K^+ channels. Autoradiographic data indicates a predominate localisation of A_1 receptors on distal dendrites (Onodera and Kogure, 1988) which has been used to explain the more negative reversal potential obtained for Adenosine against control I/V plots (Zgombick et al, 1989).

Given the similarity of the experimental and theoretical reversal values in both normal and high K^+ containing aCSF additional effects of NAd on other neuronal conductances apart from a resting K^+ conductance appear to be unnecessary to explain this depolarisation. Voltage clamp data shows step currents evoked in the presence of NAd to differ from control currents in an ohmic

manner over the duration of the step command indicating that there is no apparent effect on the time and the voltage dependent component. The NAd evoked current appears to be linear reversing, as predicted, at E_{K^+}. This may not completely rule out effects on the inward rectifier. In the LGNd NAd depolarizes neurones through a suppression of a resting K^+ conductance via α_1 receptors (McCormick and Prince, 1988). In the presence of α_1 blockers NAd also has a depolarizing action this time through a β receptor/cAMP pathway mediated augmentation of the time and voltage dependent inward rectifier, I_h (Pape and McCormick, 1989).

Depolarising actions of NAd due to a decrease in a resting potassium conductance similar to those seen in FM's have been recorded in vitro from neurones of the rat dorsal vagal motor nucleus (Fukuda et al, 1987) substantia gelatinosa (North and Yoshimura, 1984) dorsal raphe nucleus (Yoshimura et al, 1985) hypothalamic supraoptic nucleus (Randle et al, 1986); cat and guinea-pig thalamic neurones (McCormick and Prince, 1988) cat vesical parasympathetic ganglion neurones (Akasu et al, 1985) SPN's (Yoshimura et al, 1987) and cultured spinal cord neurones from foetal mice (Pun et al, 1985; Legendre et al, 1988). As with the 5-HT responses of hippocampal pyramidal cells, some of these studies show multiple responses to NAd including solely hyperpolarising, depolarizing as well as biphasic responses. It is thus again worthy of note that only depolarizing responses to NAd were obtained from FM's, suggesting that the receptor population mediating NAd actions within the FMN is homogeneous between different motoneurones and on different parts of the same neurone. This may be under some presynaptic control as in mouse spinal cord cultures while the total number of neurones responding to NAd either by depolarisation or

hyperpolarisation was unchanged by co-culture with Locus Coeruleus explants, the proportion which responded by depolarisation was significantly increased (Pun et al, 1985).

The reversal potential in all the above studies was dependent on extracellular K^+ though in only one could a true reversal of the depolarisation be obtained by holding at potentials more negative than E_{K^+} (Akasu et al, 1985). Interestingly, current-voltage plots taken in control aCSF and in the presence of NAd from LGNd neurones showed the same tendency to run parallel after the point of intersection as was seen in FM's. Perhaps since NAd modulates I_h in these neurones, which is activated at more hyperpolarised levels, this could be the cause of the rectification of the NAd current-voltage curve. Extracellular Cs^+ blocks I_h and thus the augmentation by NAd, whether this would prevent rectification of the I/V plot in the absence of α_1 antagonists has not been investigated. As mentioned previously whether a similar modulation of the time and voltage dependent inward rectifier occurs in FM's is not apparent and thus requires further investigation before such a hypothesis can be proposed.

The nature of the potassium conductance which is modulated has not been studied in any detail in most cases. It appears unaffected by the removal of Ca^{++} from the aCSF though the depolarisation in cultured spinal cord "pacemaker" neurones is blocked by Cd^{++} indicating some Ca^{++} dependence (Legendre et al, 1988). More detailed studies show extracellular TEA and 4-AP (Legendre et al, 1988) and extracellular Cs^+ (Akasu et al, 1985) not to prevent NAd depolarisation, though in both cases extracellular Ba^{++} was an effective antagonist. This was suggested to be effective through a block of an M-like current in cultured spinal

cord neurones, (Legendre et al, 1988) but not in vesical parasympathetic ganglion neurones where NAd responses were maintained even in the presence a blockade of I_M by carbachol (Akasu et al, 1985). The latter shows similarity to a Ba^{++} sensitive inwardly rectifying K^+ conductance, suppression of which mediates 5-HT and Substance P evoked depolarisation in nucleus accumbens and cultured nucleus basalis neurones, respectively (North and Uchimura, 1989; Stanfield et al, 1985). Were this to be the case in FM's, that the K^+ conductance modulated by 5-HT and NAd inwardly rectifies, an explanation for the rectification of I/V curves at negative potentials becomes apparent. Slow excitatory post synaptic potentials due to neurally evoked release of NAd have been demonstrated in the DRN (Yoshimura et al, 1985), in SPN's of the ventral horn (Yoshimura et al, 1987) as well as in the co-cultures of spinal cord and locus coeruleus (Pun et al, 1985). All display the characteristics of the slow excitatory action of exogenously applied NAd.

The depolarisation seen in all the above cases was blocked by α adrenoceptor antagonists and usually more specifically by α_1 subtype blockers. The pharmacology of the NAd evoked depolarisation of FM's was not investigated in the current series of experiments however, the similarity between this response and others reported above suggests it may also be mediated through an α_1 receptor. This is supported by the ineffectiveness of methysergide, which has negligible affinity for α-adrenergic receptors (see Bradley et al, 1986), against the NAd evoked depolarisation. Despite relatively low levels of α_1 binding sites in the hindbrain generally,

elevations in density were observed along the base of the medulla especially in the facial and vagal motonuclei (Young and Kuhar, 1980).

In addition, to these excitatory effects NAd can modulate neuronal and muscle cell excitability through actions on other membrane conductances usually mediated via different adrenoceptor subtypes. Ca^{++} currents can be increased (Gray and Johnston, 1987) or reduced (Galvan and Adams, 1982), actions mediated through β and α receptors respectively on different cell types. β_1 receptor activation leads to a reduction of the slow Ca^{++} and Na^{+} dependent K^{+} conductances in cortical neurones (Foehring et al, 1988) and also the slow Ca^{++} dependent K^{+} conductance in hippocampal pyramidal cells (Haas and Konnerth, 1983) while in SPN's a Ca^{++} and Na^{+} dependent after depolarisation is induced in the presence of NAd (Yoshimura et al, 1987). No actions on spike afterpotentials were observed in FM's.

The amplitude of the 5-HT evoked depolarisation is dose-dependent

The mean depolarisations evoked by 100, 150 and 200μM 5-HT each tested at a single dose on different FM's were similar. However, when single FM's were tested with multiple concentrations of 5-HT a dose-response (D/R) relationship could be established. These studies showed the sensitivity of FM's to 5-HT to be in the range 100 to 250μM. Despite some variability between neurones maximum responses were usually obtained with concentrations of 200 to 250μM, while in most neurones concentrations lower than 100μM produced only a small or no depolarisation. The D/R curve for the hyperpolarisation of DR neurones using a similar interface chamber was seen to be between 10 and 100μM (Rainnie, 1988). Other studies of similar 5-HT evoked depolarisations in the hippocampus (Andrade

and Nicoll, 1987) and nucleus accumbens (North and Uchimura, 1989) show D/R curves even further to the left in the range 1 to 100μM. However, these studies used a submerged slice preparation which appears to confer greater sensitivity of responses presumably by reducing diffusion barriers which are potential problems with an interface type preparation.

D/R studies also highlighted the fact that different neurones appeared to have different maximal amplitudes of 5-HT evoked depolarisation. Possible reasons for this may involve variations in receptor and/or channel numbers as well as differences in spatial distribution from cell to cell.

Explanations of the difference in sensitivity between different FM's are less apparent. Variation in dendritic localization of 5-HT receptors may account for some variation in the response measured at the soma as discussed earlier. However, this variation in sensitivity may only be apparent, caused by penetration barriers in the slice preparation. The only route of access of superfused 5-HT to the slice in an interface chamber is from below. Distribution through the slice is dependent on the ability of the aCSF to move through the matrix of the slice by capillarity. Also present in the slice will be active uptake mechanisms and metabolic systems which remove or breakdown 5-HT from the aCSF. As the use of uptake inhibitors or metabolic blockers such as MAO inhibitors was not employed it is likely that the actual concentration of 5-HT within the slice will fall as the distance from the superfusing aCSF increases. Thus the concentration of 5-HT surrounding the impaled neurone may not be the concentration actually present in the aCSF reservoir. As such variations in the effective concentrations of 5-HT between different FM's should be treated with caution.

Based on this D/R study a test dose of 150 or 200μM 5-HT was chosen as being suitable for pharmacological investigations into the receptor subtype responsible for depolarisation using a range of putative 5-HT antagonists. It could be assumed that, provided the amplitude of the response to the test-dose did not greatly exceed the average response and thus extend towards the maximum of the range, these concentrations were not supramaximal and would not prevent antagonism being observed due to the presence of an excess of agonist.

Differences in the NAd and 5-HT D/R relationships

Of added interest is the greater potency of NAd at evoking similar size depolarisations to those evoked by 5-HT. This may reflect a higher affinity of NAd for its receptor and/or greater efficiency of receptor/channel coupling. (Though differences in uptake and metabolism of NAd compared to 5-HT cannot be ruled out). While the evidence suggests that both receptor types are linked to the same type of K^+ channel no attempt was made to demonstrate occlusion of the 5-HT evoked response by NAd which would support this proposal. Convergence of signals from two or more distinct receptors has been shown to be linked to both K^+ channel closure as in the effects of LHRH and Ach on I_M in frog sympathetic ganglion cells (Kuffler and Sejnowski, 1983) or the action of 5-HT and muscarine on the Ba^{++} sensitive rectifying K^+ conductance of nucleus accumbens neurones (North and Uchimura, 1989, 1990) as well as K^+ channel opening seen in the 5-HT_{1A} and $GABA_B$ receptor mediated hyperpolarisation of hippocampal pyramidal cells (Andrade et al, 1986) and DR neurones (Rainnie, 1988). However, it could be argued that on the basis proposed earlier of differential localization of receptor types there may also be separate pools of the K^+ channel

with which they interact through localized second messenger production. Such a situation has been seen in hippocampal pyramidal neurones where despite linkage via a PTX sensitive G protein pathway to an identical K^+ conductance the maximum hyperpolarisation evoked by Adenosine (A_1) receptor activation can be partially added to by 5-HT_{1A} receptor activation but not vice-versa (Zgombick et al, 1989). It is suggested that 5-HT_{1A} receptors are linked to an additional sub-population of channels not available to A_1 receptors. If a direct stoichiometric relationship exists between receptor and channel then a difference in receptor numbers may explain this. Alternatively, if lower levels of second messenger are produced by Adenosine receptor activation not all K^+ channels will be activated. Given the differential localization of A_1 and 5-HT_{1A} receptors on these neurones (Onodera and Kogure, 1988; Pazos and Palacios, 1985) it may be that a proportion of K^+ channels available to 5-HT_{1A} receptor mediated second messenger production are too distant from the A_1 receptor mediated site of production and are thus not activated. It is of interest to the work on FM's that there is also a difference in the D/R curves for 5-HT and Adenosine the latter being further to the right similar to the position of the 5-HT D/R curve with respect to NAd for depolarisation of FM's.

<u>The receptor mediating 5-HT evoked depolarisation belongs to the 5-HT_2 family</u>

The receptor mediating the 5-HT evoked depolarisation was investigated using a range of antagonists and agonists with differential selective affinities for the ligand binding and functionally defined receptor subtypes.

8-OH-DPAT has been shown to possess high agonist affinity for 5-HT_{1A} binding sites (Middlemiss and Fozard, 1983). Electrophysiological studies show it to be a potent agonist of 5-HT_{1A} mediated hyperpolarization in the DRN (Rainnie, 1988; Williams et al, 1989) and LSN (Joels et al, 1987) while it is a partial agonist of the similar response seen in hippocampal CA_1 neurones (Andrade and Nicol, 1987a; Colino and Halliwell, 1987). The fact that neither agonist nor antagonist actions of 8-OH-DPAT were detected on FM's suggests a 5-HT_{1A} receptor of the type mentioned above is not responsible for depolarisation. Dipropyl-5-CT a 5-HT analogue with high agonist affinity at 5-HT_{1A} sites and lower affinity at other 5-HT_1 sites (Hagenbach et al, 1986) was also ineffective at mimicking the 5-HT evoked depolarisation. A small response may have been detected at equimolar doses with 5-HT but this represented only 20% of the 5-HT response and is thus inconsistent with an action through a 5-HT_{1A} receptor.

Another putative 5-HT receptor agonist, 2-CH_3-5-HT has been shown to mimic fast excitatory 5-HT actions through 5-HT_3 receptors and also the slow excitatory response seen in guinea-pig sub-mucous ganglion neurones through an unidentified receptor type (Surprenant & Crist, 1988). It was however inactive on FM's apparently ruling out an action of 5-HT through 5-HT_3 receptors.

Methysergide is a selective 5-HT receptor antagonist originally defined on peripheral preparations as being selective for D or 5-HT_2 type receptors. Ligand binding and further functional studies have shown that in fact it has high affinity for both 5-HT_1 and 5-HT_2 receptor subtypes but low affinity for 5-HT_3 sites (see Fozard and Gray, 1989). Superfusion with methysergide <u>in vitro</u> caused selective antagonism of the 5-HT evoked depolarisation leaving the

similar response to noradrenaline unaffected. This antagonism was dose dependent with a partial block of the 5-HT response being observed at 10μM and a complete block at 50 and 100μM. The onset of antagonism by methysergide was rapid requiring only short (15-20 minutes) preincubation times and once effective was sustained even after prolonged periods of superfusion with drug-free aCSF. In a few cases partial recovery of the test 5-HT depolarisation was obtained. The competitive nature of this antagonism was demonstrated by the surmounting of antagonism with increased concentrations of 5-HT. In vivo, iontophoretic and intravenous application of methysergide, antagonized 5-HT evoked depolarisation but this was also associated with a direct methysergide induced reduction in motoneurone excitability (VanderMaelen and Aghajanian, 1980). In vitro no effects of methysergide alone were observed. This suggests that either a tonic serotonergic facilitation of facial motoneurones is present in vivo but not in vitro or that iontophoretic application of methysergide has a non-specific effect or motoneurone excitability possibly through a local anaesthetic type affect observed previously on hippocampal neurones in vivo (Segal, 1976). The latter is supported by the fact that in vivo methysergide also slightly suppressed the noradrenaline evoked increase in excitability whereas in vitro it was unaffected.

Partial agonist effects of methysergide have been reported in several peripheral systems (see Bradley et al, 1986), acting through a 5-HT_1-like receptor. Similarly in the hippocampus agonist responses were observed of the 5-HT_{1A} receptor mediated neuronal hyperpolarization (Andrade & Nicoll, 1987a) though other reports claim methysergide acts as an antagonist of this response (Segal, 1980).

LY-53857 is a freely water soluble 5-HT antagonist based on the LSD/Methysergide structure. However it is said to have a greater affinity for 5-HT_2 and 5-HT_{1C} sites than for 5-HT_{1A} and $_{1B}$ sites and as for methysergide, negligible affinity for α adrenoceptors (Cohen et al, 1983; Hoyer, 1988). The ability of LY-53857 to antagonise the response evoked by 5-HT with a similar potency and speed of onset as methysergide further points to the receptor responsible being a 5-HT_{1C} or 5-HT_2 receptor. Preliminary reports of agonist effects of LY-53857 (Rasmussen and Aghajanian, 1988) were not confirmed in these studies. Methiothepin has high affinity for 5-HT_1 and 5-HT_2 receptors similar to Methysergide (Bradley et al, 1986) however, it was found to be inactive against the 5-HT evoked depolarisation. Great care was made to prevent adhesion of this drug to the walls of the perfusion reservoir and tubing though this may explain the ineffectiveness of this drug. However, <u>in vivo</u> the facilitation of glutamate evoked firing of FM's was not antagonised by iontophoretic methiothepin (McCall & Aghajanian, 1980a) and the depolarisations observed in hippocampal neurones (Andrade & Nicoll, 1987a) and spinal motoneurones (Connell & Wallis, 1988) were also insensitive to methiothepin.

In an attempt to differentiate between the 5-HT_{1C} and 5-HT_2 receptors two ligands with selective affinity for 5-HT_2 receptors, ketanserin and spiperone were tested. Somewhat surprisingly spiperone failed to antagonise the 5-HT evoked depolarisation even after prolonged superfusion times. The effects of ketanserin were less clear. Some suppression of the 5-HT response was obtained at all doses though full blockade could not be achieved even when the concentration was increased and superfusion was extended for prolonged periods. In contrast, <u>in vivo</u> studies claimed

iontophoretically applied ketanserin to be an antagonist of the 5-HT evoked facilitation of FM firing (Penington & Reiffenstein, 1986). Such an observation is not entirely inconsistent with our data as ketanserin did depress the evoked depolarisation in vitro and such an effect may be sufficient to prevent glutamate evoked firing tested at a single dose. Autoradiographic data shows that while ketanserin binding sites in the FMN have been claimed to identify a 5-HT_2 site (Fischette et al, 1987), ^3H mesulergine binding to what is presumed to be the same site is only partially displaced by ketanserin and spiperone even though 5-HT can fully displace it (Pazos et al, 1985). It has recently been claimed that two 5-HT_2 sites exist (Pierce and Peroutka, 1989) based on the selective binding of the hallucinogen ^3H-DOB to a distinct 5-HT_2 site. This site has lower affinity for ketanserin and spiperone than the classically defined 5-HT_2 site and has been termed the 5-HT_{2A} site. It has been shown in vivo that another hallucinogen, DOM, which has some selectivity for 5-HT_2 sites mimics the facilitatory effects of 5-HT on glutamate evoked firing of FM's through a methysergide sensitive receptor (Penington and Reiffenstein, 1986) and a brief report in vitro suggests this is through the same mechanism as 5-HT (Rasmussen and Aghajanian, 1988). It is thus tempting to speculate that the ineffectiveness of spiperone and poor antagonism by ketanserin reflects the possibility that the action of 5-HT on FM's is mediated through a 5-HT_{2A} receptor.

An alternative explanation for the poor antagonism by ketanserin and spiperone of the 5-HT response may be postulated based on their relative solubilities in aqueous and non-aqueous media and the use of an interface type chamber. To obtain stable recordings from these neurones it was found necessary to employ an

interface chamber. As described earlier this has the disadvantage that the only route of access for bath applied drugs is from below, equilibration being dependent on passive distribution through the slice matrix of the aCSF largely by capillary attraction and diffusion. As such the actual drug concentration at the receptor site at different levels in the slice will be governed by its relative aqueous and lipid solubilities along with any affinity for active uptake or metabolic mechanisms. While the latter may be a problem for application of endogenous transmitters as described earlier it is not likely to affect antagonists. However, given the aqueous nature of the superfusing aCSF, solubility in water is an important factor in determining the concentration of ligand which may reach the receptor. Of equal importance is solubility of the ligand in the lipid phase of the slice. Ketanserin and spiperone show low aqueous solubility (Ketanserin 10μM; Spiperone 25μM) and more importantly high lipid solubility. Carrier solvents were used to raise the aqueous solubility in aCSF (DMSO, final concentration 0.01%) though this could not control precipitation which may occur once the final dilution has been achieved. In addition to a low aqueous solubility the concentration of these ligands at different levels in the slice may be even lower due to sequestration in the lipid at lower levels in the slice and in direct contact with the aCSF. Thus depending on the recorded neurones position in the slice differential effects of these antagonists may be explained by differences in the concentration at that site.

This problem was recognised prior to use of these antagonists. The use of maximal concentrations coupled with prolonged exposure times were aimed at minimising such effects. It should be added that for similar exposure times 10μM spiperone was an effective

antagonist of 5-HT evoked hyperpolarization in DR neurones using the same perfusion chamber (Rainnie, 1988). This points to the suggestion that the 5-HT evoked depolarisation of FM's may well be mediated by a receptor insensitive to spiperone. In contrast the high aqueous solubility of methysergide and LY-53857 ($\simeq$ 4mM) ensures rapid and fairly uniform distribution throughout the slice and a closer correlation of concentration at the receptor with the aCSF drug level.

The results show that the depolarisation of FM's is unlikely to be mediated by 5-HT_3 receptors. Primarily ICS 205-930 is ineffective as an antagonist and 2-CH_3-5-HT as an agonist. Since methysergide also has negligible affinity for 5-HT_3 (M) receptor sites, the antagonism seen by this ligand is not through a 5-HT_3 receptor. More circumstantially the characteristic electrophysiological consequences of 5-HT_3 receptor activation described earlier do not involve the same mechanisms described in FM's. While such 5-HT_3 responses have only been described on peripheral preparations or clonal cell lines it is as well to suggest that, as pointed out by North and Uchimura (1989) and equally relevant to this study, the protocol used would not be optimal for observing 5-HT_3 mediated effects which display rapid desensitisation. Indeed Wallis and Dun (1988) studying 5-HT responses in rabbit coeliac ganglion neurones showed that the transient 5-HT_3 mediated response was only observed in response to brief iontophoretic applications of 5-HT and not when prolonged bath applications were made.

In vivo studies have shown that the 5-HT mediated facilitation of glutamate evoked firing can be antagonised by iontophoretic and systemic application of methysergide, cyproheptadine and cinanserin

(McCall and Aghajanian, 1980a) while iontophoretic application of metergoline was also effective in the same study. Of these antagonists only cinanserin shows any distinct selectivity for 5-HT_2 over 5-HT_{1C} receptors though as the concentrations of the drug at the receptor site is uncertain a classification based on rank order concentrations cannot be established with any certainty. The hallucinogens LSD and mescaline have been shown to have complicated effects in vivo (McCall & Aghajanian, 1980b). At low systemic and iontophoretic doses a prolonged sensitization of FM's to 5-HT and NAd is observed while at higher doses LSD acts as an antagonist and mescaline as an agonist of the facilitatory effect. Systemic application of 5-MeODMT also evokes a depolarisation of FM's in vivo which is blocked by methysergide (VanderMaelen and Aghajanian, 1982) though again without data on the concentration dependence of this effect no definitive classification of receptor pharmacology can be substantiated.

Fig. 7.1

A

RESISTANCE CHANGE 5-HT

Y=bX

n	107
a	0.0000
b	-12.3944
r	-0.7087
p	0.0000
SD	3.1947
SE	0.5772

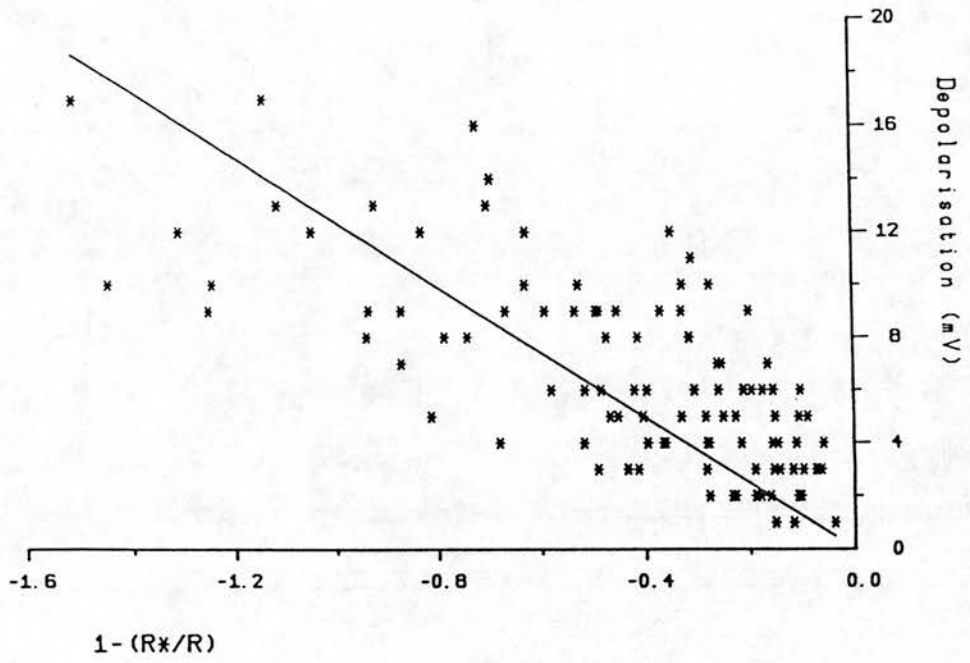

B

RESISTANCE CHANGE 5-HT

Y=a+bX

n	107
a	3.0837
b	-7.8784
r	-0.7087
p	0.0000
SD	2.5685
SE	0.7605

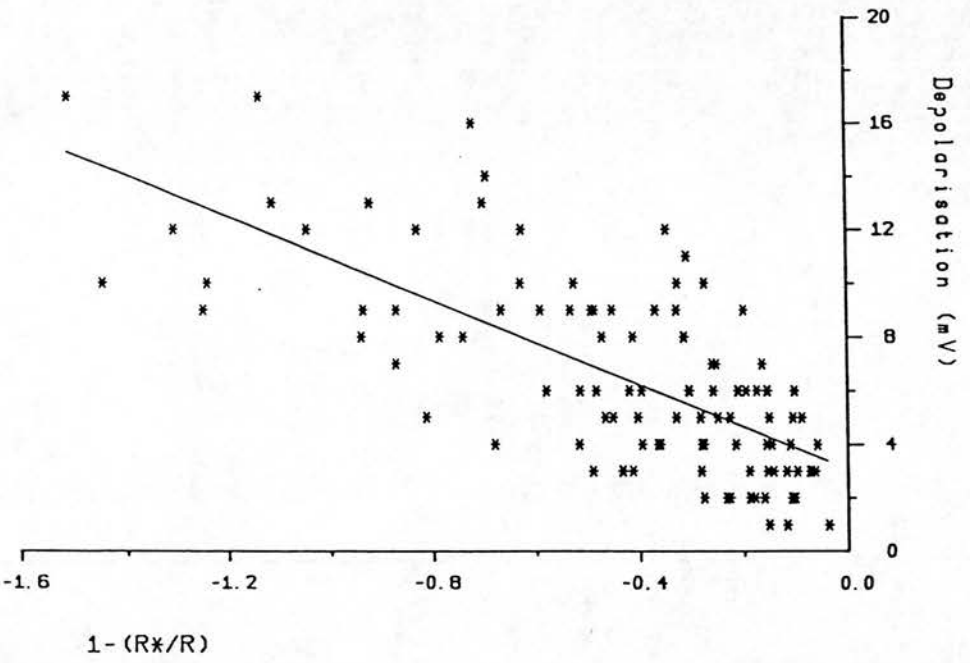

Figure 7.1

A) Plot of the ratio of the resistance change (1-(R*/R) against depolarisation amplitude for 107 FM's superfused with 5-HT. The regression line (see panel inset for statistics) has been forced through the origin and has a slope of -12.4mV.
B) As for A except the regression line has not been forced through the origin but is described by the equation Y = a + bX. Values of a and b are shown in the panel inset.

Fig. 7.2

A

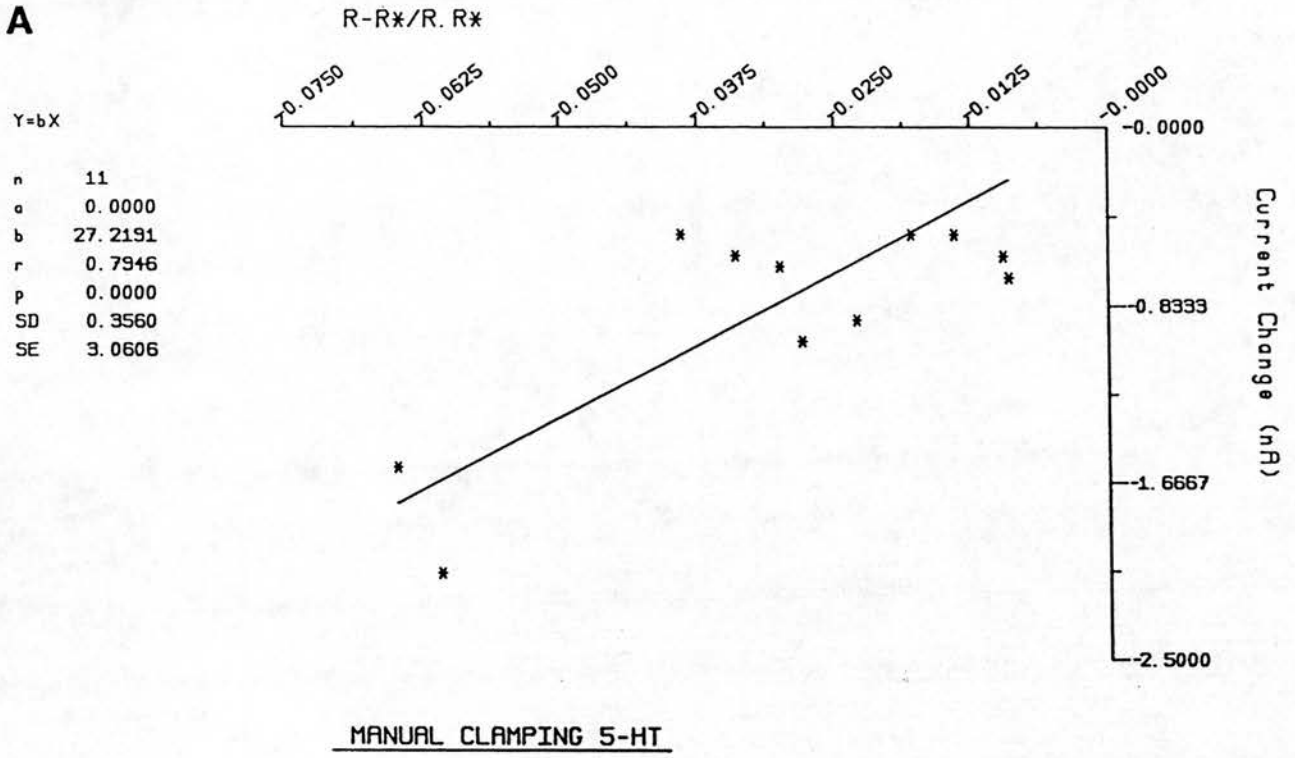
R-R*/R.R*
-0.0750
-0.0625
-0.0500
-0.0375
-0.0250
-0.0125
-0.0000
-0.0000
-0.8333
-1.6667
-2.5000
Current Change (nA)
Y=bX
n 11
a 0.0000
b 27.2191
r 0.7946
p 0.0000
SD 0.3560
SE 3.0606
MANUAL CLAMPING 5-HT

B

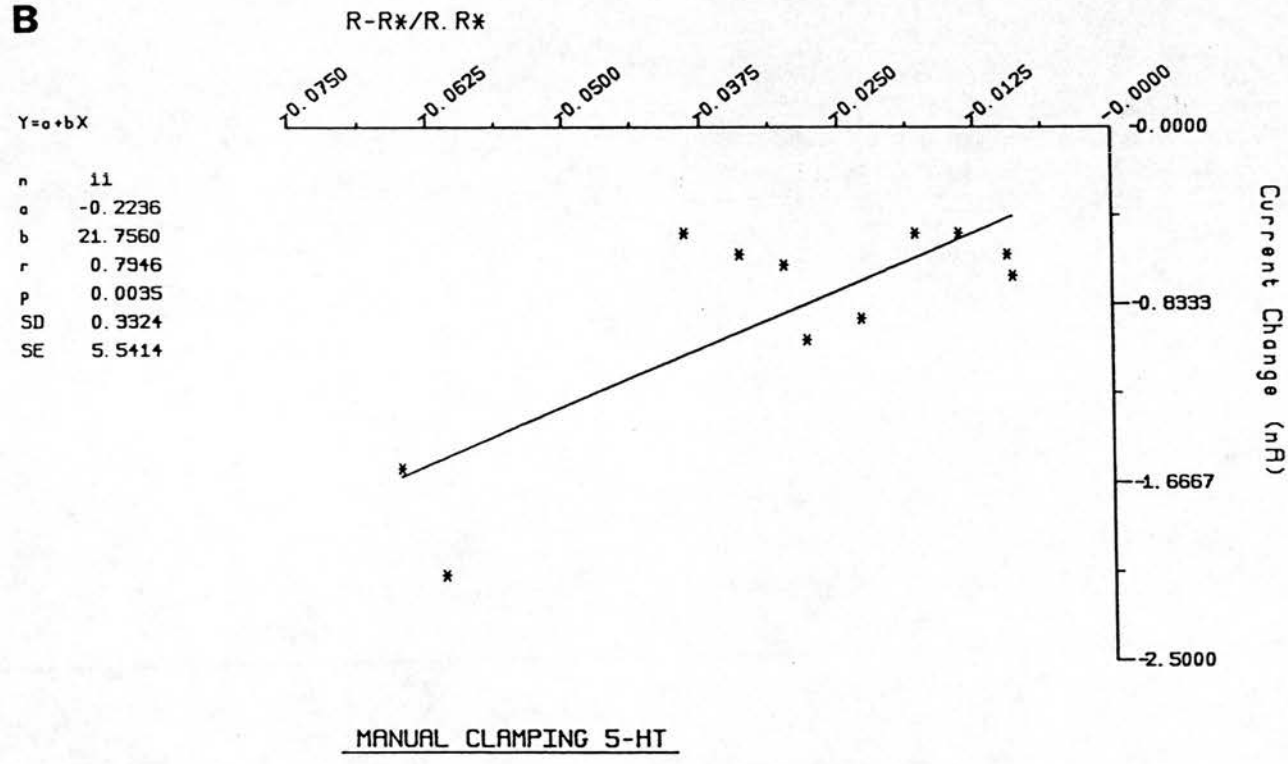
R-R*/R.R*
-0.0750
-0.0625
-0.0500
-0.0375
-0.0250
-0.0125
-0.0000
-0.0000
-0.8333
-1.6667
-2.5000
Current Change (nA)
Y=a+bX
n 11
a -0.2236
b 21.7560
r 0.7946
p 0.0035
SD 0.3324
SE 5.5414
MANUAL CLAMPING 5-HT

Figure 7.2

A) Plot of the ratio of the conductance change evoked by 5-HT, expressed in terms of resistance R-R*/R.R*, against the current required to manually clamp the FM's to the resting potential. The regression line (see panel inset for statistics) has been forced through the origin and has a slope of 27.2mV.
B) As for A except the regression line has not been forced through the origin but can be described by the equation y = a + bX according to the values in the panel inset.

Fig. 7.3

A

RESISTANCE CHANGE NA

Y=bX

n	23
a	0.0000
b	-7.0415
r	-0.4592
p	0.0000
SD	2.0794
SE	0.7181

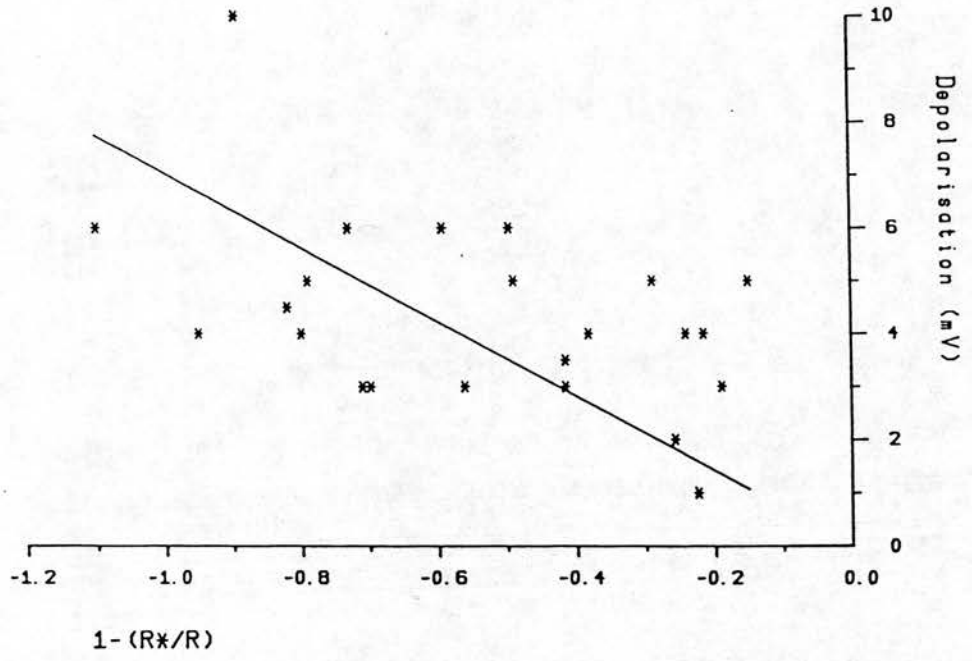

B

RESISTANCE CHANGE NA

Y=a+bX

n	23
a	2.7264
b	-3.0026
r	-0.4592
p	0.0275
SD	1.6417
SE	1.2676

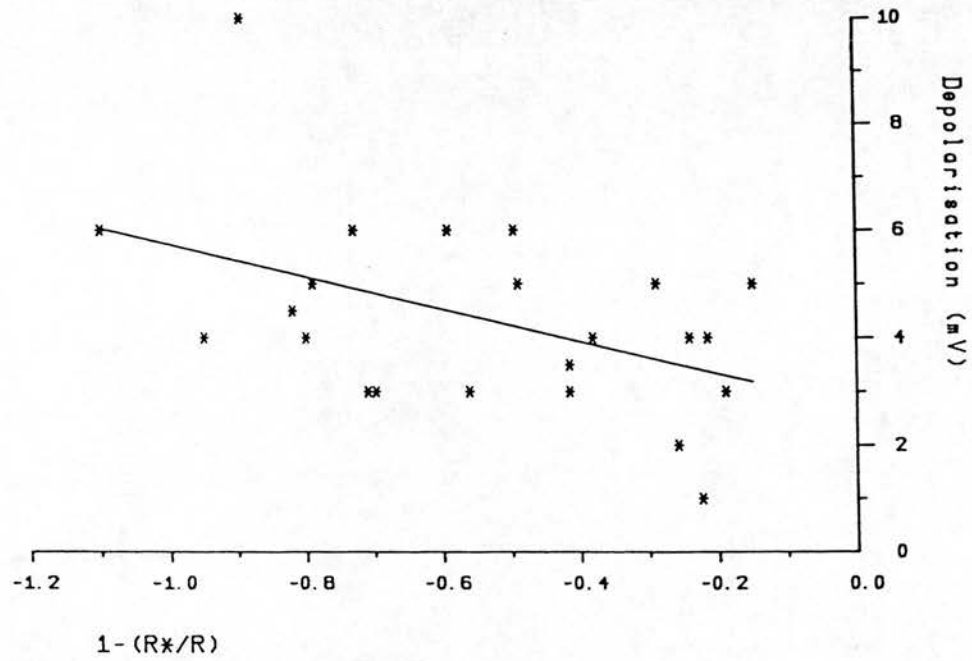

Figure 7.3

A) Plot of the ratio of the resistance change 1-(R/R*) against depolarisation amplitude for 23 applications of NAd to 21 FM's. The regression line (see panel inset for statistics) has been forced through the origin and has a slope of -7mV.
B) As for A except the regression line has not been forced through the origin but can be described by the equation y = a + bX according to the values in the panel inset.

TABLE 7.1 Classification of 5-HT mediated depolarizations and hyperpolarizations by mechanism, cell type and receptor sub-type using specific ligands

Mechanism		DEPOLARIZATION Decrease in gK^+			Increase in I_h	Increase in I_{cat^+}	HYPERPOLARIZATION Increase in gK^+		
Cell Type		FMN	N.Acc.	Hippo	PrH/LGNd	Sub-Muc. Plex.	DRN	LSN	Hippo
References		[1]	[2]	[3]	[4]	[5]	[6]	[7]	[3]
Sub-type	LIGAND								
5-HT_{1a}	8-OH-DPAT	NE	NE	NE	NE		+	+	+/-
	Buspirone			NE			+	+	+/-
	Ipsapirone			NE	NE			+/-	+/-
	Gepirone			NE					+/-
	Dipr-5-CT	NE					+		
5-HT_{1b}	RU24969			-				NE	NE
	TFMPP			NE	NE				NE
5-HT_{1}	5-CT		NE	NE	+		+		+
5-HT_{1c}	mCPP		NE	NE					
$5\text{-HT}_{1a/2}$	Spiperone	NE	-	NE	-	NE	-		-
$5\text{-HT}_{1c/2}$	LY 53857	-							
$5\text{-HT}_{1/2}$	Methysergide	-		NE	-	NE	NE		+?
	Methiothepin	NE		NE					-
	Mianserin		-	NE	NE	NE			-
	Cyproheptadine			NE		NE			-
5-HT_{2}	Ketanserin	-?	-	NE	NE	NE			NE
5-HT_{3}	ICS-205 930	NE	NE	NE/-		-			NE
	GR38032					-			
	2-CH3-5-HT	NE			NE	+			

NE = No Effect

\+ = Agonist

\- = Antagonist

+/- = Partial Agonist

[1] Kelly et al, 1988
Larkman and Kelly, 1988
Larkman 1990

[2] North and Uchimura, 1989

[3] Colino and Halliwell, 1987
Andrade and Nicoll, 1987a,b
Beck, 1988

[4] Bobker and Williams, 1989
Pape and McCormick, 1989

[5] Derkach et al, 1989
Surprenant and Crist, 1988

[6] Rainnie, 1988
Williams et al, 1988

[7] Joels et al, 1987

CONCLUDING REMARKS

CONCLUDING REMARKS

Facial motoneurones *in vitro* are depolarised by superfusion of 5-HT and NAd, an action associated with an increase in neuronal input resistance and a lengthening of the membrane time constant. These actions underlie the increase in excitability of FM's observed *in vivo* in response to iontophoretic 5-HT and NAd. Determination of the reversal potentials of these actions using I/V plot methods is complicated by a prominent inward rectifier seen in FM's. The evidence presented here supports an action of both neurotransmitters on a resting K^+ conductance though differences between the reversal potentials obtained may reflect different somatodendritic locations of the receptors mediating these actions or an additional conductance increase evoked by 5-HT. Further studies are required to provide an answer to this problem.

The pharmacological data presented here including the use of putative selective 5-HT_2 antagonists does not lead to the classification of the receptor type responsible for 5-HT evoked depolarisation of facial motoneurones. The results obtained on FM's are summarised in Table 7.1 where they are compared with the data so far obtained from intracellular studies of other 5-HT-evoked depolarisations and hyperpolarisations. The evidence points towards either a 5-HT_{1C} or 5-HT_2 receptor type though given the biochemical, pharmacological and molecular biological similarities between these receptor types it is hardly surprising that a distinction cannot be made on the basis of the electrophysiological data alone. The results of pharmacological experiments illustrate the difficulty faced in defining functional receptor profiles in the absence of highly selective receptor subtype ligands. While radioligand binding studies can define binding site subtypes on the

basis of differential affinities to a range of ligands the additional penetration barriers presented in the electrophysiologically viable slice preparation used here make a similar categorisation impossible. However, in agreement with other studies where a decrease in a K^+ conductance evoked by 5-HT is observed in central neurones (North and Uchimura, 1989; Davies et al, 1987; Andrade and Nicoll, 1987a), the ineffectiveness of 8-OH-DPAT, dipropyl-5-CT and spiperone indicate that a 5-HT_{1A} receptor does not appear to be responsible. The lack of effect of 2-CH_3-5-HT and ICS 205 930 as well as the antagonism by methysergide rule out mediation by a 5-HT_3 receptor. The low potency of ketanserin and lack of antagonism by spiperone suggest a 5-HT_{1C} receptor may be responsible for 5-HT evoked depolarisation of FM's. The low potency of 5-HT suggests against this idea however this may be a consequence of diffusion barriers (e.g. uptake, metabolism) within the slice preparation. Activation of 5-HT_{1C} receptors expressed on the Xenopus oocyte surface after injection with rat brain mRNA has been shown to evoke an inward current mediated by closure of Ba^{2+}-sensitive K^+ channels (Parker et al, 1990). The relationship of this data to the work here is even more pertinent in that it appears that the K^+ channels in question are also likely to be of injected mRNA origin. By assuming that the 5-HT_{1C} receptor belongs to the 5-HT_2 receptor "family" the results obtained with methysergide, LY 53857 and ketanserin emphasise the similarity between the receptors mediating 5-HT evoked depolarisation of FM's and equivalent actions in nucleus accumbens and cortical neurones. However, the same studies highlight the different pharmacology underlying the depolarisation of hippocampal neurones, observations comparable to the apparent heterogeneity of the hippocampal 5-HT_{1A} receptor

compared to other electrophysiologically defined 5-HT_{1A} receptors in, say, the DRN and LSN.

REFERENCES

Aghajanian, G.K., Haigler, H.J. & Bloom, F.E. (1972). Lysergic acid diethylamide and serotonin: direct actions on serotonin-containing neurons in rat brain. Life Sciences 11, 615-622.

Aghajanian, G.K. & Lakoski, J.M. (1984). Hyperpolarisation of serotonergic neurones by serotonin and LSD: studies in brain slice showing increased K^+ conductance. Brain Research 305, 181-185.

Aghajanian, G.K., & McCall, R.B. (1980). Serotonergic synaptic input to facial motoneurons: localization by electron microscopic autoradiography. Neuroscience 5, 2155-2162.

Aghajanian, G.K. & Rasmussen, K. (1989). Intracellular studies in the facial nucleus illustrating a simple new method for obtaining viable motoneurones in adult rat brain slices. Synapse 3, 331-338.

Akasu, T., Gallagher, J.P., Nakamura, T., Shinnick-Gallagher, P. & Yoshimura, M. (1985). Noradrenaline hyperpolarisation and depolarisation in cat vesicle parasympathetic neurones. Journal of Physiology 361, 165-184.

Andrade, R., Malenka, R.C. & Nicoll, R.A. (1986). A G protein couples serotonin and $GABA_B$ receptors to the same channels in hippocampus. Science 234, 1261-1264.

Andrade, R. & Nicoll, R.A. (1987a). Pharmacologically distinct actions of serotonin on single pyramidal neurones of the rat hippocampus recorded in vitro. Journal of Physiology 394, 99-124.

Andrade, R. & Nicoll, R.A. (1987b). Novel anxiolytics discriminate between postsynaptic serotonin receptors mediating different physiological responses on single neurones of the rat hippocampus. Naunyn-Schmeideberg's Archives of Pharmacology 336, 5-10.

Aston-Jones, G., Ennis, M., Pieribone, V.A., Thompson-Nickell, W. & Shipley, M.T. (1986). The brain nucleus locus coeruleus:Restricted afferent control of a broad efferent network. Science 234, 734-737.

Barrett, E.F. & Barrett, J.N. (1976). Separation of two voltage-sensitive potassium currents, and demonstration of a tetrodotoxin-resistant calcium current in frog motoneurones. Journal of Physiology 255, 737-744.

Barrett, E.F., Barrett, J.N. & Crill, W.E. (1980). Voltage-sensitive outward currents in cat motoneurones. Journal of Physiology 304, 251-276.

Barrett, J.N. & Crill, W.E. (1974). Specific membrane properties of cat motoneurones. Journal of Physiology 239, 301-324.

Barrett, J.N. & Crill, W.E. (1980). Voltage-clamp of cat motoneurone somata:properties of the fast inward current. Journal of Physiology 304, 231-249.

Baskys, A., Niesen, C.E., Davies, M.F. & Carlen, P.L. (1989). Modulatory actions of serotonin on ionic conductances of hippocampal dentate granule cells. Neuroscience 29, 443-451.

Beck, S.G. (1989). 5-Carboxyamidotryptamine mimics only the 5-HT elicited hyperpolarisation of hippocampal pyramidal cells via 5-HT1A receptor. Neuroscience Letters 99, 101-106.

Benson, D.M., Blitzer, R.D. & Landau, E.M. (1988). An analysis of the depolarization produced in guinea-pig hippocampus by cholinergic receptor stimulation. Journal of Physiology 404, 479-496.

Bobker, D.H. & Williams, J.T. (1989). Serotonin augments the cationic current I_h in central neurones. Neuron 2, 1535-1540.

Bradley, K. & Somjen, G.G. (1961). Accommodation in motoneurones of the rat and the cat. Journal of Physiology 156, 75-92.

Bradley, P.B., Engel, G., Feniuk, W., Fozard, J.R., Humphrey, P.P.A., Middlemiss, D.N., Mylecharane, E.J., Richardson, B.P. & Saxena, P.R. (1986). Proposals for the classification and nomenclature of functional receptors for 5-hydroxytryptamine. Neuropharmacology 25, 563-576.

Brown, D.A. & Constanti, A. (1980). Intracellular observations on the effects of muscarinic agonists on rat sympathetic neurones. British Journal of Pharmacology 70, 593-608.

Brown, D.A. & Griffiths, W.H. (1983a). Calcium-activated outward current in voltage-clamped hippocampal neurones of the guinea pig. Journal of Physiology 337, 287-301.

Brown, D.A. & Griffiths, W.H. (1983b). Persistent slow inward calcium current in voltage-clamped hippocampal neurones of the guinea pig. Journal of Physiology 337, 303-320.

Brown, H. & DiFrancesco, D. (1980). Voltage-clamp investigations of membrane currents underlying pace-maker activity in rabbit sino-atrial node. Journal of Physiology 308, 331-351.

Burke, R.E. & P. Rudomin. (1977). Spinal neurones and synapses. In Handbook of Physiology, Sect.1, The Nervous System, Vol.1, Cellular Biology of Neurons Part 2. J.M. Brookhart, and V.B. Mountcastle, editors. American Physiol.Soc., Bethesda. 877-944.

Burke, R.E. & Ten Bruggencate, G. (1971). Electrotonic characteristics of alpha motoneurones of varying size. Journal of Physiology 212, 1-20.

Castle, N.A., Haylett, D.G. & Jenkinson, D.H. (1989). Toxins in the characterisation of potassium channels. Trends in Neurosciences 12, 59-65.

Cohen, M.L., Fuller, R.W. & Kurz, K.D. (1983). LY53857,a selective and potent serotonergic ($5\text{-}HT_2$) receptor antagonist, does not lower blood pressure in the spontaneously hypertensive rat. Journal of Pharmacology and Experimental Therapeutics 227, 327-332.

Colino, A. & Halliwell, J.V. (1987). Differential modulation of three separate K-conductances in hippocampal CA1 neurones by serotonin. Nature 328, 73-77.

Connell, L.A. & Wallis, D.I. (1988). Responses to 5-hydroxytryptamine evoked in the hemisected spinal cord of the neonate rat. British Journal of Pharmacology 94, 1101-1114.

Connell, L.A. & Wallis, D.I. (1989). 5-Hydroxytryptamine depolarizes neonatal rat motoneurones through a receptor unrelated to an identified binding site. Neuropharmacology 28, 625-634.

Connor, J.A. & Stevens, C.F. (1971). Voltage clamp studies of a transient outward membrane current in gastropod neural somata. Journal of Physiology 213, 21-30.

Constanti, A. & Galvan, M. (1983). Fast inward-rectifying current accounts for anomalous rectification in olfactory cortex neurones. Journal of Physiology 385, 153-178.

Coombs, J.S., Curtis, D.R. & Eccles, J.C. (1957). The generation of impulses in motoneurones. Journal of Physiology 139, 232-249.

Coombs, J.S., Curtis, D.R. & Eccles, J.C. (1957). The interpretation of spike potentials of motoneurones. Journal of Physiology 139, 198-231.

Coombs, J.S., Curtis, D.R. & Eccles, J.C. (1959). The electrical constants of the motoneurone membrane. Journal of Physiology 145, 505-528.

Coombs, J.S., Eccles, J.C. & Fatt, P. (1955). The electrical properties of the motoneurone membrane. Journal of Physiology 130, 291-325.

Courville, J. (1966). The nucleus of the facial nerve; the relation between cellular groups and peripheral branches of the nerve. Brain Research 1, 338-354.

Crepel, F. & Penit-Soria, J. (1986). Inward rectification and low threshold calcium conductance in rat cerebellar Purkinje cells. An *in vitro* study. Journal of Physiology 372, 1-23.

Crill, W.E. & Schwindt, P.C. (1983). Active currents in mammalian central neurons. Trends in Neurosciences 6, 236-240.

Crist, J. & Surprenant, A. (1987). Evidence that 8-hydroxy-(n-dipropylamino)tetralin (8-OH-DPAT) is a selective α_2-adrenoceptor antagonist on guinea-pig submucous neurones. British Journal of Pharmacology 92, 341-347.

Crunelli, V., Forda, S., Kelly, J.S. & Wise, J.C.M. (1983). A programme for the analysis of intracellular data recorded from *in vitro* preparations of central neurons. Journal of Physiology 340, 13P (Abstract).

Davies, M., Wilkinson, L.S. & Roberts, M.H.T. (1988a). Evidence for depressant 5-HT1-like receptors on rat brainstem neurones. British Journal of Pharmacology 94, 492-499.

Davies, M., Wilkinson, L.S. & Roberts, M.H.T. (1988b). Evidence for excitatory 5-HT2-receptors on rat brainstem neurones. British Journal of Pharmacology 94, 483-491.

Davies, M.F., Deisz, R.A., Prince, A. & Peroutka, S.J. (1987). Two distinct effects of 5-hydroxytryptamine on single cortical neurones. Brain Research 423, 347-352.

Derkach, V., Surprenant, A. & North, R.A. (1989). 5-HT_3 receptors are membrane ion channels. Nature 339, 706-709.

DiFrancesco, D. (1981). A study of the ionic nature of the pace-maker current in calf Purkinje fibres. Journal of Physiology 314, 377-393.

Dodd, J., Dingledine, R. & Kelly, J.S. (1981). The excitatory action of acetylcholine on hippocampal neurones of the guinea pig and rat maintained in vitro. Brain Research 207, 109-127.

Dun, N.J., Kiraly, M. & Ma, R.C. (1984). Evidence for a serotonin mediated slow excitatory potential in the guinea-pig coeliac ganglia. Journal of Physiology 351, 61-76.

Dutar, P. & Nicoll, R.A. (1988). Classification of muscarinic responses in hippocampus in terms of receptor subtypes and second-messenger systems: Electrophysiological studies in vitro. Journal of Neuroscience 11, 4214-4224.

Enevoldson, T.P., Gordon, G. & Sanders, J. (1984). The use of retrograde transport of horseradish peroxidase for studying the dendritic trees and axonal courses of particular groups of tract cells in the spinal cord. Exp. Br. Res. 54, 529-537.

Fanardjian, V.V. & Manvelyan, L.R. (1987a). Mechanisms regulating the activity of facial nucleus motoneurones-3.Synaptic influences from the cerebral cortex and subcortical structures. Neuroscience 20, 835-843.

Fanardjian, V.V. & Manvelyan, L.R. (1987b). Mechanisms regulating the activity of facial nucleus motoneurones-4. Influences from the brainstem structures. Neuroscience 20, 845-853.

Fanardjian, V.V., Manvelyan, L.R. & Kasabyan, S.A. (1983a). Mechanisms regulating the activity of facial nucleus motoneurones-1.Antidromic activation. Neuroscience 9, 814-822.

Fanardjian, V.V., Manvelyan, L.R. & Kasabyan, S.A. (1983b). Mechanisms regulating the activity of facial nucleus motoneurones-2.Synaptic activation from the caudal trigeminal nucleus. Neuroscience 9, 823-835.

Fischette, C.T., Nock, B. & Renner, K. (1987). Effects of 5,7-dihydroxytryptamine on serotonin$_1$ and serotonin$_2$ receptors throughout the rat central nervous system using quantitative autoradiography. Brain Research 421, 263-279.

Foehring, P.C., Schwindt, P.C. & Crill, W.E. (1989). Norepinephrine selectively reduces slow Ca^{2+} and Na^{+}-mediated K^{+} currents in cat neocortical neurons. J. Neurophysiol. 61, 245-256.

Fozard, J.R. & Gray, J.A. (1989). 5-HT_{1C} receptor activation : a key step in the initiation of migraine ? Trends in Pharmacological Sciences 10, 307-309.

Forsythe, I.D. & Redman, S.J. (1988). The dependence of motoneurone membrane potential on extracellular ion concentrations studied in isolated rat spinal cord. Journal of Physiology 404, 83-99.

Friauf, E. (1986). Morphology of motoneurones in different subdivisions of the rat facial nucleus stained intracellularly with HRP. Journal of Comparative Neurology 253, 231-241.

Friauf, E. & Herbert, H. (1985). Topographic organisation of facial motoneurones to individual pinna muscles in rat(Rattus rattus) and bat(Rousettus aegyptiacus). Journal of Comparative Neurology 240, 161-170.

Fruns, M., Krieger, C. & Sears, T.A. (1987). Identification and electrophysiological investigations of embryonic mammalian motoneurones in culture. Neuroscience Letters 83, 82-88.

Fukuda, A., Minami, T., Nabekura, J. & Oomura, Y. (1987). The effects of nor-adrenaline on neurones in the rat dorsal motor nucleus of the vagus, in vitro. Journal of Physiology 393, 213-231.

Fulton, B.P. (1987). Development of inward rectification in A cells of isolated rat dorsal root ganglia. Journal of Physiology 370, 150P.(Abstract)

Fulton, B.P. & Walton, K. (1986). Electrophysiological properties of neonatal rat motoneurones studied in vitro. Journal of Physiology 370, 651-678.

Galvan, M. & Adams, P.R. (1982). Control of calcium current in rat sympathetic neurons by norepinephrine. Brain Research 244, 135-144.

Gerschenfeld, H.M. & Paupardin-Tritsch, D. (1974). Ionic mechanisms and receptor properties underlying the response of molluscan neurons to 5-HT. Journal of Physiology 243, 427-456.

Ginsborg, B.L. (1967). Ion movements in junctional transmission. Pharmacological Reviews 19, 289-316.

Ginsborg, B.L. (1973). Electrical changes in the membrane in junctional transmission. Biochimica et Biophysica Acta 300, 289-317.

Ginsborg, B.L., House, C.R. & Silinsky, E.M. (1974). Conductance changes associated with the secretory potential in the cockroach salivary gland. Journal of Physiology 236, 723-731.

Granit, R., Kernell, D. & Smith, R.S. (1963). Delayed depolarisation and the repetitive response to intracellular stimulation of mammalian motoneurones. Journal of Physiology 168, 890-910.

Gray, R. & Johnston, D. (1987). Noradrenaline and α-adrenoreceptor agonists increase activity of voltage-dependent calcium channels in hippocampal neurons. Nature 327, 620-622.

Gueritaud, J.P. (1988). Electrical activity of rat ocular motoneurones recorded in vitro. Neuroscience 24, 837-852.

Haas, H.L. & Konnerth, A. (1983). Histamine and noradrenaline decrease calcium-activated potassium conductance in hippocampal pyramidal cells in the hippocampus. Nature 302, 432-434.

Haas, H.L., Schaerer, B. & Vosmansky, M. (1979). A simple perfusion chamber for the study of nervous tissue slices in vitro. Journal of Neuroscience Methods 1, 323-325.

Hagenbach, A., Hoyer, D., Kalkman, H.O. & Seiler, M.P. (1986). N,N dipropyl-5-carboxamidotryptamine (DP-5CT), an extremely potent and selective 5-HT_{1A} agonist. British Journal of Pharmacology 87, 139P (Abstract).

Hagiwara, W., Miyazaki, S. & Rosenthal, P. (1976). Potassium current and the effect of caesium on this current during anomalous rectification of the egg cell membrane of a starfish. Journal of General Physiology 67, 621-638.

Halliwell, J.V. & Adams, P.R. (1982). Voltage-clamp analysis of muscarinic excitation in hippocampal neurons. Brain Research 250, 71-92.

Harada, Y. & Takahashi, T. (1983). The calcium component of the action potential in spinal motoneurones of the rat. Journal of Physiology 335, 89-100.

Hestrin, S. (1981). The interaction of potassium with the activation of anomalous rectification in frog muscle membrane. Journal of Physiology 317, 497-508.

Hinrichsen, C.F.L. & Watson, C.D. (1983). Brain stem projections to the facial nucleus of the rat. Brain Behaviour and Evolution 22, 153-163.

Hodgkin, A.L. & Huxley, A.F. (1952a). Currents carried by sodium and potassium ions through the membrane of the giant axon of Loligo. Journal of Physiology 116, 449-472.

Hodgkin, A.L. & Huxley, A.F. (1952b). The components of membrane conductance in the giant axon of Loligo. Journal of Physiology 116, 473-496.

Holstege, G.H., Tan, J., Van Ham, J. & Bos, A. (1984). Mesencephalic projections to the facial nucleus in the cat. An autoradiographical tracing study. Brain Research 311, 7-22.

Hotson, J.R., Prince, D.A. & Schwartzkroin, P.A. (1979). Anomalous inward rectification in hippocampal neurons. J. Neurophysiol. 42, 889-895.

Hounsgaard, J., Hultborn, H., Jespersen, B. & Kiehn, O. (1988). Bistability of α-motoneurones in the decerebrate cat and in the acute spinal cat after intravenous 5-hydroxytryptophan. Journal of Physiology 405, 345-367.

Hounsgaard, J., Hultborn, H. & Kiehn, O. (1986). Transmitter-controlled properties of α-motoneurones causing long lasting motor discharge to brief excitatory inputs. In Progress in Brain Research V64. H.J. Freund, U. Buttner, B. Cohen, and J. Noth, editors. Elsevier Science Publishers B.V. (Biomedical Division). 39-49.

Hounsgaard, J. & Kiehn, O. (1989). Serotonin-induced bistability of turtle motoneurones caused by a nifedipine-sensitive calcium plateau potential. Journal of Physiology 414, 265-282.

Hounsgaard, J., Kiehn, O. & Mintz, I. (1988). Response properties of motoneurones in a slice preparation of the turtle spinal cord. Journal of Physiology 398, 575-589.

Hounsgaard, J. & Mintz, I. (1988). Calcium conductance and firing properties of spinal motoneurones in the turtle. Journal of Physiology 398, 591-603.

Hoyer, D. (1988). Molecular pharmacology and biology of 5-HT_{1C} receptors. Trends in Pharmacological Sciences. 9, 89-94.

Isokawa-Akesson, M. & Komisaruk, B.R. (1987). Difference in projections to the lateral and medial facial nucleus:anatomically seperate pathways for rhythmical vibrissa movements in rats. Exp. Br. Res. 65, 385-398.

Ito, M. & Oshima, T. (1965). Electrical behaviour of the motoneurone membrane during intracellularly applied current steps. Journal of Physiology 180, 607-635.

Iwata, N., Kitai, S.T. & Olson, S. (1972). Afferent component of the facial nerve:its relation to the spinal trigeminal and facial nucleus. Brain Research 43, 662-667.

Jahnsen, H. (1980). The action of 5-hydroxytryptamine on neuronal membranes and synaptic transmission in area CA1 of the hippocampus in vitro. Brain Research 197, 83-94.

Joels, M. & Gallagher, J.P. (1988). Actions of serotonin recorded intracellularly in rat dorsal lateral septal neurons. Synapse 2, 45-53.

Joels, M., Shinnick-Gallagher, P. & Gallagher, J.P. (1987). Effect of serotonin and serotonin-analogues on passive membrane properties of lateral septal neurons in vitro. Brain Research 417, 99-107.

Joels, M., Twery, M.J., Shinnick-Gallagher, P. & Gallagher, J.P. (1986). Multiple actions of serotonin on lateral septal neurones in rat brain. European Journal of Pharmacology 129, 203-204.

Joels, M. & Urban, I.J.A. (1985). Monoamine-induced responses in lateral septal neurons: influence of iontophoretically applied vasopressin. Brain Research 344, 120-126.

Johnson, S.M., Katayama, Y. & North, R.A. (1980). Multiple actions of 5-hydroxytryptamine on myenteric neurones of the guinea-pig ileum. Journal of Physiology 304, 459-470.

Johnston, D. & Brown, T.H. (1983). Interpretation of voltage-clamp measurements in hippocampal neurons. J. Neurophysiol. 50, 464-486.

Kelly, J.S. (1982). Intracellular recording from neurons in brain slices in vitro. In Handbook of Psychopharmacology,Vol.15. L.L. Iversen, S. Iversen, and S.H. Snyder, editors. Plenum Publishing Corporation, 95-183.

Kelly, J.S., Larkman, P.M. & Rainnie, D.G. (1988). Hyperpolarizing and depolarizing responses to 5-hydroxytryptamine in the rat brain stem in vitro. British Journal of Pharmacology 95, 500P.(Abstract)

Kilpatrick, G.J., Jones, B.J. & Tyers, M.B. (1987). Identification and distribution of 5-HT_3 receptors in rat brain using radioligand binding. Nature 330, 746-748.

Klein, M. & Kandel, E.R. (1980). Mechanism of potassium current modulation underlying presynaptic facilitation and behavioural sensitisation in Aplysia. Proceedings of the National Academy of Sciences. USA. 77, 6912-6916.

Kubota, K. & Brookhart, J.M. (1963). Recurrent facilitation of frog motoneurones. J. Neurophysiol. 26, 877-893.

Kuffler, S.W. & Sejnowski, T.J. (1983). Peptidergic and muscarinic excitation at amphibian sympathetic synapses. Journal of Physiology 341, 257-278.

Lakoski, J.M. & Aghajanian, G.K. (1985). Effects of ketanserin on neuronal responses to serotonin in the prefrontal cortex, lateral geniculate and dorsal raphe nucleus. Neuropharmacology 24 No.4, 265-273.

Lamb, T.D. (1985). An inexpensive digital tape recorder suitable for neurophysiological signals. Journal of Neuroscience Methods 15, 1-14.

Lancaster, B. & Adams, P.R. (1986). Calcium-dependent current generating the after-hyperpolarisation of hippocampal neurones. J. Neurophysiol. 55, 1268-1282.

Larkman, P.M. & Kelly, J.S. (1988). The effects of serotonin (5-HT) and antagonists on rat facial motoneurones in the in vitro brainstem slice. Journal of Neuroscience Methods 24, No.2, 199 (Abstract).

Larkman, P.M., Penington, N.J. & Kelly, J.S. (1988). The effects of 5-hydroxytryptamine (5-HT) on rat facial motoneurones in the in vitro brain slice of the rat. Neuroscience Letters Suppl.32, S9.(Abstract)

Larkman, P.M., Penington, N.J. & Kelly, J.S. (1989a). Electrophysiology of adult rat facial motoneurones:the effects of serotonin(5-HT)in a novel in vitro brainstem slice. Journal of Neuroscience Methods 28, 133-146.

Larkman, P.M., Rainnie, D.G., Penington, N.J. & Kelly, J.S. (1989b). The ionic mechanism underlying the 5-hydroxytryptamine induced depolarisation of rat facial motoneurones in vitro. Serotonin Club, Florence 1, 33.(Abstract)

Lee, M., Strahlendorf, J.C. & Strahlendorf, H.K. (1986). Modulatory action of serotonin on glutamate-induced excitation of cerebellar purkinje cells. Brain Research 361, 107-113.

Legendre, P., Dupouy, B. & Vincent, J.D. (1988). Excitatory effect of noradrenaline on pacemaker cells in spinal cord primary cultures. Neuroscience 24, 647-658.

Legendre, P., Guzman, A., Dupouy, B. & Vincent, J.D. (1989). Excitatory effect of serotonin on pacemaker neurons in spinal cord cell culture. Neuroscience 28, 201-209.

Leysen, J.E., Awouters, F., Kennis, L., Laduron, P.M., Vandenberk, J. & Jannsen, P.A.J. (1981). Receptor binding profile of R 41 468,a novel antagonist at 5-HT_2 receptors. Life Sciences 28, 1015-1022.

Lindquist, C. (1973). Contraction properties of cat facial muscles. Acta physiologica scandinavica 89, 482-490.

Llinas, R. (1988). The intrinsic electrophysiological properties of mammalian neurons: Insights into central nervous system function. Science 242, 1654-1664.

Llinas, R. & Yarom, Y. (1981). Electrophysiology of mammalian inferior olivary neurones in vitro : different types of voltage sensitive conductances. Journal of Physiology 315, 549-567.

Llinas, R., Yarom, Y. & Sugimori, M. (1981). Isolated mammalian brain in vitro: new technique for analysis of electrical activity of neuronal circuit function. Fed. Proc. 40, 2240-2245.

Ma, R.C. & Dun, N.J. (1986). Excitation of lateral horn neurons of the neonatal rat spinal cord by 5-Hydroxytryptamine. Developmental Brain Research 24, 89-98.

Madison, D.V., Lancaster, B. & Nicoll, R.A. (1987). Voltage clamp analysis of cholinergic action in the hippocampus. Journal of Neuroscience 7, 733-741.

Magherini, P.C., Precht, W. & Schwindt, P.C. (1976). Electrical properties of frog motoneurones in the in situ spinal cord. J. Neurophysiol. 39, 459-473.

Martin, M.R. & Lodge, D. (1977). Morphology of the facial nucleus of the rat. Brain Research 123, 1-12.

Martin, M.R., Lodge, D., Headley, P.Max. & Biscoe, T.J. (1977). Pharmacological studies on facial motoneurones in the rat. European Journal of Pharmacology 42, 291-298.

Mayer, M.L. & Westbrook, G.L. (1983). A voltage-clamp analysis of inward (anomalous) rectification in mouse spinal sensory ganglion neurones. Journal of Physiology 340, 19-45.

McCall, R.B. & Aghajanian, G.K. (1979a). Serotonergic facilitation of facial motoneurone excitation. Brain Research 169, 11-27.

McCall, R.B. & Aghajanian, G.K. (1979b). Denervation supersensitivity to serotonin in the facial nucleus. Neuroscience 4, 1501-1510.

McCall, R.B. & Aghajanian, G.K. (1980a). Pharmacological characterisation of serotonin receptors in the facial motor nucleus:a microiontophoretic study. European Journal of Pharmacology 65, 175-183.

McCall, R.B. & Aghajanian, G.K. (1980b). Hallucinogens potentiate responses to serotonin and norepinephrine in the facial motor nucleus. Life Sciences 26, 1149-1156.

McCormick, D.A. (1989). Cholinergic and noradrenergic modulation of thalamocortical processing. Trends in Neurosciences 12, 215-221.

McCormick, D.A. & Prince, D.A. (1988). Noradrenergic modulation of firing pattern in guinea-pig and cat thalamic neurons, in vitro. J. Neurophysiol. 59, 978-996.

Mesulam, M-M. (1978). Tetramethylbenzidine (TMB) for HRP neurohistochemistry. A non-carcinogenic blue reaction product with superior sensitivity for visualising neural afferents and efferents. J. Histochem. Cytochem. 26, 106-117.

Middlemiss, D.N. & Fozard, J.R. (1983). 8-Hydroxy-2-(di-n-propylamino)tetralin discriminates between subtypes of the 5-HT_1 recognition site. European Journal of Pharmacology 90, 151-153.

Mosfeldt-Laursen, A. & Rekling, J.C. (1989). Electrophysiological properties of hypoglossal motoneurones of guinea pigs studied in vitro. Neuroscience 30, 619-637.

Nelson, P.G. & Burke, R.E. (1967). Delayed depolarisation in cat spinal motoneurones. Expl. Neurol. 17, 16-26.

Nelson, P.G. & Frank, K. (1967). Anomalous rectification in cat spinal motoneurones and the effect of polarizing currents on excitatory postsynaptic potentials. J. Neurophysiol. 30, 1097-1113.

Nishimura, Y., Schwindt, P.C. & Crill, W.E. (1989). Electrical properties of facial motoneurones in brainstem slices from guinea pig. Brain Research 502, 127-142.

North, R.A. & Uchimura, N. (1989). 5-Hydroxytryptamine acts at 5-HT_2 receptors to decrease potassium conductance in rat nucleus accumbens neurones. Journal of Physiology 417, 1-12.

North, R.A. & Uchimura, N. (1990). Muscarine acts at M1 receptors to reduce potassium conductance in rat nucleus accumbens neurones. Journal of Physiology 422, 369-380.

North, R.A. & Yoshimura, M. (1984). The actions of noradrenaline on neurones of the rat substantia gelatinosa in vitro. Journal of Physiology 349, 43-55.

O'Brien, R.J. & Fischbach, G.D. (1986). Isolation of embryonic chick motoneurones and their survival in vitro. Journal of Neuroscience 6, 3265-3274.

Onodera, H. & Kogure, K. (1988). Differential localisation of adenosine A_1 receptors in the rat hippocampus:quantitative autoradiographic study. Brain Research 458, 212-217.

Pape, H-C. & McCormick, D.A. (1989). Noradrenaline and serotonin selectively modulate thalamic burst firing by enhancing a hyperpolarization-activated cation current. Nature 340, 715-718.

Parker, I., Panicker, M.M. & Miledi, R. (1990). Serotonin receptors expressed in Xenopus oocytes by mRNA from brain mediate a closing of K^+ membrane channels. Molecular Brain Research 7, 31-38.

Paxinos, G. & Watson C. (1982). The rat brain in stereotaxic coordinates, Academic Press, Sydney.

Pazos, A., Cortes, R. & Palacios, J.M. (1985). Quantitative autoradiographic mapping of serotonin receptors in the rat brain.II. Serotonin-2 receptors. Brain Research 346, 231-249.

Pazos, A. & Palacios, J.M. (1985). Quantitative autoradiographic mapping of serotonin receptors in the rat brain.I. Serotonin-1 receptors. Brain Research 346, 205-230.

Pedigo, N.W., Yamamura, H.I. & Nelson, D.L. (1981). Discrimination of multiple [^{3}H]5-hydroxytryptamine binding sites by the neuroleptic Spiperone in rat brain. Journal of Neurochemistry 36, 220-226.

Pellmar, T.C. (1987). Peroxide alters neuronal excitability in the CA1 region of guinea pig hippocampus in vitro. Neuroscience 23, 447-456.

Penington, N.J. & Reiffenstein, R.J. (1986). Possible involvement of serotonin in the facilitatory effect of a hallucinogenic phenethylamine on single facial motoneurones. Canadian Journal of Physiology and Pharmacology 64, 1302-1309.

Peroutka, S.J. (1988). 5-hydroxytryptamine receptor subtypes : molecular, biochemical and physiological characterisation. Trends in Neurosciences 11, 496-500.

Peroutka, S.J. & Snyder, S.H. (1979). Multiple serotonin receptors:differential binding of [^{3}H]5-hydroxytryptamine, [^{3}H]lysergic acid diethylamide and [^{3}H]spiroperidol. Molecular Pharmacology 16, 687-699.

Pierce, P.A. & Peroutka, S.J. (1989). Evidence for distinct 5-hydroxytryptamine$_2$ binding site subtypes in cortical membrane preparations. Journal of Neurochemistry 52, 656-658.

Pieribone, V.A., Van Bockstaele, E.J., Shipley, M.T. & Aston-Jones, G. (1989). Serotonergic innervation of rat locus coeruleus derives from non-raphe brain areas. Society of Neurosciences Abstracts 15, 168.17 (Abstract).

Pitler, T.A. & Landfield, P.W. (1987). Probable Ca^{2+}-mediated inactivation of Ca^{2+} currents in mammalian brain neurones. Brain Research 410, 147-153.

Pogosyan, V.I. & Fanardjian, V.V. (1986). Afferent connections of cat facial nucleus : a study using retrograde axonal transport of HRP. Nierofiziologiya 1, 35-45.

Pollock, J.D., Bernier, L. & Camardo, J.S. (1985). Serotonin and cyclic adenosine 3':5'-monophosphate modulate the potassium current in tail sensory neurons in the pleural ganglia of aplysia. Journal of Neuroscience 5, 1862-1871.

Pun, R.Y.K., Marshall, K.C., Hendelman, W.J., Guthrie, P.B. & Nelson, P.G. (1985). Noradrenergic responses of spinal neurons in locus coeruleus-spinal cord co-cultures. Journal of Neuroscience 5, 181-191.

Rainnie, D.G. (1988). The biophysical and pharmacological properties of presumptive serotonergic neurones recorded intracellularly from the dorsal raphe nucleus in the in vitro slice preparation, PhD Thesis, University of Edinburgh.

Randle, J.C.R., Bourque, C.W. & Renaud, L.P. (1986). α_1-Adrenergic receptor activation depolarizes supraoptic neurosecretory neurons in vitro. American Journal of Physiology 251, R569-R574.

Rasmussen, K. & Aghajanian, G.K. (1988). Serotonin excitation of facial motoneurones:mediation through a 5-HT2 receptor. Society of Neurosciences Abstracts 14, 610:247.8 (Abstract).

Roberts, M.H.T. & Straughan, D.W. (1967). Excitation and depression of cortical neurones by 5-hydroxytryptamine. Journal of Physiology 193, 269-294.

Rogawski, M.A. (1985). The A-current:how ubiquitous a feature of excitable cells is it ? Trends in Neurosciences 8, 214-219.

Ropert, N. (1988). Inhibitory action of serotonin in CA1 hippocampal neurones in vitro. Neuroscience 26, 69-81.

Rosene, D.L. & Mesulam, M-M. (1978). Fixation variables in HRP neurohistochemistry.1. Effects of fixation time and perfusion procedures upon enzyme activity. J. Histochem. Cytochem. 26, 28-39.

Schwindt, P.C. & Crill, W.E. (1980). Properties of a persistent inward current in normal and TEA-injected motoneurons. J. Neurophysiol. 43, 1700-1724.

Schwindt, P.C. & Crill, W.E. (1981). Differential effects of TEA and cations on ionic currents of cat motoneurones. J. Neurophysiol. 46, 1-16.

Schwindt, P.C. & Crill, W.E. (1982). Factors influencing motoneuron rhythmic firing: results from a voltage clamp study. J. Neurophysiol. 48, 875-890.

Schwindt, P.C., Spain, W.J. & Crill, W.E. (1988). Influence of anomalous rectifier activation on afterhyperpolarizations of neurons from cat sensorimotor cortex in vitro. J. Neurophysiol. 59, 468-481.

Segal, M. (1975). Serotonergic input to the hippocampus:a combined physiological and pharmacological study. Brain Research 94, 115-131.

Segal, M. (1976). 5-HT antagonists in rat hippocampus. Brain Research 103, 161-166.

Segal, M. (1980). The action of serotonin in the rat hippocampal slice preparation. Journal of Physiology 303, 423-439.

Segal, M., Azmitia, E.C. & Whitaker-Azmitia, P.M. (1989). Physiological effects of selective 5-HT_{1A} and 5-HT_{1B} ligands in rat hippocampus:comparison to 5-HT. Brain Research 502, 67-74.

Semba, K. & Egger, M.D. (1986). The facial "motor" nerve of the rat:control of vibrissal movement and examination of motor and sensory components. Journal of Comparative Neurology 247, 144-158.

Semba, K., Sood, V., Shu, N.Y., Nagele, R.G. & Egger, M.D. (1984). Examination of geniculate ganglion cells contributing sensory fibres to the rat facial "motor" nerve. Brain Research 308, 354-359.

Siegelbaum, S.A., Camardo, J.S. & Kandel, E.R. (1982). Serotonin and cAMP close single K^+ channels in Aplysia sensory neurones. Nature 299, 413-417.

Spain, W.J., Schwindt, P.C. & Crill, W.E. (1987). Anomalous rectification in neurones from cat sensorimotor cortex in vitro. J. Neurophysiol. 57, 1555-1576.

Stafstrom, C.E., Schwindt, P.C., Chubb, M.C. & Crill, W.E. (1985). Properties of persistent sodium conductance and calcium conductance of layer V neurons from cat sensorimotor cortex in vitro. J. Neurophysiol. 53, 153-170.

Stanfield, P.R., Nakajima, Y. & Yamaguchi, K. (1985). Substance P raises neuronal excitibility by reducing inward rectification. Nature 315, 498-501.

Steinbusch, H.W.M. (1981). Distribution of serotonin-immunoreactivity in the central nervous system of the rat:-cell bodies and terminals. Neuroscience 6, 557-618.

Storm, J.F. (1987). Action potential repolarisation and a fast after-hyperpolarisation in rat hippocampal pyramidal cells. Journal of Physiology 385, 733-759.

Surprenant, A. & Crist, J. (1988). Electrophysiological characterisation of functionally distinct 5-hydroxytryptamine receptors on guinea-pig submucous plexus. Neuroscience 24, 283-295.

Swanson, L.W. & Hartman, B.K. (1975). The central adrenergic system.An immunofluorescence study of the location of cell bodies and their efferent connections in the rat utilising dopamine-β-hydroxylase as a marker. Journal of Comparative Neurology 163, 467-506.

Takada, M., Itoh, K., Yasui, Y., Mitani, A., Somura, S. & Mizuno, N. (1984). Distribution of premotor neurones for orbicularis oculi motoneurones in the cat, with particular reference to possible pathways for blink reflex. Neuroscience Letters 50, 251-255.

Takahashi, T. (1978). Intracellular recording from visually identified motoneurones in rat spinal cord slices. Proc. R. Soc. Lond. B. 202, 417-421.

Takahashi, T. & Berger, A.J. (1990). Direct excitation of rat spinal motoneurones by serotonin. Journal of Physiology 423, 63-76.

Takeuchi, Y., Kojima, M., Matsuura, T. & Sano, Y. (1983). Serotonergic innervation on the motoneurones in the mammalian brainstem. Light and electron microscopic immunohistochemistry. Anatomy and Embryology 167, 321-333.

Traub, R.D. & Llinas, R. (1977). The spatial distribution of ionic conductances in normal and axotomised motoneurones. Neuroscience 2, 829-849.

VanderMaelen, C.P. & Aghajanian, G.K. (1980). Intracellular studies showing modulation of facial motoneurone excitability by serotonin. Nature 287, 346-347.

VanderMaelen, C.P. & Aghajanian, G.K. (1982). Intracellular studies on the effects of systemic administration of serotonin agonists on rat facial motoneurons. European Journal of Pharmacology 78, 233-236.

VanderMaelen, C.P. & Aghajanian, G.K. (1982). Serotonin-induced depolarisation of rat facial motoneurones in vivo:comparison with amino acid transmitters. Brain Research 239, 139-152.

Wallen, P., Buchanan, J.T., Grillner, S., Hill, R.H., Christenson, J. & Hokfelt, T. (1989). Effects of 5-hydroxytryptamine on the afterhyperpolarisation, spike frequency regulation, and oscillatory membrane properties in lamprey spinal cord neurons. J. Neurophysiol. 61, 759-768.

Wallis, D.I. & Dun, N.J. (1988). A comparison of fast and slow depolarisations evoked by 5-HT in guinea-pig coeliac ganglion cells in vitro. British Journal of Pharmacology 93, 110-120.

Wallis, D.I. & North, R.A. (1978). The action of 5-hydroxytryptamine on single neurones of the rabbit superior cervical ganglion. Neuropharmacology 17, 1023-1028.

Walton, K. & Fulton, B.P. (1983). Hydrogen peroxide as a source of molecular oxygen for in vitro mammalian CNS preparations. Brain Research 278, 387-393.

Walton, K. & Fulton, B.P. (1986). Ionic mechanisms underlying the firing properties of rat neonatal motoneurones studied in vitro. Neuroscience 19, 669-683.

Watson, C.R.R., Sakai, S. & Armstrong, W. (1982). Organisation of the facial nucleus in the rat. Brain Behaviour and Evolution 20, 19-28.

White, S.R. & Neuman, R.S. (1980). Facilitation of spinal motoneurone excitability by 5-hydroxytryptamine and noradrenaline. Brain Research 188, 119-127.

Williams, J.T., Colmers, W.F. & Pan, Z.Z. (1988). Voltage- and ligand-activated inwardly rectifying currents in dorsal raphe neurons in vitro. Journal of Neuroscience 8, 3499-3506.

Wood, J.D. & Mayer, C.J. (1979). Serotonergic activation of tonic-type enteric neurones in guinea-pig small bowel. J. Neurophysiol. 42, 582-593.

Yakel, J.L. & Jackson, M.B. (1988). 5-HT_3-receptor mediated responses in cultured hippocampus and a clonal cell line. Neuron 1, 615-621.

Yakel, J.L., Trussell, L.O. & Jackson, M.B. (1988). Three serotonin responses in cultured mouse hippocampal and striatal neurones. Journal of Neuroscience 8 No.4, 1273-1285.

Yarom, Y. & Llinas, R. (1987). Long-term modifiability of anomalous and delayed rectification in guinea-pig inferior olive neurones. Journal of Neuroscience 7, 1166-1177.

Yarom, Y., Sugimori, M. & Llinas, R. (1985). Ionic currents and firing patterns of mammalian vagal motoneurones in vitro. Neuroscience 16, 719-737.

Yoshimura, M., Higashi, H. & Nishi, S. (1985). Noradrenaline mediates slow excitatory synaptic potentials in rat dorsal raphe neurones in vitro. Neuroscience Letters 61, 305-309.

Yoshimura, M. & Nishi, S. (1982). Intracellular recordings from lateral horn cells of the spinal cord in vitro. Journal of the Autonomic Nervous System 6, 5-11.

Yoshimura, M., Polosa, C. & Nishi, S. (1986). Electrophysiological properties of sympathetic preganglionic neurones in the cat spinal cord in vitro. Pflugers Archives 406, 91-98.

Yoshimura, M., Polosa, C. & Nishi, S. (1987). Slow EPSP and the depolarising action of noradrenaline on sympathetic preganglionic neurones. Brain Research 414, 138-142.

Yoshimura, M., Polosa, C. & Nishi, S. (1987). Noradrenaline-induced afterdepolarisation in cat sympathetic preganglionic neurons in vitro. J. Neurophysiol. 57, 1314-1324.

Young, W.S. & Kuhar, M.J. (1980). Noradrenergic α_1 and α_2 receptors:light microscopic autoradiographic localization. Proceedings of the National Academy of Sciences. USA. 77, 1696-1700.

Zgombick, J.M., Beck, S.G., Mahle, C.D., Craddock-Royal, B. & Maayani, S. (1989). Pertussis toxin-sensitive guanine nucleotide-binding protein(s) couple adenosine A_1 and 5-hydroxytryptamine$_{1A}$ receptors to the same effector systems in rat hippocampus: biochemical and electrophysiological studies. Journal of Pharmacology and Experimental Therapeutics 35, 484-494.

Zhang, L. & Krnjevic, K. (1986). Effects of 4-aminopyridine on the action potential and the after-hyperpolarization of cat spinal motoneurones. Canadian Journal of Physiology and Pharmacology 64, 1402-1406.

Zhang, L. & Krnjevic, K. (1987). Apamin depresses selectively the after-hyperpolarisation of cat spinal motoneurones. Neuroscience Letters 74, 58-62.